ANALYSIS OF THE ROLE OF PELLINO2 IN THE ACTIVATION OF THE NLRP3 INFLAMMASOME

A thesis presented to Maynooth University, Maynooth for the degree of Doctor of Philosophy

By

Ronan Bergin, B.Sc., M.Sc.

Institute of Immunology, Department of Biology,

Maynooth University

October 2015

Supervisor: Professor Paul Moynagh

Head of Department: Professor Paul Moynagh

DECLARATION

This thesis has not been previously submitted to this or any other university for examination for a higher degree. The work presented here is entirely my own except where otherwise acknowledged. This thesis may be made available for consultation within the university library. It may be copied or lent to other libraries for purposes of consultation.

Ronan Bergin

CONTENTS

Acknowledgments

Paul, I want to thank you for giving me the chance to work in your laboratory on such an exciting project. Your belief in me gave me the confidence to try new techniques and approaches which I may otherwise have shied away from. Your knowledge, patience, and good humour have all played a huge part in shaping my understanding of what it means to be a scientist. It has been an honour to learn from you over the past four years and I hope to continue to do so during the years which follow.

Ruaidhri, without your help and guidance I would not be where I am today and without your work on Pellino2, there would be no thesis to speak of! You pushed me to apply for this PhD and offered me an immeasurable amount of guidance during it. You have been both a great friend and a source of inspiration over the course of my PhD and will continue to be throughout the rest of my career.

Marc, your friendship helped keep me sane during some of the longer days in the lab. You have always provided insight into the arcane world of cellular biology and were always on hand to provide assistance whenever I needed help. Keep on Freefallin'! Enda, both during my Masters and PhD you were there to offer advice and assistance to me. There are few things I like more than to get into debates with you, which kept me entertained on dull days. I feel I have to mention your unforgettable stint as a radio DJ, I wish I recorded the "Rockfield Sessions" I really do!

I'd like to thank everyone in the Molecular Immunology lab, all of whom have made me feel welcome right from the very beginning. Figs, you are one of the most knowledgeable people I know and extremely dedicated to your work. Your assistance on the Pellino2 study has been greatly helpful, especially the overexpression work with IRAK1 presented here in figure 3.32 (b and c). Thank you

so much for your help and advice. Nezira, thank you for your help throughout my PhD as well as all of our entertaining chats! Bingwei and Yang thank you both for your help during the years and Bingwei, thank you especially for your excellent management of the Pellino colonies in the BRU, which can be a thankless job at times! Mark, you provided me with helpful insight into experimental design and were always on hand if I needed any help around the lab. It was also nice to have someone else who shared my enjoyment of random pub quiz questions! Claire and Johanna, even though you guys joined the group during my last two years, you both brought a lot of positive energy to the lab, which in turn made my experience all the more enjoyable.

Mam and Dad, you guys have always supported me throughout my life, and especially throughout my many years in college. I often look to you guys as examples of how I should live my life and how to be a better person. The values and love you have shown me throughout my life have made me who I am today. Thank you both for always standing by me and believing in me.

Karen, you've always supported me, especially through the last four years. Without you I wouldn't have started down this path in the first place and your belief in me has kept me going. We have both achieved so much by each other's sides and I can't wait to spend the rest of my life with you and continue to accomplish our dreams together. I love you more than you can know.

Abstract

The innate immune system is the first line of defence against invading pathogens and is responsible for both initial pathogen recognition and mounting an effective immunological response. The recognition of conserved pathogen-associated molecular patterns can be carried out by a number of families of innate immune receptors, including Toll-like receptors. Toll-like receptors can respond to a diverse range of microbial signals and elicit a targeted immune response against the invading pathogen. A key regulator of inflammation is IL-1β, which can be secreted from activated cells and mediate a strong inflammatory response. The regulation of its release is a tightly controlled signalling event, as its dysregulation has been linked with the pathogenesis of a variety of diseases including Alzheimer's disease and rheumatoid arthritis. The signalling complex which controls IL-1β release is known as the inflammasome, which requires two signals to facilitate its activation. The work in this thesis demonstrates a role for the E3 ubiquitin ligase Pellino2 in the specific activation of the NLRP3 inflammasome. Using a newly generated Pellino2-deficient mouse, it was determined that Pellino2 played no role during TLR induced NF-κB or MAPK signalling. However, *Peli2*$^{-/-}$ mice were more resistant to the lethal effects of LPS induced septic shock and this correlated with reduced serum IL-1β levels. Pellino2-deficient mice were shown to exhibit diminished NLRP3 inflammasome activation, correlating with reduced levels of NLRP3 ubiquitination and thus, lower levels of IL-1β secretion. While Pellino2 does not directly mediate the ubiquitination of NLRP3, it was observed that Pellino2-deficiency promoted the increased interaction of NLRP3 with hyperphosphorylated IRAK1. The data presented in this thesis defines for the first time a physiological role for Pellino2 in innate immune signalling with a particular function in mediating activation of the NLRP3 inflammasome.

Abbreviations

a/g:	Protein A/G beads
AIM2:	Absent in melanoma 2
Apaf1	Apoptosome regulator apoptotic protease activating factor 1
APC:	Antigen presenting cell
APS:	Ammonium persulfate
ASC:	Apoptosis-associated speck-like protein containing a CARD
ATP:	Adenosine triphosphate
BAC:	Bacterial artificial chromosome
BMDC:	Bone marrow derived dendritic cells
BMDM:	Bone marrow derived macrophages
BSA:	Bovine serum albumin
Ca^{+}:	Calcium
cAMP:	3'-5'-cyclic adenosine monophosphate
CARD:	Caspase activation and recruitment domain
cDNA:	Complementary DNA
CGD:	Chronic granulomatous diseases
CHAPS:	3-[(3-cholamidopropyl)dimethylammonio]-1-propanesulfonate
CLR:	C-type lectin receptors
CM:	Conditioned media
CNS:	Central nervous system
CoIP:	Co-immunoprecipitation
CpG:	2′-deoxyribo cytidine-phosphate-guanosine
CREB:	cAMP response element-binding protein
CTB:	Cholera toxin B

DAI:	DNA-dependent activator of IFN-regulatory factors
DAMPs:	Danger-associated molecular patterns
DC:	Dendritic cell
DD:	Death domain
DISC:	Death-inducing signalling complex
DMEM:	Dulbecco's Modified Eagle's medium
DMSO:	Dimethyl sulfoxide
DNA:	Deoxyribonucleic acid
dNTPs :	Deoxyribonucleic triphosphates
dsDNA:	Double stranded B-DNA
dsRNA:	Double-stranded RNA
DSS	Disuccinimidyl suberate
dToll:	*Drosophila* toll
DUB:	Deubiquitinating enzyme
E.coli:	*Escherichia coli*
EAE:	Experimental autoimmune encephalomyelitis
EDTA:	Ethylenediaminetetraacetic acid
ELISA:	Enzyme-linked immunosorbant assay
EMCV:	Encephalomyocarditis virus
EMSA:	Electrophoresis mobility shift assay
ER:	Endoplasmic reticulum
ERK:	Extracellular signal regulated kinase
EtOH:	Ethanol
EV:	Empty vector
FBS:	Foetal bovine serum
FHA:	Forkhead-associated
FOXP3:	Factor forkhead box P3
g:	Gravitation

GAPDH:	Glyceraldehyde 3-phosphate dehydrogenase
GM-CSF:	Granulocyte-macrophage colony-stimulating factor
h:	Hour
HCl:	Hydrochloric acid
HEK:	Human embryonic kidney
HEPES:	Hydroxyeicosapentaenoic acid
HIN-200:	Hematopoietic interferon-inducible nuclear proteins with a 200 amino acid repeat
HIV:	Human Immunodeficiency Virus
HPRT:	Hypoxanthine-guanine phosphoribosyltransferase
HRP:	Horseradish-peroxidase
HSP60:	Heat shock protein 60
HSV-1:	Herpes simplex virus
IAV:	Influenza A virus
IB:	Immunoblot
IBD:	Inflammatory bowel disease
iBMDM:	Immortalised BMDM
IFI16	Interferon gamma-inducible protein 16
IFN:	Interferon
Ig:	Immunoglobulin
IKK:	IκB kinase
IL:	Interleukin
IL-1R:	IL-1 receptor
IP:	Immunoprecipitation
IRAK:	IL-1 receptor associated kinase
IRF:	Interferon-regulatory factor
IκB:	Inhibitor of κB
JNK:	c-Jun n-terminal kinase

K^+:	Potassium
Kb:	Kilobase
KD:	Kilodalton
KSAH:	Kaposi sarcoma-associated herpesvirus
LB:	Lysogeny broth
LBP:	LPS binding protein
LCMV:	Lymphocytic choriomeningitis virus
LMP1:	Latent membrane protein 1
LPS:	Lipopolysaccharide
LRR:	Leucine-rich repeat
LUBAC:	Linear ubiquitin assembly complex
mA:	Milliamp
MAL:	Myd88 adaptor like
MAP:	mitogen-activated protein
MAPK:	Mitogen activated protein kinase
MAP3K:	mitogen-activated protein kinase kinase kinase
MAVS:	Mitochondrial anti-viral signalling
M-CSF:	Macrophage colony-stimulating factor
Mda5:	Melanoma differentiation−associated gene 5
MD-2	Myeloid differentiation factor 2
mDC:	Myeloid/convention dendritic cells
MDP:	Muramyl dipeptide
MEF:	Murine embryonic fibroblast
$MgCL_2$:	Magnesium chloride
min:	Minute
ml:	Millilitre
MLS:	Macrolide, lincosamide, and streptogramin group
mM:	Millimolar

mRNA:	Messenger RNA
MSU:	Monosodium urate crystals
MyD88:	Myeloid differentiation protein 88
Na_3VO_4:	Sodium orthovanadate
NaCl:	Sodium chloride
NADPH:	Nicotinamide adenine dinucleotide phosphate
NAIP:	Neuronal apoptosis inhibitor proteins
NBD:	Nucleotide-binding Domain
NaOH:	Sodium hydroxide
NF-κB:	Nuclear factor kappa B
ng:	Nanogram
NLR:	Nucleotide-binding oligomerization domain-like receptor
NLRC:	NOD, LRR and CARD-containing
NLRP:	NOD, LRR and PYD domains-containing protein
nM:	Nanomolar
NOD:	Nucleotide-binding oligomerization domain
NP-40:	Nonidet P-40 (octyl phenoxypolyethoxylethanol).
OD:	Optical density
PAGE:	Polyacrylamide gel electrophoresis
Pam_2CSK4:	S-[2,3-bis(palmitoyloxy)propyl]cysteine-4
PAMP:	Pathogen-associated molecular pattern
PBMC:	Peripheral blood mononuclear cells
PBS:	Phosphate buffered saline
PCR:	Polymerase chain reaction
pDC:	Plasmacytoid dendritic cell
PMSF:	Phenylmethylsulfonyl fluoride
Poly(I:C):	Polyinosinic-polycytidylic acid
Poly(dA-dT):	Poly(deoxyadenylic-deoxythymidylic)

PRR:	Pattern-recognition receptor
PYHIN:	Pyrin and HIN domain-containing protein
RANTES:	Regulated upon activation normal T cell expressed and secreted
RBL:	Red blood cell lysis
RIG-I:	Retinoic acid-inducible gene 1
RING:	Really interesting new gene
RIP1:	Receptor-interacting protein-1
RLR:	RIG-I like receptor
RNA:	Ribonucleic acid
rRNA:	Ribosomal RNA
RNAi:	RNA interference
ROS:	Reactive oxygen species
RPMI:	Roswell park memorial institute
RSV:	Respiratory syncytial virus
RT:	Room temperature; reverse transcriptase
sec:	Second
SDS:	Sodium dodecyl sulphate
siRNA:	Small interfering RNA
SeV:	Sendai Virus
SLE:	Systemic lupus erythematosus
SNP:	Single nucleotide polymorphisms
ssRNA:	Single-stranded RNA
STAT:	Signal transduction and transcription
SYC:	Spleen tyrosine kinase
T3SS:	Type III secretion system
TAE:	Tris-acetate-EDTA
TAB1:	TAK1 binding protein 1
TANK:	TRAF family member-associated NF-κB activator

TAK1:	TGFβ-activated kinase
TBEV:	Tick-borne encephalitis virus
Taq:	*Thermophilus aquaticus*
TBK1:	TANK-binding kinase 1
TBS:	Tris-buffered saline
TBST:	Tris-buffered saline containing Tween 20
Tc:	Threshold cycle
TE:	Tris-EDTA
TEMED:	N N N' N' - Tetramethylethylene-diamine
TIR:	Toll-IL-1 receptor domain
TLR:	Toll-like receptor
TMB:	3 3' 5 5'-Tetramethylbenzidine
TNF-α:	Tumour necrosis factor alpha
TNFR:	Tumour necrosis factor receptor
TRADD:	TNFR1-associated death domain protein
TRAF:	TNF receptor associated factor
TRAM:	TRIF-related adaptor molecule
TRIKA:	TRAF6-regulated IKK activator
TRIF:	TIR domain-containing adaptor inducing IFN-β
Ubc:	Ubiquitin conjugating enzyme
UBC:	Ubiquitin-conjugating enzyme
UEV1a:	Ubiquitin conjugating enzyme variant 1a
UV:	Ultraviolet light
V:	Volts
v:	Volume
VSV:	Vesicular stomatitis virus
w:	Weight
WNV:	West Nile virus

WT:	Wild-type
μg:	Microgram
μl:	Microliter
μM:	Micromolar

Chapter 1: Introduction

1.1 The Immune System

The immune system is multifaceted, consisting of many molecules, cells and organs which together, orchestrate protection against infective pathogens. Early research in the field lead to the broad characterisation of two separate phases of the immune response: the innate and adaptive systems. This is not a true dichotomy however, as there is a great degree of interaction and crosstalk between both (Lanier and Sun, 2009). The distinction between these two branching systems lies primarily in the degree of specificity to antigens, the speed of the response and the generation of a long lasting immunological memory (Kurtz, 2005). The innate immune system acts rapidly, targeting a wide range of pathogens through recognition of distinct conserved pathogenic components. This is mediated by antigen presenting cells (APC) such as macrophages and dendritic cells (DC), which can interact directly with invading pathogens and facilitate an appropriate response (Guilliams *et al.*, 2014). The adaptive response occurs later and is primarily mediated by the B and T lymphocytes. A T-cell response requires stimulation by activated APCs, which present pathogen-derived peptides to the T-cell and dictate their differentiation and polarisation (Kapsenberg, 2003). Activated T-cells assist B-cells in the production of antibodies which are targeted against specific epitopes present on the invading microorganism. Antibody production is a key event in the generation of an immunological memory and is the basis of effective vaccination (Nutt *et al.*, 2015). The importance of T-cells in immunity is highlighted during human immunodeficiency virus (HIV) infection, where the CD4 subset of T-cells are severely diminished, resulting in the increased susceptibility to a secondary opportunistic infection (Pope and Haase, 2003). The ability of the immune system to be able to define self from non-self is vital in the generation of a long lasting immune response, as a breakdown in this system can lead to autoimmunity (Wu *et al.*, 2009).

1.2 The Innate Immune System

The innate immune system is a highly evolutionarily conserved system which is the first line of defence during a pathogen invasion and is responsible for the broad spectrum clearance of the vast majority of microbes. The protective layers of the innate immune system extends from physical barrier to entry such as the skin and mucosal barriers (Peterson and Artis, 2014), to the more complex interplay between varieties of specialised cells (Nguyen *et al.,* 2002). The innate immune system was originally thought to be a simplistic response which only served to prime the more complex adaptive response. As a result, the bulk of early research into the immune system focused on this adaptive response (O'Neill *et al.,* 2013). A key question which was unanswered at the time was how the secretion of pro-inflammatory factors such as interleukin-1β (IL-1β) were regulated (Dinarello, 1991). The concept of cells recognising microbial products as priming signal to link an early and late immune response was first pioneered by Charles Janeway in 1989 (Janeway, 1989). The discovery of toll-like receptors (TLRs) and their ability to recognise conserved pathogen associated molecular patterns (PAMPs) opened the door to a major new area of immune research, innate immune signalling (Lemaitre *et al.,* 1996; Medzhitov *et al.,* 1997). Stimulated TLRs were shown to lead to the activation of a variety of immune-related genes and thus result in the secretion of cytokines and chemokines which can contribute to cell trafficking, inflammation and anti-viral responses (Hoshino *et al.,* 1999). This initial signalling by pattern recognition receptors (PRRs) underlies and directs the functions of a range of innate immune cells including macrophages and DCs, leading to an effective adaptive response. Continued research into PRRs has led to a more complete and nuanced understanding of the complexity of this initial signalling event.

1.4 Pattern Recognition Receptors

Mounting appropriate and specialised responses to specific pathogens is vital in maintaining an adequate immune response. This is achieved by a range of PRRs which can recognise PAMPs from bacterial, viral, fungal and parasitic origin. The controlled induction of inflammation through the signalling of these molecules provides protection against infection and can lead to tissue regeneration following this acute response (Medzhitov, 2008). It is essential that the motifs which PRRs recognise are distinct from self-molecules, as any breakdown in the differentiation between self and non-self would lead to an auto-immune environment, potentially leading to detrimental outcomes such as septic shock (Rittirsch *et al.,* 2008). While effective allorecognition is vital, an important distinction must be made with respect to certain danger associated molecular patterns (DAMPs), some of which originate from the host in times of cellular stress or tissue damage during pathogenic insult (Srikrishna and Freeze, 2009). These signals often arise during an immune response and as such can be recognised by certain PRRs (Mills, 2011). The cellular localisation of PRRs is also fundamentally important in facilitating their pathogenic recognition. Bacterial and fungal PAMPs are often encountered extracellularly and thus, the associated PRRs are localised to the plasma membrane. Contrastingly, viral PAMPs are generally recognised by PRRs located in the cytoplasm (Nishiya and DeFranco, 2004). PRRs are highly expressed in sentinel cells such as macrophages and DCs, but are also present on B-cells (Dorner *et al.,* 2009).

Currently, five families of PRRs have been described: TLRs, nucleotide-binding oligomerisation domain (NOD)-like receptors (NLRs), Pyrin and HIN domain-containing protein (PYHIN) family, retinoic acid-inducible gene 1 (RIG-I)-like receptors (RLRs) and C-type lectin receptors (CLRs) (Kutikhin and Yuzhalin, 2012; Mogensen, 2009). Each family consists of numerous members, all recognising a diverse range of ligands. Upon activation, complex signalling cascades are initiated downstream of the PRR, which can culminate in the upregulation of inflammatory cytokines, chemokines and type 1 interferons (IFN) (Perry *et al.,* 2005). This leads to the development of a cytokine milieu capable of inducing a pro-inflammatory state

and can influence the future immune responses to the invading pathogens. The signalling involved is rapid and can trigger immune responses based on the receptors activated as well as cross-talk between receptors (Tan *et al.*, 2014).

1.5 Toll-like Receptors and Their History

TLRs were the first family of PRRs to be identified and are the most well studied to date. Early research into the area of innate immunity focused on the determination of a cellular receptor to the gram negative bacterial cell membrane lipopolysaccharide (LPS) due to its useful adjuvant properties (Seppälä and Mäkelä, 1984). The cell surface molecule CD14 was shown to be indispensable in eliciting a cellular response to LPS (Wright *et al.,* 1990), but the LPS receptor itself proved elusive. Determining the receptor through the use of classical binding studies proved difficult due to the hydrophobic nature of LPS (Beutler, 2011). The first key discovery which led to the identification of the TLRs arose from research carried out in the fruit fly *Drosopila melanogaster*. The sequencing of the receptor IL-1R type 1 (IL-1R1), was shown to share homology with the *D. melanogaster* protein Toll, previously thought to only function as a maternal effect gene in embryonic development (Anderson *et al.*, 1985).

In 1996, Hoffman and Lemaitre published their seminal paper demonstrating the role of Toll signalling in the production of the antifungal molecule peptide drosomycin in adult Drosophila during fungal infection (Lemaitre *et al.*, 1996). This work highlighted for the first time that Toll and IL-1R not only shared common structural similarities, but functional ones. This work was expanded upon by Medzhitov and Janeway in 1997, when they cloned and characterised the first human Toll-like protein, now known as TLR4. It was shown that transfection of a constitutively activated form of TLR4 into human cells could activate NF-κB and lead to the induction of pro-inflammatory cytokines as well as B7.1 (CD80), an important co-stimulatory molecule for the maturation and activation of naïve T cells (Medzhitov *et al.*, 1997). This was the first link between the innate and adaptive response, verifying

Janeway's early hypothesis of the importance of innate signalling in shaping the adaptive response (Medzhitov *et al.,* 1997). This discovery sparked a great interest in the field of PRRs and quickly resulted in the identification of a family of TLRs (Rock *et al.,* 1998).

TLRs are transmembrane receptors which localise either on the cell surface or within intracellular compartments. TLRs consist of an extra-cellular domain composed of tandem leucine-rich repeats (LRRs), a membrane spanning component and a cytosolic Toll/IL-1R (TIR) domain. The extracellular domain is responsible for ligand recognition and its crystal structure shows that LRRs form a loop structure (Bell *et al.,* 2005; Choe *et al.,* 2005). Upon ligand binding, TLRs dimerise to form either homodimers or heterodimers which facilitates the cytosolic TIR domains to act as a scaffold allowing the formation of a signalling complex (Xu *et al.,* 2000). To date, 13 mammalian TLRs have been identified. TLRs1-9 have a shared function between mice and humans, but while TLR10 is present in humans, it is a non-functional pseudogene in mice. TLR11-13 are functional in mice, but human *TLR11* is also a non-functional pseudogene, while *TLR12* and *TL13* does not exist in the human genome (Akira *et al.,* 2006; Kawai and Akira, 2009).

1.5.1 TLR2 Forms Heterodimers to Detect an Extensive Range of Ligands

Early work implicated LPS as a ligand of TLR2 (Yang *et al.,* 1998), but this was clarified using TLR2 knockout mice, which were equally sensitive to LPS as wild type (WT) mice (Takeuchi *et al.,* 1999). Instead, the latter study demonstrated a role for TLR2 in detecting gram-positive bacteria and further research has shown that TLR2 can identify a wide range of agents and ligands. These include measles virus (Bieback *et al.,* 2002), bacterial tri-acylated lipoproteins (Aliprantis *et al.,* 1999; Lien *et al.,* 1999), lipoteichoic acid and peptidoglycan as well as the fungal cell wall component zymosan (Underhill *et al.,* 1999). TLR2 is capable of recognising such a

diverse range of ligands due in part to its ability to form heterodimers with other TLRs. It has been suggested that homodimers of TLR2 may also form, but to date, this has not been demonstrated (M. S. Jin *et al.,* 2007). TLR2 is capable of forming heterodimers with TLR1, TLR6 and TLR10 (Oliveira-Nascimento *et al.,* 2012). Interestingly, while the various TLR2-containing heterodimers facilitates the recognition of an array of ligands, the functional downstream signalling responses are the same, implicating the evolutionary expansion of recognition, while maintaining the downstream signalling response (Farhat *et al.,* 2008).

TLR1/2 recognises triacylated lipoproteins as well as mycobacterial products while TLR2/6 recognises diacylated lipoproteins. Synthetic lipopeptides can be used to specifically target either TLR1/2 or TLR2/6 heterodimers. Pam3CSK4 is a synthetic triacylated lipopeptide which can bind TLR1/2 (M. S. Jin *et al.,* 2007) while Pam2CSK4 is a synthetic diacylated lipoprotein and binds TLR2/6 (Kang *et al.,* 2009). CD36 is a member of the scavenger receptor type B family and is known to act as a co-receptor for diacylglyceride signalling in combination with TLR2/6. The requirement of CD36 to act as a co-receptor during triacylglyceride recognition is redundant however, demonstrating the selectivity with which this signalling can occur (Hoebe *et al.,* 2005). To date, both the specific ligand and the signalling consequences for the TLR2/10 heterodimer are unknown (Guan *et al.,* 2010).

Zymosan is a yeast-derived polysaccharide consisting of β-glucan and mannan (Brown *et al.,* 2002) and is recognised by both TLR2/6 and dendritic-cell-associated C-type lectin-1 (Dectin-1). Dectin-1 is a membrane bound receptor capable of direct binding to β-glucans and the induction of a spleen tyrosine kinase (SYK) dependent signalling pathway (Underhill *et al.,* 2005). The response to zymosan occurs synergistically between both dectin-1 and TLR2/6, resulting in an augmented inflammatory response and improved microbial phagocytosis (Gantner *et al.,* 2003). Dectin-1 has also been shown to co-localise with TLR2 upon zymosan stimulation, highlighting the possibility of the formation of a signalling complex similar to other TLR2 heterodimers (Brown *et al.,* 2003).

1.5.2 TLR 3 Recognises Double-Stranded RNA

TLR3 is an endosomal PRR and was first shown to recognise double-stranded RNA (dsRNA), which is an intermediate pattern that occurs during the replication cycle of many viruses (Weber *et al.,* 2006). TLR3 signalling was also demonstrated to lead to the activation of NF-κB and the production of type I IFNs (Alexopoulou *et al.,* 2001). This discovery implicated TLR3 as a key regulator in the recognition and response to a variety of viruses. Since this initial characterisation, TLR3 has also been shown to recognise non-viral signals such as self mRNA released from necrotic cells as a DAMP (Karikó *et al.,* 2004). Interestingly, this effect is not seen during apoptotic events, implicating a role for TLR3 in the response to tissue stress or injury (Cavassani *et al.,* 2008). A synthetic analogue of dsRNA often used to activate TLR3 *in vitro* is known as polyriboinosinic:polyribocytidylic acid (poly(I:C)). The effectiveness of the activation is dependent on the molecular mass of the poly(I:C) used, with longer forms inducing a more robust TLR3 dependent response (Zhou *et al.,* 2013). While TLR3 is a highly expressed receptor in most innate immune cells, it is not expressed in either neutrophils (Hayashi *et al.,* 2003) or plasmacytoid dendritic cells (pDC) (Edwards *et al.,* 2003).

The importance of the contribution of TLR3 to *in vivo* viral clearance remains controversial. Encephalomyocarditis virus (EMCV) and mouse cytomegalovirus (MCMV) infection of the *TLR3*$^{-/-}$ mouse model have shown that the absence of TLR3 leads to reduced survival, correlating with increased viral load and reduced antiviral cytokine secretion (Hardarson *et al.,* 2007; Tabeta *et al.,* 2004). However, another study comparing the role of TLR3 in various murine viral infections showed that *TLR3*$^{-/-}$ mice show no difference in susceptibility to reovirus, lymphocytic choriomeningitis virus (LCMV) and vesicular stomatitis virus (VSV), implicating a redundancy in TLR3 signalling (Edelmann *et al.,* 2004). The *TLR3*$^{-/-}$ mouse model has also been shown to be largely resistant to West Nile virus (WNV), as a TLR3 mediated inflammatory response is required for a compromised blood-brain barrier leading to encephalitis and death (Wang *et al.,* 2004). Pneumonia induced by influenza A virus showed that while *TLR3*$^{-/-}$ mice exhibited reduced viral clearance

in the lungs, they showed increased rates of survival in this acute model due to a reduction in secreted inflammatory mediators (Le Goffic *et al.*, 2006).

Similar to data from mice, the functional role of TLR3 in humans remains ambiguous. A polymorphism of *TLR3* at Leu412Phe has been shown to confer protection against HIV-1 (Sironi *et al.*, 2012) and tick-borne encephalitis virus (TBEV) (Kindberg *et al.*, 2011). Conversely, this polymorphism is also associated with increased susceptibility to enteroviral myocarditis due to reduced activation of NF-κB and type I IFN (Gorbea *et al.*, 2010). Human TLR3 has been shown to be critical in the immunity to herpes simplex virus 1 (HSV-1) in children, as demonstrated by independent TLR3 genetic mutations in patients exhibiting HSV-1 encephalitis (Zhang *et al.*, 2007).

1.5.3 TLR4: The LPS Receptor

TLR4 is one of the most well studied TLRs and is primarily responsible for the recognition of LPS (Chow *et al.*, 1999; Hoshino *et al.*, 1999; Poltorak *et al.*, 1998). As mentioned previously, early work focusing on LPS recognition showed that TLR2 potentially played a role in LPS signalling. However this was shown not to be the case as it was demonstrated that mutation of the *TLR4* gene impaired LPS recognition while *TLR2* mutation did not (Heine *et al.*, 1999; Poltorak *et al.*, 1998; Underhill *et al.*, 1999).

LPS is a major component of the gram-negative bacterial cell wall and low concentrations are capable of inducing a robust and rapid inflammatory response, making LPS a key signal in the early response to infection (Kamio and Nikaido, 1976; Raetz and Whitfield, 2002). LPS is composed of three domains: the lipid A hydrophobic anchor, a nonrepeating oligosaccharide and the distal polysaccharide, known as the O antigen (Raetz and Whitfield, 2002). The lipid A component of LPS can be subjected to extensive modification by the bacteria both during and after synthesis. These modifications which include acylation (Guo *et al.*, 1998) and the

modification of phosphate groups (Gunn *et al.*, 1998) can lead to a diverse range of lipid A structures which can vary greatly between bacteria. These modifications can result in immune evasion and environmental adaption (Guo *et al.*, 1998). While TLR4 can directly recognise the lipid A moiety of LPS, modifications to bacterial lipid A can impair or entirely disrupt this binding (Hajjar *et al.*, 2002).

Myeloid differentiation factor 2 (MD-2) contains no transmembrane or intracellular domains and forms a complex with the extracellular component of TLR4 (Kim *et al.*, 2007). LPS binding protein (LBP) is a soluble protein circulating at low concentrations in serum. Upon infection, LBP recognises and binds LPS (Lamping *et al.*, 1998) and traffics LPS to the membrane-bound receptor CD14 (Pugin *et al.*, 1993). This further transports the LPS to the TLR4-MD-2 complex resulting in signal transduction.

While TLR4 plays a key role in the response to gram-negative bacteria, it has also been shown to respond to several other PAMPs such as the F protein of respiratory syncytial virus (RSV) (Kurt-Jones *et al.*, 2000) and teichuronic acid, a cell wall component of the gram-positive bacteria *Micrococcus luteus* (Yang *et al.*, 2001). Various host derived endogenous signals can also illicit a TLR4 response, such as heat shock protein 60 (HSP60) (Ohashi *et al.*, 2000), Fibrinogen type III extra domain A (Okamura *et al.*, 2001), saturated fatty acids (Tsukumo *et al.*, 2007) and minimally oxidized low-density lipoproteins (Choi *et al.*, 2009) which are usually secreted during tissue damage. These ligands are all structurally dissimilar, highlighting the potential for ligands to bind different regions of the receptor or, as the case with TLR4-MD-2, use different accessory molecules to facilitate binding (Kim *et al.*, 2007).

1.5.4 TLR5 Modulates the Gut Microflora

TLR5 is localised at the cell surface and recognises flagellin from gram-negative and gram-positive bacteria (Hayashi *et al.*, 2001). The flagellum consists of filaments of

the protein flagellin; it extrudes from the surface of bacteria and functions as a source of motility and adhesion (Ramos *et al.,* 2004). Rotation of these filaments at hundreds of revolutions per second generates taxis (Yonekura *et al.,* 2003). The number of individual flagella on a single *Candidatus Ovobacter* for example can exceed 400 and form prominent flagellar tufts (Fenchel and Thar, 2004).

The focus of most TLR5 research has centred on its function in the intestine. A healthy gut microbiome contains low levels of flagella (Bambou *et al.,* 2004), however a recent study shows that *TLR5*$^{-/-}$ mice exhibit increased numbers of commensals expressing higher levels of flagella (Cullender *et al.,* 2013). This is associated with an increased rate of intestinal breaching of bacteria leading to dysbiosis. Interestingly, the loss of TLR5 in these mice also correlates to reduced levels of anti-flagellin IgA. The authors concluded that the anti-flagellin antibodies maintain gut homeostasis by first binding and immobilising flagellated bacteria and then as a signalling molecule which can alter the composition of the gut microbiome. This hints at a complex crosstalk between the microbiota and the host immune system.

Single nucleotide polymorphisms (SNPs) in TLR5 may serve as useful biomarkers for a wide range of diseases. For example, the single dominant nucleotide polymorphism in TLR5 (TLR5^{R392X}) (Hawn *et al.,* 2003) is one of the most frequent polymorphisms to occur in the TLR family and is associated with Legionnaires disease, urinary tract infections (Hawn *et al.,* 2009, 2003), colorectal cancer (Klimosch *et al.,* 2013) and bronchopulmonary dysplasia (Sampath *et al.,* 2012). The possible role of TLR5 in cancers is particularly intriguing, as the composition of the gut microbiota has been shown to shape the response to both chemotherapy and immunotherapy (Viaud *et al.,* 2013).

1.5.5 Endosomal TLR 7/8/9

Like TLR3, TLR7, 8 and 9 are located on the endosomes of cells. However, they differ from TLR3 in their ligand recognition as well as their downstream signalling pathways. TLR7 and 8 form a heterodimer that recognises the synthetic imidazoquinoline family of antiviral derivatives, loxoribine and GU-rich ssRNAs (Diebold *et al.,* 2004; Heil *et al.,* 2004, 2003; Hemmi *et al.,* 2002) while TLR9 is a homodimer (Latz *et al.,* 2007) and recognises unmethylated CpG-rich dsDNA (Hemmi *et al.,* 2000).

While myeloid DCs express TLR8 (Ganguly *et al.,* 2009), pDCs have a limited TLR expression profile but predominantly express TLR7 and TLR9. This small population of cells compromise only between 0.2 and 0.8% of all mononuclear cells in the blood. However, they are capable of producing high levels of Type I IFNs in response to a viral infection, making them specialised viral sensing cells (Birmachu *et al.,* 2007). Systemic lupus erythematosus (SLE) is an autoimmune disease characterised by the production of auto-antibodies (Tan *et al.,* 1982). It was found that TLR9 and TLR8-deficient mice exhibited accelerated and severe SLE disease, while TLR7 deficient mice were protected against SLE. It was also determined that in the absence of TLR9 and TLR8, TLR7 levels could be upregulated, leading to the promotion of auto-antibodies (Christensen *et al.,* 2006; Demaria *et al.,* 2010; Nickerson *et al.,* 2010).

1.5.6 Human Orphan TLR 10

TLR10 has proven difficult to study because of the lack of an available mouse model due to *TLR10* being present as a pseudogene in mice. As such, there is comparatively little known about its signalling pathway and the determination of its agonist has remained elusive. Early work using human cells determined that TLR10 is highly expressed in B-cells and pDCs (Chuang and Ulevitch, 2001) and can interact with

TLR2 *in vitro*. However, B-cells have been shown to be unresponsive to TLR2 agonists which implicates no phenotypical interaction *in vivo* (Berkeredjian-Ding *et al.,* 2005; Hasan *et al.,* 2005). Further work clarified that TLR2 is upregulated in a certain subsets of differentiating $CD19^{inter}$ B-cells, highlighting a possible role for TLR2/TLR10 in the maturation of B-cells or germinal cell formation (Ganley-Leal *et al.,* 2006). Interestingly, TLR10 is expressed in T regulatory cells and regulated by transcription factor forkhead box P3 (FOXP3), but its physiological relevance is still unclear (Bell *et al.,* 2007).

Recent evidence has implicated TLR10 in the response to influenza virus, where it can modulate the secretion of type I and III IFNs and also pro-inflammatory cytokines (Lee *et al.,* 2014). The upregulation of TLR10 protein expression is higher following a H5N1 infection when compared with a less pathogenic H1N1 infection, highlighting the possibility that TLR10 may moderate the cellular response to certain infections.

1.5.7 Murine TLR 11/12/13

The first defined ligand for TLR11 was the intracellular protozoa *Toxoplasma gondii* profilin-like molecule (Yarovinsky *et al.,* 2005). Profilin is secreted from the parasite and is responsible for actin polymerisation and functions in parasites as a means of motility (Dobrowolski and Sibley, 1996; Plattner *et al.,* 2008). TLR11 is an intracellular receptor and requires the endoplasmic reticulum (ER) protein UNC93B1 for its functioning. However, intracellular infection of DCs with *T. gondii* did not illicit a necessary response for clearance (Pifer *et al.,* 2011). The TLR11 interaction with profilin occurs within endolysosomes, suggesting that recognition must occur prior to intracellular infection (Pifer and Yarovinsky, 2011). TLR12, another murine specific TLR, has been shown to complex with TLR11 and facilitates the recognition of profilin (Raetz *et al.,* 2013). It is interesting to note that both TLR11 and TLR5 are responsible for detection of molecules involved in the movement of pathogens. The ability to recognise motility molecules from both

protozoa and bacteria demonstrates the specific recognition of vital components of pathogens.

TLR13 recognises a 23S ribosomal RNA (rRNA) from bacteria such as *Saccharopolyspora erythraea* (Oldenburg *et al.,* 2012). The sequence of 23s rRNA that TLR13 recognises is also the binding region of macrolide, lincosamide, and streptogramin group (MLS) antibiotics. It was shown that modifications to 23s rRNA which induced MLS resistance, also rendered the bacteria undetectable to TLR13. The authors hypothesise that an ancient form of natural antibiotic resistance (D'Costa *et al.,* 2011) occurred in bacteria which rendered TLR13 redundant in many mammals, which is why it is not found in humans (Oldenburg *et al.,* 2012).

1.6 MyD88 Dependent TLR Pathway

Upon TLR engagement, complex downstream signalling pathways are initiated (Fig. 1.1). Myeloid differentiation primary response gene 88 (MyD88) is an adapter protein, which can directly bind all TLRs except TLR3 (Adachi *et al.,* 1998). Upon ligand binding, MyD88 associates with the cytoplasmic tail of the TLR and serves as a signalling platform to rapidly initiate a signalling cascade. The end-point of this pathway is the activation of NF-κB, the transcription factor vital for the production of inflammatory cytokines and anti-microbial mediators (Warner and Núñez, 2013). This MyD88 dependent pathway is a highly conserved and critically important signalling pathway responsible for the initiation of both innate and adaptive responses.

MyD88 is composed of three main domains: a death domain (DD), an intermediate domain and a TIR domain (Hardiman *et al.,* 1996). MyD88 association with TLRs occurs via a TIR-TIR domain interaction following TLR dimerisation and leads to the initiation of a larger signalling cascade (Ohnishi *et al.,* 2009). The adapter molecule MyD88-adapter-like (MAL) can also associate with MyD88 at the TIR domain during TLR4 (Fitzgerald *et al.,* 2001), TLR2/5 and TLR1/2 (Yamamoto *et*

al., 2002) activation. The protein complex which forms upon TLR receptor association is known as the myddosome and consists of the serine/threonine kinases interleukin-1 receptor-associated kinase 1 (IRAK1), IRAK2 and IRAK4. The complex first requires the oligomerisation of MyD88 molecules, which further recruits IRAK4 via DD interactions, leading to its oligomerisation (Lin *et al.,* 2010; Li *et al.,* 2002). IRAK1 and IRAK2 are then recruited to the complex, where IRAK4 can phosphorylate both, leading to the promotion of their auto-phosphorylation. Interestingly, both IRAK1 and IRAK4 have been shown to directly phosphorylate MAL and lead to its degradation, resulting in a negative regulation of TLR signalling (Dunne *et al.,* 2010). Activated IRAK1 or IRAK2 can then leave the complex and further associate with TNFR-associated factor 6 (TRAF6). The involvement of IRAK1 during this signalling event is primarily thought to result in the initiation of a rapid signalling response, while IRAK2 results in a more sustained signal and is not subject to acute degradation (Martin and Kollewe, 2001; Meylan and Tschopp, 2008). Upon activation, IRAK1 is subject to auto-phosphorylation and ubiquitination leading to its proteosomal degradation (Conze *et al.,* 2008; Yamin and Miller, 1997).

TRAF6 is an E3 ligase and in conjunction with the ubiquitin conjugating complex Ubc13-Uev1A, also known as TRAF6-regulated IKK activator 1 (TRIKA1), can auto-ubiquitinate and form free K63 linked ubiquitin chains, which are associated with signal propagation (Deng *et al.,* 2000). TRAF6 can also ubiquitinate IRAK1 (Conze *et al.,* 2008) and TRIKA2 (Wang *et al.,* 2001) in a K63 manner. TRIKA2 is a protein complex composed of TGFβ-activated kinase (TAK1), TAK1 binding protein 1 (TAB1), TAB2 and TAB3. TRAF6 associates with this complex through interaction and ubiquitination of TAK1, mediated by the binding of TAB2 and TAB3 to ubiquitinated TRAF6 (Kanayama *et al.,* 2004). This activated protein kinase complex acts as a signalling junction, dictating the regulation of both the NF-κB and AP-1 responses.

The transcription factor NF-κB is normally sequestered by IκBα in the cytosol of resting cells (Napetschnig and Wu, 2013). However pathways like IL-1 and TLRs can trigger the above MyD88-dependent pathway to promote phosphorylation and ubiquitination of IκBα leading to its degradation and the further dissociation of the

IκBα–NF-κB complex. NF-κB is then free to translocate to the nucleus and regulate gene activity (Z. J. Chen *et al.,* 1996). The NF-κB family is composed of five members, RelA, RelB, c-Rel, p50 and p52 and plays a central role in the immune response and during cellular development (Vallabhapurapu and Karin, 2009). IκBα phosphorylation is mediated by the IκB kinase (IKK) complex of proteins, which consist of IKKα (Z. J. Chen *et al.,* 1996), IKKβ (DiDonato *et al.,* 1997) and IKKγ (also known as NEMO) (Yamaoka *et al.,* 1998). TRAF6 is also capable of ubiquitinating NEMO, which facilitates the interaction of the IKK complex with TAK1 resulting in its activation (Sun *et al.,* 2004). Activated TAK1 can phosphorylate IKK (Wang *et al.,* 2001), which leads to IκBα degradation and subsequent NF-κB activation. TAK1 can also regulate activation of the mitogen-activated protein (MAP) kinase kinase kinase (MAP3K) pathway (Wang *et al.,* 2001). TAK1 phosphorylates MKK6, which leads to the activation of the c-Jun N-terminal kinase (JNK), P38 and extracellular signal-regulated kinase (ERK) activation, leading to the activation of the transcription factor AP-1.

MyD88 has also been shown to play a role in antiviral interferon regulatory factor (IRF) signalling. MyD88 is capable of associating with IRF7 through death domain interaction in a complex also involving TRAF6 (Kawai *et al.,* 2004). This MyD88-IRF7 association occurs strongly in differentiated pDCs upon TLR9 and TLR7/8 stimulation (Hemmi *et al.,* 2003; Hochrein *et al.,* 2004). IRF7 activation leads to a type-I interferon production and is required for a robust anti-viral immune response (Honda *et al.,* 2005). The activation of another member of the IRF family, IRF5 by TLRs has also been shown to be dependent on MyD88 signalling and mediated by TRAF6 (Balkhi *et al.,* 2008; Schoenemeyer *et al.,* 2005).

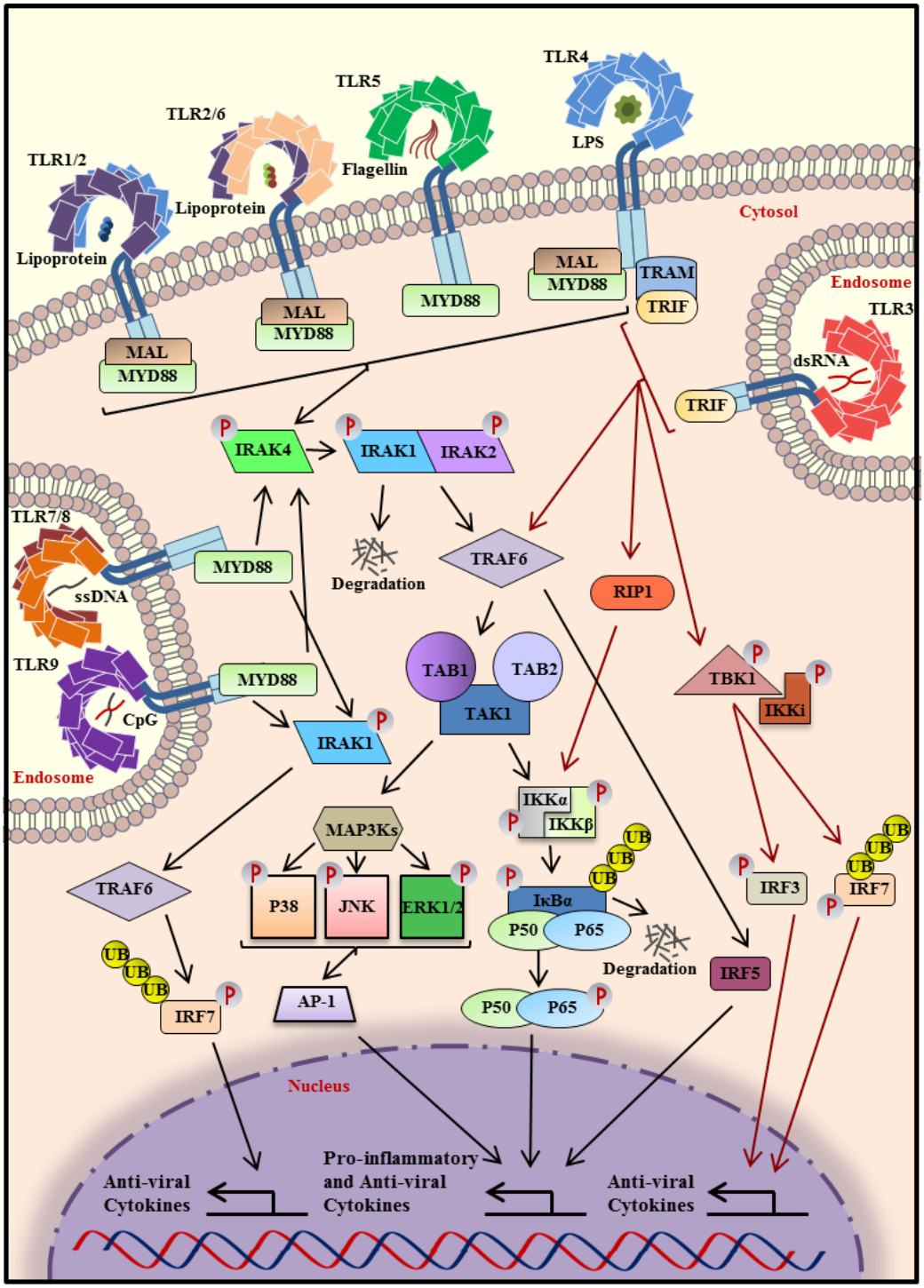

Fig 1.1 TLR1-9 Signalling Pathways

See sections 1.6 and 1.7 for detailed descriptions of the signalling pathways shown here. Red arrows indicate TRIF dependent signalling, while black arrows represent MyD88 signalling. Yellow circles containing "UB" represent ubiquitination, whole circles containing "P" represent phosphorylation.

1.7 TRIF Dependent TLR Pathway

TLR3 signals via the adapter molecule TIR-domain-containing adapter-inducing interferon-β (TRIF) which leads to the activation of both IRF3 and NF-κB (Hoebe *et al.,* 2003; Yamamoto *et al.,* 2003). TLR4 is also capable of signaling through TRIF but requires prior association with a bridging adapter molecule TRIF-related adaptor molecule (TRAM) (Rowe *et al.,* 2006; Yamamoto *et al.,* 2003b). Upon LPS/TLR binding, the MyD88 pathway is initiated. TLR4 can then be endocytosed and can activate TRAM-TRIF dependent signaling in early endosomes. Therefore, cellular localization can play a key role in the recruitment of downstream adapter molecules to the TLR TIR domains (Kagan *et al.,* 2008).

Receptor-interacting protein-1 (RIP1) along with TRAF6, can associate with TRIF and cooperate synergistically in the downstream activation of NF-κB (Meylan *et al.,* 2004; Sato *et al.,* 2003). Polyubiquitination of RIP1 is necessary for the recruitment of TAK1 and IKK complexes, leading to their activation (Ea *et al.,* 2006). The requirement of RIP1 and not the IRAK family of proteins differentiates TLR3 dependent NF-κB activation from the other TLRs (Meylan *et al.,* 2004). TANK-binding kinase 1 (TBK1) and IKKε also associates with TRIF and lead to the phosphorylation of IRF3 and the induction of an antiviral response (Fitzgerald *et al.,* 2003; Sharma *et al.,* 2003).

1.8 Inflammasome-mediated Processing of IL-1β and IL-18

The secretion of the inflammatory cytokine IL-1β is tightly regulated due to its ability to induce systemic inflammation. IL-1β is produced in an inactive form (pro IL-1β) and sequestered in the cytoplasm before cleavage and activation by caspase-1. The steps leading to this activation were unknown until the concept of an inflammasome was first proposed by Jürg Tschopp and colleagues in 2002 (Martinon *et al.,* 2002). This landmark work demonstrated the capacity of the protein

NOD, LRR and PYD domains-containing protein 1 (NLRP1) to regulate the secretion of IL-1β. NLRP1 was shown to form a protein complex with the adapter protein apoptosis-associated speck-like protein containing a CARD (ASC) which could lead to the activation of caspase-1 and thus result in the processing of IL-1β. This fundamental discovery heralded the beginning of a new branch of immune research that has furthered our understanding of the response to infection as well as autoimmunity.

The production and secretion of IL-1β and IL-18 are more tightly regulated than most other inflammatory cytokines. Their activation is dependent upon both protein translation and a secondary activating signal (Martinon *et al.,* 2009; Schroder and Tschopp, 2010). The secretion of these cytokines after activation is known as unconventional protein secretion and is independent of the (ER)/Golgi-dependent pathway but dependent on caspase-1 (Keller *et al.,* 2008). The precise mechanisms by which protein trafficking out of the cell occurs after processing by the inflammasome is still a subject of debate (Lopez-Castejon and Brough, 2011). Understanding these regulatory events is vitally important, due to the destructive effect these cytokines can have on the host, as the dysregulation of these cytokines has been implicated in a variety of auto-inflammatory diseases (Mills *et al.,* 2013; Sedimbi *et al.,* 2013). Monocytes and macrophages are major producers of IL-1β and IL-18 (Kahlenberg and Dubyak, 2004), but other cell types have also been shown to display inflammasome activity under specific conditions, such as keratinocytes (Feldmeyer *et al.,* 2007).

The inflammasome is a multi-protein complex, capable of responding to a wide variety of danger signals (Figure 1.2) and inducing a pro-inflammatory state which can further trigger a necrotic form of cell death called pyroptosis (Y. Chen *et al.,* 1996; Fink and Cookson, 2006). A number of members of the NLR protein family make up the majority of the known sensors capable of inducing the assembly of an inflammasome upon recognition of a triggering molecule (Martinon *et al.,* 2002). ASC, which is an essential component for all canonical inflammasomes, then associates with the activated sensor and oligomerises to form a large complex that manifests as a large single protein speck in microscopic analysis (Sahillioglu *et al.,*

2014; Yamamoto *et al.,* 2004). Interestingly, this polymerisation is a characteristic of prion formation and mutation of the regions associated with this prion activity negates its signalling potential (Cai *et al.,* 2014). Pro-caspase 1 is then recruited to this multi-protein scaffold and cleaved to its active form, which can subsequently cleave and activate pro-IL-1β and pro-IL-18 (van de Veerdonk *et al.,* 2011).

A key feature of inflammasome signalling is the requirement of two distinct signals before assembly and subsequent cleavage events can occur; this highlights the degree of regulation involved in IL-1β and IL-18 release and emphasises their importance as key mediators of inflammation (van de Veerdonk *et al.,* 2011). Signal 1 or the priming signal is required for the initial transcription of inflammasome components such as pro-IL-1β and NLRP3. This signal involves activation of NF-κB due to the stimulation of PRRs such as TLRs (Schroder and Tschopp, 2010). Signal 2 can range from DAMPs such as alum (Franchi and Núñez, 2008) and extracellular ATP (Mariathasan *et al.,* 2006) to PAMPs such as nigericin (Mariathasan *et al.,* 2006) and flagellin (Zhao *et al.,* 2011). This signal leads to the maturation of IL-1β and IL-18. While signal 1 is required for optimal IL-18 secretion, unlike IL-1β, pro-IL-18 does not require upregulation during signal 1 as it is constitutively expressed (Kahlenberg *et al.,* 2011).

There is a high degree of diversity in the range of PAMPs and DAMPs which can lead to inflammasome activation; this is due to the number of different sensors which can initiate inflammasome assembly. Despite this variation in recognition, the key protein-protein interactions within the different activated inflammasomes are analogous (Latz *et al.,* 2013). The adapter ASC is composed of a pyrin domain and a caspase activation and recruitment domain (CARD) (Masumoto *et al.,* 1999). Homotypic interaction with the upstream sensor molecule occurs mainly through pyrin interaction (Vajjhala *et al.,* 2014). The proteins NOD, LRR and CARD-containing 4 (NLRC4) and RIG-I are the exceptions, as their interaction with ASC is facilitated by CARD interaction (Poeck *et al.,* 2010; Pothlichet *et al.,* 2013; Proell *et al.,* 2013). Interaction between caspase-1 and ASC occurs through CARD interaction, resulting in the self-cleavage of caspase-1.

A number of inflammasomes have been characterised to date and include NLRP1, NLRP3, NLRP6, and NLRC4. Other inflammasomes have also been described that are not part of the NLR family (Latz *et al.*, 2013). These include two PYHIN family members, absent in melanoma 2 (AIM2) and interferon gamma-inducible protein 16 (IFI16) and RIG-I (Latz *et al.*, 2013; Martinon *et al.*, 2009).

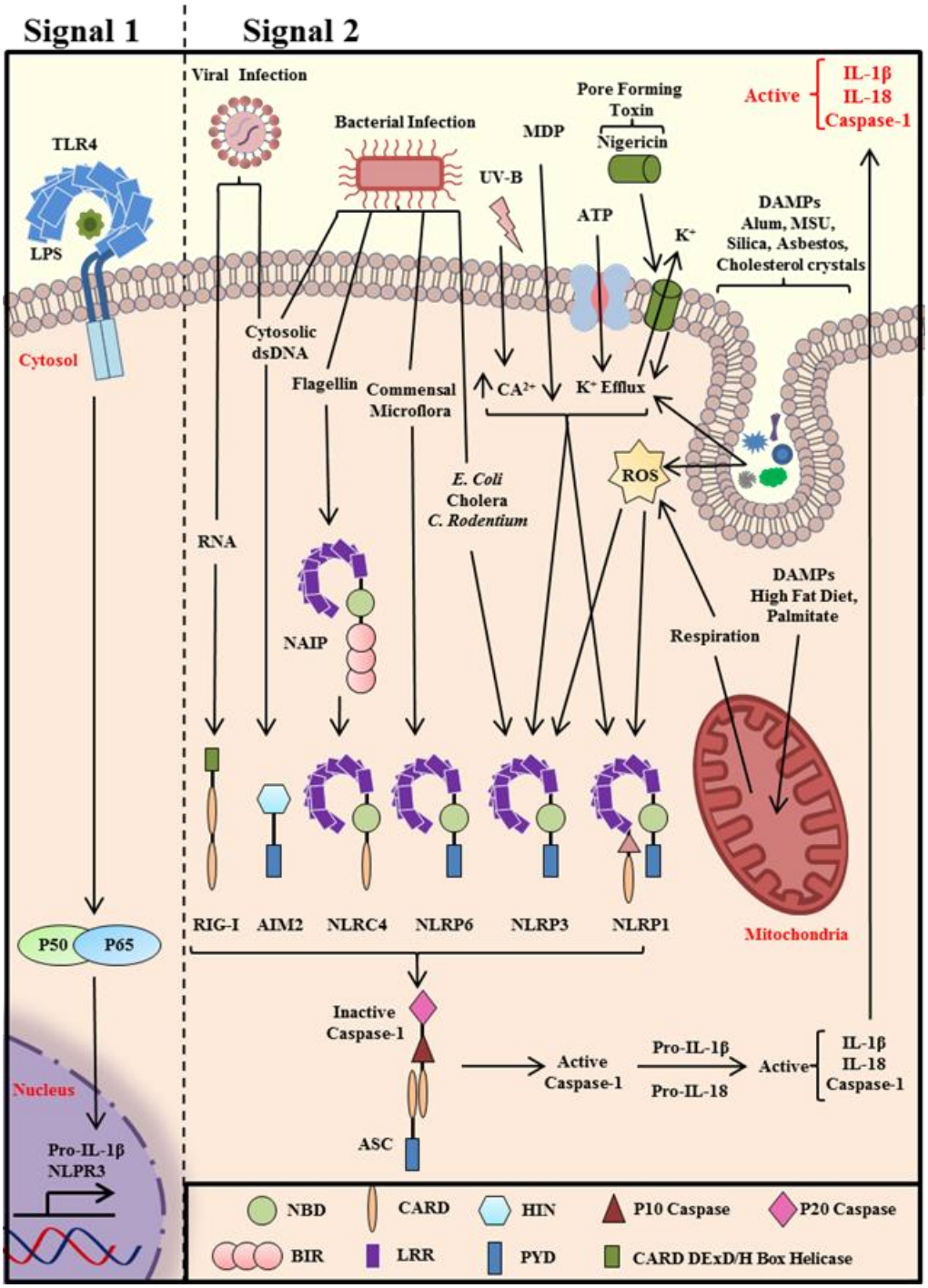

Figure 1.2 Activation and signalling of the inflammasome

See section 1.8 for a detailed description of the factors with lead to inflammasome assembly as well as the mechanism by which signal transduction occurs.

1.8.1 NLRP1: The First Known Inflammasome

NLRP1 was the first protein to be associated with inflammasome activation (Martinon *et al.,* 2002). It is a member of the NLR family of proteins and shares structural similarities with the other members. There are 14 members of this family, with each member containing a LRR and nucleotide-binding domain (NBD). NLRP1 is unique among inflammasome forming members of the NLR family as it contains both PYD and a C-terminal CARD domain (Chu *et al.,* 2001).

The only known activators of NLRP1 to date is muramyl dipeptide (MDP) a bacterial cell wall component (Martinon *et al.,* 2004). However, determining the function of human NLRP1 using standard murine models is complicated by the genetic differences between mouse and human NLRP1 (Boyden and Dietrich, 2006). The mouse genome contains NLRP1a, NLRP1b and NLRP1c which are all orthologs to human NLRP1. Studies into murine NLRP1b have described *Bacillus anthracis* toxin as an activator. NLRP1b lack a PYD domain, which further complicates the comparison between human and murine NLRP1 signalling (Boyden and Dietrich, 2006).

NLRP1 exists in an auto-repressed state in the cell and the precise mechanisms of its activation remain controversial. It has been hypothesised that the LRR domain is the site of ligand binding, as is the case in TLRs (Tschopp *et al.,* 2003). However, a recent study shows that while MDP can bind NLRP1 directly *in vitro*, the crystal structure of the LRR domain of NLRP1 lacks a MDP binding site (Reubold *et al.,* 2014). Instead of acting as a direct binding site, the LRR domain may instead sterically hinder activation of NLRP1 prior to ligand binding, as selective deletion of the LRR domain has been shown to result in spontaneous NLRP1 oligomerisation (Faustin *et al.,* 2007). Another possibility is that cytosolic receptor nucleotide-binding oligomerisation domain-containing protein 2 (NOD2) is the key MDP receptor and upon recognition leads to the association with NLRP1, facilitating its activation (Ferwerda *et al.,* 2008). Furthermore, NLRP1 has been shown to result in caspase 1 cleavage, independent of ASC association. However, interaction with ASC leads to a more robust response (Faustin *et al.,* 2007; Van Opdenbosch *et al.,* 2014).

Caspase-1 activation can also lead to pyroptosis, which has been shown to be supressed by Bcl-2 and Bcl-X_L. These anti-apoptotic proteins can directly bind NLRP1 and function to downregulate its activity (Bruey *et al.,* 2007). Conversely, NLRP1 can also interact with the apoptosome regulator apoptotic protease activating factor 1 (Apaf1) and facilitate enhanced induction of apoptosis (Chu *et al.,* 2001). Despite having few known activators, NLRP1 has been implicated in many auto-inflammatory conditions. SNPs in NLRP1 have been shown to be a risk factor in autoimmune Addison's disease (Żurawek *et al.,* 2010) and rheumatoid arthritis (Sui *et al.,* 2012) and can increase the susceptibility of patients with vitiligo to associated autoimmune diseases (Y. Jin *et al.,* 2007).

1.8.2 NLRP3 Responds to Cellular Stress

NLRP3 is the most characterised and studied of the inflammasomes to date; despite this, many of the molecular mechanisms by which ligand recognition and activation occurs remains poorly understood. NLRP3 contains LRR, PYD and NBD domains and requires both ASC and caspase-1 for initiation of the inflammasome (Masumoto *et al.,* 2003). NLRP3 has a wide range of known triggers for its activation including extracellular adenosine triphosphate (ATP), nigericin (Mariathasan *et al.,* 2004) and monosodium urate crystals (MSU) (Martinon *et al.,* 2006); this ability to respond to numerous diverse PAMPs and DAMPs distinguishes this receptor among all the inflammasomes as the most versatile. The NLRP3 dependent inflammasome was also shown to play a role in the modulation of the response to intracellular adenoviral DNA and the subsequent IL-1β response, which demonstrates the importance of the inflammasome in viral immunity (Muruve *et al.,* 2008). It is thought that NLRP3 does not directly associate with its various activators, but instead can be activated by a generic pathway of cell stress or perhaps facilitated by other activating proteins (Horvath *et al.,* 2011). Many models for activation have been proposed and demonstrated, including: mitochondrial damage and the release of reactive oxygen species (ROS) (Zhou *et al.,* 2011), potassium (K^+) efflux (Pétrilli *et al.,* 2007),

calcium (Ca^{2+}) signalling (Lee *et al.*, 2012) and lysosomal disruption during incomplete phagocytosis (Hornung *et al.*, 2008). A combination of some or all of these pathways may contribute to the complex signalling of NLRP3.

After ROS was shown to play a role in IL-1β secretion (Cruz *et al.*, 2007), the first hypothesised pathway to link the generation of ROS to the inflammasome was via nicotinamide adenine dinucleotide phosphate (NADPH) oxidase. As a result of incomplete phagocytosis of crystals, NADPH oxidase was thought to produce ROS and thus lead to the activation of NLRP3 (Dostert *et al.*, 2008; Hewinson *et al.*, 2008). This hypothesis has been challenged recently, with studies indicating that the use of ROS inhibitors blocked NLRP3 upregulation during the priming stage, but did not affect the activation and assembly of NLRP3 when administered after priming (Bauernfeind *et al.*, 2011). Conversely, the absence of NADPH in mouse models has been shown to result in a hyper inflammatory state due to increased γδ T-cell activity (Romani *et al.*, 2008). Patient data has supported this model, as patients with chronic granulomatous diseases (CGDs) display a defective NADPH system and yet exhibit increased IL-1β release (van de Veerdonk *et al.*, 2010). While the role of NADPH in the inflammasome remains controversial, a different pathway involving both ROS and the mitochondria has recently been demonstrated (Zhou *et al.*, 2011). It has been suggested that ROS itself is not an absolute requirement for NLRP3 activation, as the oxazolidinone antibiotic linezolid does require ROS signalling. Destabilisation of the mitochondria however is required, since cyclosporine A stabilisation of the mitochondria or inhibition of the mitochondrial surface protein cardiolipin blocked NLRP3 activation. This suggests that direct interaction with the mitochondria may be vital for inflammasome assembly to proceed (Iyer *et al.*, 2013).

Intracellular ion homeostasis has also been shown to play a role in the initiation of NLRP3 inflammasome assembly. Increased levels of Ca^{2+} in the cytosol is capable of promoting NLRP3 assembly while also downregulating cellular cyclic AMP (cAMP), a known inflammasome inhibitor (Lee *et al.*, 2012). Interestingly, a recent study demonstrated that increased concentration of extracellular Ca^{2+} is also capable of leading to inflammasome assembly through the signalling of G protein-coupled calcium sensing receptors (Rossol *et al.*, 2012). The authors determined that necrotic

cells could be a source of this calcium, which implicates calcium signalling in the amplification of the inflammatory response and potentially in sterile inflammation. K^+ efflux was shown to regulate IL-1β secretion before the discovery of the inflammasome (Walev *et al.,* 1995) and has since been directly shown to regulate the NLRP3 inflammasome assembly (Pétrilli *et al.,* 2007). Recent work has implicated K^+ efflux as being the common signalling trigger required to achieve inflammasome activation in response to particulate matter and bacterial pore-forming toxins (Muñoz-Planillo *et al.,* 2013). Indeed, lysosomal disruption during incomplete phagocytosis promotes inflammasome activation (Hornung *et al.,* 2008) by triggering the opening of K^+ pores leading to a drop in cytosolic K^+ (Muñoz-Planillo *et al.,* 2013). While the NLRP3 inflammasome has been studied extensively, many questions relating to its activating triggers and assembly still remain.

Recent clinical research has demonstrated that dysregulation of NLRP3 signalling can both initiate and exacerbate a wide variety of auto-inflammatory and metabolic conditions. Accumulation of the endogenous particulate MSU in joints has long been known to be a major causative agent in Gout (Wollaston, 1797) and MSU itself is known to induce NLRP3 signalling in macrophages (Martinon *et al.,* 2006).

Studies linking NLRP3 polymorphisms with autoimmune diseases have yielded inconsistent results, with some studies demonstrating a link (Bidoki *et al.,* 2016; Roberts *et al.,* 2010), while others showed contrary results (Pontillo *et al.,* 2012; Wang *et al.,* 2015). However, a recent meta-analysis has highlighted an association of an NLRP3 polymorphism (rs10754558 C/G) with an increased risk of autoimmune disorders (Lee and Bae, 2016).

1.8.3 NLRP6 Maintains Gut Homeostasis

Structurally, NLRP6 is similar to NLRP3 as it contains LRR, PYD and NBD domains but the precise nature of its early activation remains unclear (Chen, 2014). Early work demonstrated the capacity for NLRP6 to co-localise with ASC (Grenier

et al., 2002), yet to date there has been no conclusive biochemical evidence which elucidates its role in the assembly of an inflammasome.

Much of the interest in NLRP6 relates to its role in intestinal homeostasis. *Nlrp6* deficient mice exhibited colitogenic gut microflora profiles with increased levels of Bacteroidetes (Prevotellaceae family) which has been associated with inflammatory bowel disease (IBD) (Kleessen *et al.,* 2002). A more severe inflammatory phenotype is also observed upon induction of dextran sodium sulfate (DSS) colitis (Elinav *et al.,* 2011). Interestingly, co-housing *Nlrp6*$^{-/-}$ with wild type mice for 4 weeks lead to the transference of this colitogenic microbiota profile to the wild type, subsequently enhancing the inflammatory effect of DSS induced colitis. This alteration of the microflora can also lead to an increase in secreted IL-6, which modifies the proliferation of resident epithelial cells, leading to increased tumorigenesis (B. Hu *et al.,* 2013).

Conversely, NLRP6 may also contribute to suppressing the immune response during bacterial infection. *Nlrp6*$^{-/-}$ mice when exposed to *Escherichia coli*, *Listeria monocytogenes* and *Salmonella typhimurium* were shown to be highly resistant to infection (Anand *et al.,* 2012). This correlated with an increase in circulating neutrophils and a more robust NF-κB response upon TLR stimulation.

1.8.4 NLRC4 and the NAIP family

Similar to the other NLRs which form an inflammasome, NLRC4 contains a LRR and NBD. However, it lacks a PYD and instead contains a CARD domain (Z. Hu *et al.,* 2013). The interplay between NLRC4 and the neuronal apoptosis inhibitor proteins (NAIPs) results in the formation of an inflammasome in response to a variety of different PAMPs of bacterial origin. Flagellin within the cytosol was first shown to lead to a NLRC4 dependent caspase 1 cleavage independent of TLR5 (Franchi *et al.,* 2006). Further work has shown that NAIP5 and NAIP6 function upstream of NLRC4 in the response to *L. pneumophila* and are indispensable in

facilitating the formation of the inflammasome in response to this bacteria. Contrastingly, NLRC4 recognition of *P. aeruginosa* and *S. typhimurium* can occur independently of both NAIP5 and NAIP6 (Lightfield *et al.*, 2008). This is due to the capacity of NLRC4 to respond to the type III secretion systems (T3SS) from Gram-negative bacterial origin (Miao *et al.*, 2010b). T3SS is capable of injecting various virulence factors into the cytosol of cells, which can shape the cells response to the pathogen. It consists of more than 20 proteins which exists as a needle shaped complex present on the bacterial envelope (Galán and Wolf-Watz, 2006; Miao *et al.*, 2010b). NAIP2 was identified as the specific receptor for the bacterial needle protein CprI in humans, which facilitated the action of NLRC4 (Zhao *et al.*, 2011). Flagellin did not associate with NAIP2, which highlights the NAIP family as critical inflammasome components capable of dictating the specific response to bacterial signals.

The interaction between the NAIP family and NLRC4 remains poorly understood. It has been hypothesised that upon ligand binding, NAIPs are released from an auto-inhibitory state and oligomerise, which further allows the oligomerisation of NLRC4 (Guo *et al.*, 2015). Similar to NLRP1, the LRR domain may inhibit the function of the NAIPs and NLRC4, as shown through deletion studies (Kofoed and Vance, 2011). Phosphorylation of NLRC4 has also been demonstrated to be critical for caspase-1 recruitment to the inflammasome (Qu *et al.*, 2012), but this phosphorylation has been shown to occur independently of NAIP5. Interestingly, a two-step model has been hypothesised where subsequent interaction with NAIP5 or NAIP1/2 is required to produce the conformational change of phosphorylated NLRC4, which facilitates its activation (Matusiak *et al.*, 2015).

As with the other inflammasomes, NLRC4 is capable of processing IL-1β and IL-18 into their active forms. However, NLRC4 may contribute to bacterial clearance independent of these cytokines. *S. typhimurium* for example was shown to replicate in macrophages, but were cleared by neutrophils due to the generation of ROS (Miao *et al.*, 2010a). Caspase-1 induced pyroptosis of the infected macrophages functioned not only in the clearance of infected cells, but also served as a mechanism

to release intracellular bacteria into the extracellular space allowing for subsequent phagocytosis by neutrophils.

1.8.5 AIM2 and IFI16: The DNA sensors

Unlike the other inflammasomes discussed, AIM2 and IFI16 are not members of the NLR family, but instead belong to a family of hematopoietic interferon-inducible nuclear proteins with a 200-amino acid repeat (HIN-200). They contains a PYD and a HIN domain (Albrecht *et al.,* 2005; Ludlow *et al.,* 2005) and due to this are also known as the PYHIN family of proteins (Hornung *et al.,* 2009). AIM2 has been shown previously to function in the regulation of cell growth (Choubey *et al.,* 2000) and to possibly play a role in colorectal tumorigenesis (Mori *et al.,* 2001) by mediating the regulation of interferon-stimulated genes (ISGs) (J. Lee *et al.,* 2012). IFI16 has been implicated in various cancers and functions in the response to DNA damage (Fujiuchi *et al.,* 2004).

The recognition of cytoplasmic DNA can be mediated by a number of different receptors including TLR9 (Hochrein *et al.,* 2004), DNA-dependent activator of IFN-regulatory factors (DAI) (Takaoka *et al.,* 2007) and NLRP3 (Muruve *et al.,* 2008). Whilst NLRP3 plays a role in responding to intracellular adenoviral DNA, it is not involved in the recognition of transfected poly(deoxyadenylic-deoxythymidylic) (poly(dA-dT)), a synthetic analogue of double stranded B-DNA (dsDNA). Instead, the IL-1β release upon poly(dA-dT) transfection requires both ASC and caspase-1 and this is triggered by the upstream inflammasome sensor AIM2 (Fernandes-Alnemri *et al.,* 2009; Hornung *et al.,* 2009). Since its discovery as a novel cytoplasmic dsDNA receptor, AIM2 has been shown to be involved in the response against *Francisella tularensis* (Fernandes-Alnemri *et al.,* 2010), *Listeria monocytogenes* (Kim *et al.,* 2010; Sauer *et al.,* 2010) and *Legionella pneumophila* (Ge *et al.,* 2012).

The crystal structure of AIM2 complexed with dsDNA has been determined and is the first inflammasome receptor that has been demonstrated to directly bind to its ligand (Jin *et al.,* 2012). Further structural and binding studies show that the PYD and HIN domains strongly interact prior to dsDNA association, indicating its auto-inhibition, similar to other inflammasomes (Jin *et al.,* 2013, 2012). AIM2 is thought to oligomerise and act as a platform for ASC binding and further caspase-1 signalling. This platform is also capable of activating caspase-8 independent of caspase-1 and leads to apoptosis of the cell (Pierini *et al.,* 2012). Interestingly, a similar interplay between apoptosis and pyroptosis is observed upon NLRP1 inflammasome assembly, which highlights the important role inflammasomes can play in orchestrating cell death.

IFI16 is primarily localised in the nucleus and has been shown to act as a dsDNA sensor, utilising STING, TBK-1 and IRF3 to induce and IFN-β response (Unterholzner *et al.,* 2010). Notably, this study determined that unlike AIM2, IFI16 did not interact with ASC upon cytoplasmic transfection of dsDNA. Recent work has shown that in response to kaposi sarcoma-associated herpesvirus (KSAH) which replicates in the nucleus, IFI16 can associate with ASC and form an inflammasome (Kerur *et al.,* 2011). The reason for this disparity is possibly due to the requirement of a foreign DNA signal in the nucleus. This study also represents the first demonstration of an inflammasome assembling in the nucleus.

1.8.6 The RIG-I Inflammasome

The role of RIG-I in the production of type I interferon in response to viral infection is well understood (Loo and Gale, 2011). It is a DExD/H box RNA helicase containing two CARD domains and shares both structure and function with melanoma differentiation-associated gene 5 (Mda5) (Kawai *et al.,* 2005). RIG-I can detect dsRNA from replicating viruses in the cytosol and upon recognition, associate via CARD-CARD interaction with mitochondrial antiviral signalling (MAVS) (Seth *et al.,* 2005; Yoneyama *et al.,* 2004). This association causes the formation of a

signalling platform on the mitochondria leading to the recruitment of IKKε and IKKα/IKKβ which can phosphorylate IRF3 and IκB respectively, triggering the activation of a pro-inflammatory and anti-viral response (Meylan *et al.,* 2005).

An emerging role of RIG-I is its potential to form an inflammasome and result in IL-1β maturation. Unlike the IRF/IFN signalling of RIG-I described above, inflammasome assembly through RIG-I is independent of MAVS signalling (Poeck *et al.,* 2010). However, recent work has shown that during infection of lung epithelial cells by Influenza A virus (IAV), RIG-I initially signals through a MAVS dependent pathway, leading to a type I interferon response (Pothlichet *et al.,* 2013). Secreted IFN-β initiates a positive feedback loop, further upregulating RIG-I, which is required for its inflammasome assembly. This demonstrates the potential of RIG-I to be involved during both signal 1 and signal 2.

1.8.7 The Non-canonical and Emerging Inflammasomes

The initial characterisation of the function of caspase-1 in published IL-1β studies used *Casp1*$^{-/-}$ mice (Kuida *et al.,* 1995; Li *et al.,* 1995). It was recently determined that these mice were in fact *Casp1*$^{-/-}$*Casp11*$^{-/-}$ double knock out mice, an error which occurred due to the close proximity of both genes in the genome (Kayagaki *et al.,* 2011). Using a *Casp11* bacterial artificial chromosome (BAC) transgene, the authors generated a functional *Casp1* knockout which confirmed the role of caspase-1 in IL-1β and IL-18 secretion. Interestingly, this work also implicated caspase-11 functioning in a non-canonical inflammasome, independent of caspase-1, NLRP3 and ASC. Caspase-11 activation has since been shown to lead to detrimental levels of cell death due to intracellular *Salmonella* infection in the absence of caspase-1 (Broz *et al.,* 2012).

It was recently discovered that intracellular LPS could activate a non-canonical inflammasome (Kayagaki *et al.,* 2013). Only the specific serotype LPS O111:B4 in combination with cholera toxin B (CTB) could elicit this response, due to O111:B4

binding CTB which acts as a raft facilitating the entry of LPS into the cell. Transfection of any LPS serotype achieved this activation, demonstrating the existence of an intracellular LPS receptor which acts independent of TLR4. Caspase-11 is only found in mice, however recent work on the human homologues caspase-4 and -5 has shown that both are involved in IL-18 secretion independent of caspase-1, which potentially links their functionally with caspase-11 (Knodler *et al.,* 2014). LPS recognition is directly mediated by caspase-11/4/5 binding to LPS in a CARD dependent manner, resulting in their oligomerisation and subsequent activation (Shi *et al.,* 2014).

The requirement of a third activating signal in the inflammasome has also been hypothesised. During Gram-negative bacterial infection, type I IFNs are secreted in a TLR4 dependent manner, leading to its autocrine association with the interferon receptors IFNα/βR1 and IFNα/βR2 (Rathinam *et al.,* 2012). This leads to the downstream upregulation and activation of caspase-11, which synergises with the NLRP3 inflammasome, facilitating heightened IL-1β release. This non-canonical pathway is dependent on TRIF signalling through TLR4, but not MyD88 (Broz *et al.,* 2012).

NLRP7 and NLRP12 have also recently been shown to form inflammasomes in response to bacterial lipopeptides (Khare *et al.,* 2012) and *Yersinia pestis* (Vladimer *et al.,* 2012) respectively. Future work is likely to uncover other inflammasome forming proteins which may have implications in other inflammatory diseases.

1.8.8 Crosstalk between TLRs and NLRP3

As discussed, the assembly of the inflammasome requires two distinct signals; the first is a priming signal that results in downstream activation of NF-κB. This signalling can be achieved upon stimulation of a variety of TLRs, but also IL-1R and tumour necrosis factor receptor (TNFR) (Bauernfeind *et al.,* 2009). It was originally thought that signal 1 served only to upregulate pro-IL-1β which would be cleaved

upon recognition of a second signal. However, recent work has challenged this simplistic model and has shown it to be incomplete. There is in fact a complex and nuanced crosstalk involving inflammasome components which occurs during priming. A variety of post-translational modifications resulting from initial TLR signalling are capable of modulating the assembly of the inflammasome (De Nardo *et al.,* 2014).

The first protein based post-translational modification described was the conserved 76-amino-acid polypeptide protein ubiquitin (Ciehanover *et al.,* 1978; Hershko *et al.,* 1980). The covalent addition of ubiquitin to a target protein is known as ubiquitination, and is fundamentally important in a wide range of cellular functions, including innate signalling. The formation of ubiquitin chains can be linked through various lysine residues on the ubiquitin protein, leading to a variation in cellular outcomes. Lysine 48 (K48) linked ubiquitination is generally considered to signal for proteosomal degradation (Chau *et al.,* 1989), while K63 linked polyubiquitination is associated with signal transduction and protein stability (Chen, 2005). It is an ancient process which is conserved even in plant immunity (Trujillo and Shirasu, 2010).

Deubiquitination of NLRP3 by the deubiquitinating enzyme (DUB) BRCC3 has been shown to be essential to the initiation of the NLRP3 inflammasome (Juliana *et al.,* 2012; Py *et al.,* 2013). This deubiquitination occurs after signal 2, allowing NLRP3 to oligomerise and associate with ASC. Knockdown of BRCC3 inhibits the activation of the NLRP3 inflammasome and thus regulates IL-1β secretion. Interestingly, NLRC4 and AIM2 activation were not affected by the pharmacological inhibition of DUBs, which demonstrates the difference in regulation between inflammasome sensors.

Priming of ASC prior to its interaction with NLRP3 is also a key molecular switch required for aggregation of stable specks and thus the formation of the inflammasome. Phosphorylation of ASC occurs in a Jnk/Syk dependent manner and is required for ASC oligomerisation, possibly via association and trafficking along microtubules to the site of speck formation (Hara *et al.,* 2013). Ubiquitination by the linear ubiquitin assembly complex (LUBAC) also plays an important role in the priming of ASC. Linear ubiquitination, or M1-linked ubiquitination, results from the

linking of the N-terminal methionine of one ubiquitin and the C-terminal Gly76 of another forming head to tail linear linkages (Kirisako *et al.*, 2006; Pickart and Fushman, 2004). LUBAC consists of a combination of the proteins HOIP, HOIL-1L and Sharpin (Gerlach *et al.*, 2011) and together can lead to the linear ubiquitination of ASC. These ubiquitin complexes remain complexed to ASC during speck formation, potentially demonstrating that a complete deubiquitination event is not required prior to complex formation (Rodgers *et al.*, 2014).

A20, which is also known as TNFAIP3, is a known negative regulator of the innate response. It is capable of regulating NF-κB signalling by both functioning as a DUB and deubiquitinating RIP and also catalysing the formation of K48 ubiquitination of RIP, leading to its degradation (Wertz *et al.*, 2004). Cells from A20-deficient mice showed spontaneous activation of the NLRP3 inflammasome is response to TLR stimulation alone, implicating it as a possible regulator of the inflammasome (Duong *et al.*, 2015). A20 was shown to associate with both caspase-1 and pro-IL-1β and localises with the inflammasome complex upon activation. Further, it was also observed that pro-IL-1β associates in a complex with RIPK1, RIPK3, caspase-1, caspase-8 and K63 ubiquitin. Pro-IL-1β could indeed be ubiquitinated during signal 1 prior to NLRP3 inflammasome assembly and this ubiquitination was increased in A20 deficient cells, which can support signal propogation and lead to increased IL-1β processing. This work demonstrates the regulatory role which A20 plays during inflammasome priming by inhibiting IL-1β ubiquitination.

Our understanding of the molecular modifications which trigger an active inflammasome are still incomplete, but it is clear that there is a complex interplay occurring between the priming and activating signals which can shape the response. Ubiquitination of IL-1β, NLRP3 and ASC during LPS priming has been shown to critically regulate inflammasome activation (Duong *et al.*, 2015; Hara *et al.*, 2013; Py *et al.*, 2013). To date, no specific E3 ligase has been identified which can facilitate this ubiquitination. To this end, the focus of the work presented in this thesis is to investigate the role of the E3 ligase Pellino2 in the ubiquitination and subsequent regulation of the NLRP3 inflammasome.

1.9 The Pellino Family

Ubiquitination of a target protein requires the actions of 3 separate enzymes: an El ubiquitin-activating enzyme, an E2 ubiquitin-conjugating enzyme and an E3 ubiquitin–protein 1igase (Ciechanover *et al.*, 1982; Hershko *et al.*, 1983). In humans, there are two E1 enzymes which are capable of initiating the ubiquitin conjugating cascade, Uba6 and Ube1 (Jin *et al.,* 2007). The E1 protein binds both ubiquitin and ATP and catalyses the adenylation of the ubiquitin c-terminal, leading to its activation (Ciechanover *et al.,* 1982). E1 then recruits one of a number of E2 enzymes, facilitating the transfer of the activated form of ubiquitin to the E2 (Wijk and Timmers, 2010). The final step involves an E3 protein ligase, which facilitates the transfer of ubiquitin from E2 to a target substrate (Hochstrasser, 2006). There are approximately 35 active E2 enzymes in humans (Wijk and Timmers, 2010) and hundreds of E3 proteins. E3 proteins are a large and diverse group, due to their requirement to bind to a large variety of target substrates (Berndsen and Wolberger, 2014).

The Pellino family of proteins were first characterised as a component of the Dorsal/Cactus signalling complex in *Drosophila melanogaster,* which is a critical signalling system during embryogenesis (Prothmann *et al.,* 2006). Dorsal is a member of the Rel family of proteins and is inhibited in the cytoplasm by the protein cactus prior to activation, similar to NF-κB in mammals (Lemaitre *et al.,* 1996). Using Pelle as a bait in a yeast two-hybrid screen, Pellino was demonstrated to be a Pelle (IRAK) interacting protein (Großhans *et al.,* 1999). Pellino homologues were also identified in *Caenorhabditis elegans* (Rich *et al.,* 2000) and the notochord of *Ciona intestinalis* (Hotta *et al.,* 2000). Vital components of TLR signalling have been largely conserved between vertebrates and invertebrates (Medzhitov and Janeway, 2000) and this is also the case for the Pellino family, which highlights them as evolutionarily important molecules. Three mammalian Pellino proteins have been discovered and genetically mapped. The genes *PELI1* and *PELI2* that encode the proteins Pellino1 and Pellino2 were first successfully mapped to chromosomes 2 and 14 in humans (Resch *et al.,* 2001; Rich *et al.,* 2000). *PELI3* was the final

annotated member of the family, which was mapped to chromosome 11 in humans and encodes two splice variants of Pellino3, the larger Pellino3a and the smaller Pellino3b (Jensen and Whitehead, 2003a).

Early work suggested that functionally the Pellino family acted as scaffolding proteins during TLR signalling. However, through homology analysis it was proposed that Pellino proteins contain a CHC2CHC2 really interesting new gene (RING)-like finger motif, differing slightly from a classical C3HC4 RING domain (Schauvliege *et al.,* 2007, 2006). The RING domain is a feature of a sub-family of E3 ubiquitin ligases and the presence of a putative RING-like domain in Pellino proteins suggested that they may have E3 ligase activity. Indeed, the Pellino proteins were demonstrated to polyubiquitinate IRAK-1 when co-expressed with either Pellino1, 2 or 3 (Schauvliege *et al.,* 2006). Further, Pellino proteins exhibiting a single point mutation in the RING domain were co-expressed with IRAK1 in order to assess the E3 ligase function of the Pellino proteins. The Pellino RING motif was determined to be dispensable in IRAK1 binding, but crucial to the inducing IRAK1 polyubiquitination. Pellino1 was further demonstrated to act as an E3 ligase which could catalyse Lys63-linked polyubiquitin chains on IRAK1 and IRAK4, allowing for the subsequent phosphorylation and ubiquitination of Pellino1 (Butler *et al.,* 2007; Schauvliege *et al.,* 2006). All members of the Pellino family are structurally similar; they each contain a RING domain and a forkhead-associated (FHA) domain, which is usually associated with phosphothreonine-binding activity. This cryptic FHA domain was not apparent from the primary sequence, but was resolved through x-ray crystallography of the 15–275 amino acid n-terminal region (Lin *et al.,* 2008). Mutation of the amino acid involved in phosphothreonine binding inhibits IRAK1 interaction, indicating that it is the FHA and not the RING domain which mediates protein-protein interaction with IRAK1 (Lin *et al.,* 2008). Pellino3 shares an amino acid identity of 84% and 85% with Pellino1 and Pellino2 respectively. Pellino3 also has a longer N-terminal domain by 27 and 25 amino acid compared to Pellino1 and Pellino2. The third exon of Pellino3a also contains a 24 amino acid insert in the N-terminus (Jensen and Whitehead, 2003a).

1.9.1 Pellino1 Modulates NF-κB Activity

Despite the structural similarities between the members of the Pellino family, many recent studies have focused on the characterisation of the distinct physiological functions of the individual members (Humphries and Moynagh, 2015). Using both siRNA knockdown and protein overexpression, Pellino1 was initially shown to be required during TLR and IL-1R signalling for the activation of NF-κB (Jiang *et al.*, 2003). Pellino1 was hypothesised to target the IRAK4-TRAF6 complex due to the homology of the Pellino family with the Pelle protein in Drosophila (Großhans *et al.*, 1999). Pellino1 was shown to be capable of interacting with IRAK1, IRAK4, TRAF-6, and TAK1 (Jiang *et al.*, 2003). Smad2 was also shown to be capable of inhibiting the interaction with Pellino1 and the IRAK1/TRAF6 complex, leading to an inhibition of NF-κB signalling (Choi *et al.*, 2006). MAPK signalling was unaffected during knockdown of Pellino1, indicating a targeted effect on NF-κB (Jensen and Whitehead, 2003b).

The generation of a Pellino1 knockout mouse has led to a more complete understanding of the physiological relevance of Pellino1. Pellino1 was demonstrated to play a pivotal role in the TLR activation of NF-κB through the interaction and ubiquitination of RIP1, which facilitated activation of the IKK complex and thus NF-κB (Chang *et al.*, 2009a). Pellino1 was indespensible for TLR3-NF-κB signalling, but only partially required during TLR4 signalling, while IRF3 activation was unaffected in the Pellino1-deficient mouse. Interestingly, this work demonstrated that Pellino1 was not required for IL-1R, TLR2 or TLR9 signalling, highlighting the Myd88 independent function of Pellino1 (Chang *et al.*, 2009a). However, the recent generation of a Pellino1 kinase-dead knock-in mouse has questioned the role of Pellino1 in TLR3 signalling (Enesa *et al.*, 2012). Pellino1[F397A] mutant knock-in mice exhibited an inactive Pellino1 RING domain which abolished its E3-ligase activity. This mouse model demonstrated a reduced IFNβ response upon TLR3 signalling, while no difference was observed in RIP1 polyubiquitination or IKK complex and MAP kinase activation. This discrepancy between knockout and knock-in mutant needs to be addressed, but potentially highlights a functional role of

Pellino1 independent of its E3-ligase activity (Enesa *et al.,* 2012). The total loss of Pellino1 may also result in the differential upregulation or compensation of the other Pellino1 proteins, leading to their exaggerated function.

Pellino1 also plays a role in the negative regulation of T cell activation. Pellino1 was demonstrated to be capable of acting as an E3 ligase for the NF-κB subunit c-Rel and promote c-Rel's polyubiquitination by K48 ubiquitin linkage (Chang *et al.,* 2011). This leads to its degradation in activated T-cells and the suppression of NF-κB activation. Pellino1-deficiency led to accumulation of c-Rel and a spontaneous activation of T-cells. *Peli1*$^{-/-}$ mice also developed T cell mediated autoimmunity and presented with splenomegaly, as well as increased immune cell infiltration to organs. Serum autoantibody levels were similarly increased (Chang *et al.,* 2011). Pellino1-deficiency has been shown to be protective in experimental autoimmune encephalomyelitis (EAE). It was determined that Pellino1 is specifically required for NF-κB activation in microglial cells, which are mediators of EAE induction (Xiao *et al.,* 2013). Pellino1 was shown to function downstream of TRAF6 and mediate TRAF3 degradation and the activation of c-IAP. This results in the activation of MAPK signalling, leading to the upregulation of pro-inflammatory genes and contributing to the pathogenesis of EAE. This work highlights the difficulty in clarifying the role of Pellino1 as its functional relevance can be tissue specific.

1.9.2 The Physiological Role of Pellino2 Remains to be delineated

To date, Pellino2 has been primarily studied in the context of IL-1 and TLR signalling using over-expression and RNAi-based knockdown approaches. Pellino2 has been shown to interact with IRAK1 when overexpressed and was determined to be required during IL-1 and TLR signalling (Yu *et al.,* 2002). Using shRNA knockdown techniques, Pellino2 was shown to be required for IL-1 and TLR4 induced polyubiquitination of IRAK1 (Kim *et al.,* 2012). A Pellino2 RING mutant,

which lacks E3 ligase activity, was incapable of promoting IRAK1 ubiquitination. This highlights the importance and requirement of the E3 ligase activity of Pellino2 during this ubiquitination event. The activation of the MAPK pathways, JNK and ERK, by TLR4 and IL-1β, were also inhibited in the Pellino2-knockdown cells. Finally, the levels of secreted IL-6 and TNFα were decreased in knockdown cells, which was attributed to impaired mRNA stability (Kim *et al.,* 2012). Pellino2 has also been shown to interact with BCL10 during TLR4 signalling and induce NF-κB activation (Liu *et al.,* 2004).

However, the physiological role of Pellino2 remains ambiguous. To date, no research using a Pellino2-deficient mouse has been published. The work in this thesis aims to clarify the functional roles of Pellino2-deficiency in the immune system.

1.9.3 Pellino3 and its Role in Innate Immune Signalling

Early work into establishing the function of Pellino3 focused primarily on its role in TLR and IL-1 signalling (Butler *et al.,* 2005; Xiao *et al.,* 2008). This is due to discovery of Pellino3 as an IRAK1 interactor (Jensen and Whitehead, 2003a). It was originally shown that Pellino3 could activate both c-jun and Elk-1, but not NF-κB. It was hypothesised that differential levels of expressed Pellino3 in tissues could direct a cellular response towards either a MAPK dependent response in the case of high Pellino3 expression or a NF-κB response in tissues exhibiting low Pellino3 expression (Jensen and Whitehead, 2003a). Over-expression studies further established a role for Pellino3 in the P38 MAPK pathway and the activation of cAMP response element-binding protein (CREB) (Butler *et al.,* 2005). Pellino3b overexpression also inhibited IL-1-induced IRAK1 degradation, via stabilisation in a Lys-63-linked polyubiquitination dependent manner. This resulted in the inhibition of TAK1-dependent NF-κB activation (Xiao *et al.,* 2008). Pre-treatment of the macrophage cell line RAW 264.7 with oxLDL (oxidized low density lipoproteins) inhibits TLR4 signalling through TRIF, resulting in reduced levels of IFNβ (Tzieply *et al.,* 2012). The authors proposed that this inhibition is mediated by Pellino3 via

mono-ubiquitination of TRAF family member-associated NF-κB activator (TANK) which hinders the recruitment of TBK1 and TRAF3, inhibiting the activation of IRF3. While these studies are vital in shaping our understanding of Pellino biology, a more physiologically relevant model was required to further elucidate the role of Pellino3. To do this, a Pellino3-deficient mouse was generated in our laboratory and these mice demonstrated normal viability, growth and development. This mouse has since been used to demonstrate the importance of Pellino3 in a variety of innate immune processes (Figure 1.3).

Pellino3-deficiency was shown to have no effect on the production of pro-inflammatory cytokines via TLR stimulation (Siednienko *et al.,* 2012). However, type I interferons induced by TLR3 stimulation was shown to be augmented in Pellino3-deficient cells, which implicated Pellino3 as a negative regulator of TLR3 signalling. A new pathway was elucidated showing that TRAF6 can ubiquitinate IRF7 and promote nuclear translocation and induce type I IFN. Pellino3 was shown to induce K63-linked polyubiquitination of TRAF6, which blocks the interaction of TRAF6 with IRF7 and so repress nuclear translocation and type I IFN expression (Siednienko *et al.,* 2012).

Due to previous work demonstrating the requirement of Pellino1 in the ubiquitination of RIP1 (Chang *et al.,* 2009a), the possible role of Pellino3 in RIP biology has also been examined. It was shown that Pellino3 targets RIP1 to control cell fate in response to TNF stimulation (Yang *et al.,* 2013b). TNF was first described in 1975 as having a strong cytotoxic effect on tumours (Carswell *et al.,* 1975). It is now understood to have a wide range of actions including the modulation of apoptosis, cell survival and immune signalling (Flynn *et al.,* 1995; Nagata and Golstein, 1995; Sugarman *et al.,* 1985). While TNFα is capable of binding both TNFR1 and TNFR2, only TNFR1 contains death domains, which facilitate the formation of protein complexes resulting in the signalling for cell death (Tartaglia *et al.,* 1993). Upon TNFR1 stimulation, TNFR1-associated death domain protein (TRADD) is recruited to the receptor and in turn recruits RIP1 (Hsu *et al.,* 1996; Liu *et al.,* 1996). RIP1 is ubiqutinated via a complex of E3 ubiquitin ligases including TRAF2, TRAF5, cIAP1, and cIAP2, resulting in the recruitment of IKKβ and

activation of NF-κB (Ea *et al.,* 2006; Vince *et al.,* 2009; Zheng *et al.,* 2010). However, unmodified RIP1 can hinder NF-κB activity and instead leads to the formation of the death-inducing signalling complex (DISC) containing Fas-associated death domain (FADD) and caspase-8. This complex leads to the activation of caspase-8 and the initiation of apoptosis (Kim *et al.,* 2000; Kischkel *et al.,* 1995). In effect, the ubiquitination of RIP1 represents a signalling crossroads which can influence cell death or survival. Pellino3, via its FHA domain, was shown to interact with RIP1 and block recruitment of RIP1 into DISC thus promoting cell survival. This role of Pellino3 is independent of its E3 ligase activity, which highlights the diverse functionality of this protein (Yang *et al.,* 2013b).

Pellino3 is also capable of directly binding RIP2 and is required for the induction of its ubiquitination in a NOD2 dependent manner (Yang *et al.,* 2013a). NOD2 is cytosolic receptor, responsible for the recognition of bacterial peptidoglycan and the subsequent activation of NF-κB (Inohara *et al.,* 2001; Ogura *et al.,* 2001) NOD2 has been shown to play an important role in gut homeostasis and loss-of-function mutants of NOD2 have been linked with Crohn's disease (Ogura *et al.,* 2001a). Following ubiquitination, RIP2 further recruits TAK1, TAB2 and TAB3 and leads to NF-κB and MAPK activation. Interestingly, analysis of the colons of patients with Crohn's disease showed a downregulation of Pellino3 levels when compared to healthy controls. This corresponds to experimental colitis models carried out in mice, where *Peli3*$^{-/-}$ mice showed enhanced inflammation during late stage colitis, despite a reduction in NOD2 signalling (Yang *et al.,* 2013a).

Pellino3-deficient mice subjected to a high-fat diet (HFD) show exacerbated inflammation and insulin resistance. Pellino3 levels were also shown to be reduced in the adipose tissue of HFD mice, which also correlated with reduced Pellino3 expression in human abdominal adipose tissue from obese patients (Yang *et al.,* 2014). IL-1β transcription levels are a key factor in mediating insulin resistance and inflammation (Lagathu *et al.,* 2006; Xu *et al.,* 2003). This transcription of IL-1β during obesity is mediated in part by HIF-1α stability and translocation to the nucleus (Cramer *et al.,* 2003; Semenza and Wang, 1992; Tannahill *et al.,* 2013). Pellino3 was shown to interact with and ubiquitinate TRAF6, which blocks further

ubiquitination of HIF-1α, resulting in its degradation. Pellino3-deficient cells exhibit increased stabilisation and ubiquitination of HIF-1α, resulting in increased IL-1β levels and inflammation (Yang *et al.*, 2014). These studies illustrate the importance of Pellino3 in acting as a molecular switch which can influence not just the fate of an individual cell, but also the overall immune response. The recent evidence elucidating the roles of Pellino3 in patients demonstrates its potential as a therapeutic target in the future.

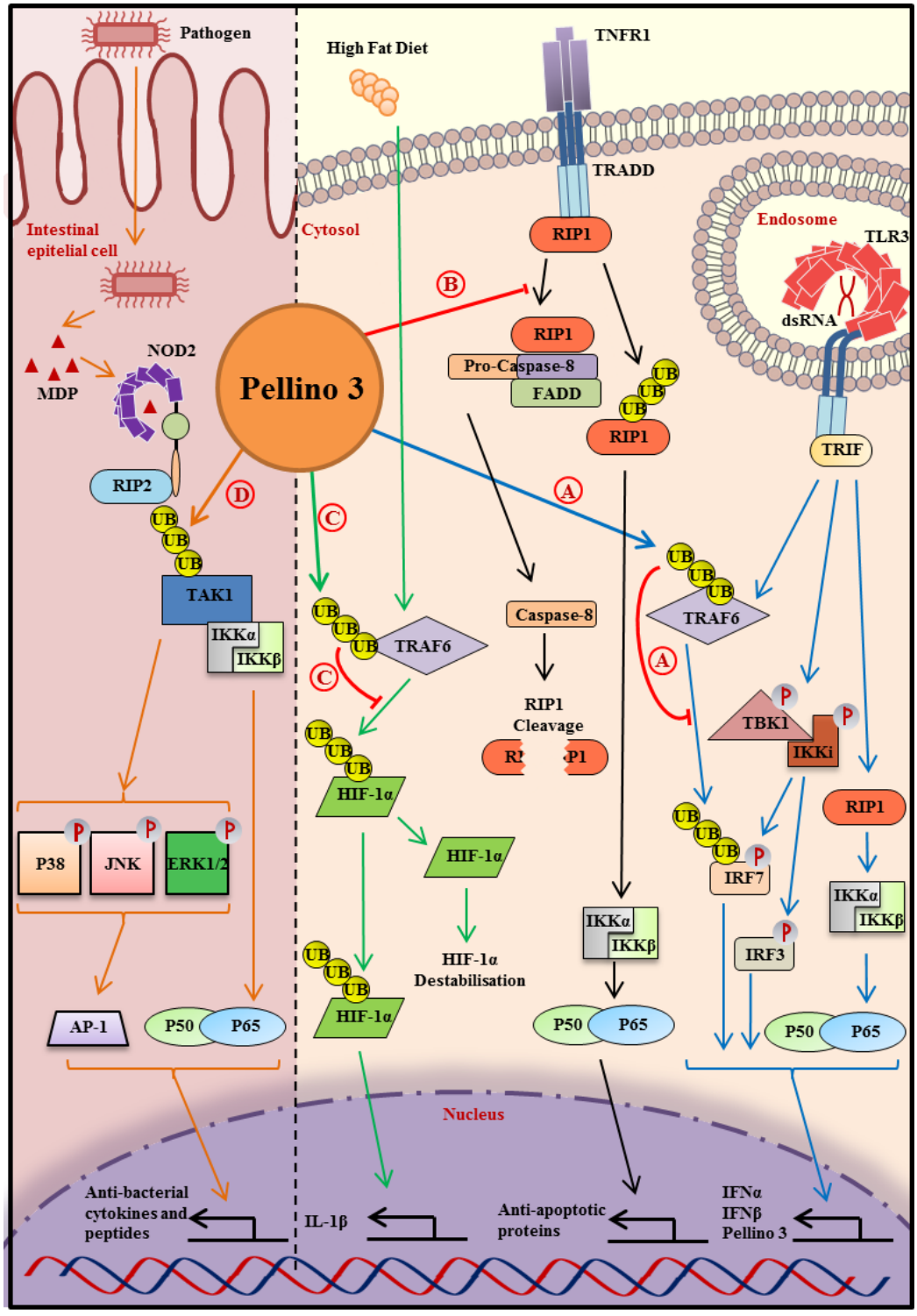

Fig 1.3 The roles of Pellino3 in innate immune signalling

Described in detail in section 1.9.3**.** Red arrows represent inhibition (A) Blue arrows indicate TLR3 signalling. (B) Black arrows indicate TNF signalling. (C) Green arrows indicate HFD signalling. (D) Orange arrows indicate NOD2 signalling.

1.10 Project aims

Recent research has elucidated distinct roles for both Pellino1 and Pellino3 in innate immune signalling. However, due to the lack of a knockout mouse model for Pellino2, its physiological relevance remains to be delineated. In light of this, we used a newly generated Pellino2-deficient mouse to address the following objectives:

- To define the effect of Pellino2-deficiency on TLR and IL-1R signalling

- To explore the role of Pellino2 in inflammasome activation

- To investigate the physiological relevance of Pellino2-deficiency

Chapter 2: Materials and Methods

2.1 Materials

2.1.1 Reagents

Reagents	Supplier
Agar	Sigma-Aldrich
Agarose	Promega
Ampicillin	Sigma-Aldrich
APS	Sigma-Aldrich
BSA	Sigma-Aldrich
Bradford reagent dye	Bio-Rad
Bromophenol blue	Sigma-Aldrich
CHAPS	Sigma-Aldrich
Chloroform	Sigma-Aldrich
CLO97	Invivogen
Coomassie Blue (G250)	Sigma-Aldrich
CpG type A ODN 1585	Invivogen
CpG type B ODN 1666	Invivogen

DirectPCR Lysis Reagent (Tail)	Viagen Biotech
DMEM	Invitrogen
DMSO	Sigma-Aldrich
DNA ladder & Loading dye	Promega
dNTPs	Promega
DSS	Sigma-Aldrich
DTT	Sigma-Aldrich
E.coli-TOP10 competent cells	Invitrogen
EDTA	Sigma-Aldrich
Ethanol	Sigma-Aldrich
Ethidium bromide	Sigma-Aldrich
FBS	Invitrogen
Flagellin	Invivogen
Glycerol	Sigma-Aldrich
Glycine	Sigma-Aldrich
GoTaq® polymerase	Promega
GoTaq® Green Master Mix	Promega

HEPES	Sigma-Aldrich
HCl	Merck
H_2O_2	Sigma-Aldrich
Igepal	Sigma-Aldrich
Isopropanol	Sigma-Aldrich
Kanamycin	Sigma-Aldrich
Lipofectamine 2000	Invitrogen
LPS	Enzo Life Sciences
LB	Sigma-Aldrich
Magnesium Chloride	Sigma-Aldrich
Methanol	The British Drug Houses (BDH)
Molecular Biology Grade Water (RNase and DNase Free)	Sigma-Aldrich
OptiMEM	Invitrogen
Pam_2CSK4	Invivogen
Pam_3CSK4	Invivogen
PBS	Oxoid

Penicillin / Streptomycin / Glutamine	Invitrogen
PMSF	Sigma-Aldrich
Poly(I:C)	Invivogen
Prestained molecular weight marker	Invitrogen
Protease inhibitor cocktail	Roche
Protein A/G-agarose	Santa Cruz
Proteinase K	Qiagen
Protogel	National Diagnostics
Random primers	Invitrogen
RNase Zap	Ambion
SDS	Sigma-Aldrich
Milk powder	Sigma-Aldrich
NaCl	Sigma-Aldrich
NaOH	Sigma-Aldrich
Na_3VO_4	Sigma-Aldrich
Na_3PO_4	Sigma-Aldrich
H_2SO_4	Sigma-Aldrich

Synthetic oligonucleotides	MWG Biotech
TEMED	Sigma-Aldrich
TMB	Sigma-Aldrich
Tris-base	Sigma-Aldrich
Tris-HCl	Sigma-Aldrich
Trition-X-100	Sigma-Aldrich
Trypsin/EDTA	Invitrogen
Tween-20	Sigma-Aldrich
Zymosan	Invivogen
Blasticidin	Invivogen
Zeocin	Invivogen
2-Mercaptoethanol	Gibeco
Ponceau s	Sigma-Aldrich
Acetic Acid	Fisher-Scientific
WesternBright ECL HRP Substrate	Advansta

2.1.2 Kits

Kit	Supplier
Murine CXCL1 ELISA Kit	R&D Systems
Murine IL-1β ELISA Kit	R&D Systems
Murine IL-6 ELISA Kit	R&D Systems
Murine RANTES ELISA Kit	R&D Systems
Murine TNFα ELISA Kit	R&D Systems
Plasmid Plus Midi Kit	Qiagen
SensiMix SYBR No-ROX Kit	Bioline

2.1.3 Antibodies

2.1.3.1 Antibodies for Immunoblotting

Primary Antibody	Supplier	Dilution	Diluent
ASC	Santa Cruz	1:200	5% Milk TBST
Caspase-1 p10	Santa Cruz	1:200	5% Milk TBST

Caspase-1 p20	Adipogen	1:1000	5% Milk TBST
ERK	Cell Signalling	1:1000	5% BSA TBST
FLAG M2	Sigma-Aldrich	1:2000	5% Milk TBST
IKK-β	Cell Signalling	1:1000	5% BSA TBST
IκB-α	Santa Cruz	1:200	5% Milk TBST
IL-1β	Adipogen	1:1000	5% Milk TBST
IRAK-1	Cell Signalling	1:1000	5% Milk TBST
JNK	Cell Signalling	1:1000	5% BSA TBST
Myc-Tag (9B11	Cell Signalling	1:2000	5% Milk TBST
NLRP3	Adipogen	1:1000	5% Milk TBST
Phospho-p38	Cell Signalling	1:1000	5% BSA TBST
Phospho-ERK	Cell Signalling	1:1000	5% BSA TBST
Phospho-IκB-α	Cell Signalling	1:1000	5% BSA TBST
Phospho-JNK	Cell Signalling	1:1000	5% BSA TBST
Phospho-cJUN	Cell Signalling	1:1000	5% BSA TBST
Phospho-IKK-α/β	Cell Signalling	1:1000	5% BSA TBST
Ubiquitin	Santa Cruz	1:200	5% Milk TBST

K48 Ubiquitin	Abcam	1:1000	5% Milk TBST
K63 Ubiquitin	Abcam	1:1000	5% Milk TBST
β-actin	Sigma-Aldrich	1:5000	5% Milk TBST

Secondary Antibody	**Supplier**	**Dilution**	**Diluent**
IRDye® 680RD Goat anti-Mouse	Li-cor	1:5000	5% Milk TBST
IRDye® 800CW Goat anti-Rabbit	Li-cor	1:5000	5% Milk TBST
IRDye® 800CW Donkey anti-Goat	Li-cor	1:5000	5% Milk TBST
Anti-mouse HRP	Cell Signalling	1:2000	5% Milk TBST

2.1.3.2 IFN-β ELISA Antibodies

Antibody	**Supplier**	**Dilution**	**Function**
Rat anti-Mouse IFN-β	Santa Cruz	1:1000	Capture
Rabbit anti-Mouse IFN-β	PBL Interforn Source	1:2000	Detection
anti-Rabbit HRP	Promega	1:2000	Reporter

2.1.4 Cell Lines

Name	Description
HEK293	Human embryonic kidney 293 cells
L929	Murine aneuploid fibrosarcoma cell line
J558	Myeloma cell line induced by by mineral oil injection in BALB/c mice, transduced with murine GM-CSF sequence.

2.1.5 Primer Sequences

2.1.5.1 Real-Time PCR Primers

Targeted Gene	Sense Primer Sequence 5'-3' Antisense Primer Sequence 5'-3'
HPRT	AGGGATTTGAATCACGTTG TTTACTGGCAACATCAACAG
IL-1β	GGATGATGATGATAACCTGC CATGGAGAATATCACTTGTTGG
NLRP3	GATGCTGGAATTAGACAATG GTACATTTCACCCAACTGTAG

Peli1	ACATGCCAACGGAGTGAAGC
	AGCGGCCAATCTGGAACA
Peli2	AACGACCCATACACACCACG
	TGTCCATCAGGGTTTTTCCAT
Peli3	CCTTGTCCATGTAAGTTTCTC
	CAGAGTTCAGAAGTCTGGAACT

2.1.5.2 Genomic DNA PCR Primers

Allele Targeted	**Sense Primer Sequence 5'-3'** **Antisense Primer Sequence 5'-3'**
HPRT	GCTTGCTGGTGAAAAGGACCTCTCGAAG
	CCCTGAAGTACTCATTATAGTCAAGGGCAT
WT Peli2 Primers (A + B)	CGTGTCCATCACTCTTAAATGAA
	GCACCATTGTACCTAAAGTAGAGAC
KO Peli2 Primers (C + D)	GCCTCTACAGGATGCTCATTT
	GGACAGTCATGCTAGTCTGAGG

2.1.6 Buffers

Buffer Name	Ingredients
Block buffer (Immunoblotting)	TBS, 0.1% (v/v) Tween-20 with 5 % (w/v) non-fat dry milk
Block buffer (ELISA)	PBS, 1% (w/v) BSA, Filtered Sterilised using 0.02 μm filter
Protein lysis buffer	50 mM HEPES pH 7.5, 10% (v/v) Glycerol, 0.5% (w/v) CHAPS, 0.5% (v/v) Triton-X-100, 250 mM NaCl. Prior to use: 1 mM Na_3VO_4, 1 mM PMSF and protease inhibitor mixture cocktail
Laemmli sample buffer	62.5 mM Tris-HCl, pH 6.8, 10% (w/v) glycerol, 2% (w/v) SDS, 0.7 M β-mercaptoethanol and 0.001% (w/v) bromophenol blue
Phosphate buffered saline (PBS)	2.7 mM KCl, 1.5mM KH_2PO_4, 137 mM NaCl and 8 mM Na_2HPO_4, pH 7.4
Ponceau stain	0.1% (w/v) Ponceau S in 5% (v/v) acetic acid
SDS running buffer	25 mM Tris, 192 mM glycine, 0.1% SDS
Tris-acetate-EDTA (TAE) Buffer	40 mM Tris base, 0.1% (v/v) glacial acetic acid, 1 mM EDTA
Tris buffered saline (TBS)	25 mM Tris, pH7.4, containing 0.14M NaCl

Tris-EDTA (TE) buffer	10 mM Tris-HCl, 1 mM EDTA pH 8.0

2.1.7 Gifts

2.1.7.1 Cells

HEK293: Prof. Douglas Golenbock (The University of Massachusetts Medical School, Worcestor, Massachusettes 01605, USA)

WT iBMDM: Dr. Sinead Miggin (National University of Ireland Maynooth, Co. Kildare, Ireland)

2.1.7.2 Constructs

Human NLRP3: Dr. Ruaidhri Jackson (Yale School of Medicine, New Haven, Connecticut, USA)

Human WT IRAK1: Dr. Marion Butler (National University of Maynooth, Co. Kildare, Ireland

Human WT IRAK1 kinase-dead: Dr. Marion Butler (National University of Maynooth, Co. Kildare, Ireland

Myc-tagged human WT Pellino2: Dr. Marion Butler (National University of Maynooth, Co. Kildare, Ireland

2.2 Methods

2.2.1 Cell Culture

2.2.1.1 Culture of HEK293T

HEK293T cells were cultured in DMEM supplemented with 10% (v/v) heat inactivated FBS, penicillin G (100 μg/ml) and streptomycin (100 μg/ml) in a 37°C humidified chamber under a 5% CO2 atmosphere. Cell morphology and confluence were monitored daily. Once cells reached approximately 80% confluence, adherent cells were passaged using a 1% (w/v) Trypsin/EDTA solution in PBS. Cells were cultured for a maximum of 25 passages in order to avoid excessive genetic drift.

2.2.1.2 Culture of immortalised BMDMs (iBMDMs)

iBMDM cells from WT and IRAK1$^{-/-}$ were cultured in RPMI supplemented with 10% (v/v) heat inactivated FBS, penicillin G (100 μg/ml) and streptomycin (100 μg/ml) in a 37°C humidified chamber under a 5% CO2 atmosphere. Cell morphology and confluence were monitored daily. Once cells reached approximately 80% confluence, adherent cells were passaged using a cell scraper with PBS. Cells were cultured for a maximum of 25 passages in order to avoid excessive genetic drift.

2.2.1.3 Culture of L929 Cells for Production of M-CSF containing conditioned media (M-CSF CM)

L929 cells were cultured in DMEM supplemented with 10% (v/v) heat inactivated FBS, penicillin G (100 μg/ml) and streptomycin (100 μg/ml) in a 37°C humidified chamber under a 5% CO2 atmosphere. Cell morphology and confluence were

monitored daily. Once cells reached approximately 80% confluence, adherent cells were passaged using a cell scraper with PBS. For the generation of M-CSF CM, cells were counted using a haemocytometer and seeded at $5x10^5$ cells/ml with 40 ml DMEM in a $T175^2$ culture flask for 7 days. CM was removed from the cells and was centrifuged at 600 g for 5 min. The supernatant was removed and subjected to further centrifugation at 600 g for 5 min in order to ensure the removal of any remaining cells. The supernatant was stored at -80°C for up to 6 months. Cells were cultured for a maximum of 25 passages in order to avoid excessive genetic drift

.

2.2.1.4 Culture of J558 Cells for Production of GM-CSF-containing conditioned media (GM-CSF CM)

J558 cells were cultured in RPMI supplemented with 10% (v/v) heat inactivated FBS, penicillin G (100 μg/ml) and streptomycin (100 μg/ml) in a 37°C humidified chamber under a 5% CO2 atmosphere. Blasticidin (10 μg/ml) was used every 4 passages to select for GM-CSF producing cells. Cell morphology and confluence were monitored daily. Once cells reached approximately 80% confluence, non-adherent cells were passaged by centrifugation at 600 g for 5 min. Prior to the generation of GM-CSF CM, cells were passaged in Blasticidin-free media for two passages. Cells were counted using a haemocytometer and seeded at $1x10^6$ cells/ml with 40 ml RPMI in a $T175^2$ culture flask for 7 days. Once cells reached approximately 80% confluence CM was removed and was centrifuged at 600 g for 5 min. The supernatant was removed and subjected to further centrifugation at 600 g for 5 min in order to ensure the removal of any remaining cells. The supernatant was stored at -80°C for up to 6 months. Cells were cultured for a maximum of 25 passages in order to avoid excessive genetic drift.

2.2.1.5 Generation and culture of primary BMDMs

Age (8-12 weeks) and gender matched WT and *Peli2*$^{-/-}$ mice were sacrificed by cervical dislocation. Mice were first sterilised with 70% EtOH before removal of the femur and tibia under aseptic conditions in a laminar flow hood. Bone marrow was removed by flushing the bones with a 27¾ gauge needle containing 20 ml PBS. Cells were then pelleted by centrifugation at 600 g for 5 min. Red blood cell lysis (RBL) was carried out by resuspending the pellets in 1ml of Sigma-Aldrich RBL buffer and incubated at room temperature for 1 min. Lysis was terminated by the addition of 20 ml DMEM supplemented with 10% (v/v) heat inactivated FBS, penicillin G (100 μg/ml) and streptomycin (100 μg/ml) and cells were centrifuged again at 600 g for 5 min. Pellets were re-suspended in 10 ml DMEM and cells were counted using a haemocytometer. WT and *Peli2*$^{-/-}$ cells were seeded at $2x10^6$ cells/ml with 25 ml DMEM in a $T175^2$ culture flask. Supernatant media from cultured L929 cells containing M-CSF was added to a final concentration of 20% (v/v). Cells were cultured in a 37°C humidified chamber under a 5% CO2 atmosphere for 3 days before media was carefully removed without displacing adherent cells. 25 ml of fresh DMEM supplemented with 20% M-CSF (v/v) was gently added and cells were cultured for a further 4 days, supplementing cells with additional 10 ml of M-CSF supplemented DMEM on day 3. Optimal cell growth was determined by examining cell morphology. Differentiated BMDM cells were collected by cell scraping and seeded in M-CSF free DMEM for further use.

2.2.1.6 Generation and culture of primary BMDC

Age (8-12 weeks) and gender matched WT and *Peli2*$^{-/-}$ mice were sacrificed by cervical dislocation. Mice were first sterilised with 70% EtOH before removal of the femur and tibia under aseptic conditions in a laminar flow hood. Bone marrow was removed by flushing the bones with a 27¾ gauge needle containing 20 ml PBS. Cells were then pelleted by centrifugation at 600 g for 5 min. RBL was carried out by resuspending the pellets in 1ml of Sigma-Aldrich RBL buffer and incubated at RT for 1 min. Lysis was terminated by the addition of 20 ml RPMI supplemented

with 10% (v/v) heat inactivated FBS, penicillin G (100 μg/ml) and streptomycin (100 μg/ml) and cells were centrifuged again at 600 g for 5 min. Pellets were re-suspended in 10ml RPMI and cells were counted using a haemocytometer. WT and *Peli2*$^{-/-}$ cells were equalised and seeded at 2x10^6 cells/ml with 40 ml RPMI in a T175^2 culture flask. Supernatant media from cultured J558 cells containing GM-CSF was added to a final concentration of 20% (v/v). Cells were cultured in a 37°C humidified chamber under a 5% CO2 atmosphere for 3 days after which the cells were scraped and pelleted by centrifugation at 600 g for 5 min. Pellets were re-suspended in 10 ml RPMI and cells were counted using a haemocytometer. WT and *Peli2*$^{-/-}$ cells were equalised and seeded at 2x10^6 cells/ml with 40 ml RPMI in 2 T175^2 culture flasks. Fresh RPMI supplemented with 20% GM-CSF (v/v) was gently added and cells were cultured for a further 4 days. Optimal cell growth was determined by examining cell morphology. Differentiated non-adherent BMDC cells were collected and seeded in GM-CSF free RPMI for further use.

2.2.2 Molecular Biological Methods

2.2.2.1 DNA Isolation for Genotyping

3 week old mice were earpunched and the tissue sample was placed in a sterile eppendorf tube. Crude DNA samples were prepared by adding 100 μl of DirectPCR™ Lysis Reagent containing Proteinase K (0.4 mg/ml) was added to each sample and incubated at 55°C for between 5 and 12 hours. Proteinase K was inactivated by incubating at 85°C for 45 min. Extracted DNA was then diluted 1:10 in DNase free water prior to being used as the template for genotyping PCR reactions.

2.2.2.2 Total Cellular RNA Extraction

To avoid contamination of RNA samples, all reagents and labware used were certified as RNase free. Gloves were worn and changed frequently in order to avoid introducing RNase contamination. All surfaces were decontaminated with RNase Zap.

BMDM, BMDCs and iBMDM cells were seeded at $1x10^6$ cells/ml with 3 ml media in 6-well plates for all mRNA analysis experiments. Harvesting for total RNA was carried out by first washing with PBS, scraping the cells and centrifuging at 6,500 g for 5 minutes at 4°C. Cell pellets were re-suspended with 500 µl of Trizol and incubated at RT for 5 minutes to ensure full homogenisation. 150 µl of chloroform was added and the mixture was first inverted and then vortexed for 5 sec. Samples were incubated at RT for 10 minutes, during which time phase separation begins. This is completed by centrifugation at 12,000 g for 15 minutes at 4°C. 150 µl of the upper aqueous phase was transferred to a new sterile tube, avoiding contamination with the red phenol-chloroform phase or the interphase. 150 µl of isopropanol was added to the aqueous phase and the mixture was first inverted and then vortexed for 5 sec. Samples were incubated at RT for 5 minutes, followed by centrifugation at 12,000 g for 15 minutes at 4°C. The isopropanol was carefully removed without disturbing the precipitated RNA pellet. 900 µl of 75% (v/v) EtOH was added to the pellet and vortexed briefly. Samples were centrifuged at 6,500 g for 5 min at 4°C, after which the ethanol was removed and the RNA pellets were air dried in a laminar flow hood for 10 minutes. The RNA pellet was re-suspended in 20 µl of RNase free water and incubated at 60°C for 10 minutes. A Nanodrop™ spectrophotometer was used to quantify the concentration of RNA in each sample. The ratio of the absorbance at 260 and 280 nm was used to assess the purity of the RNA sample, where a ratio of 1.8-2.0 indicated pure RNA. RNA samples were stored at -80°C.

2.2.2.3 First Strand cDNA Synthesis from Total Cellular RNA

Complementary DNA (cDNA) is a DNA copy synthesised from mRNA. This reaction was carried out in a sterile microcentrifuge tube. 2 µg of quantified total cellular RNA was diluted in nuclease-free water to a final volume of 12 µl. 1 µl of random primers (0.5 µg) was added to the sample and incubated at 70°C for 5 min, followed by incubation of the sample on ice. The random primers consist of a mixture of hexamers and anchored-dT primers which results in an even coverage of the RNA template. The following master premix was prepared:

Reagent	**Volume (µl)**
Bioscript Reverse Transcriptase (200u/µl)	0.5
dNTPs (10mM)	1
5X Bioscript Reaction Buffer	4
Nuclease-free water	1.5

After addition of the premix to the sample, mixtures were incubated at 25°C to facilitate primer annealing. The mixture was incubated at 42°C for 45 min. The reaction was then terminated by incubation at 85°C for 5 min, followed by chilling on ice. cDNA samples were stored at -20°C or immediately amplified by PCR.

2.2.2.4 Polymerase Chain Reaction (PCR)

2.2.2.4.1 DNA Amplification by PCR

Previously generated cDNA or whole genomic DNA (outlined in 2.2.2.1 and 2.2.2.3) were subjected to amplification using predesigned DNA primers (2.1.5.1) to target specific amplification of the region of interest. The reagents of the reaction premix described below were added on ice.

Reagent	**Volume (µl)**
5X GoTaq® Reaction Buffer	5
MgCl2 Solution (25mM)	2
Sense Primers (100 pmol/µl)	.25
Anti-Sense Primers (100 pmol/µl)	.25
dNTPs (10mM)	1
GoTaq® DNA Polymerase (5u/µl)	.15
Template DNA	2
Nuclease-free Water	14.35

Using a thermal cycler, samples were first incubated at 95°C for 5 minutes to facilitate denaturation of template DNA. Samples were then subjected to 30 cycles of first 95°C for 30 sec, followed by 60°C for 30 sec and 72°C for 1 min. Each stage of this cycling step encompassed denaturation, annealing and extension of the product,

respectively. A final extension of the product was carried out at 72°C for 10 min before the reaction was quenched by incubation at 4°C. PCR products were stored at -20°C or immediately quantified through gel electrophoresis or real-time PCR.

2.2.2.4.2 Qualitative Analysis by Agarose Gel Electrophoresis

Agarose gel electrophoresis was used for the purpose of genotyping to determine the presence or absence of amplified regions of interest from whole genomic DNA. Agarose gels were prepared using 1.5% (w/v) agarose in TAE buffer. This was achieved by heating the solution until the agarose had fully dissolved and subsequently cooled to below 50°C. SYBR® Safe DNA Gel Stain (1:10,000 dilution) was added to allow visualisation of DNA and the gel was poured into a pre-assembled gel tray with well combs. Solidified gel was placed into electrophoresis rig which was filled with TAE buffer. Samples were loaded alongside a 1 kb molecular size marker and subjected to electrophoresis at 90 volts. DNA product bands were visualised using ultraviolet (UV) light (254 nm) and image acquisition was carried out using a Syngene G box gel documentation system.

2.2.2.4.3 Quantitative Real-time PCR Analysis

Previously generated cDNA (outlined in section 2.2.2.4.1) were subjected to quantitative real-time PCR analysis, allowing for a comparative quantification between various DNA samples during the PCR amplification process. Specifically designed primers correlating to a targeted region of interest (Section 2.1.5) were used. The reagents of the reaction premix described below were added on ice.

Reagent	Volume (µl)
2X SensiMix™ SYBR® No-ROX	10
Sense Primers (4 pmol/µl)	2.5
Anti-Sense Primers (4 pmol/µl)	2.5
Nuclease-free Water	3

18 µl of the above reaction premix was added to a PLATE followed by 2 µl of previously prepared template DNA. The PCR was carried out using an Applied Biosystems Step One™ real-time PCR instrument. Samples were first incubated at 95°C for 5 minutes to facilitate denaturation of template DNA. Samples were then subjected to 30 cycles of first 95°C for 30 sec, followed by 57°C for 30 sec and 72°C for 45 sec. Each stage of this cycling step encompassed denaturation, annealing and extension of the product, respectively. SYBR green binds to double stranded DNA product during the annealing and extension stage, which after absorbance of 497 nm blue light, can be measured by emitted 520 nm green light. The cycling step was followed by a melt curve analysis, which requires the products to be heated from 60°C to 90°C. One peak on the melt curve verified the presence of a single amplification product. Relative quantification of the targeted gene expression activity was determined using the Crossing Threshold (CT) method. The generated CT value reflected the target well exceeding a preprogramed fluorescence threshold, indicating the presence of a sufficient number of the target amplicons. The cycle which the CT value was reached was recorded and ΔCT value could be determined by subtracting the control gene CT value from the targets. The relative fold change of the genes was further determined using $2^{-\Delta CT}$.

2.2.2.5 Transformation of *Escherichia coli* for Propagation of Plasmids

One Shot® TOP10 chemically competent *E.coli* were used for plasmids propagation. 100 ng (1 µl) of plasmid was added to 5 µl of TOP10 cells on ice. DNA and bacteria were mixed with a pipette and incubated on ice for 30 min. Mixing was carried out gently as cells are highly sensitive to temperature and mechanical lysis. Cells were heat-shocked for 30 seconds at 42°C and placed on ice for 2 min. 150 µl of pre-warmed SOC medium at 37ºC was added to cells which were then incubated at 37 ºC on an Exceller E25 shaker at 220 revolutions per minute (rpm) for 1 h. 150 µl of the mix was then spread out on pre-warmed LB agar plates (LB broth with 1.5% (w/v) agar) containing 100 µg/ml ampicillin. The plates were inverted and incubated overnight at 37ºC. Colonies were then be selected from the plates for plasmid purification. Plates were stored at 4ºC for up to four weeks

2.2.2.6 Large-scale Purification of DNA from *E. coli*

100 ml LB broth containing ampicillin (50 µg/ml) was inoculated with a colony of transformed *E. coli* colony from section 2.2.2.5. The culture was incubated at 37 ºC on an Exceller E25 shaker at 220 rpm overnight. Large-scale plasmid purification was carried out using the high-speed plasmid midi kit from Qiagen. The bacterial cells were pelleted by centrifugation at 3,000 g for 25 min. The supernatant was discarded and plasmid DNA extraction was carried out as per manufacturer's instructions. A Nanodrop™ spectrophotometer was used to quantify the concentration of DNA in each sample. The ratio of the absorbance at 260 and 280 nm was used to assess the purity of the DNA sample, where absorbance of 1 unit at 260 nm is ~50 µg/ml. DNA samples were stored at -20°C.

2.2.2.7 Transient Transfection of Mammalian Cells

HEK293 cells were seeded at $2x10^5$ cells/ml (3 ml) in 6-well plates and incubated overnight. 1 ml of media was removed from each well. 1 μg of plasmid DNA for transfection was diluted in 250 μl of OptiMEM and mixed gently. 4 μl of Lipofectamine2000 was diluted into a separate vial containing 250 μl of OptiMEM. After a 5 min incubation, the solutions were combined dropwise and incubated for 20 min. 500 μl of the DNA-Lipofectamine complexes were gently added to each well and left for 24 h before harvesting.

2.2.3 Biochemical Methods

2.2.3.1 Protein Extraction

2.2.3.1.1 Extracellular Protein Extraction

To avoid protein degradation, all equipment was pre-chilled and all steps in the extraction process were carried out on ice unless otherwise stated. In the case of adherent cells, extracellular protein was generated by removing conditioned medium, centrifuging at 6,500 g for 10 minutes at 4°C to remove any non-adhered cells, transferring the supernatant to fresh 1.5 ml tubes and storing at -20°C.To generate intracellular protein extracts, adherent cells (after removal of conditioned medium), were washed gently with PBS and then scraped in 1 ml PBS and transferred to fresh 1.5 ml tubes. Samples were centrifuged at 6,500 g for 10 minutes at 4°C, after which the PBS was removed. In the case of semi-adherent cells, the media containing non-adherent cells was removed and added to a 15 ml tube. Cells were scraped in 1 ml PBS and transferred to the same 15 ml tube. Samples were centrifuged at 6,500 g for 10 minutes at 4°C, after which the PBS was removed. Cells were re-suspended in 1 ml PBS, transferred to a new 1.5 ml tube and once again centrifuged at 6,500 g for 10 minutes at 4°C and the PBS was removed. In the case of both adherent and semi-adherent cells, cellular pellets were re-suspended in 90 μl lysis buffer and incubated on ice for 30 min under constant agitation on an orbital shaker. Lysates were then

centrifuged at 12,000 g for 10 min at 4°C. 80 µl of the supernatant consisting of soluble proteins was transferred to fresh 1.5 ml tubes and stored at -20°C. The insoluble protein pellet was washed with 1ml PBS and then centrifuged at 12,000 g for 10 min at 4°C. PBS was removed and the wash step was repeated. Samples were then analysed for whole insoluble protein expression by SDS-PAGE or subject to chemical cross-linking analysis.

2.2.3.1.2 Irreversible Chemical Crosslinking of Insoluble Protein Complex

Washed insoluble pellets from above were re-suspended with 500 µl of PBS containing non-cleavable protein cross-linker disuccinimidyl suberate (DSS) (4 mM). Samples were incubated at RT for 30 minutes under constant agitation on an orbital shaker. Samples were pelleted by centrifugation at 5000 g for 10 minutes. Cross-linked pellets were re-suspended in 50 µl 2x sample buffer and were incubated for 10 minutes at 100°C.

2.2.3.2 Protein Immunoprecipitation

2.2.3.2.1 Co-Immunoprecipitation to Investigate Protein-Protein Interactions

For overexpression studies, cells were transfected with protein expression constructs as in section 2.2.2.7 and after 24 h cells were harvested as below. To investigate endogenous interactions, cells were seeded at 1 x 10^6 cells/ml (10 ml) in 10 cm tissue culture dishes and left overnight. After ligand stimulation, cells were placed on ice and the media was removed. Cells were gently washed with 3 ml ice cold PBS prior to being scraped in 1 ml PBS. Cells were transferred to 1 ml microfuge tubes and subjected to centrifugation at 6,500 g for 5 min. Excess PBS was removed without disturbing the pellet which was then re-suspended in 200 µl CoIP lysis buffer. Samples were left on ice on an orbital shaker under constant agitation for 20 min,

ensuring complete lysis of cells. This cellular lysate was then subjected to centrifugation at 12,000 g for 10 min. 20 µl of the protein lysate supernatant was removed and stored at this point to be used later as an input whole cell lysate control. The remaining protein lysate was removed from the insoluble pellet and transferred to a fresh 1.5 ml tubes. The volume of the sample was inceased to 1 ml using CoIP lysis buffer. Immunoprecipitation of the protein of interest was then carried out by addition of 1 µg of a respective antibody to each tube. Samples were incubated overnight at 4°C under constant agitation using a sample rocker. 40 µl of protein A/G beads were added to each sample followed by a further incubation at 4°C for 6 h under constant agitation. Samples were centrifuged at 12,000 g for 1 minute and the supernatant was removed. 1 ml of CoIP lysis buffer was added to the bead pellet followed by several inversions of the tube. Samples were once again subjected to centrifugation and the wash step was repeated three more times. After the final wash step, all the supernatant was removed and 40 µl of 2X sample buffer was added to the beads. Samples were incubated at RT for 20 min before being vortexed and boiled for 5 minutes. Samples were then either stored at -20°C or directly subjected to SDS-PAGE.

2.2.3.2.2 Immunoprecipitation to Investigate Post Translational Modifications

For overexpression studies, cells were transfected with protein expression constructs as in section 2.2.2.7 and after 24 h cells were harvested as below. To investigate endogenous post translational modifications (PTM) of a protein of interest, cells were seeded at 1 x 10^6 cells/ml (10 ml) in 10 cm tissue culture dishes and left overnight. After ligand stimulation, cells were placed on ice and the media was removed. Cells were gently washed with 3 ml ice cold PBS prior to being scraped in 1 ml PBS. Cells were transferred to 1 ml tubes and subjected to centrifugation at 6,500 g for 5 min. Excess PBS was removed without disturbing the pellet which was then re-suspended in 200 µl CoIP lysis buffer. Samples were left on ice on an orbital shaker under constant agitation for 20 min, ensuring complete lysis of cells. This

cellular lysate was then subjected to centrifugation at 12,000 g for 10 min. 20 µl of the protein lysate supernatant was removed and stored at this point to be used as a whole cell lysate control. The remaining 180 µl of protein lysate was removed from the insoluble pellet and transferred to a fresh 1.5 ml tubes. 20 µl of 10% (w/v) SDS was added to samples and left at RT for 5 min. Samples were then boiled for 5 min to facilitate complete disassociation of proteins. The sample was then split into two separate tubes and the volume of each tube was increased to 1 ml using CoIP lysis buffer in order to dilute remaining SDS. Immunoprecipitation of the protein of interest was then carried out by addition of 1 µg of a respective antibody to each tube. Samples were incubated overnight at 4°C under constant agitation using a sample rocker. 40 µl of protein A/G beads were added to each sample followed by a further incubation at 4°C for 6 h under constant agitation. Samples were centrifuged at 12,000 g for 1 minute and the supernatant was removed. 1 ml of CoIP lysis buffer was added to the bead pellet followed by several inversions of the tube. Samples were once again subjected to centrifugation and the wash step was repeated three more times. After the final wash step, all the supernatant was removed and the duplicate samples were recombined and wash once more. After centrifugation and complete removal of the supernatant, 40 µl of 2X sample buffer was added to the beads. Samples were incubated at RT for 20 min before being vortexed and boiled for 5 minutes. Samples were then either stored at -20°C or directly subjected to SDS-PAGE.

2.2.3.3 SDS-Polyacrylamide Gel Electrophoresis (SDS-PAGE)

SDS-PAGE was conducted as outlined by Laemmli (Laemmli, 1970) and modified by Studier (Studier, 1973). Samples and pre-stained molecular ladder (10-180 kDa) were denatured in SDS-PAGE sample buffer by boiling for 5-10 min prior to loading into individual wells. Electrophoresis was performed at a constant 60 V through a 5% SDS polyacrylamide stacking gel and then through a 8-15% resolving gel at 90 V for 1.5-2 h. The percentage of the resolving gel was chosen based on the size of

the targeted protein of interest, where higher percentage gels were used to priortise resolution of proteins of lower molecular weights.

2.2.3.3.1 Immunoblotting

Following separation by electrophoresis, the migrated proteins were transferred electrophoretically to nitrocellulose membranes by a Pierce G2 Fast Blotter semi-dry transfer unit. Electrical current (Amps) and transfer times varied depending on the size of the protein of interest. Pre-cut Whatmann paper and nitrocellulose were equilibrated with Pierce 1-Step Transfer Buffer 10 min prior to use. 3 layers of Whatmann paper were placed on the bottom surface of the transfer unit followed by a single layer of nitrocellulose. The resolving gel was washed briefly in transfer buffer before being place on the nitrocellulose while avoiding bubbles. 3 more layers of Whatmann paper were placed on top and the unit was closed. Transfer was carried out as per the settings below.

Number of Gels	Volts	Amps	< 20 kDA	20-100 kDA	> 100 kDA
1	25	1.3	5 min	7 min	10 min
2	25	2.5	5 min	7 min	10 min
3	25	3.8	5 min	7 min	10 min
4	25	5	5 min	7 min	10 min

After transfer was completed, membranes were briefly washed with deionised H_2O before incubation with Blocking Buffer for 30 minutes on an orbital shaker at RT to inhibit non-specific antibody binding to a membrane. Membranes were then

incubated with primary antibody overnight in TBST containing 5% (w/v) skimmed milk powder as per dilutions given in section 2.13. The membranes were washed in TBST for 5 minutes under constant agitation. This wash step was repeated 3 times. Membranes were then incubated with a secondary antibody specific to the primary antibody (anti-mouse, anti-rabbit, anti-goat) in TBST containing 5% (w/v) skimmed milk powder at RT for 1 h. The membranes were again washed in TBST 3 times for 5 minutes under constant agitation. Protein bands were then visualised using the Odyssey infrared imaging system from Licor Biosciences or using enhanced chemiluminescence (ECL).

2.2.3.4 Enzyme-Linked Immunosorbent Assay (ELISA)

2.2.3.4.1 TNF-α, IL-6, RANTES, CXCL1 and IL-1β ELISA

Cell supernatant or serum samples were collected and stored at -80°C prior to analysis. 96-well NUNC "Maxisorb" plates were coated with 100 µl capture antibody diluted to a working concentration in PBS. Dilutions of capture antibody were lot specific. Plates were covered to avoid evaporation and placed on an orbital shaker overnight at RT. Antibody was aspirated from the plate and each well was washed three times with a wash buffer (0.05% Tween® 20 in PBS). After the final wash, plate was inverted and blotted against clean paper towels to ensure the removal of excess wash buffer. Plates were blocked by adding 300 µl of block buffer (1% (w/v) BSA in PBS filter sterilised (0.2 µm)) for 2 h. Reagent diluent was prepared for the IL-1β plate (0.1% (w/v) BSA in Tris-buffered Saline (20mM Trizma base, 150mM NaCl) filter sterilised (0.2 µm)) and the TNF-α, IL-6, RANTES, CXCL1 plates (1% (w/v) BSA in PBS filter sterilised (0.2 µm)). Samples were diluted in reagent diluent and added to each well. Standards were diluted in reagent diluent along a seven point standard curve using 2-fold serial dilutions with a top standard of 2000 pg/ml. Plates were covered to avoid evaporation and placed on an orbital shaker overnight at 4°C. Plates were washed as above and 100 µl of detection antibody was diluted to a working concentration in reagent diluent. Dilutions of capture antibody were lot specific. Plates were incubated for 2 h at RT and the wash

step was repeated. Streptavidin-HRP conjugate was diluted in reagent diluent as per lot specific instructions and 100 µl was added to each well. Plates were incubated in the dark at RT for 20 min and the wash step was repeated. 100 µl TMB (1.25 mM/l) solution was added to each well and the plates were covered and incubated at RT for 20 min. 50 µl 1 N H_2SO_4 stop solution was added to stop the reaction. The optical density (OD) value of each well was measured at 450 nm with a correction at 590 nm. A ELx800TM microplate reader with Gen5 Data Analysis Software was used to carry out the reading. The sample concentrations were determined by interpolating the sample absorbance from the known concentrations of the standard curve. Standards were assayed in duplicate while samples were analysed in triplicate. Data presentation and analysis were carried out using Graphpad Prism 5 software.

2.2.3.4.2 IFN-β ELISA

Cell supernatant or serum samples were collected and stored at -80°C prior to analysis. 96-well NUNC "Maxisorb" plates were coated with 100 µl of rat anti-mouse IFN-β (0.1 µg/ml) diluted in PBS. Plates were covered to avoid evaporation and placed on an orbital shaker overnight at RT. Antibody was aspirated from the plate and each well was washed three times with a wash buffer (0.05% Tween® 20 in PBS). After the final wash, plate was inverted and blotted against clean paper towels to ensure the removal of excess wash buffer. Plates were blocked by adding 300 µl of reagent diluent (1% (w/v) BSA in PBS filter sterilised (0.2 µm)) for 2 h. Samples were diluted in reagent diluent and added to each well. Standards were diluted in reagent diluent along a seven point standard curve using 2-fold serial dilutions with a top standard of 3000 pg/ml. Plates were covered to avoid evaporation and placed on an orbital shaker overnight at 4°C. Plates were washed as above and 100 µl of rabbit anti-mouse IFN-β (500 ng/ml) diluted in PBS was added to each well. Plates were incubated for 2 h at RT and the wash step was repeated. Streptavidin-HRP conjugate was diluted 1:2000 in reagent diluent and 100 µl was added to each well. Plates were incubated in the dark at RT for 20 min and the wash step was repeated. 100 µl TMB (1.25 mM/l) solution was added to each well and the plates were covered and

incubated at RT for 20 min. 50 µl 1 N H_2SO_4 stop solution was added to stop the reaction. The OD value of each well was measured at 450 nm with a correction at 590 nm. A ELx800TM microplate reader with Gen5 Data Analysis Software was used to carry out the reading. The sample concentrations were determined by interpolating the sample absorbance from the known concentrations of the standard curve. Standards were assayed in duplicate while samples were analysed in triplicate. Data presentation and analysis were carried out using Graphpad Prism 5 software.

2.2.3.5 Bradford Assay

Bradford assays were performed to quantitate protein concentration (Bradford, 1976). Known concentrations of BSA standards and samples were diluted in 20 µl of water and mixed with 180 µl of Bradford assay reagent. The OD value of each well was measured at 590 nm. A ELx800TM microplate reader with Gen5 Data Analysis Software was used to carry out the reading. The sample concentrations were determined by interpolating the sample absorbance from the known concentrations of the standard curve. Standards were assayed in duplicate while samples were analysed in triplicate. Data and analysis were carried out using Graphpad Prism 5 software.

2.2.3.6 LDH Assay

Phenol-free DMEM was used to avoid background signal in the detection phase of the assay. LDH release from cells was determined using a Pierce™ LDH Cytotoxicity Assay Kit. 10X Lysis Buffer was added to an untreated well 45 min prior to harvest to act as the maximum LDH activity control. Supernatant samples were collected and stored at -80°C prior to analysis. 50 µl of sample was added to a flat bottom 96 well plate followed by addition of 50 µl of reaction mixture. Samples were incubated at RT in the dark under gentle agitation for 30 min. 50 µl of stop solution was added to each well and The OD value of each well was measured at 490

nm with a correction at 680 nm. A ELx800TM microplate reader with Gen5 Data Analysis Software was used to carry out the reading. Samples were analysed in triplicate. Data presentation and analysis were carried out using Graphpad Prism 5 software.

2.2.3.7 *In vitro* Assay

In vitro ubiquitination assay was carried out on ice by incubating 500 ng UBE1 (E1), 400 ng Ubc13/Uev1A (E2), 2 µg ubiquitin, 300 ng NLRP3 and 300 ng Pellino2-myc (20 nM) in reaction buffer (5 mM Tris-HCl, pH 8.0, 2 mM MgCl, 2 mM ATP, Proteinase inhibitor-EDTA free 1/10 dilution) made up to 20 µl volume in Samples were incubated at 37℃ for 1 h. Samples were then immunoprecipitated (as in section 2.2.3.2.2) and analysed by western blot.

2.2.4 *In Vivo* Methods

2.2.4.1 LPS Induced Sepsis Model

2.2.4.1.1 Survival analysis

Age (8-10 weeks), weight and sex matched. Mice were rehoused in pairs and allowed to acclimatise to the new surroundings overnight to avoid stress. Mice were weighed again prior to injection to determine LPS dose. Injection of either PBS control or 20 mg/kg ultrapure LPS was carried out i.p. using a 27 g needle. Mice were monitored every 8 hours and documented using an animal welfare scoring system. Animals were monitored for adverse clinical signs, matted fur, abnormal behaviour, response to stimulus and weight loss. Any animal with a total cumulative health score exceeding a pre-defined threshold was culled. All mice were culled at the 72 h end-point of the experiment. Data presentation and analysis were carried out

using Graphpad Prism 5 software. All experiments were performed in accordance with the regulations and guidelines of the Irish Department of Health and protocols approved by the Research Ethics committee of National University of Ireland Maynooth.

2.2.4.1.2 Serum collection

Mice were age (8-10 weeks), weight and sex-matched. Mice were rehoused in pairs and allowed to acclimatise to the new surroundings overnight to avoid stress. Mice were weighed again prior to injection to determine LPS dose. Injection of either PBS control or 20 mg/kg ultrapure LPS was carried out i.p. using a 27 g needle. After 18 hours, mice were sacrificed by cervical dislocation and blood was extracted. Whole blood was incubated at RT for 30 min to allow clotting. This was followed by centrifugation at 2,000 g for 10 minutes at 4°C. The resulting serum supernatant was removed and stored at -80°C.

2.2.4.1.3 Isolation of Mouse Peritoneal Cavity Cells

Mice were age (8-10 weeks), weight and sex-matched. Mice were rehoused in pairs and allowed to acclimatise to the new surroundings overnight to avoid stress. Mice were weighed again prior to injection to determine LPS dose. Injection of either PBS control or 20 mg/kg ultrapure LPS was carried out i.p. using a 27 g needle. After 18 h the mouse was euthanised, sprayed with 70% EtOH and mounted on a Styrofoam block. The peritoneum was exposed by removing the outer skin and injected using a 27 g needle with 5 ml ice cold PBS (containing 3% FCS). The peritoneum was massaged to dislodge any attached cells and then the fluid was collected using a 25 g needle. The cell suspension was subjected to centrifugation at 2000 g for 10 minutes and the supernatant was discarded. Cells were then counted and stained for flow cytometric analysis.

Chapter 3: Results

Analysis of the Role of Pellino2 in the Activation of the NLRP3 Inflammasome

3.1 Prologue

The innate immune system represents the initial detection and response to a pathogen and is required for the subsequent initiation of the adaptive immune response. Inflammasomes are cytosolic supramolecular protein structures which play a critical role in the detection of danger-associated signals, as well as pathogen signals. A number of different inflammasome forming proteins have been discovered, including NLRP1, NLRP3, NLRP6, NLRC4, AIM2 and RIG-I (Latz *et al.,* 2013). While the activating signals and formation of each inflammasome can differ, each culminates in the activation and secretion of IL-1β and IL-18, both of which strongly contribute to inflammation. A form of cell death called pyroptosis is also thought to be associated with inflammasome activation (Miao *et al.,* 2010a). The signalling of NLRP3 differs to classical PRRs, as it requires two signals: A priming signal (signal 1) and an activating signal (signal 2). The priming signal is primarily via NF-κB activation, usually through TLR signalling. NF-κB activation is required for the transcription of vital inflammasome components. This dual signal response is a tightly controlled signalling event, requiring recognition of a pathogen associated ligand as well as a danger signal (F. Bauernfeind *et al.,* 2009).

The NLRP3 inflammasome is capable of responding to a wide variety of different activating signals and as such, is thought to not bind any one ligand directly. It is therefore believed that a cellular event, such as potassium efflux, calcium signalling or lysosomal disruption may instead lead to its activation (Martinon *et al.,* 2009). This leads to the upregulation of NLRP3 as well as the inactive pro-IL-1β. After priming, a second signal is required which leads to NLRP3 oligomerisation, which recruits the protein ASC and acts as a nucleus for ASC aggregation. This large protein complex can be visualised as a speck in the cytoplasm of the cell under fluorescence microscopy (Sahillioglu *et al.,* 2014). Interestingly the speck itself is capable of acting as an activating signal of the NLRP3 inflammasomes of neighbouring cells when released during pyroptosis, resulting in an amplified inflammatory response (Baroja-Mazo *et al.,* 2014). This NLRP3-ASC complex can

further act as a platform which recruits caspase-1 and converts it to its enzymatically active form, allowing for the further activation of IL-1β.

Despite the research into NLRP3 inflammasome, the molecular details underpinning NLRP3 activation remain to be fully delineated. The post-translational events specifically regulating NLRP3 activation remain a key topic in research, as this can occur independently of protein translation. Deubiquitination of NLRP3 by BRCC3 has been shown to be vital to its assembly (Juliana *et al.,* 2012; Py *et al.,* 2013). Phosphorylation may also play a role in the activation of NLRP3, however this has not been directly observed (De Nardo *et al.,* 2014). The kinase activity of Syk (Gross *et al.,* 2009), protein kinase R (PKR) (He *et al.,* 2013) and TAK1 (Gong *et al.,* 2010) have also been shown to induce NLRP3 activation. These studies demonstrate the complexity involved in NLRP3 signalling, as well as the importance of post-translational modifications in facilitating its activation.

Three mammalian Pellino proteins have been discovered and genetically mapped. (Jensen and Whitehead, 2003a). All members of the Pellino family are structurally similar; they each contain a RING domain and a FHA domain, which contains phosphothreonine-binding modules and mediates protein-protein interaction (Lin *et al.,* 2008). Each Pellino protein also contains a RING domain, which are a feature of E3 ubiquitin ligases (Schauvliege *et al.,* 2006). The functions of both Pellino1 and Pellino2 have been physiologically identified, but the function of Pellino2 remains ambiguous. Pellino2 has primarily been studied in the context of IL-1 and TLR signalling (Yu *et al.,* 2002) using shRNA knockdown and over-expression techniques. Pellino2 was shown to be required for IL-1 and TLR4 induced polyubiquitination of IRAK1. The phosphorylation JNK and ERK were also inhibited during both TLR4 and IL-1β signalling in Pellino2-knockdown cells (Kim *et al.,* 2012). Pellino2 was also shown to interact with BCL10 during LPS signalling (Liu *et al.,* 2004). The work in this thesis aims to investigate the physiological role of Pellino2 using a newly generated *Peli2*$^{-/-}$ mouse.

3.2 Results

3.2.1 Generation and phenotypic observation of *Peli2*$^{-/-}$ Mice

Peli2$^{-/-}$ mice were generated by Taconic Artemis using proprietary technology. In order to characterise the genotype of the mice used in this study, PCR analysis of DNA isolated from murine ear punches was carried out. PCR analysis using WT (*Peli2*$^{+/+}$) and heterozygous (*Peli2*$^{+/-}$) genomic DNA as a template resulted in the production of a fragment when using primers (a + b), corresponding with the WT *Peli2* product (Fig. 3.1a). Primers (c + d) amplified a fragment in knockout (*Peli2*$^{-/-}$) and heterozygous (*Peli2*$^{+/-}$) genomic DNA, corresponding with the knockout *Peli2* product. *Peli2*$^{-/-}$ was determined by the absence of the WT *Peli2* fragment and the presence of the knockout *Peli2* fragment. DNase free water (H_20) was used as a negative control in place of the genomic DNA template. Primers amplifying the housekeeping gene HPRT were used as a positive control. mRNA levels were also examined in cells in order to assess the levels of Pellino2 mRNA expression and confirm knockdown. mRNA levels of Pellino2 were assessed by RT-PCR in BMDMs from WT and *Peli2*$^{-/-}$ bone marrow. Total abrogation of Pellino2 mRNA was observed in *Peli2*$^{-/-}$ cells, further demonstrating that Pellino2 expression has been effectively knocked out in *Peli2*$^{-/-}$ mice (Fig. 3.1b). Finally, *Peli2*$^{-/-}$ mice were monitored for the spontaneous generation of any aberrant phenotype. Pellino2 is not required for development since Pellino2-deficient mouse are viable, with breeding rates comparable with WT mice. No weight differences were observed between WT and Pellino2-deficient mice after 10 weeks of normal chow diet (Fig. 3.1c). Taken together, these results show that Pellino2 gene expression is absent in the Peli2$^{-/-}$ mice and that these mice are viable and develop normally.

3.2.2 Loss of Pellino2 has no effect on TLR-induced expression of pro-inflammatory cytokines

Given that the other Pellino proteins have been shown to affect TLR signalling, the initial screens to elucidate a physiological role for Pellino2 focused on its potential involvement on mediating TLR-induced expression of pro-inflammatory cytokines. BMDMs cultured from WT and *Peli2*$^{-/-}$ bone marrow were stimulated for 24 h with ligands for TLR2/6 (Pam2CSK4), TLR 2/1 (Pam3CSK4), TLR2/Dectin-1 (Zymosan), TLR3 (Poly(I:C)), TLR4 (LPS), TLR5 (Flagellin), TLR8 (CLO75), TLR7/8 (CLO97) and TLR9 (CpG) and assessed for IL-6 and TNF-α expression. IL-6 and TNF were initially chosen as both are well characterised pro-inflammatory cytokines that are strongly induced by TLRs. Cytokine protein levels were assessed by ELISA. Each TLR ligand promoted strong expression of IL-6 (Fig. 3.2a) and TNF-α (Fig. 3.2b) in macrophages from WT mice and comparable expression levels were observed in *Peli2*$^{-/-}$ macrophages suggesting that Pellino2 is not involved in the TLR-induced expression of these pro-inflammatory cytokines. The effect of Pellino2 deficiency on TLR-induced chemokine expression was also evaluated. Using RANTES (Fig. 3.3a) and CXCL1 (Fig. 3.3b) as TLR-responsive chemokines, the various TLR ligands were shown to induce comparable levels of their expression in WT and *Peli2*$^{-/-}$ BMDMs. These results indicate that TLR induction of both pro-inflammatory cytokines as well as chemokines are unaffected by the absence of Pellino2.

3.2.3 Loss of Pellino2 has no effect on IFNβ secretion upon TLR stimulation

In addition to the creation of a pro-inflammatory environment, TLR signalling can also play a key role in the recognition or viruses and the induction of anti-viral type I IFNs. Innate immune receptors that play key roles in mediating anti-viral responses

by inducing type I IFNs include TLR2/Dectin-1, TLR3, TLR4, TLR8, TLR7/8 and TLR9. BMDMs cultured from WT and *Peli2*$^{-/-}$ bone marrow were stimulated for 24 h with ligands for TLR2/Dectin-1 (Zymosan), TLR3 (Poly(I:C)), TLR4 (LPS), TLR8 (CLO75), TLR7/8 (CLO97) and TLR9 (CpG). Protein secretion levels of IFN-β were assessed by ELISA. Each ligand lead to a detectable increase in IFN-β, however there was no observable difference in responsiveness between WT and *Peli2*$^{-/-}$ BMDMs (Fig 3.4). This again suggests that Pellino2 does not contribute to the induction of TLR-responsive cytokines.

3.2.4 Loss of Pellino2 has no effect on the induction of RLR, NLR or cytokine responsive genes.

Given the findings that Pellino2 does not appear to mediate TLR signalling, the role of Pellino2 was next explored in other innate immune receptor families including the intracellular RIGI-like receptors (RLRs) and NOD-like receptors (NLRs). Various agents and ligands were chosen to stimulate these pathways. ppp-dsRNA and Sendai virus (SeV) activate RIG-i (Baum *et al.,* 2010), MDP activates NOD2 (Girardin *et al.,* 2003) while transfected poly(I:C) is capable of activating MDA-5 (Gitlin *et al.,* 2006). Poly(dA:dT) transfection initiates a number of pathways including IPS-1 (Kumar *et al.,* 2006) and RIG-I (Ablasser *et al.,* 2009). BMDMs cultured from WT and *Peli2*$^{-/-}$ bone marrow were treated with transfection reagent alone or subjected to transfection for 24 h with ppp-dsRNA, Poly(I:C), Poly(dA:dT) and MDP. Cell supernatants were then assessed for IL-6 (Fig. 3.5a) and IFN-β (Fig. 3.5b). The transfected ligands induced the expression of these cytokines but there were no observable differences in responsiveness of WT and Pellino2-deficient cells. As a more physiologically relevant model, SeV was also studied as a viral-inducer of IFN-β expression. Again, WT and Pellino2-deficient cells showed similar levels of IFN-β expression in response to SeV challenge (Fig. 3.6). These data indicate that Pellino2 does not mediate the induction of NLR or RLR-responsive genes.

Since over-expression and knockdown studies have implicated a role for Pellino2 in cytokine signalling, especially pathways that employ the transcription factor NF-κB, Pellino2 was next examined for possible involvement in cytokine signalling pathways that activate NF-κB. BMDMs were screened for IL-6 secretion using 24 h treatments of IL-1β and TNF-α. Both WT and Pellino2-deficient BMDMs showed similar responsiveness to IL-1 and TNF (Fig. 3.7), which is in contrast to previous knockdown studies (Kim *et al.,* 2012) and questions the role of Pellino2 in these pathways.

3.2.5 Loss of Pellino2 leads to reduced secretion of IL-1β upon NLRP3 inflammasome activation

The data above suggests that Pellino2 plays no role in regulating the expression of pro-inflammatory cytokines in response to stimulation of cytokine receptors, TLRs, NLRs or RLRs. While these assays focused on the expression of cytokines that are induced and secreted from cells via classical secretory mechanisms, IL-1β is a cytokine whose secretion is regulated differently than the other cytokines previously examined. IL-1β is initially translated in a precursor pro-IL-1β form that lacks a leader sequence and does not enter the classical secretory pathway upon upregulation. Instead it requires a secondary signal to allow its activation from an inactive to an active form. The assembly of an inflammasome is responsible for the processing of pro-IL-1β into its mature, bioactive form, with the NLRP3 inflammasome being the best studied to date. The role of Pellino2 in NLRP3 inflammasome activation of processing of IL-1β was next examined.

Two different immune cell types, BMDCs (Fig. 3.8a) and BMDMs (Fig. 3.8b) from WT and *Peli2*$^{-/-}$ bone marrow were stimulated with LPS for 3 hours. Cells were then left untreated or subjected to 40 min co-stimulation with either ATP or the bacterial pore forming toxin nigericin, each of which lead to the functional assembly of the NLRP3 inflammasome (Mariathasan *et al.,* 2006). Protein secretion levels of IL-1β

were assessed by ELISA. Both ATP and nigericin co-stimulation with LPS resulted in the secretion of IL-1β fom WT cells whereas ATP or nigericin alone were ineffective. However, a significant reduction of IL-1β secretion was observed in *Peli2*$^{-/-}$ cells. This data indicates that Pellino2 is required for optimal IL-1β secretion upon NLRP3 assembly.

BMDCs were more sensitive to IL-1β secretion through LPS stimulation alone. This is possibly due to a more constitutively active inflammasome in this cell type, similar to what has been described in monocytes (Kahlenberg and Dubyak, 2004). Due to this, all further cellular work carried out using *Peli2*$^{-/-}$ was in BMDMs to allow for more specific elucidation of the role of Pellino2 in inflammasome activation.

3.2.6 Loss of Pellino2 is protective in an LPS induced sepsis model

The physiological relevance of the role of Pellino2 in the secretion of IL-1β was then examined using an *in vivo* sepsis model. In a previous study investigating the role of Pellino1, *Peli1*$^{-/-}$ mice have been shown to be resistant to LPS induced septic shock when compared with WT mice (Chang *et al.,* 2009a). Due to the relevance of Pellino1 in this model, the effect of Pellino2 deficiency was investigated. To monitor survival, WT and *Peli2*$^{-/-}$ mice were challenged with either intraperitoneal saline (control) or a lethal dose of LPS (20 mg/kg). Mice were monitored every 8 hours, with responsiveness and weight loss assessed. By 48 h, all WT mice had succumbed to the lethal effects of LPS, while 50% of Pellino2 mice survived until the 72 h endpoint (Fig. 3.9). During the experiment, both WT and *Peli2*$^{-/-}$ mice lost a comparable percentage of weight (Fig. 3.10a). However, *Peli2*$^{-/-}$ mice which survived the LPS lethal shock were able to recover their weight by day 7 (Fig. 3.10b).

The mechanistic basis to the protective effects of Pellino2 against LPS-induced lethality was next explored by measuring the expression of pro-inflammatory cytokines in response to the *in vivo* administration of LPS. A separate cohort of animals was challenged with either intraperitoneal saline (control) or a dose of LPS (20 mg/kg). After 18 hours mice were sacrificed and serum was collected. ELISA assays were carried out on these samples to assess the levels of IL-6 (Fig. 3.11a), TNFα (Fig. 3.11b), RANTES (Fig. 3.11c), CXCL1 (Fig. 3.11d) and IL-1β (Fig. 3.11c). Increased serum cytokine levels were detected in all LPS challenged mice. The LPS-induced levels of IL-6, TNFα, RANTES and CXCL1 showed no significant difference between WT and *Peli2*$^{-/-}$ mice. However, *Peli2*$^{-/-}$ mice showed a significant reduction in serum IL-1β levels.

The protein Gr1 is highly expressed on the cell surface of neutrophils. Due to neutrophil infiltration playing a key role in sepsis (Pruitt *et al.*, 1995), cellular trafficking of Gr1^{+} cells was examined. A separate cohort of animals was challenged with either intraperitoneal saline (control) or a dose of LPS (20 mg/kg). After 18 hours mice were sacrificed and peritoneal cavity cells were isolated and stained with anti-GR1. Cells were then analysed by flow cytometry. While there is a reduction in the levels of GR1^{+} cells in the peritoneum of *Peli2*$^{-/-}$ mice, this difference did not reach statistical significance (Fig 3.12). This may be due to the contribution of other chemokines such as RANTES which are unaffected by Pellino2-deficiency. Taken together, these results were consistent with cell-based data that proposes a specific role for Pellino2 in mediating the secretion of bioactive IL-1β and not other pro-inflammatory cytokines. The decreased IL-1β levels in *Peli2*$^{-/-}$ mouse serum is consistent with reduced LPS-induced neutrophilia and lethality in these mice.

3.2.7 Loss of Pellino2 negatively affects Klebsiella-induced IL-1β secretion

Examining the inflammasome using a dual signal approach is important in order to elucidate the precise molecular mechanisms of its activation. However, it was also necessary to examine a more physiologically relevant scenario in order to confirm if Pellino2 deficiency can impact the innate immune response to pathogenic challenge. *Klebsiella pneumonia* was used as it has been shown previously in studies to illicit an NLRP3 dependent IL-1β response (Hua *et al.,* 2015; Willingham *et al.,* 2009). BMDMs from WT and *Peli2*$^{-/-}$ bone marrow were infected with *K. pneumonia* for 1 h, after which infected media was removed and replaced with gentamicin treated media. Cells were incubated for 3 h and harvested. Cell supernatants were then assessed for IL-1β levels by ELISA. Low levels of secreted IL-1β were detected (Fig. 3.13a). Pellino2-deficient cells exhibited reduced secretion of IL-1β when compared with WT. The reduced expression of mature IL-1β in the absence of Pellino2 is likely due to deficiency in signal 2-induced activation of the inflammasome since Pellino2-deficiency has no effect on the ability of *K. Pneumonia* to induce Signal 1-type effects such as induction of pro-IL-1β (Fig 3.13b) or NLRP3 (Fig 3.13c) at the mRNA and protein (Fig 3.13d) level. These results show that Pellino2 is required for optimal activation of the inflammasome during infection with *K. pneumonia,* which highlights a physiologically-relevant role for Pellino2 in inflammasome signalling.

3.2.8 Cell death is unaffected by reduced IL-1β in *Peli2*$^{-/-}$ cells

Assembly of the inflammasome and secretion of IL-1β has been shown to be linked with a necrotic form of cell death, known as pyroptosis (Miao *et al.,* 2010a). Pellino2 was thus probed for its potential role in pyroptosis. BMDMs from WT and *Peli2*$^{-/-}$

bone marrow were stimulated with LPS for 3 hours and left untreated or subjected to co-stimulation with either ATP for 40 min. Cells were harvested and stained with Annexin and PI in order to determine apoptosis. No difference in cell death between WT and Pellino2-deficent cells was observed (Fig 3.14a). LDH release from cells was also analysed. BMDMs from WT and *Peli2*$^{-/-}$ bone marrow were stimulated with LPS for 3 hours. Cells were then left untreated or subjected to co-stimulation with either ATP for 40 min. Supernatants were harvested and used in the LDH assay. No difference was observed in the LDH release between WT and Pellino2-deficient cells and interestingly, inflammasome activation led to low overall LDH release from cells (Fig 3.14b).. Previous studies exploring LDH release during NLRP3 inflammasome activation in BMDMs which used similar time-points have confirmed the finding that LDH release from cells shows no significant increase following pre-treatment with LPS and 40 minute co-stimulation with ATP when compared with unstimulated cells (Baroja-Mazo *et al.,* 2014). These results demonstrate that the difference observed in the secretion of IL-1β in WT and Pellino2-deficent cells is not due to a difference in cellular viability.

3.2.9 Pellino2 selectively regulates activation of the NLRP3 inflammasome

While the above data suggests that Pellino2 has a role in the functioning of the NLRP3 inflammasome, it was important to determine if it has a role in the production of IL-1β via other inflammasome forming proteins. To this end cells were transfected with different ligands to trigger other canonical pathways of inflammasome activation. AIM2 is triggered by the synthetic dsDNA ligand Poly(dA:dT) (Hornung *et al.,* 2009) while bacterial flagellin activates NLRC4 (Zhao *et al.,* 2011). BMDMs from WT and *Peli2*$^{-/-}$ bone marrow were stimulated with LPS, the ligand for TLR4 for 3 hours. Cells were then treated with transfection reagent alone or subjected to transfection with either Flagellin or Poly(dA:dT) for 18 h. Cell supernatants were then assessed for IL-1β levels by ELISA. All co-stimulations

induced IL-1β protein secretion, but there was no detectable difference between WT and *Peli2*$^{-/-}$ macrophages (Fig. 3.15). LPS in combination with the transfection agent showed an increase in IL-1β, possibly due to the liposomes acting as a danger signal (Zhong *et al.,* 2013). These results are consistent with the findings that Pellino2 plays a specific role in the canonical inflammasome activation by NLRP3.

3.2.10 Pellino2 does not affect NF-κB signalling through TLR4

The molecular and mechanistic basis to the regulatory effects of Pellino2 on NLRP3-mediated processing of IL-1β was next investigated. The regulation of the NLRP3 inflammasome signalling is dependent upon two distinct signalling events which culminate in the activation and assembly of inflammasome components. Signal 1, or the priming signal, is dependent upon TLR activation and has been shown to play a key role in the upregulation and activation of NLRP3 (Bauernfeind *et al.,* 2009; Qiao *et al.,* 2012). Pellino2 has previously been implicated in having a role in NF-κB signalling (Liu *et al.,* 2004; Yu *et al.,* 2002) so its role in this pathway was first explored. The phosphorylation of IκBα and IKKβ are key indicators of NF-κB signalling and were chosen for examination. BMDMs from WT and *Peli2*$^{-/-}$ bone marrow were stimulated with LPS over the indicated time-points (Fig. 3.16) and protein lysates were generated and probed with the appropriate antibodies. Pellino2 had no effect on the phosphorylated or total states of IKKβ. Peak phosphorylation was observed early during the time-course, at 15 and 30 min post-stimulation. There appears to be a decrease in phosphorylation by 90 min with a secondary increase apparent at 6 h. Phosphorylated and activated IKKβ can further phosphorylate its down-steam substrate IκBα, which inhibits and sequesters the activity of NF-κB in the steady state. Upon IKK activation, IκBα is rapidly phosphorylated and ubiquitinated, leading to degradation by the 26S proteasome and thus facilitates the translocation of NF-κB to the nucleus (Zandi *et al.,* 1997). Pellino2 does not have a role in the phosphorylation or degradation of IκBα. LPS induced rapid

phosphorylation of IκBα at 5 and 15 min in WT BMDMs with a second peak phosphorylation event also occurring at 6 h (3rd panel Fig. 3.16), which mirrors the kinetics seen with IKKβ. IκBα phosphorylation is followed by decreased total levels of IκBα (4th panel Fig. 3.16). Similar temporal patterns of phosphorylation and degradation of IκBα are apparent in WT and Pellino2-deficient cells. These results show that Pellino2 does not mediate TLR4-induced activation of NF-κB.

3.2.11 Pellino2 does not play a role during TLR4-induced MAPK signalling

Previous work indicated a possible role for Pellino2 in facilitating robust MAPK signalling, specifically via JNK and ERK activation (Kim *et al.,* 2012a). Also, given that recent work has shown that JNK is required for the formation of the NLRP3 inflammasome (Hara *et al.,* 2013), the role of Pellino2 in MAPK signalling was next investigated. BMDMs from WT and *Peli2*$^{-/-}$ bone marrow were stimulated with LPS over the indicated time-points (Fig. 3.17) and protein lysates were generated and probed with the appropriate antibodies. The phosphorylation of JNK, ERK and p38 all showed similar kinetic profiles. Phosphorylation was observed 15 and 30 min after stimulation and was subsequently lost. However, no difference was observed between WT and Pellino2-deficient cells. These results indicate that Pellino2 has no role in regulating the signalling and activation of MAPKs through TLR4.

3.2.12 Pellino2 does not affect IL-1β induced MAPK or NF-κB signalling

The lack of a role for Pellino2 in TLR4-induced activation of NF-kB and MAPK pathways contrasts with previous reports, using overexpression and knockdown

approaches, that proposed a role for Pellino2 in mediating activation of these pathways in response to IL-1β (Kim *et al.*, 2012). Therefore, it was important to characterise IL-1 signalling in Pellino2-deficient cells. BMDMs from WT and *Peli2*$^{-/-}$ bone marrow were stimulated with IL-1β over the indicated time-points (Fig. 3.18) and protein lysates were generated and probed with the appropriate antibodies. IκBα phosphorylation was used to determine NF-κB activity. The phosphorylation signal was highest after 5 minutes and steadily decreased over the time-course. After 90 min, Pellino2-deficient cells showed a modest reduction when compared to WT cells, but the overall level of activation is weak since there is no observable degradation of IκBα. JNK and ERK phosphorylation were used to determine the activity of the MAPK pathways in response to IL-1. IL-1 caused activation of both kinases at early time points but no difference was observed between WT and Pellino2-deficient cells. These data question the role, if any, of Pellino2 in mediating IL-1β-induced activation of NF-κB or MAPKs.

3.2.13 The expression levels of inflammasome components are not regulated by Pellino2

While NF-κB and MAPK signalling pathways were unaffected by Pellino2-deficiency, which suggests a lack of role for Pellino2 in Signal 1 of inflammasome activation, it is important to note that some of the important readouts of Signal 1 are transcriptional up-regulation of the genes encoding NLRP3 and pro-IL-1β. BMDMs from WT and *Peli2*$^{-/-}$ bone marrow were stimulated with LPS over the indicated time-points and mRNA levels for IL-1β (Fig. 3.19a) and NLRP3 (Fig. 3.19b) were assessed by RT-PCR. IL-1β mRNA levels showed a robust induction in response to LPS which peaked at 6 h. NLRP3 mRNA levels also peaked at 6 h. No difference was observed in the upregulation of the inflammasome components between WT and Pellino2-deficient cells, again supporting a lack of role for Pellino2 in mediating Signal 1 in inflammasome activation.

To further corroborate these results, the translation of these components into protein was next assessed. BMDMs from WT and *Peli2*$^{-/-}$ bone marrow were stimulated with LPS over the indicated time-points (Fig. 3.20) and protein lysates were generated and probed with the appropriate antibodies. Pro-IL-1β exists in an inactive form in the cytoplasm prior to activation by the inflammasome. The levels of pro-IL-1β mirrored the mRNA fold data, with a peak observed at 6 h. Increased NLRP3 protein levels was also induced across the time-points. LPS-induced protein levels of pro-IL-1β and NLRP3 were equivalent in WT and Pellino2-deficient cells, which indicated that Pellino2 has no role in either the transcription or translation of inflammasome components.

3.2.15 Pellino2 mediates NLRP3 Inflammasome-induced cleavage of Caspase-1 and pro-IL-1β

Given that Pellino2 is not involved in the initial upregulation of inflammasome components during signal 1, its potential role in signal 2 was next examined by characterising the importance of Pellino2 in processing of pro-caspase 1 and pro-IL-1β. BMDMs from WT and *Peli2*$^{-/-}$ bone marrow were stimulated with LPS for 3 hours. Cells were then left untreated or subjected to co-stimulation with either ATP (Fig. 3.21a) or Nigericin (Fig. 3.21b) for 40 min. Conditioned media (supernatant) and cell samples were generated and probed with the appropriate antibodies. Supernatant samples were probed for the processed (activated) forms of IL-1β and caspase-1 which are cleaved and subsequently released from the cell upon co-stimulation with LPS and ATP. Co-stimulation of WT cells with LPS and either ATP or nigericin as Signal 2 resulted in high levels of processed caspase 1 and IL-1β, but processed levels of both molecules were greatly reduced in Pellino2-deficient cells. This is consistent with earlier ELISA analysis above that demonstrated decreased IL-1β in supernatants from *Peli2*$^{-/-}$ cells (Fig. 3.8). Pro-IL-1β levels in the lysate were also probed to assess if the decreased processed levels of IL-1β were due to lack of up-regulation of pro-IL-1β protein by Signal 1. As before, the levels of

pro-IL-1β are similar in WT and *Peli2*$^{-/-}$ cells suggesting that Pellino2 targets the processing step. It should be noted that co-stimulation of cells with LPS and ATP or nigericin results in decreased levels of pro-IL-1β in the cell lysates, but this is coincident with increased secretion of processed IL-1β into the cell supernatants.

Later time-points were also used to determine if the role of Pellino2 during IL-1β processing could be influenced by a longer LPS priming step. BMDMs from WT and *Peli2*$^{-/-}$ bone marrow were stimulated with LPS for either 6 or 24 hours. Cells were then left untreated or subjected to co-stimulation with ATP for 40 min. Supernatant and lysate samples were generated and probed with the appropriate antibodies. Reduced levels of cleaved IL-1β and caspase-1 were observed in conditioned media from Pellino2-deficient cells at all time-points (Fig. 3.22). Interestingly, the difference was most apparent after 24 hours pre-treatment prior to ATP. Reduced β-Actin levels were seen at the 6 h co-stimulation time-point, indicating the possibility of cell death, presumably by pyroptosis. These results indicate that Pellino2 has a function in regulating the activity of the NLRP3 inflammasome upstream of caspase-1 and that Pellino2 can function to regulate IL-1β processing independent of varying LPS incubation times.

3.2.14 The role of Pellino2 in NLRP3 inflammasome activation is independent of priming agent

All of the previous findings have focused on the use of LPS as a primary signal and it was important to confirm that the role of Pellino2 during inflammasome activation was independent of the priming signal. In order to examine this, zymosan was used as a trigger of TLR2/6 and Dectin-1 pathways that lead to robust NF-κB activation, a pre-requisite to upregulation of pro-IL-1β and NLRP3 (Bauernfeind *et al.*, 2009).

WT and *Peli2*$^{-/-}$ bone marrow were stimulated with zymosan for 3 hours. Cells were then left untreated or subjected to 40 min co-stimulation with ATP. Supernatant and lysate samples were generated and probed with the appropriate antibodies.

Supernatant samples were probed for IL-1β while lysates were probed for IL-1β and β-Actin. Similarly to LPS pre-treatment, Pellino2-deficiency led to abrogated IL-1β secretion (Fig. 3.23). Conditioned media was also analysed by IL-1β ELISA, demonstrating reduced IL-1β secretion in Pellino2-deficient cells (Fig. 3.24), which verified the observations of the western blot. This suggests that the effects of Pellino2 on inflammasome activation are independent of the nature of Signal 1. This is further confirmed by Zymosan alone inducing the same levels of expression of pro-IL-1β and NLRP3 in WT and *Peli2*$^{-/-}$ BMDMs at both mRNA (Fig. 3.26a; 3.26b) and protein (Fig. 3.25) levels.

3.2.16 Pellino2 is required for optimal inflammasome assembly

The data presented above suggests that Pellino2 is contributes to inflammasome-mediated activation of caspase-1. It was next investigated whether the inflammasome assembly itself was affected by Pellino2 deficiency. Upon inflammasome assembly, ASC aggregates with NLRP3 and forms protein scaffolds which are insoluble in NP-40 lysis buffer (Kang *et al.*, 2015). BMDMs from WT and *Peli2*$^{-/-}$ bone marrow were stimulated with LPS for 3 hours. Cells were then left untreated or subjected to co-stimulation with ATP for 40 min. NP-40 soluble and insoluble fractions were generated and probed with the appropriate antibodies. Co-stimulation of WT cells with LPS and ATP resulted in accumulation of NLRP3 and ASC in the insoluble fraction consistent with assembly of the inflammasome complex (Fig. 3.27). Notably the levels of insoluble NLRP3 and ASC are reduced in Pellino2-deficient cells suggesting that assembly of the inflammasome is at least partially compromised in the absence of Pellino2. Interestingly, NLRP3 that is recruited to the insoluble fraction in Pellino2-deficient cells migrates as an apparent double-band which can be observed also. This may possibly indicate the presence of an additional post-translational modified form of NLRP3 when Pellino2 is absent.

To further assess the assembly of the inflammasome, the oligomerization status of ASC was compared in WT and Pellino2-deficient cells. BMDMs from WT and *Peli2*$^{-/-}$ bone marrow were stimulated with LPS for 3 hours. Cells were then left untreated or subjected to co-stimulation with ATP for 40 min. NP40 soluble and insoluble fractions were generated as above with the latter being also subjected to disuccinimidyl suberate (DSS) crosslinking. Samples were then subjected to immunoblotting with the appropriate antibodies. Costimulation of WT cells with LPS and ATP resulted in the increased oligomerization of ASC in the insoluble fraction as manifested by the appearance of dimeric, trimeric and tetrameric forms of ASC (Fig. 3.28). There were reduced ASC polymers present in the insoluble fraction of Pellino2-deficient cells, again indicating reduced inflammasome assembly. These results further support a role for Pellino2 in the optimal assembly of the NLRP3 inflammasome.

3.2.17 Pellino2 positively contributes to NLRP3 ubiquitination

Deubiquitination events have been shown to play an important role in inflammasome formation. As NLRP3 deubiquitination is required for its recruitment to the inflammasome (Py *et al.,* 2013; Rodgers *et al.,* 2014), it was important to investigate the deubiquitination event in WT and *Peli2*$^{-/-}$ cells. BMDMs from WT and *Peli2*$^{-/-}$ bone marrow were stimulated with LPS for 3 hours. Cells were then left untreated or subjected to co-stimulation with ATP for 40 min. Protein lysates were subjected to treatment with 10% SDS and boiling in order to disassociate protein-protein interactions. The samples were then immunoprecipitated using anti-NLRP3 antibody. After western blot analysis, samples could be probed for covalently bound ubiquitin modifications. LPS treatment alone induced polyubiquitination of NLRP3 in the WT cells but not in Pellino2-deficient cells (Fig. 3.29). Upon ATP stimulation, this ubiquitination in the WT cells was lost, as NLRP3 is deubiquitated and recruited to the inflammasome pellet. Pellino2-deficient cells exhibited no change in the status

of polyubiquitination upon co-stimulation. K63 ubiquitination of NLRP3 followed the same trend as pan-ubiquitin showed, as LPS treatment alone induced ubiquitination, while ATP co-stimulation induced a loss of ubiquitination. K48-linked polyubiquitantion was also examined as it has been shown to be responsible for targeting proteins for proteasomal degradation (Chau *et al.,* 1989). No K48 ubiquitination was seen at any time-point, suggesting that protein degradation of NLRP3 is not a key factor in the reduced inflammasome formation apparent in Pellino2-deficient cells. Increased polyubiquitination was apparent with ATP alone, but this does not translate to inflammasome assembly, demonstrating the importance of the LPS signal to induce ubiquitination and subsequent deubiquitination. These results suggest that Pellino2 has a role in modulating the ubiquitination of NLRP3 prior to inflammasome assembly in an LPS dependent manner.

Ubiquitination during Signal 1 plays a key role in the formation of the inflammasome, as demonstrated by new research showing that ASC speck formation requires prior ubiquitination of ASC before assembly (Guan *et al.,* 2015; Rodgers *et al.,* 2014). Ubiquitination of pro-IL-1β (Duong *et al.,* 2015) and caspase-1 (Rodgers *et al.,* 2014) are also required for NLRP3 inflammasome activity. While the deubiquitination event regulating NLRP3 activation has been well characterised, the specific E3 ligase which controls the initial ubiquitination of NLRP3 remains to be elucidated. To further investigate the ubiquitination status of NLRP3 during signal 1, an LPS time-course was used to examine the temporal ubiquitination status of NLRP3. BMDMs from WT and *Peli2*$^{-/-}$ bone marrow were stimulated with LPS for the indicated times (Fig. 3.30). Samples were then immunoprecipitated using anti-NLRP3 antibody as before and probed for covalently bound ubiquitin modifications. In WT cells, LPS induced a robust polyubiquitination of NLRP3 after 3 h which was sustained after 6 h. Pellino2-deficient cells showed no observable LPS induced NLRP3 polyubiquitination. Using an anti-K63 antibody, it was determined that LPS-induced K63-linked ubiquitination of NLRP3 in WT cells and this was absent in Pellino2 deficient cells (2nd panel Fig. 3.30).

The above work demonstrates that LPS initially induces ubiquitination of NLRP3 with a second signal like ATP subsequently promoting its deubiquitination, resulting

in inflammasome activation. We hypothesised that the LPS-induced ubiquitination of NLRP3 may be a priming event, possibly for inflammasome assembly, but that deubiquitination subsequently needs to take place to trigger downstream effects of inflammasome activation.

3.2.18 Pellino2 does not directly ubiquitinate or interact with NLRP3

The above studies indicate that LPS-induced ubiquitination of NLRP3 is absent in Pellino2-deficient cells and this is associated with reduced inflammasome activation. It was next investigated whether Pellino2 could directly mediate this ubiquitination of NLRP3 and thus necessitated a prior assessment of the potential of Pellino2 to interact with NLRP3. The capacity for Pellino2 to directly ubiquitinate NLRP3 was tested using an *in vitro* ubiquitination assay. Recombinant ubiquitin, E1, E2, Pellino2 and NLRP3 were incubated with ATP and a Tris buffer to allow for the ubiquitination event to progress. Immunoprecipitation was carried out using an anti-NLRP3 antibody in order to assess the specific ubiquitination of NLRP3. IP samples were blotted for ubiquitin and WCL samples were blotted for ubiquitin. It was observed that while Pellino2 was able to induce the formation of ubiquitin free-chains, it was unable to directly ubiquitinate NLRP3 (Fig 3.31).

Interaction studies were carried out to assess whether Pellino2 could directly bind to NLRP3. To do this, an *in vitro* binding assay testing NLRP3-Pellino2 interaction was carried out. Recombinant Pellino2 and NLRP3 were incubated with an ATP containing buffer. Co-Immunoprecipitation was carried out using an anti-NLRP3 antibody while the wash steps were retained. It was shown that recombinant Pellino2 was lost during the first wash stage and was not immunoprecipitated with NLRP3 (Fig 3.32a). The potential for NLRP3 and Pellino2 to interact in cells was next assessed by overexpression of NLRP3 and Pellino2. HEK293 cells were transfected with plasmids encoding Myc-tagged Pellino2 and NLRP3-V5. Pellino2 was

immunoprecipitated with an anti-Myc antibody and analysed for co-precipitated NLRP3 by Western blotting. NLRP3 could not be detected in these immunoprecipitates, suggesting that Pellino2 and NLRP3 do not interact with each other (Fig. 3.32b). As a positive control, Pellino2-IRAK1 interaction was investigated by similar co-immunoprecipitation analysis, since IRAK1 is a known protein interaction partner for Pellino2 (Lin *et al.,* 2008). In keeping with previous reports, Pellino2 was shown to interact with IRAK1 (Fig. 3.32c). These results indicate no interaction between NLRP3 and Pellino2.

While Pellino2 may not directly ubiquitinate NLRP3, the data presented has shown it to be involved in mediating this ubiquitination. Pellino2 may exert its function indirectly, mediated by other protein interactions with NLRP3. The inflammasome assembly is complex and may require numerous adapter molecules to facilitate its ubiquitination *in vivo*.

3.2.19 IRAK1 stabilisation is unaffected by Pellino2 deficiency

Because it has been shown both here and previously (Yu *et al.,* 2002) that Pellino2 and IRAK1 can interact, the role of IRAK1 in the NLRP3 inflammasome was next assessed. Recent work has highlighted a possible role for IRAK1 in the early activation of the inflammasome (Lin *et al.,* 2014). The authors showed that co-stimulation with LPS and ATP resulted in reduced degradation of IRAK1 when compared to LPS alone, suggesting a possible role for IRAK stabilisation in inflammasome activation. To investigate the stabilisation of IRAK1, BMDMs from WT and *Peli2*$^{-/-}$ bone marrow were stimulated with LPS alone or in combination with ATP over an indicated time-course (Fig. 3.33). Protein lysates were harvested and subjected to analysis by western blotting. Rapid IRAK1 degradation was observed after 15 min when treated with LPS alone. However, co-stimulation with both LPS and ATP resulted in modest stabilisation at 15 min. No difference was

observed in the levels of IRAK1 degradation between WT and Pellino2-deficient cells suggesting that any effects of Pellino2 on inflammasome activation are independent of stabilisation of IRAK1. Interestingly, basal levels of IRAK1 in Pellino2-deficient cells appear to be increased when compared with WT cells.

3.2.20 IRAK1 is differentially ubiquitinated in Pellino2-deficient cells

Since their discovery, Pellino proteins have been thought to play a role in IRAK1 activation (Jiang *et al.*, 2003; Lin *et al.*, 2008; Tzieply *et al.*, 2012). The role of Pellino2 in the ubiquitination of IRAK1 during priming was next assessed. BMDMs from WT and *Peli2*$^{-/-}$ bone marrow were stimulated with LPS for the indicated times (Fig. 3.34). Protein lysates were subjected to treatment with 10% SDS and boiling in order to disassociate protein-protein interactions. The samples were then immunoprecipitated using anti-IRAK1 antibody. After western blot analysis, samples were probed for covalently bound ubiquitin modifications. In both WT and Pellino2-deficient cells, LPS induced a robust polyubiquitination of IRAK1 after 15 min which was lost after 30 min. A second phase of IRAK1 ubiquitination was observed in WT cells after 1 h, but this was not apparent in Pellino2-defficient cells. The type of linkages in the polyubiquitination chains was also probed using K63 and K48-ubiquitin-specifc antibodies. LPS primarily induces strong K48 ubiquitination in WT and Pellino2-deficient cells, and this is consistent with IRAK1 degradation in these cells (Ramadan and Meerang, 2011). These data indicate that early IRAK1 ubiquitination that leads to degradation is unaffected in Pellino2-deficient cells and this is consistent with the lack of a role of Pellino on early NF-κB signalling (Section 3.2.10). However the late phase ubiquitination of IRAK1 seems to be absent in Pellino2-deficient cells and it is interesting to speculate that this may lead to reduced inflammasome activation in these cells.

3.2.21 Loss of Pellino2 leads to increased NLRP3 interaction with IRAK1

It has been shown recently that IRAK1 and NLRP3 can interact with each other, at least when both proteins are over-expressed in cell lines (Fernandes-Alnemri *et al.,* 2013) and both proteins can co-localise in BMDMs (Lin *et al.,* 2014). Because of this work, the importance of Pellino2 for the interaction of NLRP3 and IRAK1 was next assessed. BMDMs from WT and *Peli2*$^{-/-}$ bone marrow were stimulated with LPS for the indicated times (Fig 3.35). Protein lysates were then immunoprecipitated using anti-NLRP3 antibody. After western blot analysis, samples could be probed for associated proteins. In WT cells, IRAK1 was observed to interact with NLRP3 only after 6 h stimulation. This manifested as bands of lower electrophoretic mobility that are usually associated with hyperphosphorylated forms of IRAK1. Interestingly, NLRP3 in Pellino2-deficient cells showed basal IRAK1 interaction, which was lost after initial LPS treatment. This interaction was re-established after 3 h and maintained. Analysis of the whole cell lysates demonstrated once again that basal levels of IRAK1 are increased in Pellino2-deficient cells. From these data, it is interesting to speculate that LPS induces interaction of hyperphosphorylated forms of IRAK with NLRP3 at later time points to terminate inflammasome activation. In the absence of Pellino2 this interaction is already apparent and this may contribute to reduced inflammasome activation in Pellino2-deficient cells. In such a model Pellino2 may serve to suppress basal IRAK1 phosphorylation and activation and so impair this negative regulatory pathway and allow for activation of the inflammasome. The LPS-induced interaction of hyperphosphorylated forms of IRAK with NLRP3 at later time points suggests that the regulatory effect of Pellino2 is lost at later times post LPS stimulation.

3.2.22 Pellino2 levels are affected by TLR activation

The data presented above highlights a role for Pellino2 in the interaction of IRAK1 and NLRP3 during later LPS time-points. In order to investigate the effect of LPS on Pellino2 expression, mRNA induction of the Pellino family were explored over an LPS time-course. These experiments revealed that LPS strongly suppresses the expression of Pellino2 and that this effect is selective for Pellino2 since other family members are induced in response to LPS (Fig. 3.36). BMDMs cultured from WT and *Peli2*$^{-/-}$ bone marrow were stimulated for over the indicated time-course with LPS and mRNA was extracted. mRNA levels for Pellino1 (Fig. 3.36a), Pellino2 (Fig. 3.36b) and Pellino3 (Fig. 3.36c) were assessed by RT-PCR. In WT cells Pellino2 levels showed a marked decrease over the time-course, while Pellino1 and Pellino3 levels increased with stimulation. This suggests that Pellino2 has a unique role during TLR activation, independent of the other members of the family. This effect is selective for Pellino2 since other family members are induced in response to LPS.

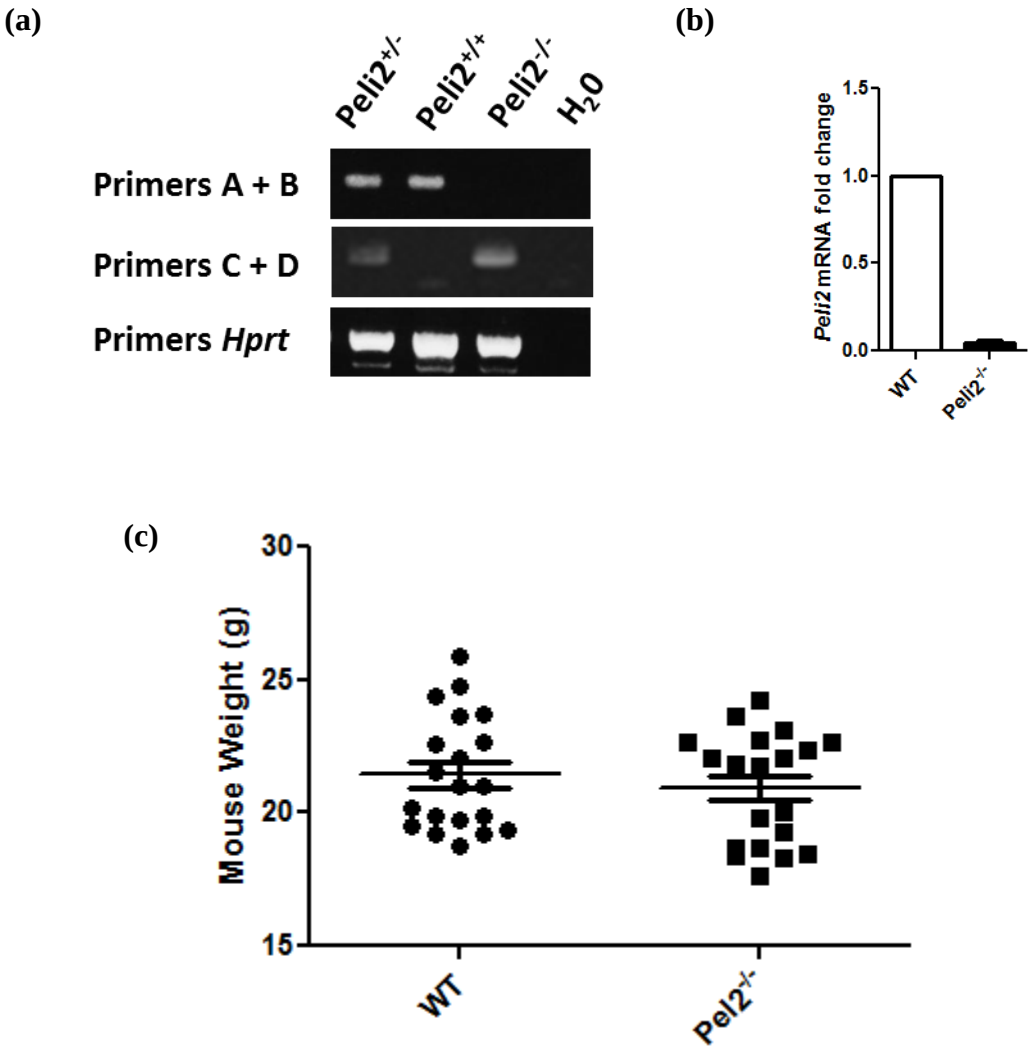

Figure 3.1 Characterisation of *Peli2*-deficient mice

(a) Genotyping by PCR analysis of genomic DNA from ear punches. Primers a and b amplify the WT *Peli2* in heterozygous mice and homozygous WT mice while primers c and d detect only the *Peli2* knockout allele. Primers for HPRT were used as a genomic DNA control. Water was used as a negative control for the PCR reaction. **(b)** Quantitative real-time PCR of Pellino2 expression in cells from BMDMs isolated from WT and *Peli2*$^{-/-}$. Analysis was carried out and mRNA levels are presented as a fold change relative to WT and normalised to HPRT expression **(c)** Sex and age matched mice were monitored for variations in weight (n=20) at 10 weeks of age.

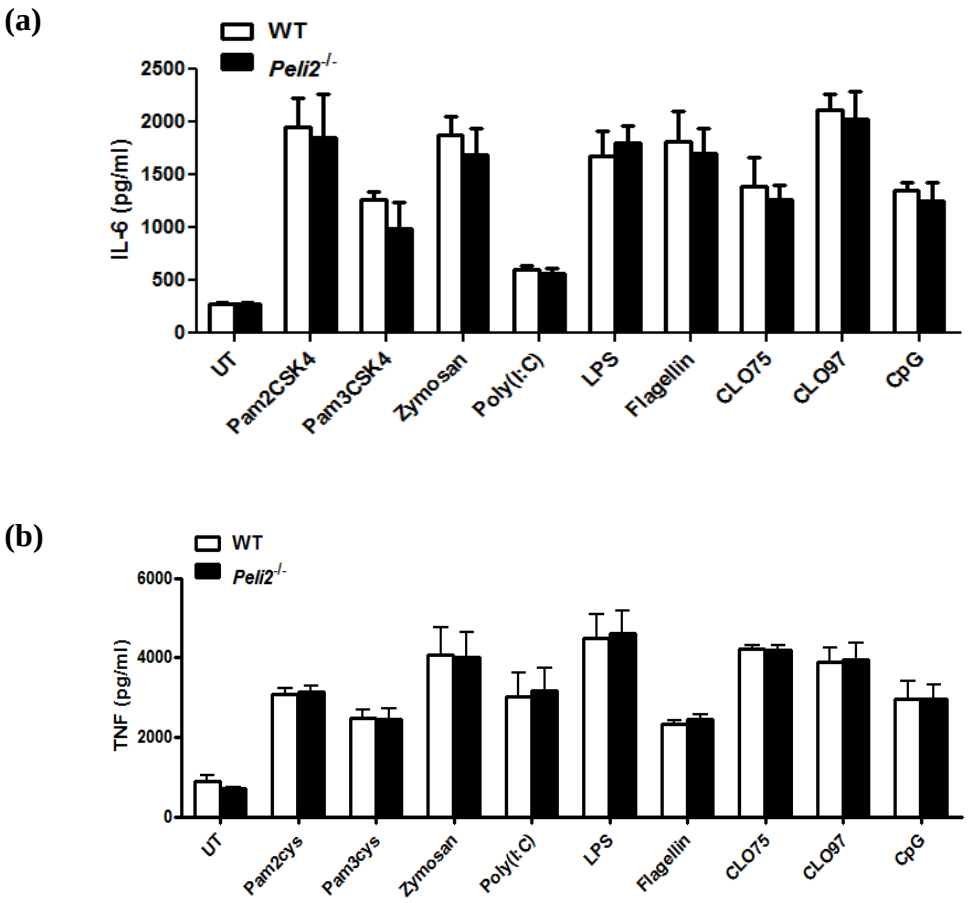

Figure 3.2 Effect of Pellino2-deficiency on TLR-induced expression of pro-inflammatory cytokines

BMDMs from WT and *Peli2*$^{-/-}$ bone marrow were left untreated (UT) or stimulated for 24 h with Pam2CSK4 (10 ng/ml), Pam3CSK4 (10 ng/ml), Zymosan (5 µg/ml), Poly(I:C) (25 µg/ml), LPS (10 ng/ml), Flagellin (5 µg/ml), CLO75 (5 µg/ml), CLO97 (5 µg/ml), CpG (5 µM). Conditioned media was assayed by ELISA for levels of **(a**) IL-6 and **(b)** TNF. Data are presented as the mean of three independent experiments +/- SEM. Statistical significance was determined using two-tailed Student's t-test.

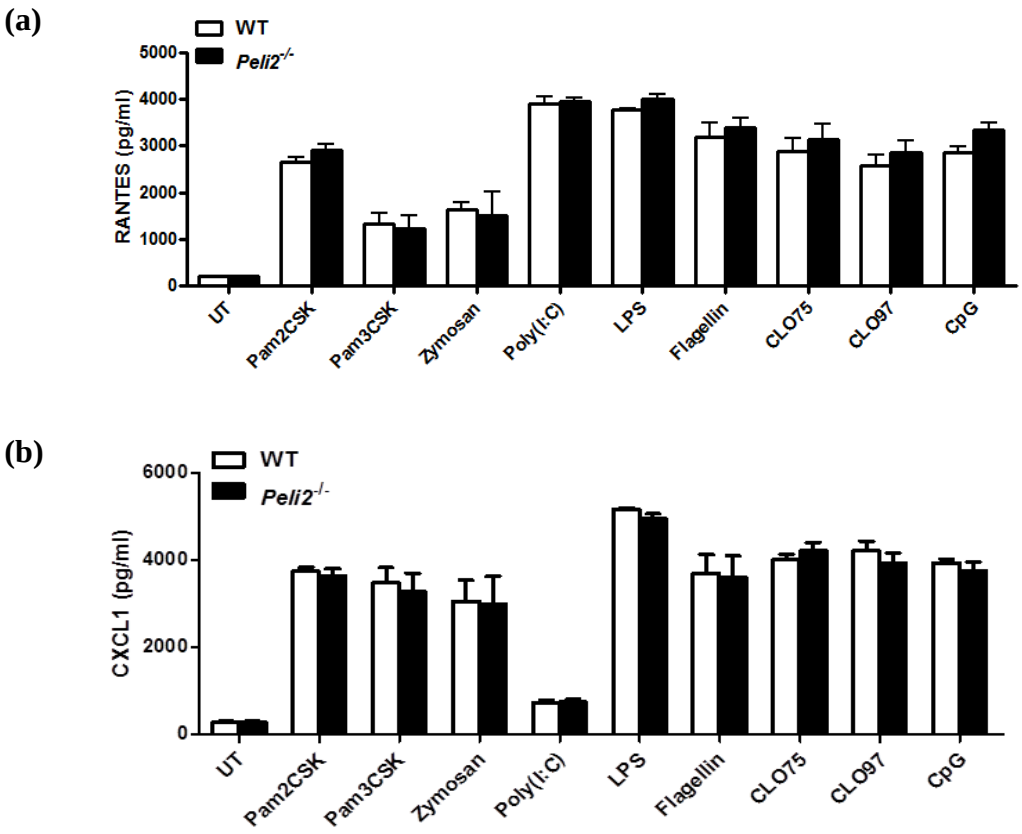

Figure 3.3 Effect of Pellino2-deficiency on TLR-induced expression of pro-inflammatory chemokines

BMDMs from WT and *Peli2*$^{-/-}$ bone marrow were left untreated (UT) or stimulated for 24 h with Pam2CSK4 (10 ng/ml), Pam3CSK4 (10 ng/ml), Zymosan (5 µg/ml), Poly(I:C) (25 µg/ml), LPS (10 ng/ml), Flagellin (5 µg/ml), CLO75 (5 µg/ml), CLO97 (5 µg/ml), CpG (5 µM). Conditioned media was assayed by ELISA for levels of **(a**) RANTES and **(b)** CXCL1. Data are presented as the mean of three independent experiments +/- SEM. Statistical significance was determined using two-tailed Student's t-test.

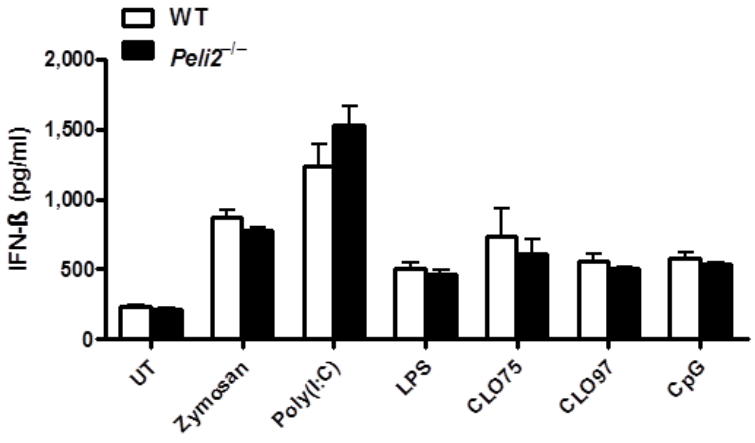

Figure 3.4 Effect of Pellino2-deficiency on TLR-induced expression of IFN-β

BMDMs from WT and *Peli2*$^{-/-}$ bone marrow were left untreated (UT) or stimulated for 24 h with Zymosan (5 µg/ml), Poly(I:C) (25 µg/ml), LPS (10 ng/ml), CLO75 (5 µg/ml), CLO97 (5 µg/ml), CpG (5 µM). Conditioned media was assayed by ELISA for levels of IFN-β. Data are presented as the mean of three independent experiments +/- SEM. Statistical significance was determined using two-tailed Student's t-test.

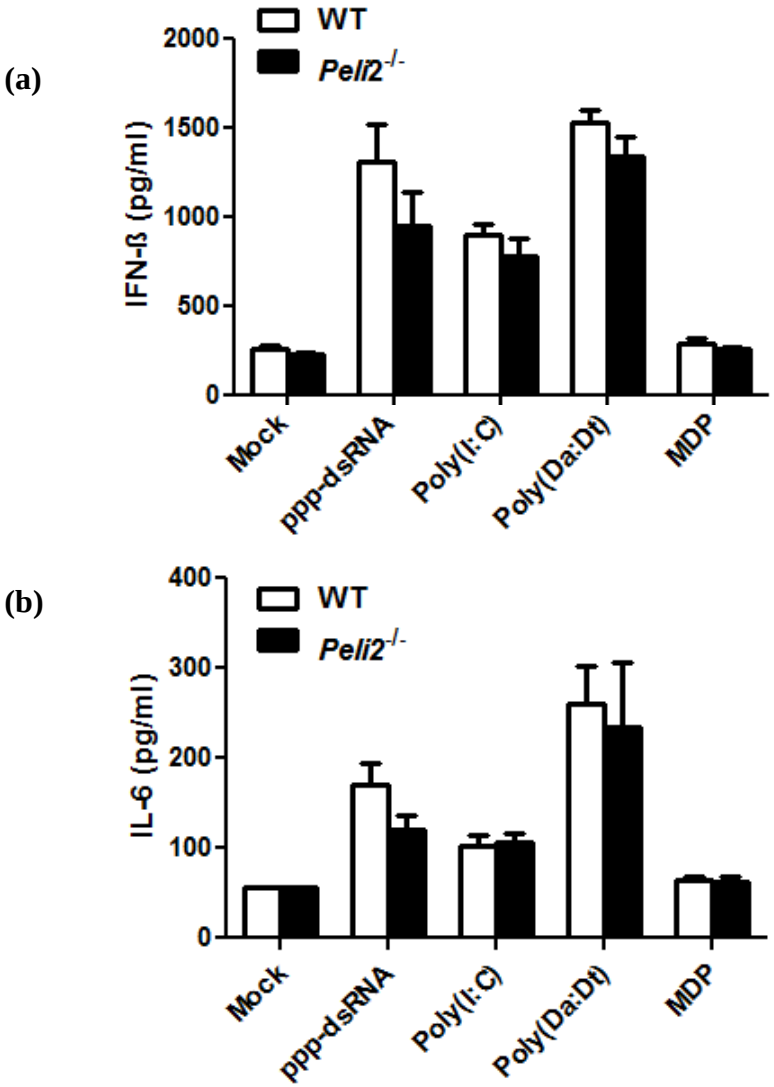

Figure 3.5 Effect of Pellino2-deficiency on cytosolic pattern recognition receptors

BMDMs from WT and *Peli2*$^{-/-}$ bone marrow were treated with transfection reagent alone (Mock) or transfected for 24 h with Poly(I:C) (25 µg/ml), Poly(Da:Dt) (4 µg/ml), MDP (50ng/ml), ppp-dsRNA (500 ng/ml). Conditioned media was assayed by ELISA for levels of **(a**) IFN-β and **(b)** IL-6. Data are presented as the mean of three independent experiments +/- SEM. Statistical significance was determined using two-tailed Student's t-test.

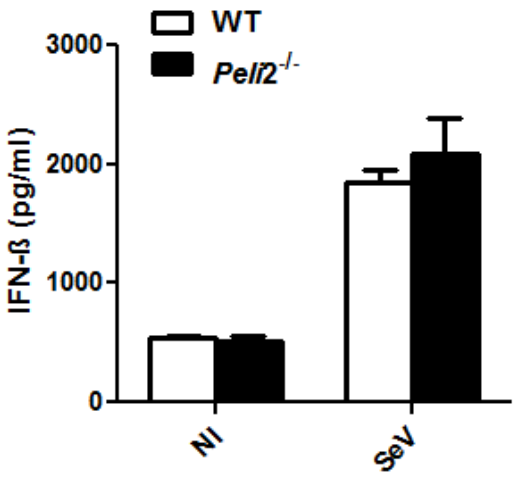

Figure 3.6 Effect of Pellino2-deficiency on SeV infection-induced expression of IFN-β

BMDMs from WT and *Peli2*$^{-/-}$ bone marrow were not infected (NI) or infected for 24 h with 1:1000 dilution SeV. Conditioned media was assayed by ELISA for levels of IFN-β. Data are presented as the mean of three independent experiments +/- SEM. Statistical significance was determined using two-tailed Student's t-test.

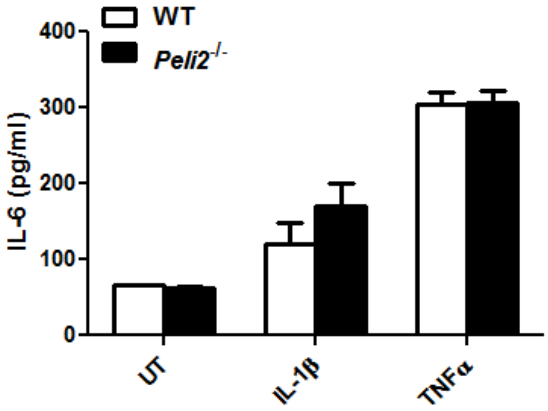

Figure 3.7 Effect of Pellino2-deficiency on cytokine-induced expression of IL-6

BMDMs from WT and *Peli2*$^{-/-}$ bone marrow were either untreated (UT) or stimulated for 24 h with IL-1β (10 ng/ml) and TNF-α (10 ng/ml). Conditioned media was assayed by ELISA for levels of IL-6. Data are presented as the mean of three independent experiments +/- SEM. Statistical significance was determined using two-tailed Student's t-test.

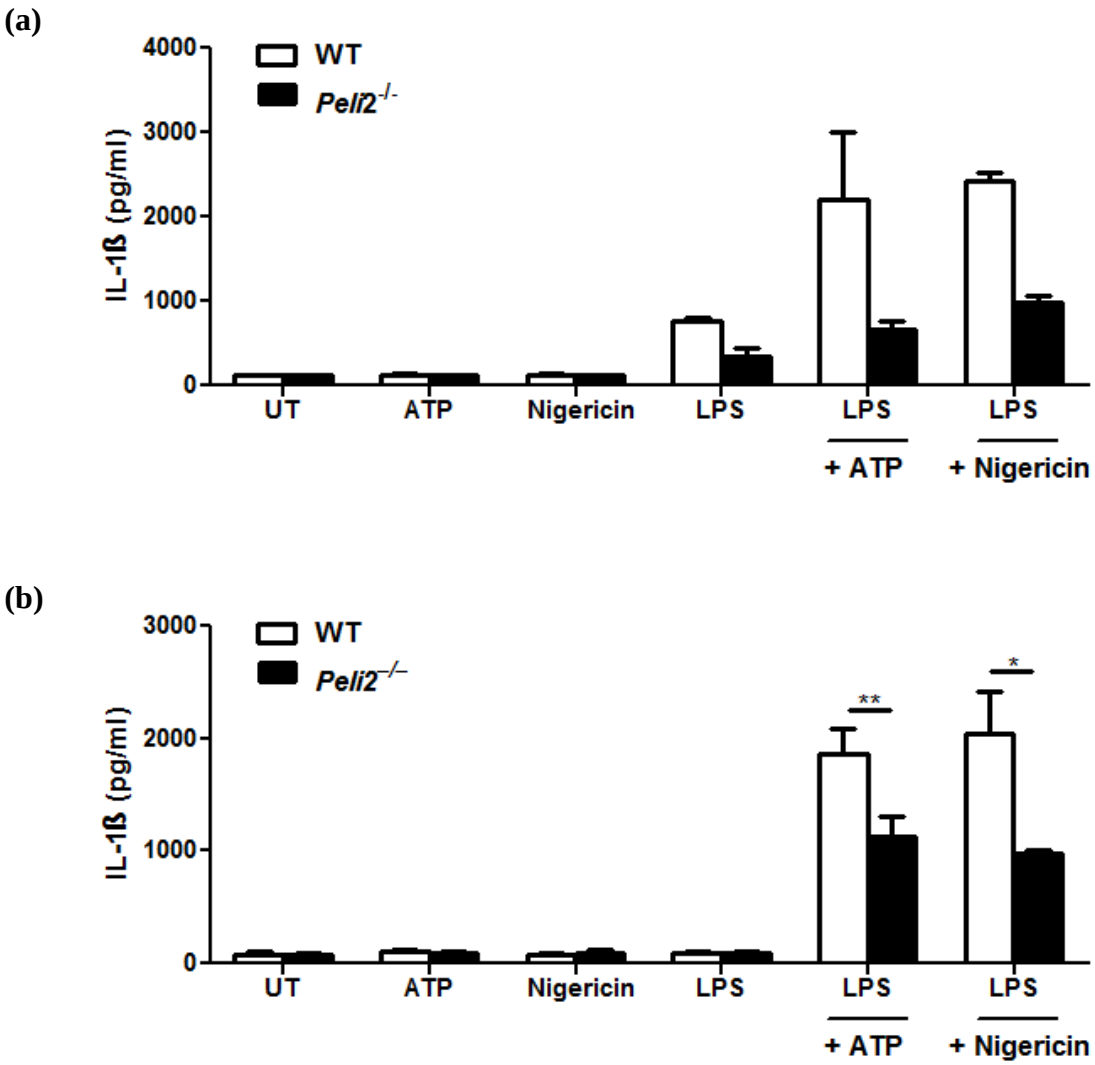

Figure 3.8 Effect of Pellino2-deficiency on IL-1β secretion during NLRP3 inflammasome activation in BMDMs and BMDCs.

(a) BMDCs or **(b)** BMDMs from WT and *Peli2*$^{-/-}$ bone marrow were either untreated (UT) or stimulated for 3 h with LPS (10 ng/ml). Cells were then left untreated or subjected to co-stimulation with either ATP (2.5 µM) or Nigericin (1 µM). Conditioned media was assayed by ELISA for levels of IL-1β. Data are presented as the mean of three independent experiments +/- SEM. Statistical significance was determined using two-tailed Student's t-test (*, $p < 0.05$; **, $p < 0.01$).

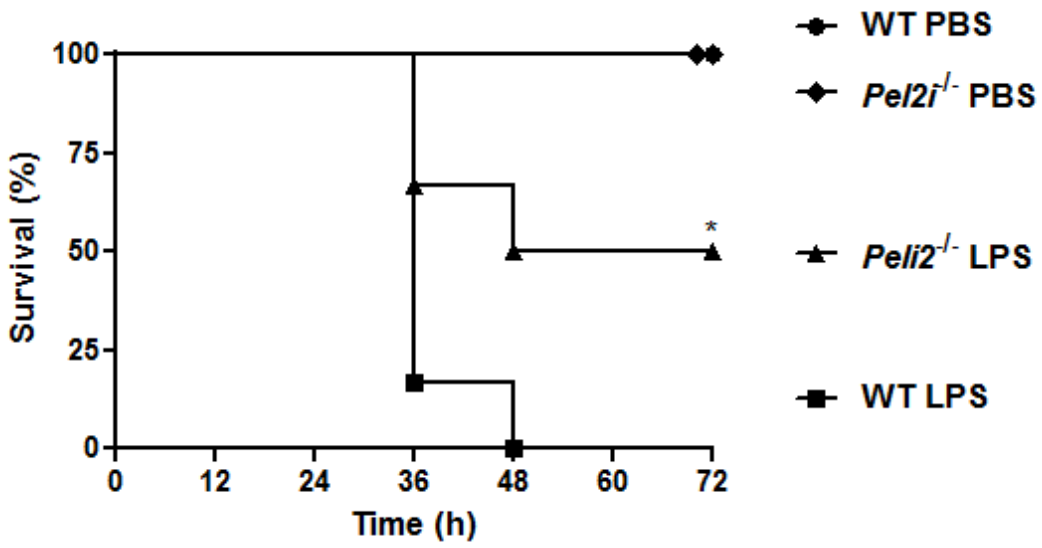

Figure 3.9 Effect of Pellino2-deficiency on survival rates of mice during LPS induced septic shock.

Survival rates of age, sex and weight matched WT and *Peli2*$^{-/-}$ mice after intraperitoneal injection with either 20mg/kg LPS (n= 8) or PBS as a control (n= 3). Mouse health was monitored and moribund mice were euthanised (*, $p < 0.05$ (Mantel-Cox test)).

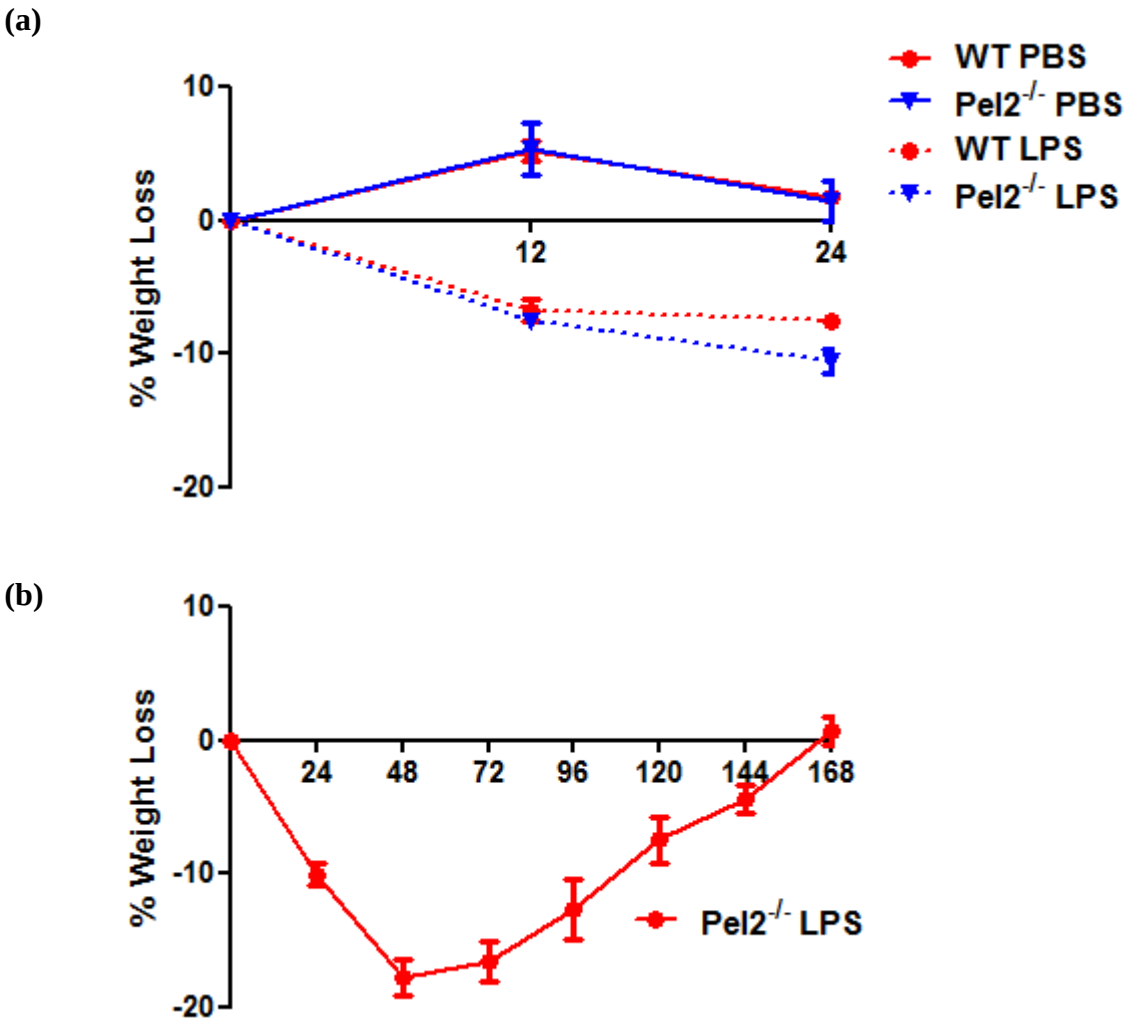

Figure 3.10 Weight loss and recovery of Pellino2-deficient mice during LPS induced septic shock.

(a) Weight loss rates of age, sex and weight matched WT and *Peli2*$^{-/-}$ mice after intraperitoneal injection with either 20mg/kg LPS (n= 8) or PBS as a control (n= 3). **(b)** *Peli2*$^{-/-}$ mice weight recovery after 20mg/kg LPS (n= 4).

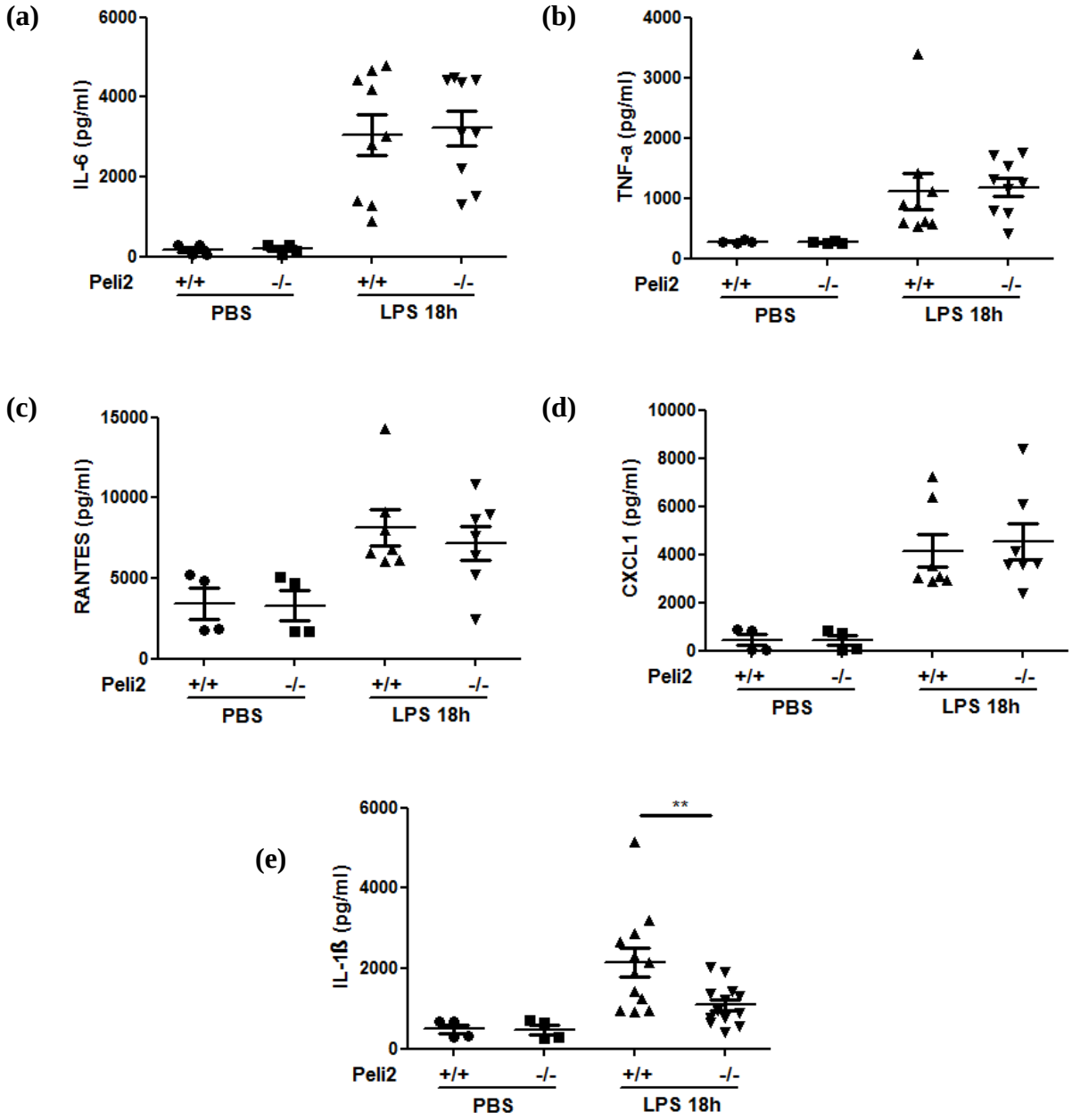

Figure 3.11 Effect of Pellino2-deficiency on serum levels of pro-inflammatory cytokines in response to administration of LPS

Serum cytokine analysis of WT and *Peli2*$^{-/-}$ mice 18 h after intraperitoneal injection with either 20mg/kg LPS (n= 11) or PBS as a control (n= 4). Mice were sacrificed and serum analysed by ELISA for **(a)** IL-6 **(b)** TNF **(c)** RANTES **(d)** CXCL1 and **(e)** IL-1β. Statistical significance was determined using two-tailed Student's t-test (**, $p < 0.01$).

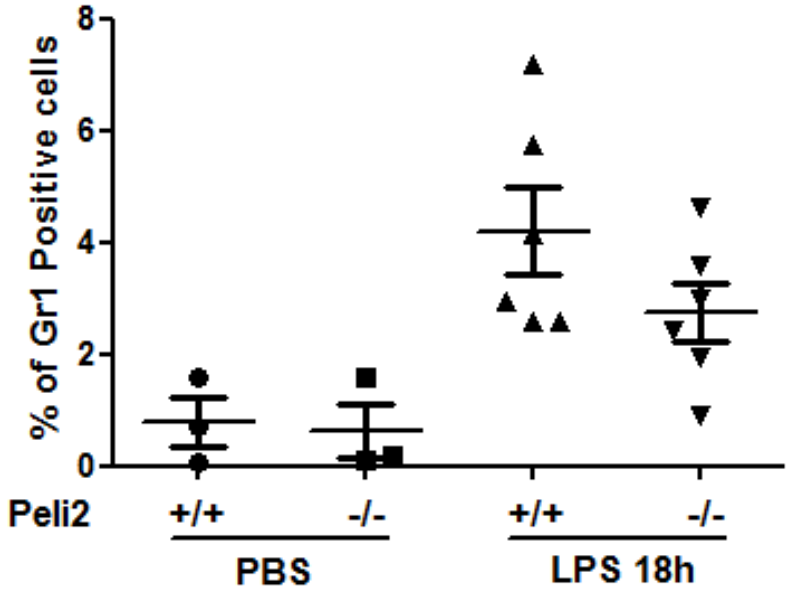

Figure 3.12 Effect of Pellino2-deficiency on peritoneal neutrophil infiltration in response to administration of LPS

Influx of $GR1^{+}$ cells into the peritoneum of of WT and *Peli2*$^{-/-}$ mice 18 h after intraperitoneal injection with either 20mg/kg LPS (n= 6) or PBS as a control (n= 3). Cells were stained with isotype controls and anti-GR1. After staining the cells were examined through flow cytometry. Data represented as a percentage of total cells. Statistical significance was determined using two-tailed Student's t-test.

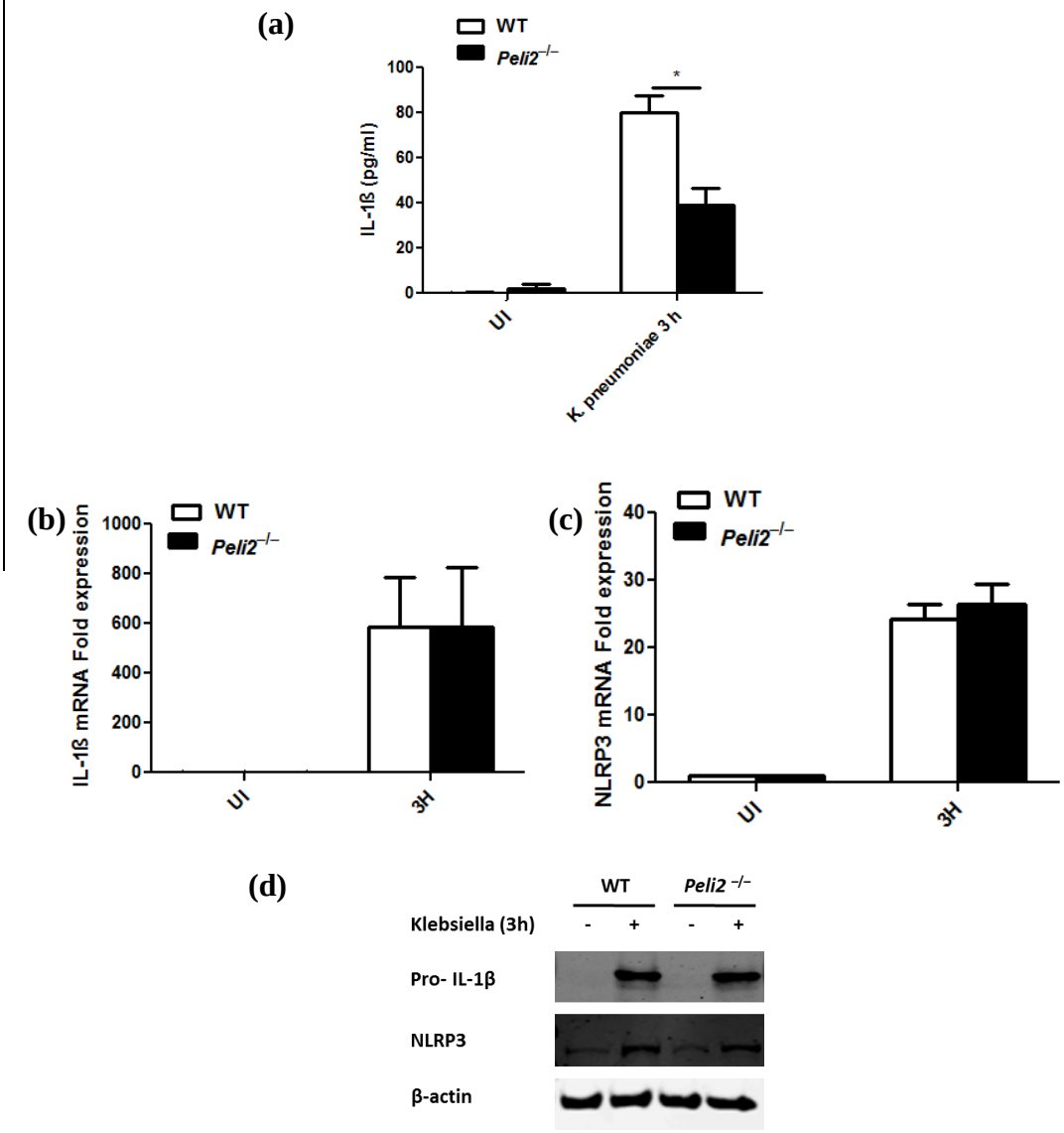

Figure 3.13 Effect of Pellino2-deficiency during *K. pneumoniae* infection.

BMDMs from WT and *Peli2*$^{-/-}$ bone marrow were either left uninfected (UI) or stimulated for 3 h with *K. pneumoniae* and TNF-α (10 ng/ml). **(a)** Conditioned media was assayed by ELISA for levels of IL-1β. Quantitative real-time PCR of **(b)** IL-1β and **(c)** NLRP3 was carried out and mRNA levels are presented as a fold change relative to WT UT and normalised to HPRT expression. **(d)** Lysates were generated and immunoblotted. Lysate samples were probed for NLRP3, IL-1β and β-actin as a loading control. Data are representative of 3 independent experiments. Data are presented as the mean of three independent experiments +/- SEM. Statistical significance was determined using two-tailed Student's t-test.

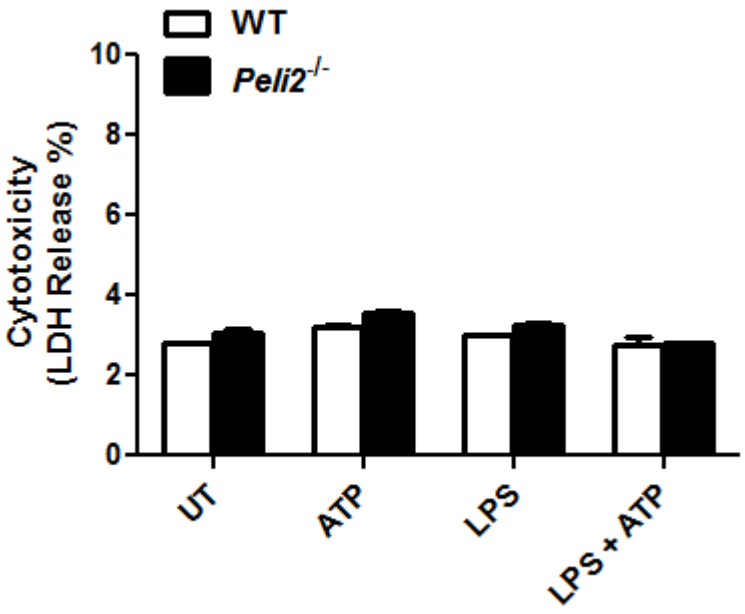

Figure 3.14 Effect of Pellino2-deficiency on inflammasome induced cell death in BMDMs.

BMDMs cultured from WT and *Peli2*$^{-/-}$ bone marrow were either untreated (UT) or stimulated for 3 h with LPS (10 ng/ml). Cells were then left untreated or subjected to co-stimulation with either ATP (2.5 µM) for 40 min. Conditioned media was assayed for LDH release from cells and presented as a percentage of maximum LDH release from lysis treated cells. Data are presented as the mean of two independent experiments +/- SEM. Statistical significance was determined using two-tailed Student's t-test.

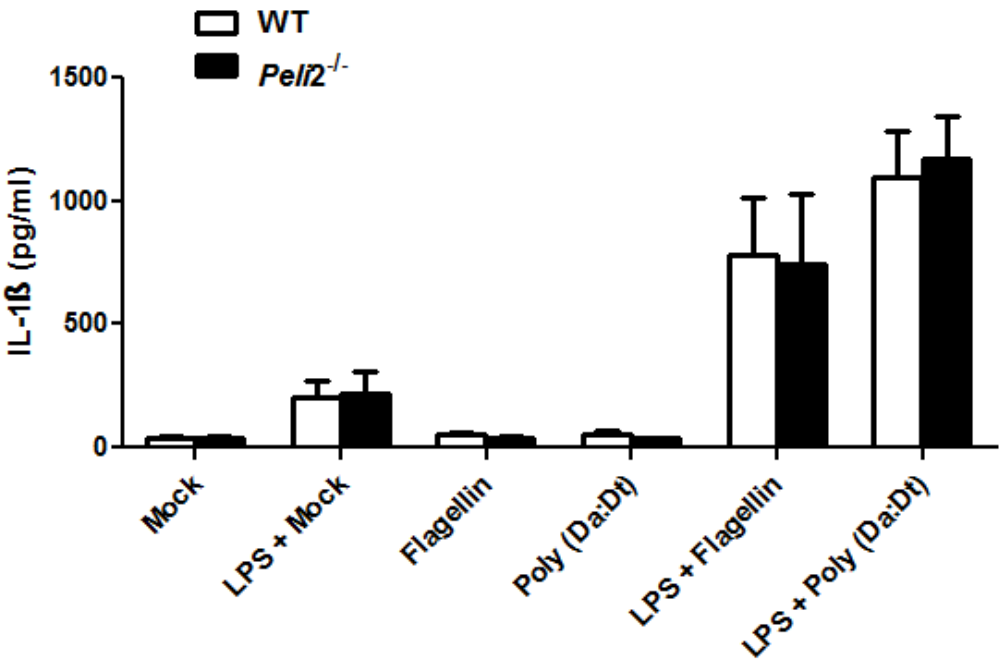

Figure 3.15 Effect of Pellino2-deficiency on the activation of AIM2 and NLRC4 inflammasomes.

BMDMs from WT and *Peli2*$^{-/-}$ bone marrow were left untreated or stimulated for 3 h with LPS (10 ng/ml). Cells were either treated with transfection reagent alone (Mock) or subjected to co-stimulation via transfection with flagellin (5 µg/ml) or poly(Da:Dt) (4 µg/ml). Conditioned media was assayed by ELISA for levels of IL-1β. Data are presented as the mean of three independent experiments +/- SEM. Statistical significance was determined using two-tailed Student's t-test.

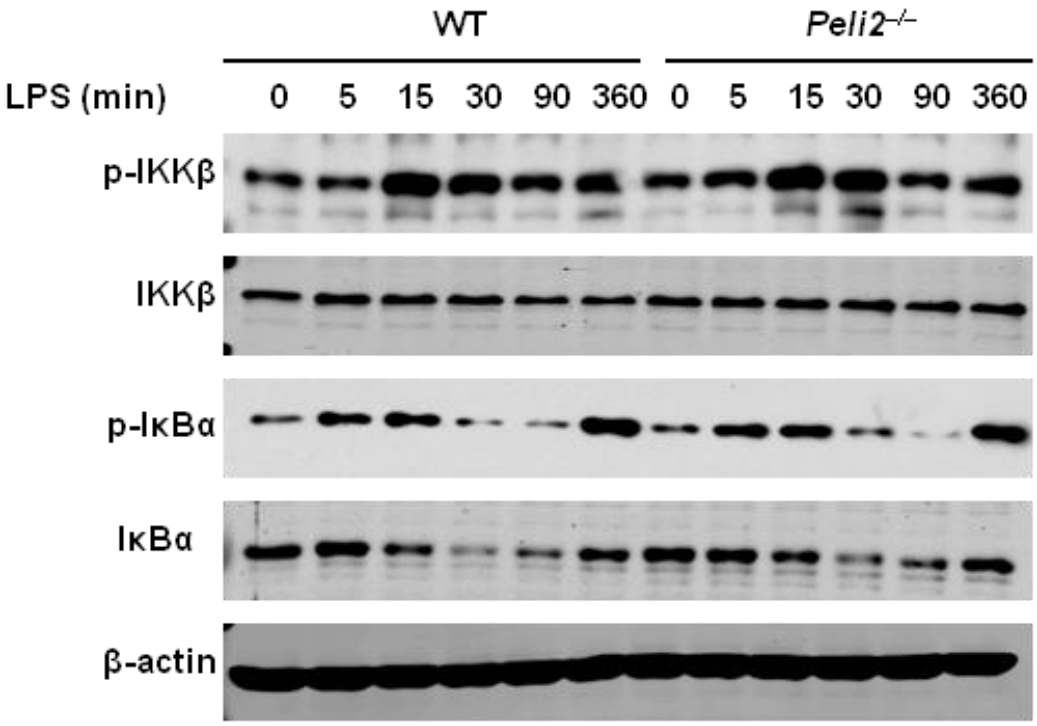

Figure 3.16 Effect of Pellino2-deficiency on TLR4 induced activation of NF-κB.

BMDMs cultured from WT and *Peli2*$^{-/-}$ bone marrow were left untreated (0) or stimulated for the indicated times with LPS (10 ng/ml). Cell lysates were generated and immunoblotted. Samples were first probed for p-IKKβ and p-IκBα followed by total levels of IKKβ, IκBα and β-actin as a loading control. Data are representative of 3 independent experiments.

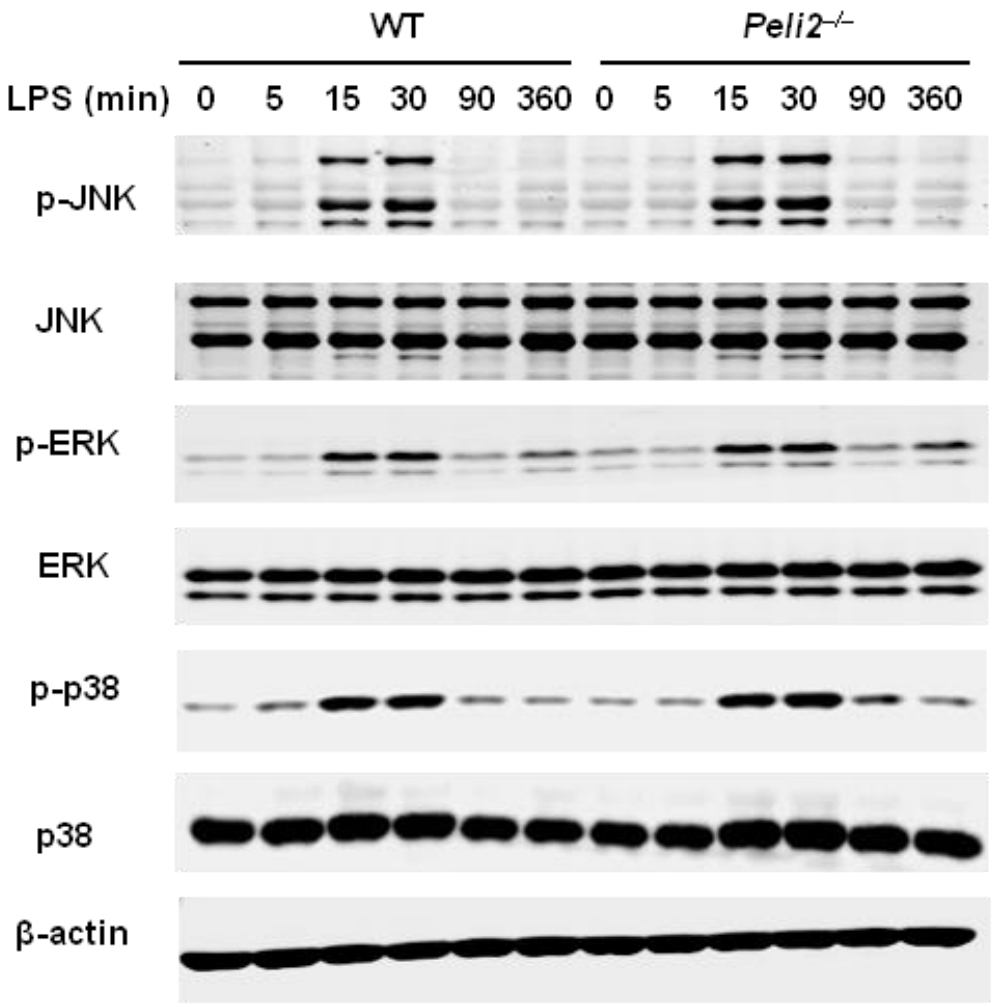

Figure 3.17 Effect of Pellino2-deficiency on TLR4 induced activation of MAPKs.

BMDMs cultured from WT and *Peli2*$^{-/-}$ bone marrow were left untreated (0) or stimulated for the indicated times with LPS (10 ng/ml). Cell lysates were generated and immunoblotted. Samples were first probed for p-JNK, p-ERK and p-p38 followed by total levels of JNK, ERK, p38 and β-actin as a loading control. Data are representative of 3 independent experiments.

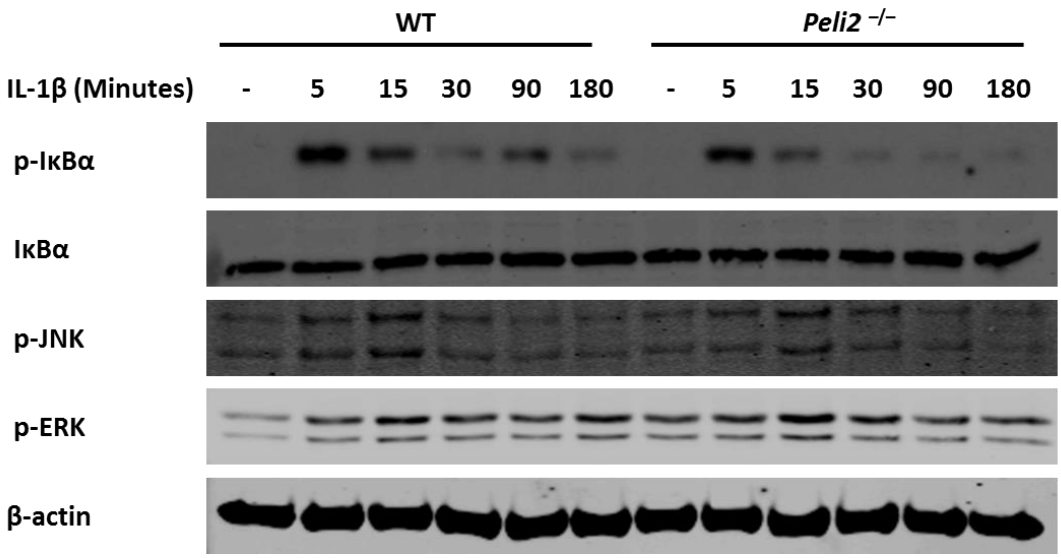

Figure 3.18 Effect of Pellino2-deficiency on IL-1β induced activation of NF-κB and MAPKs.

BMDMs cultured from WT and *Peli2*$^{-/-}$ bone marrow were left untreated (-) or stimulated for the indicated times with LPS (10 ng/ml). Cell lysates were generated and immunoblotted. Samples were first probed for p-JNK, p-ERK and p-IκBα followed by total levels of IκBα and β-actin as a loading control. Data are representative of 3 independent experiments.

(a)

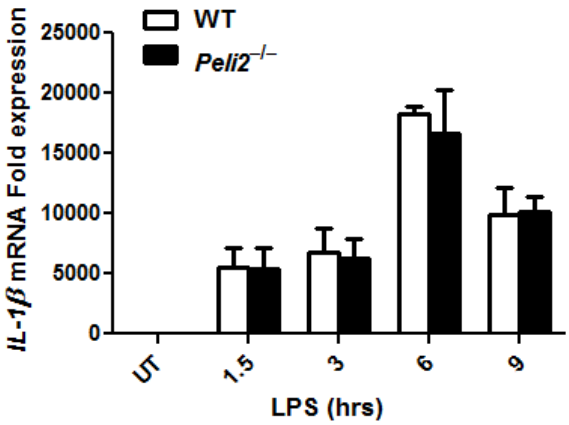

(b)

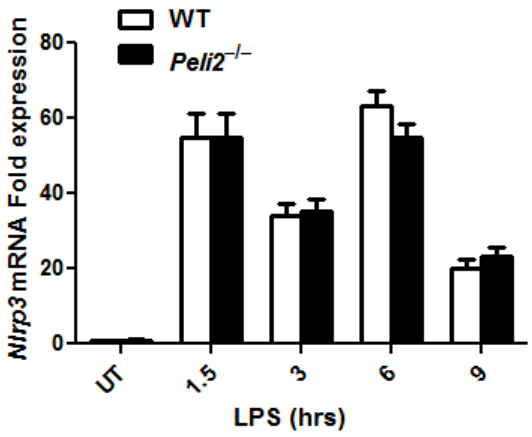

Figure 3.19 Effect of Pellino2-deficiency on TLR4 induced IL-1β and NLRP3 mRNA upregulation

Quantitative real-time PCR of **(a)** IL-1β and **(b)** NLRP3 expression in cells from BMDMs isolated from WT and *Peli2*$^{-/-}$ mice and left untreated (UT) or stimulated with LPS (10 ng/ml) over the indicated time-course. Analysis was carried out and mRNA levels are presented as a fold change relative to WT UT and normalised to HPRT expression. Data are presented as the mean of three independent experiments +/- SEM. Statistical significance was determined using two-tailed Student's t-test.

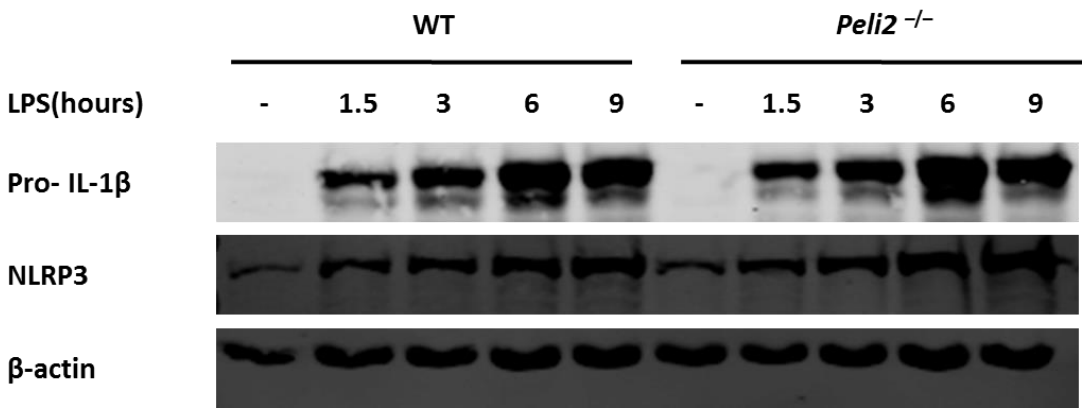

Figure 3.20 Effect of Pellino2-deficiency on TLR4 induced IL-1β and NLRP3 protein upregulation.

BMDMs cultured from WT and *Peli2*$^{-/-}$ bone marrow were left untreated (-) or stimulated with LPS (10 ng/ml) over the indicated time course. Cell lysates were generated and immunoblotted for IL-1β, NLRP3 and β-actin as a loading control. Data are representative of at least 3 independent experiments.

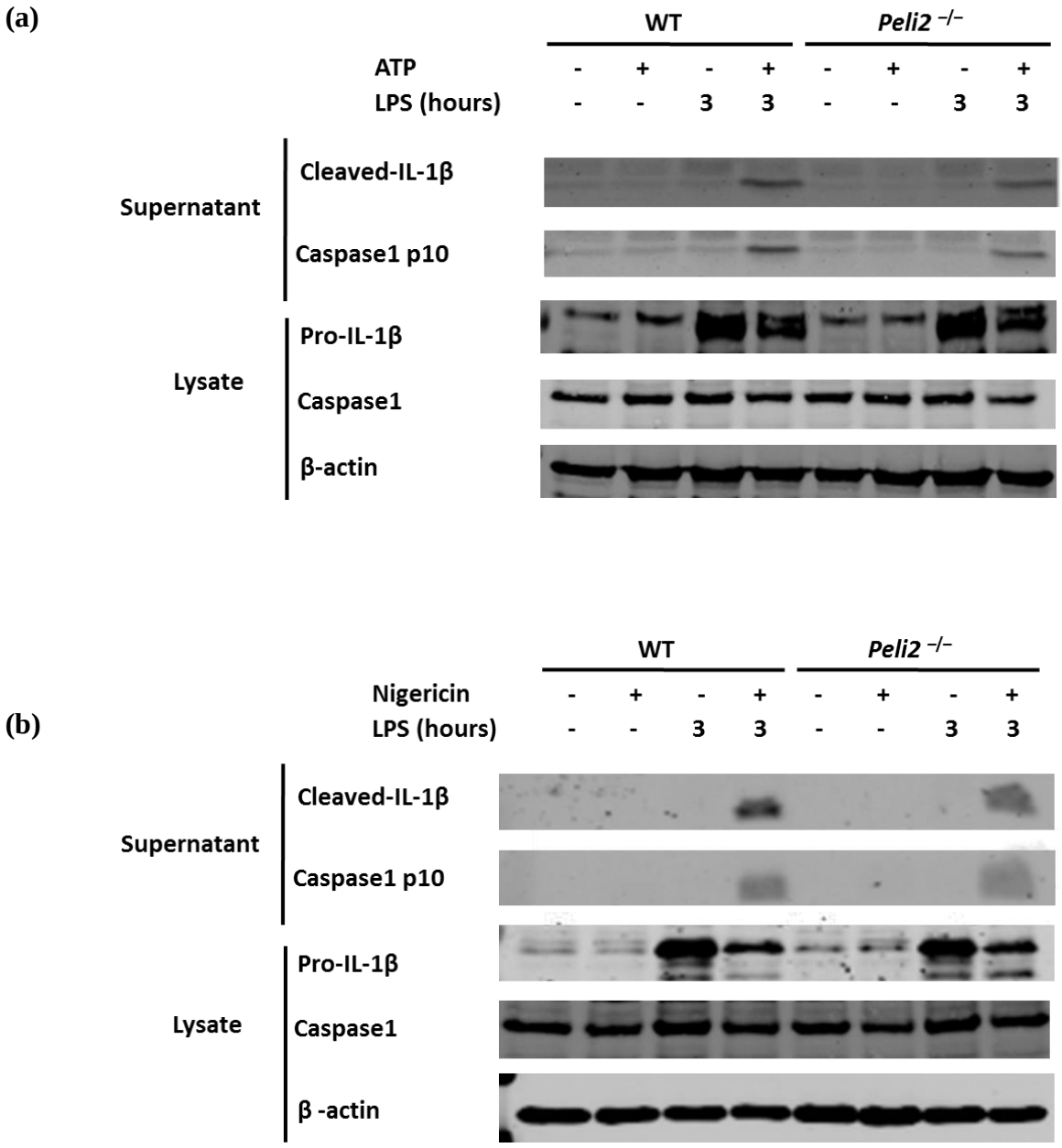

Figure 3.21 Effect of Pellino2-deficiency on the activation of the NLRP3 inflammasome in BMDMs.

BMDMs cultured from WT and *Peli2*$^{-/-}$ bone marrow were either untreated (-) or stimulated for 3 h with LPS (10 ng/ml). Cells were then left untreated or subjected to co-stimulation with either **(a)** ATP (2.5 µM) or **(b)** Nigericin (1 µM) for 40 min. Cell Supernatants and lysates were generated and immunoblotted. Supernatant samples were probed for cleaved-IL-1β and caspase 1 p10. Lysate samples were probed for pro-IL-1β and β-actin as a loading control. Data are representative of at least 3 independent experiments.

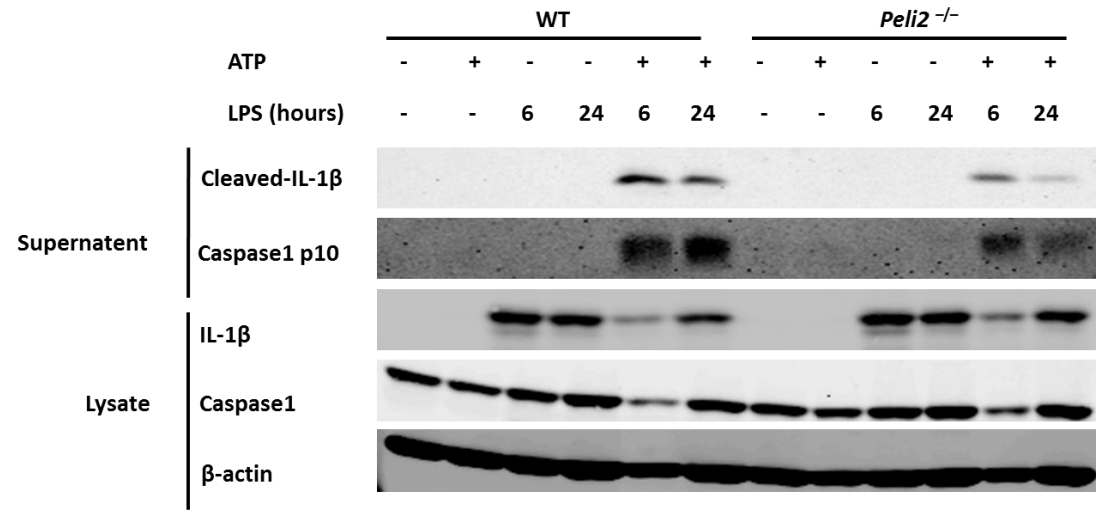

Figure 3.22 Effect of Pellino2-deficiency on the activation of the late NLRP3 inflammasome.

BMDMs cultured from WT and *Peli2*$^{-/-}$ bone marrow were left untreated (-) or stimulated for either 6 h or 24 h with LPS (10 ng/ml). Cells were then left untreated or subjected to co-stimulation with ATP (2.5 µM) for 40 min. Cell Supernatants and lysates were generated and immunoblotted. Supernatant samples were probed for cleaved-IL-1β and caspase 1 p10. Lysate samples were probed for pro-IL-1β and β-actin as a loading control. Data are representative of at least 3 independent experiments.

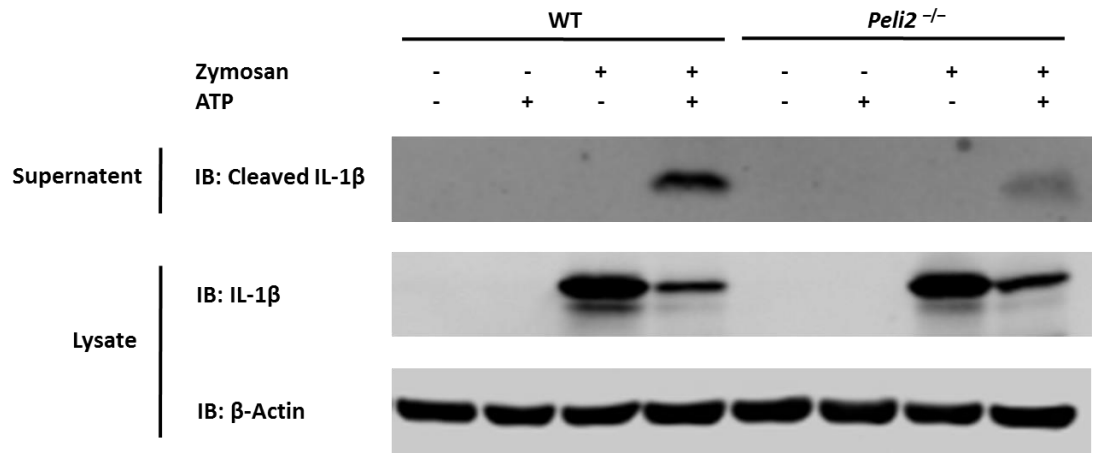

Figure 3.23 Effect of Pellino2-deficiency on the activation of the NLRP3 inflammasome using zymosan as a priming signal.

BMDMs cultured from WT and *Peli2*$^{-/-}$ bone marrow were either untreated (-) or stimulated for 3 h with Zymosan (5 µg/ml). Cells were then left untreated or subjected to co-stimulation ATP (2.5 µM) for 40 min. Cell Supernatants and lysates were generated and immunoblotted. Supernatant samples were probed for cleaved-IL-1β. Lysate samples were probed for pro-IL-1β and β-actin as a loading control. Data are representative of at least 3 independent experiments.

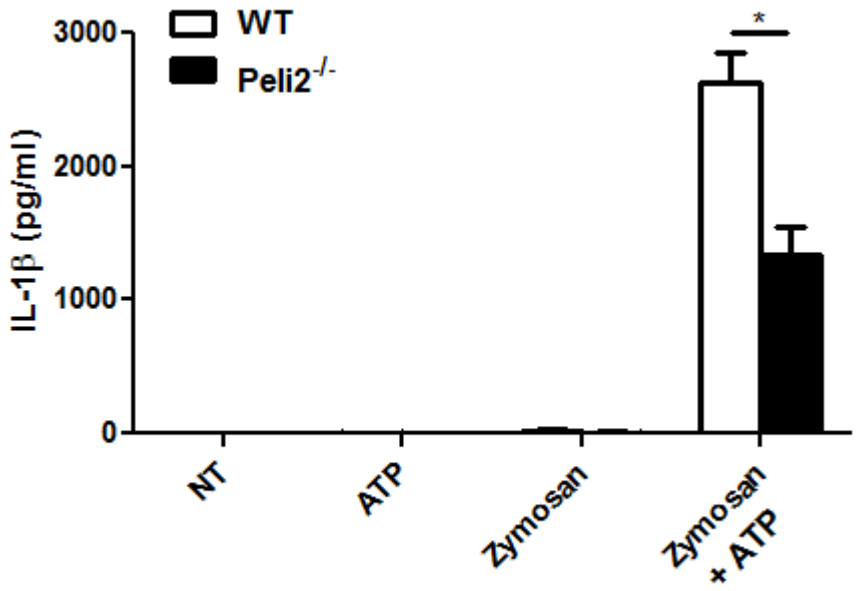

Figure 3.24 Effect of Pellino2-deficiency on IL-1β secretion during NLRP3 inflammasome activation using zymosan as a priming signal in BMDMs.

BMDMs from WT and *Peli2*$^{-/-}$ bone marrow were left non-treated (NT) or stimulated for 3 h with Zymosan (5 µg/ml), Cells were then left untreated or subjected to co-stimulation with ATP (2.5 µM). Conditioned media was assayed by ELISA for levels of IL-1β. Data are presented as the mean of three independent experiments +/- SEM. Statistical significance was determined using two-tailed Student's t-test (*, $p < 0.05$).

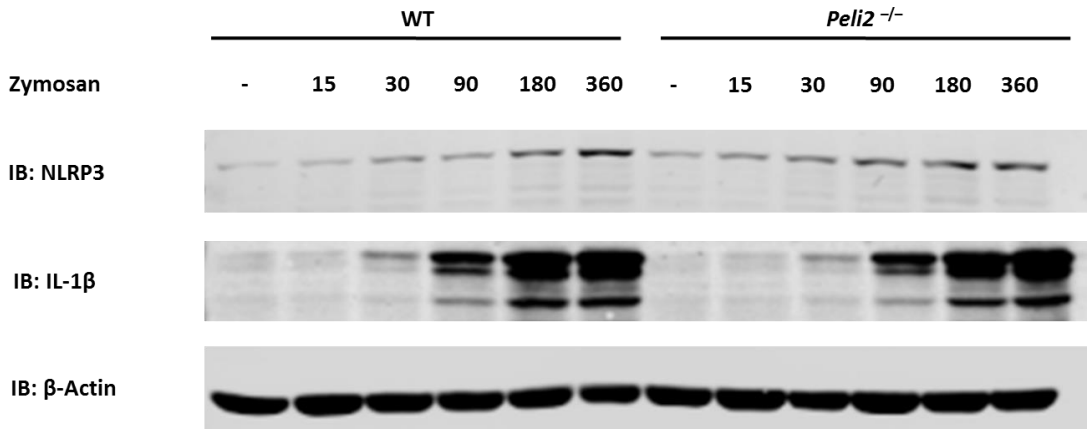

Figure 3.25 Effect of Pellino2-deficiency on zymosan induced IL-1β and NLRP3 protein upregulation.

BMDMs cultured from WT and *Peli2*$^{-/-}$ bone marrow were left untreated (-) or stimulated with Zymosan (5 µg/ml) over the indicated time course. Cell lysates were generated and immunoblotted for IL-1β, NLRP3 and β-actin as a loading control. Data are representative of at least 3 independent experiments.

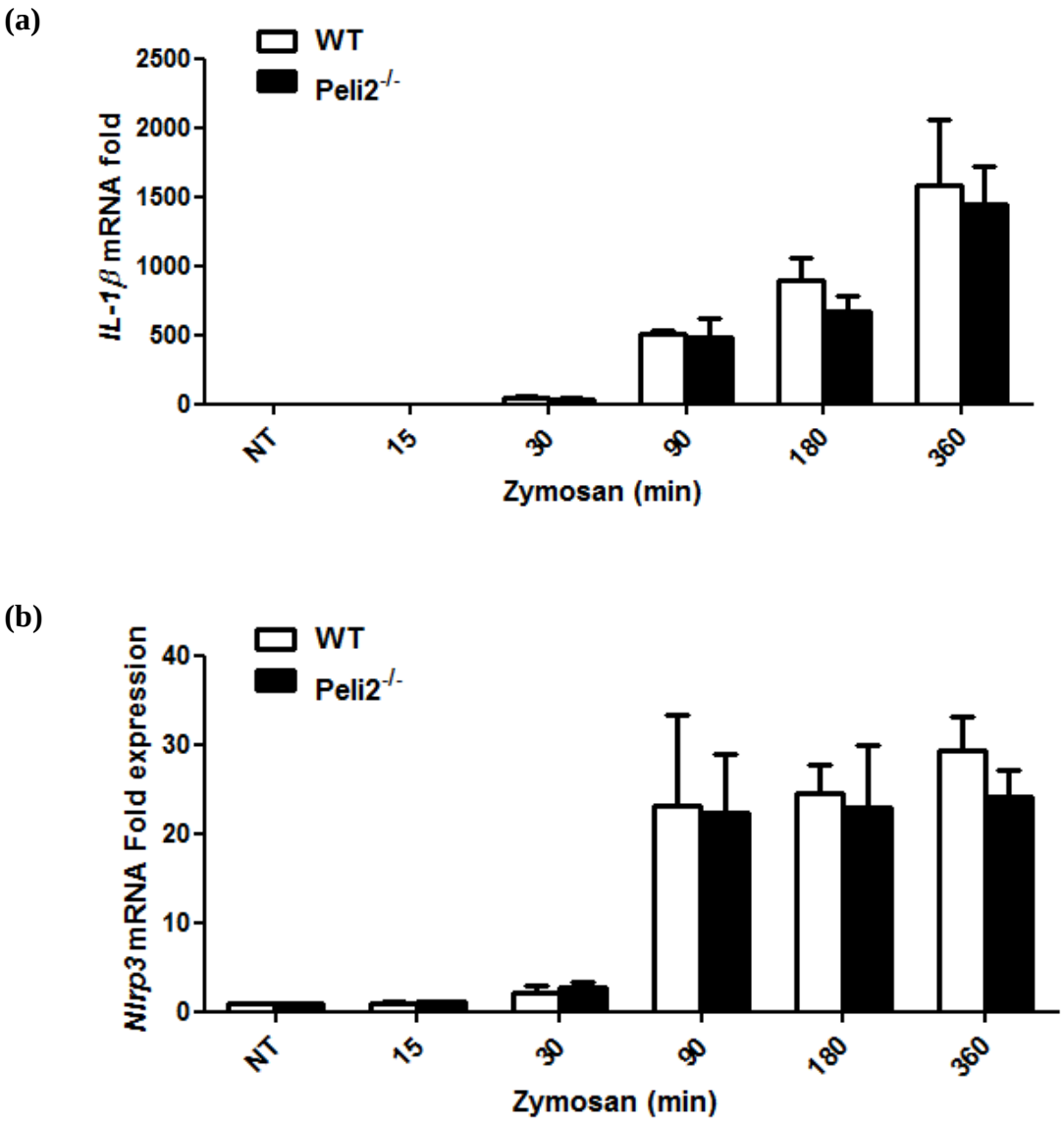

Figure 3.26 Effect of Pellino2-deficiency on zymosan induced IL-1β and NLRP3 mRNA upregulation.

Quantitative real-time PCR of **(a)** IL-1β and **(b)** NLRP3 expression in cells from BMDMs isolated from WT and *Peli2*$^{-/-}$ mice and left non-treated (NT) or stimulated with Zymosan (5 μg/ml) over the indicated time-course. Analysis was carried out and mRNA levels are presented as a fold change relative to WT NT and normalised to HPRT expression. Data are presented as the mean of three independent experiments +/- SEM. Statistical significance was determined using two-tailed Student's t-test.

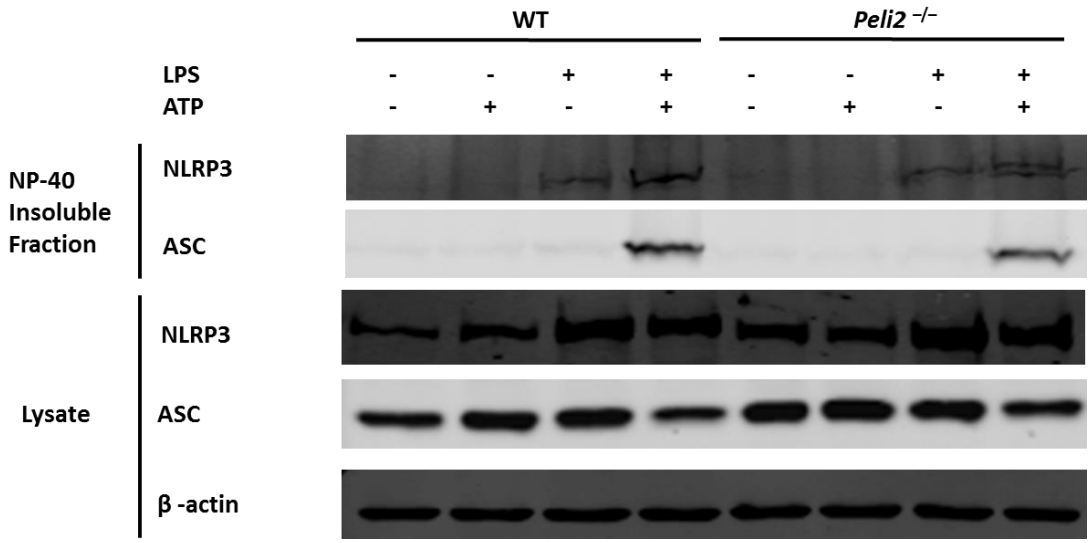

Figure 3.27 Effect of Pellino2-deficiency on the migration of NLRP3 components to the NP-40 insoluble fraction.

BMDMs cultured from WT and *Peli2*$^{-/-}$ bone marrow were left untreated (-) or stimulated for 3 h with LPS (10 ng/ml). Cells were then left untreated or subjected to co-stimulation with ATP (2.5 μM) for 40 min. NP-40 insoluble fraction and lysates were generated and immunoblotted. NP-40 insoluble fractions were probed for NLRP3 and ASC. Lysate samples were probed for NLRP3 and β-actin as a loading control. Data are representative of 3 independent experiments.

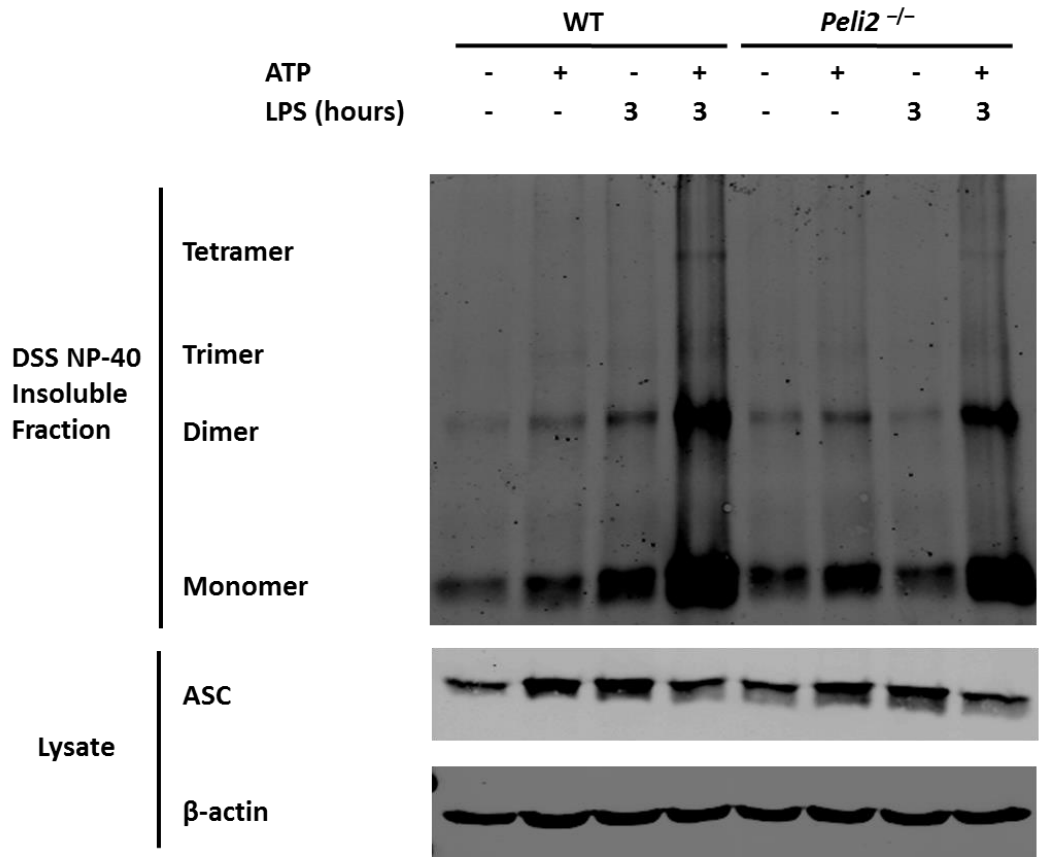

Figure 3.28 Effect of Pellino2-deficiency on ASC oligomerisation during activation of the NLRP3 inflammasome in BMDMs.

BMDMs cultured from WT and *Peli2*$^{-/-}$ bone marrow were left untreated (-) or stimulated for 3 h with LPS (10 ng/ml). Cells were then left untreated or subjected to co-stimulation with ATP (2.5 µM) for 40 min. Chemical crosslinking of NP-40 insoluble fraction was carried out using DSS (4 mM) and lysates were also generated and immunoblotted. Pellet samples were probed for ASC. Lysate samples were probed for ASC and β-actin as a loading control. Data are representative of 3 independent experiments.

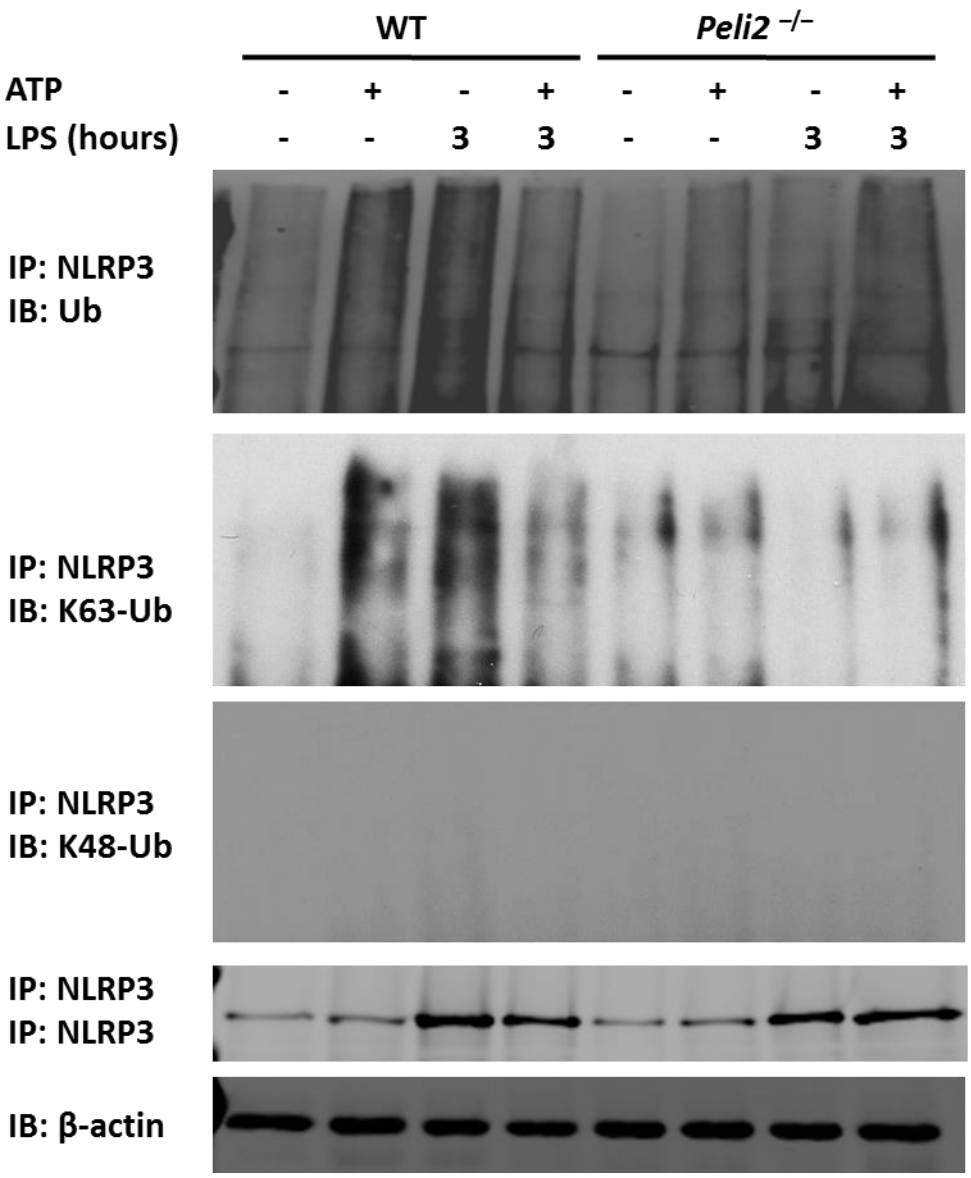

Figure 3.29 Effect of Pellino2-deficiency on the ubiquitination of NLRP3 during LPS stimulation in BMDMs.

BMDMs cultured from WT and *Peli2*$^{-/-}$ bone marrow were left untreated (-) or stimulated with LPS (10 ng/ml) for 3 h. Cells were then left untreated or subjected to co-stimulation with ATP (2.5 μM) for 40 min. Cell lysates were generated and immunoprecipitated (IP) using anti-NLRP3 antibody. IP samples were probed for Ubiquitn (Ub), K63-Ub, K48-Ub and NLRP3. Lysate samples were probed for β-actin as a loading control. Data are representative of 3 independent experiments.

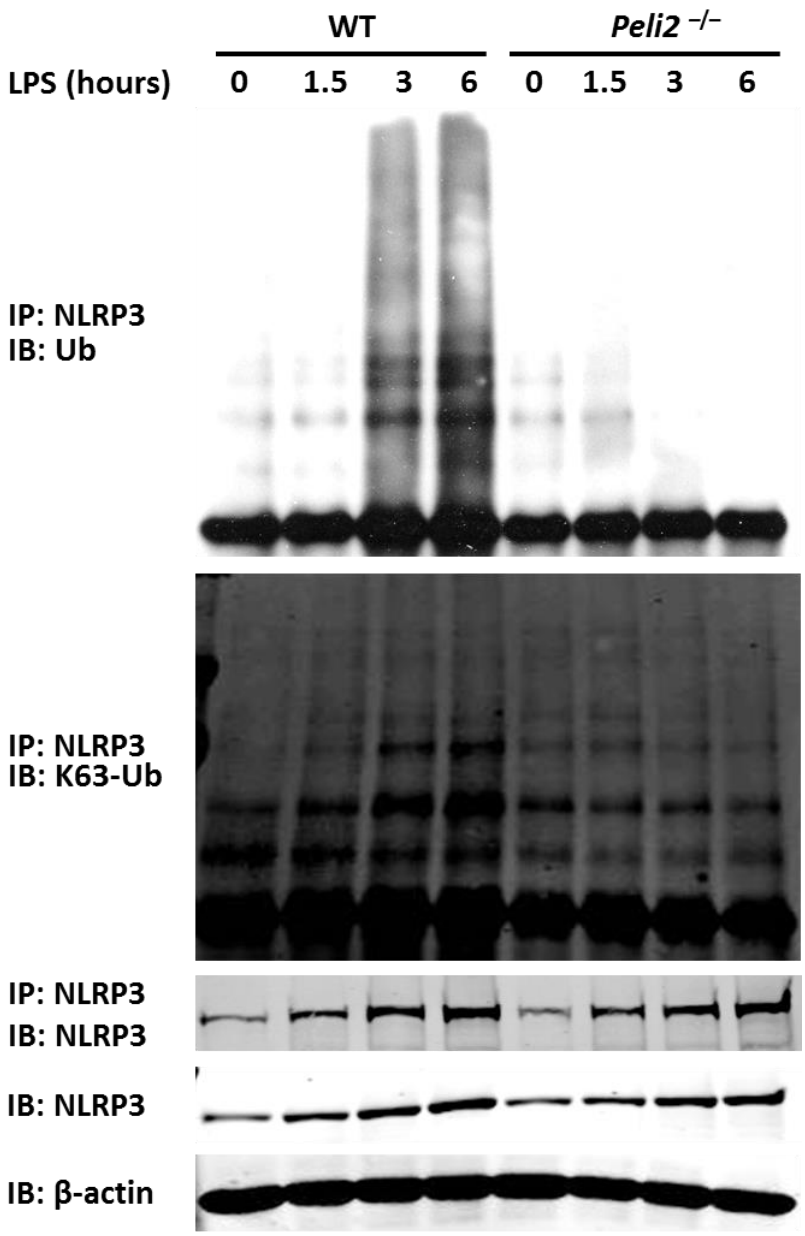

Figure 3.30 Effect of Pellino2-deficiency on the ubiquitination of NLRP3 during LPS stimulation in BMDMs.

BMDMs cultured from WT and *Peli2*$^{-/-}$ bone marrow were left untreated (0) or stimulated with LPS (10 ng/ml) for indicated times. Cell lysates were generated and immunoprecipitated (IP) using anti-NLRP3 antibody. IP samples were probed for Ubiquitn (Ub), K63-Ub and NLRP3. Lysate samples were probed for NLRP3 and β-actin as a loading control. Data are representative of 3 independent experiments.

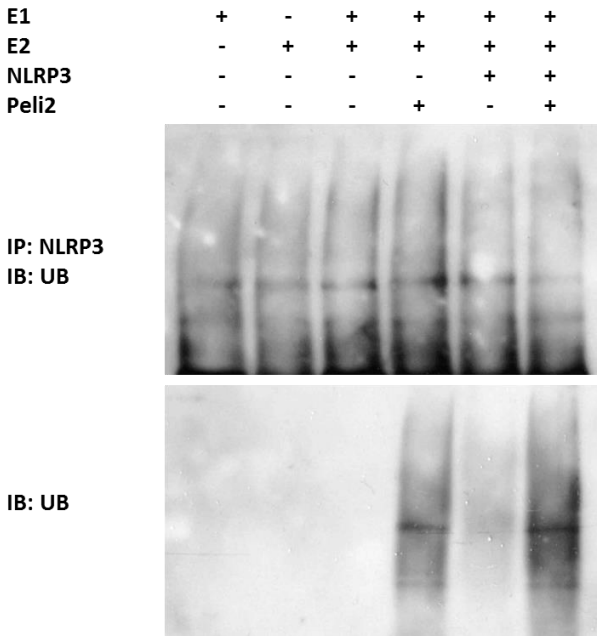

Figure 3.31 Pellino2 fails to catalyse ubiquitination of NLRP3 *in vitro*

In vitro ubiquitination assay was carried out by incubating 500ng UBE1 (E1), 400ng Ubc13/Uev1A (E2), 2µg ubiquitin, NLRP3 (200 nM) and Pellino2-myc (20 nM) in reaction buffer (5 mM Tris-HCl, pH 8.0, 2 mM MgCl, 2 mM ATP, Proteinase inhibitor-EDTA free 1/10 dilution) at 37℃ for 1 h. Immunoprecipitated (IP) was carried out using anti-NLRP3 antibody. IP samples were probed for ubiquitin (UB). Remaining sample was probed for UB to detect free-chains. Data are representative of 3 independent experiments.

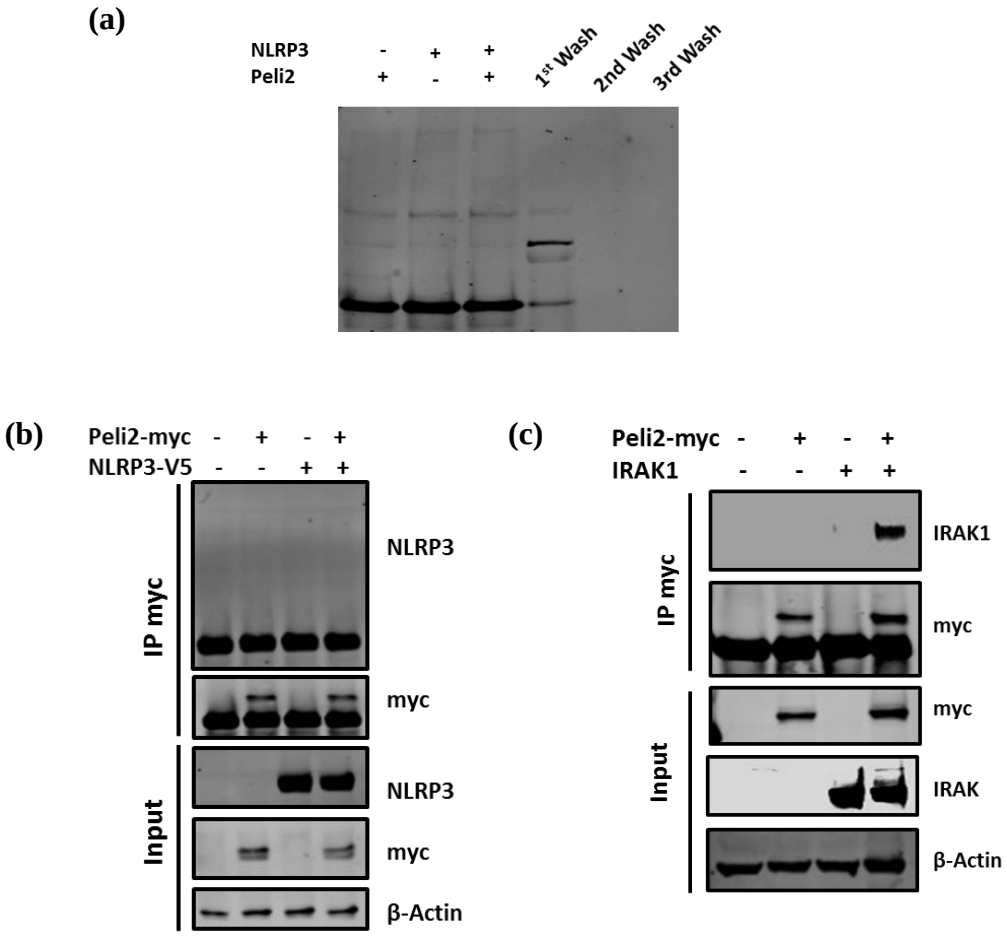

Figure 3.32 Pellino2 does not interact with NLRP3.

(a) *In vitro* ubiquitination assay was carried out by incubating NLRP3 (200 nM) and Pellino2-myc (20 nM) in reaction buffer (5 mM Tris-HCl, pH 8.0, 2 mM MgCl, 2 mM ATP, Proteinase inhibitor-EDTA free 1/10 dilution) at 37°C for 1 h.. Whole sample was immunoprecipitated using anti-NLRP3 antibody. The three wash stages during immunoprecipitation were retained. Samples were blotted with anti-Myc antibody. Data are representative of 2 independent experiments **(b)** HEKT cells were transfected with empty vector (EV) alone or in combination with expression constructs encoding Pellino2-Myc (Peli2-Myc) and NLRP3-V. Cell lysates were generated and co-immunoprecipitated with an anti-MYC antibody. Immunoprecipitated (IP) samples and WCL samples were subjected to immunoblot (IB) for presence of Myc-tagged proteins and NLRP3. β- actin was used as a loading control. **(c)** HEKT cells were transfected with empty vector (EV) alone or in combination with expression constructs encoding Pellino2-Myc (Peli2-Myc) and IRAK1. Cell lysates were generated and co-immunoprecipitated with an anti-MYC antibody. Immunoprecipitated (IP) samples and WCL samples were subjected to immunoblot (IB) for presence of Myc-tagged proteins and IRAK1. β- actin was used as a loading control. ((b)/(c) Data provided by Dr. Fiachra Humphries)

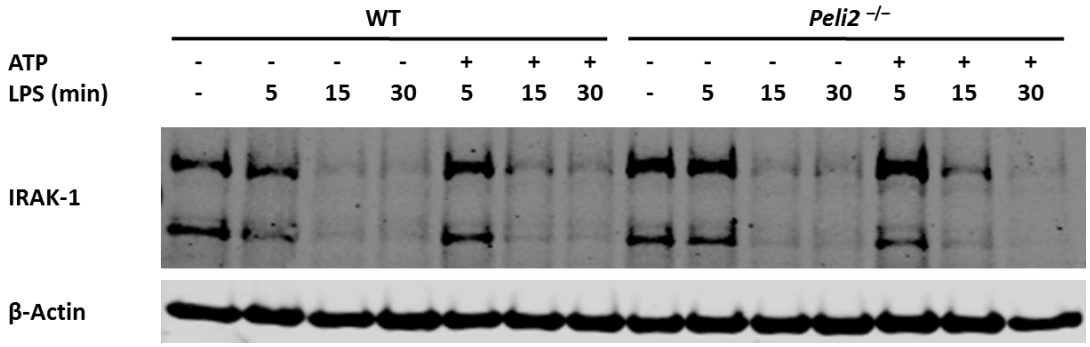

Figure 3.33 Effect of Pellino2-deficiency on IRAK1 stabilisation during early inflammasome activation in BMDMs.

BMDMs cultured from WT and *Peli2*$^{-/-}$ bone marrow were left untreated (-), stimulated for with LPS (10 ng/ml) or co-stimulate with LPS and ATP (2.5 μM) over a time-course. Lysates were generated and immunoblotted. Lysate samples were probed for IRAK-1 and β-actin as a loading control. Data are representative of 3 independent experiments.

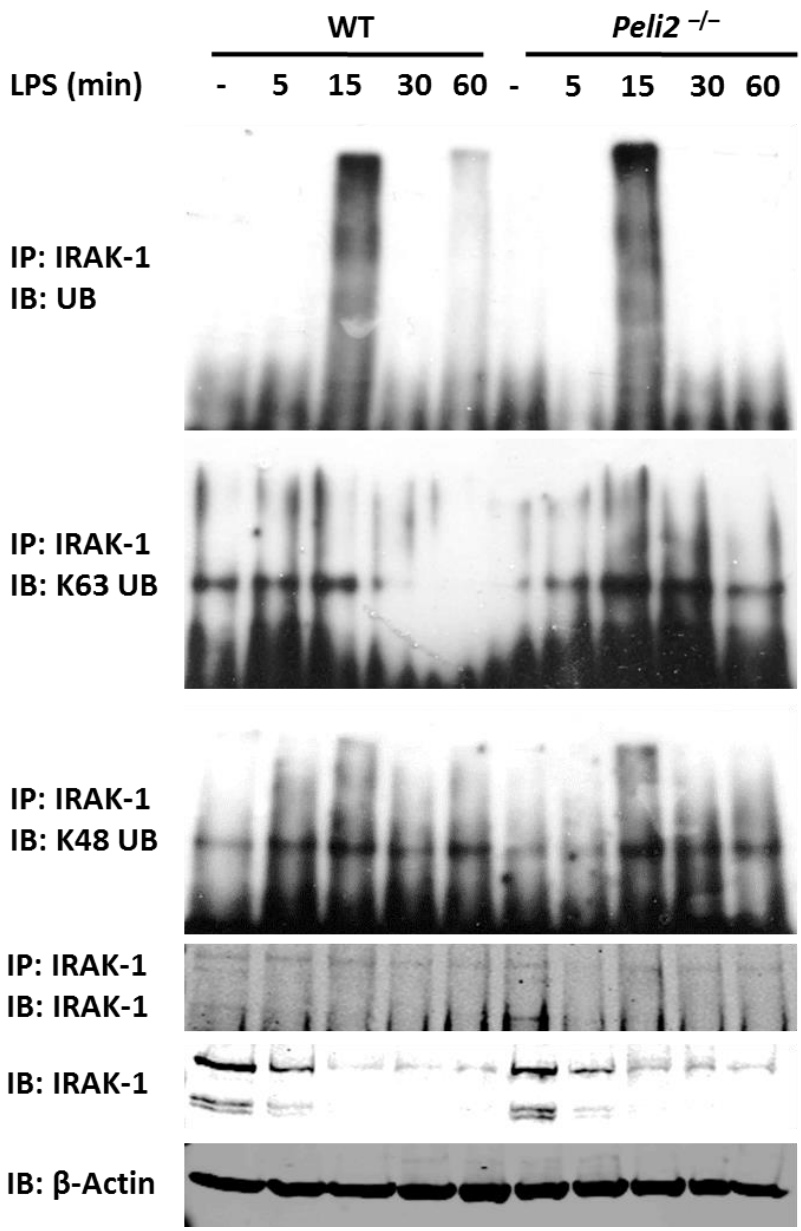

Figure 3.34 Effect of Pellino2-deficiency on the ubiquitination of IRAK1 during LPS stimulation in BMDMs.

BMDMs cultured from WT and *Peli2*$^{-/-}$ bone marrow were left untreated (-) or stimulated with LPS (10 ng/ml) for indicated times. Cell lysates were generated and immunoprecipitated (IP) using anti-IRAK1 antibody. IP samples were probed for Ubiquitn (Ub), K63-Ub, K48-Ub and NLRP3. Lysate samples were probed for IRAK-1 and β-actin as a loading control. Data are representative of 3 independent experiments.

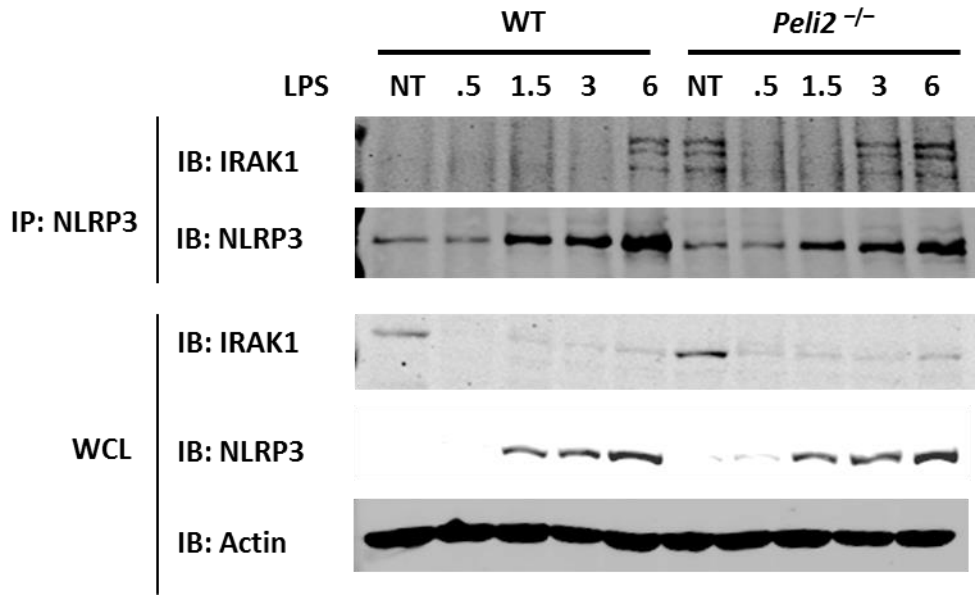

Figure 3.35 Effect of Pellino2-deficiency on the interaction of NLRP3 and IRAK1 during LPS stimulation in BMDMs.

BMDMs cultured from WT and *Peli2*$^{-/-}$ bone marrow were left untreated (-) or stimulated with LPS (10 ng/ml) for indicated times. Cell lysates were generated and coimmunoprecipitated (IP) using anti-NLRP3 antibody. IP samples were probed for IRAK1 and NLRP3. Lysate samples (WCL) were probed for IRAK-1, NLRP3 and β-actin as a loading control. Data are representative of 3 independent experiments.

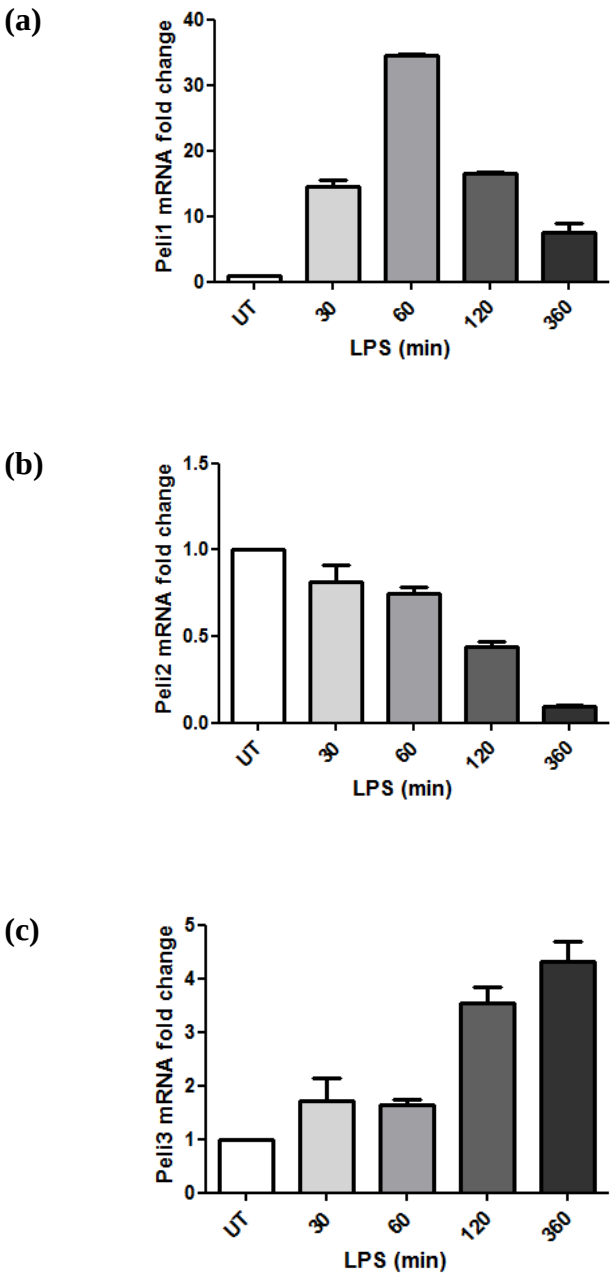

Figure 3.36 The regulation of Pellino expression by LPS in BMDMs.

Quantitative real-time PCR of **(a)** Peli1 **(b)** Peli2 and **(c)** Peli3 expression in cells from BMDMs isolated from either WT mice and left untreated (UT) or stimulated with LPS (10 ng/ml) over the indicated time-course. Analysis was carried out and mRNA levels are presented as a fold change relative to WT NT and normalised to HPRT expression. Data are presented as the mean of three independent experiments +/- SEM.

Chapter 4: Discussion

The generation of Pellino1 (Chang *et al.,* 2009b) and Pellino3-deficient mice (Siednienko *et al.,* 2012) has led to a rapid expansion of our understanding of the field of Pellino biology over the last number of years. Investigation into these proteins prior to the development of these models focused primarily on the use of overexpression and knockdown techniques. Knockout mouse models however have enhanced our understanding of the physiological relevance of both Pellino1 and Pellino3, which have been demonstrated to possess a diverse range of immunological functions. To date, a similar mouse model for the final member of the Pellino family, Pellino2, has not been published. The work in this thesis uses a newly generated Pellino2-deficient mouse model to demonstrate a novel physiological role for Pellino2 in the regulation of NLRP3 inflammasome activation. Whilst many of the molecular components of NLRP3 have been identified, the regulatory mechanisms controlling its assembly and activation have yet to be fully elucidated. The data presented here demonstrates for the first time that hyperphosphorylated IRAK1 can interact with NLRP3 at late time-points during inflammasome priming and may serve to hinder NLRP3 ubiquitination and subsequent activation (Fig. 4.1). In the absence of Pellino2, this interaction occurs prior to inflammasome priming and may contribute to the observed reduction in inflammasome assembly in these cells. It can be speculated that Pellino2 may serve to regulate the basal phosphorylation and subsequent activation of IRAK1 and thus limit the regulatory role of IRAK1 during NLRP3 inflammasome activation. In WT cells, Pellino2 is downregulated during an LPS time-course, leading to the increased interaction of hyperphosphorylated IRAK1 with NLRP3 at later time-points. However, in Pellino2-deficient cells, this hyperphosphorylation of IRAK1 is unabated which results in heightened NLRP3/IRAK1 interaction, corresponding to reduced NLRP3 ubiquitination and subsequent inflammasome activation (Fig. 4.3). This work demonstrates a novel mechanism by which Pellino2 and IRAK1 work in concert to regulate the activation of the NLRP3 inflammasome and thus influence the secretion of IL-1β.

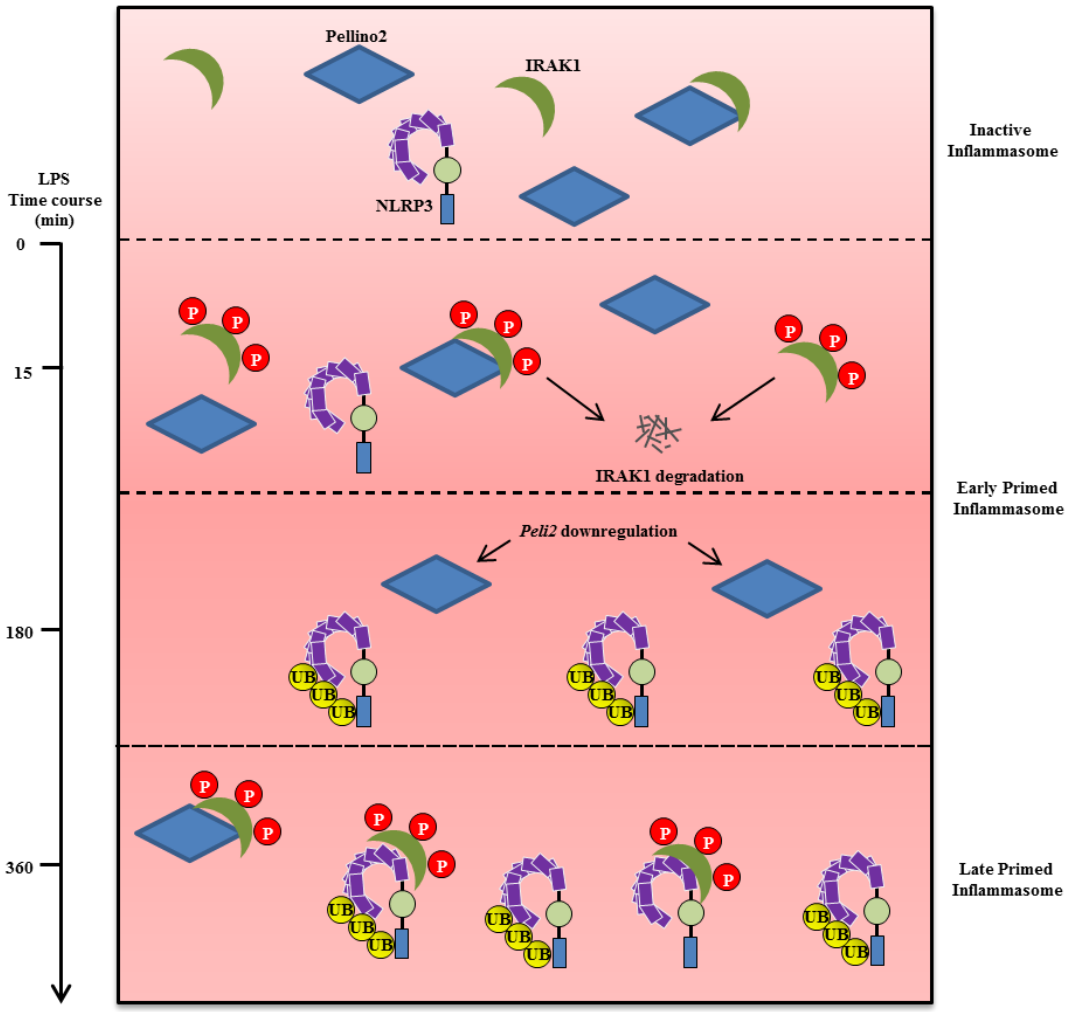

Figure 4.1 The role of Pellino2 and IRAK1 in the regulation of NLRP3 Inflammasome assembly during priming

The description of the role of both Pellino2 and IRAK1 in controlling the normal functioning of the NLRP3 inflammasome activation is highlighted in the discussion. Yellow circles containing "UB" represent ubiquitination event. Red circles containing "P" represent phosphorylation.

Prior to this work, Pellino2 was primarily studied in the context of IL-1 and TLR signalling (Kim *et al.*, 2012a; Schauvliege *et al.*, 2006). The lack of a Pellino2-deficient mouse model dictated that previous research on Pellino2 has depended on the use of overexpression and knockdown techniques. Using shRNA knockdown, Pellino2 was shown to be required for IL-1 and TLR4 induced polyubiquitination of IRAK1. The further overexpression of a Pellino2 RING mutant abolished the capacity of Pellino2 to promote this ubiquitination, highlighting the importance of the E3 ligase activity of Pellino2 during this ubiquitination event. Furthermore, the phosphorylation of two key components of the MAPK pathway, JNK and ERK were also inhibited during both TLR4 and IL-1β signalling in Pellino2-knockdown cells (Kim *et al.*, 2012b). Finally, the levels of secreted IL-6 and TNFα were decreased in knockdown cells, which was attributed to impaired mRNA stability (Kim *et al.*, 2012a). However, evidence presented in this thesis argues against a role for Pellino2 in the regulation of pro-inflammatory cytokine secretion in response to TLR or IL-1β stimulation. Only when the cells were subjected to a second signal which caused the formation of the NLRP3 inflammasome was a role for Pellino2 in IL-1β secretion revealed. LPS and IL-1β-induced activation of the NF-κB and MAPK signalling pathways were fully intact in Pellino2-deficient cells. Furthermore, TLR induced expression of IL-1β, IL-6 and NLRP3 at the mRNA and protein levels were not affected by the absence of Pellino2. Previous studies have demonstrated a similar discrepancy between overexpression and knockout models. Pellino3 for example was shown to affect MAPK signalling through the use of overexpression (Butler *et al.*, 2005), but this effect was not seen in the *Peli3*$^{-/-}$ mouse model (Siednienko *et al.*, 2012). Overexpression of any E3 ligase may result in loss of substrate specificity and so produce effects which are not directly attributable to the E3 ligase under study. Conversely, the generation of a mouse that is deficient in a single member of the Pellino family may lead to functional compensation by the remaining family members and may mask effects that are revealed by more acute knockdown approaches in cell models.

Peli1$^{-/-}$ mice were previously shown to be resistant to of LPS induced septic shock in combination with D-galactosamine. This acute model led to the death of all WT mice and 100% survival of *Peli1*$^{-/-}$ mice. A high-dose LPS model was also used which

resulted in a lethality of 50% WT and 15% of *Peli1*$^{-/-}$ mice. Cytokine analysis of the serum of mice showed severely abrogated TNF and IL-6 levels in the Pellino1-deficient mice and this was attributed to effects on NF-κB signalling (Chang *et al.*, 2009). Similar to the phenotype observed in *Peli1*$^{-/-}$, the data presented in this thesis shows that Pellino2-deficiency protected against the lethal effects and systemic inflammatory effects of LPS. However the mechanisms of protection in *Peli1*$^{-/-}$ and *Peli2*$^{-/-}$ differ. Pellino2 does not play a role in the propagation of the initial TLR signalling event and thus does not regulate NF-κB activity and instead mediates activation of NLRP3. This is consistent with a previously described role for NLRP3 in mediating LPS-induced septic shock (Gong *et al.*, 2015; Mao *et al.*, 2013). In order to demonstrate the *in vivo* relevance of the regulatory effects of Pellino2 on inflammasome activation, the high-dose LPS model of sepsis was employed. Pellino2-deficient mice showed 50% survival after 48 h, while all WT mice had succumbed to septic shock. During the experiment, *Peli2*$^{-/-}$ mice showed more responsiveness to stimuli and moved around cages more freely. All mice which survived recovered weight and showed no sign of illness after 72 h. While increased survival of *Peli2*$^{-/-}$ mice in this model mirrored similar protection in *Peli1*$^{-/-}$ mice, the measurement of serum cytokine levels again highlight differing mechanisms. Only levels of IL-1β in *Peli2*$^{-/-}$ mouse serum were shown to be reduced when compared to WT, while other pro-inflammatory cytokines such as IL-6, TNFα and RANTES were unaffected. In contrast many of these pro-inflammatory cytokines were reduced in Peli1$^{-/-}$ mice. This highlights a situation in which members of the Pellino family may show similar functional effects but with different underlying mechanisms. Despite sharing similar homology, Pellino proteins have distinct signalling roles. This could in part be due to the differing expression profiles in tissue as has been demonstrated during Pellino1 signalling in microglial cells (Xiao *et al.*, 2013). Pellino1 has been shown to regulate TLR signalling by degradation of TRAF3, which is an inhibitor of MAPK signalling. This function is specific to microglial cells, due to high levels of expressed Pellino1 in these cells.

Inflammasomes are large multi-protein complexes involved in the maturation of the pro-inflammatory cytokines IL-1β and IL-18 (Lamkanfi and Dixit, 2014). Whilst many of the molecular components of NLRP3 have been identified the regulatory

mechanisms controlling its assembly and activation remain to be fully elucidated. It is capable of responding to a wide variety of cellular and pathogenic signals, making it unlikely to bind directly to a particular DAMP. Instead, it is thought to be a cellular sensor which can be activated in response to generic signals of cellular disruption such as K+ efflux from the cell (Muñoz-Planillo *et al.,* 2013). NLRP3 activation requires a priming signal and a secondary signal. During priming, both NLRP3 and IL-1β are upregulated via NF-κB signalling through TLRs. The secondary signal involves stimulation with an NLRP3 activating agent and results in the assembly of the inflammasome complex. NLRP3 first oligomerises by association with the NBD, allowing the formation of a PYD signalling platform (Horvath *et al.,* 2011). This event leads to ASC aggregation by PYD-PYD association and the nucleation around the NLRP3 complex (Hara *et al.,* 2013). This filamentous complex can further act as a platform which recruits caspase-1 via CARD-CARD interactions and result in its activation (Lu *et al.,* 2014) (Fig. 4.2). Given that Pellino2-deficiency affected secreted levels of IL-1β, but had no impact on the NF-kB or MAPK pathways or upregulation of proIL-1β, mechanistic studies in this work especially focused on a role for Pellino2 during the secondary signal, which is required for inflammasome activation. The level of ASC oligomerisation, which results in the formation of inflammasome aggregation in the NP-40 insoluble fraction, is reduced in Pellino2-deficient cells. Caspase-1 cleavage is similarly reduced in these cells, implicating a role for Pellino2 upstream of the assembly of the inflammasome. Pellino2 has a role specifically in NLRP3 inflammasome assembly, as signalling by NLRC4 (Zhao *et al.,* 2011) and AIM2 (Hornung *et al.,* 2009) inflammasome, both of which can activate and secrete IL-1β, are unaffected in Pellino2-deficient cells. Based on these data, the molecular mechanisms regulating NLRP3 activation were explored.

NLRP3 has recently been shown to require deubiquitination prior to assembly of the inflammasome (Juliana *et al.,* 2012; Py *et al.,* 2013). However, the initial regulation of NLRP3 ubiquitination has not been studied to date and the E3 ligase responsible remains to be identified. The work presented here demonstrates that NLRP3 ubiquitination occurs during the inflammasome priming event and is associated with optimal inflammasome activation following signal 2. This initial NLRP3

ubiquitination is lost in Pellino2 deficient cells, which results in a lack of a deubiquitination event, hindering inflammasome assembly and activity. It is intriguing to speculate why NLRP3 requires both ubiquitination and subsequent deubiquitination prior to inflammasome assembly. The initial ubiquitination event may be required to bridge an interaction of NLRP3 with another unidentified adapter protein which may be required to promote the activation of NLRP3, similar to how the TAK1 and IKK complexes are recruited to ubiquitinated TRAF6 or RIP1 during NF-κB signalling (Ea *et al.,* 2006). Alternatively, ubiquitination of NLRP3 may be required to block the interaction with proteins capable of binding to and hindering NLRP3 activity. Interestingly, a recent report investigating ubiquitination of the protein Dishevelled shows that ubiquitination of its DIX domain at K54 effectively acts as a negative signal and blocks its polymerisation and signalling. DUB activity is required to cleave DIX54-UB and thus promote Dishevelled assembly (Madrzak *et al.,* 2015). It is possible that the deubiquitination step during NLRP3 activation only partially disassembles the formed ubiquitin chains, leading to an exposed mono-ubiquitin which facilitates NLRP3 oligomerisation. Mono-ubiquitination has previously been demonstrated to be involved in membrane protein trafficking into the endocytoic pathway (Kerkhof *et al.,* 2000). This highlights the possibility that NLRP3 ubiquitination and subsequent deubiquitination is required for the cellular localisation of NLRP3 which facilitates activation. Another alternative is that BRCC3 deubiquitinates NLRP3 at the LRR domain (Juliana *et al.,* 2012) which promotes a conformational change in NLRP3, which alters the auto-inhibitory state of NLRP3, leading to its potential activation. Many of the critical details underlying the mechanisms which regulate the assembly of the inflammasome remain enigmatic and will require further work to fully discern the critical steps leading to optimal activation.

While we show that Pellino2 does not directly bind to NLRP3 and cannot directly mediate its ubiquitination, it may exert its effects via an intermediary protein. To investigate this, the association of IRAK1 with NLRP3 was investigated, as IRAK1 has been shown to interact both with Pellino2 (Lin *et al.,* 2008) and NLRP3 (Fernandes-Alnemri *et al.,* 2013). We observed a hyperphosphorylated form of IRAK1 which only associated with NLRP3 at the 6 h time-point during LPS

stimulation in WT cells; while this interaction was apparent basally in Pellino2-deficient cells. In Pellino2-deficient cells this interaction was lost during early LPS signalling, but re-established after 3 h. We speculate that Pellino2 may normally function to inhibit the NLRP3/IRAK1 interaction, however as Pellino2 is downregulated during LPS signalling, this regulatory effect of Pellino2 is lost and IRAK1 can associate with NLRP3, leading to inhibition of NLRP3 signalling. However, in the absence of Pellino2, IRAK1 pre-associates with NLRP3, which hinders its signalling potential. The role of IRAK1 in early inflammasome activation has been examined by a previous report (Lin *et al.,* 2014). This study describes the role of IRAK1 as being required during NLRP3-dependent caspase-1 activation in the absence of a priming step. The roles for IRAK1 suggested by this group are not in conflict with our model, as they describe the effect of IRAK1 after 30 minutes when cells were co-stimulated with LPS and ATP, whereas we describe an alternate role for IRAK1 following a long priming event.

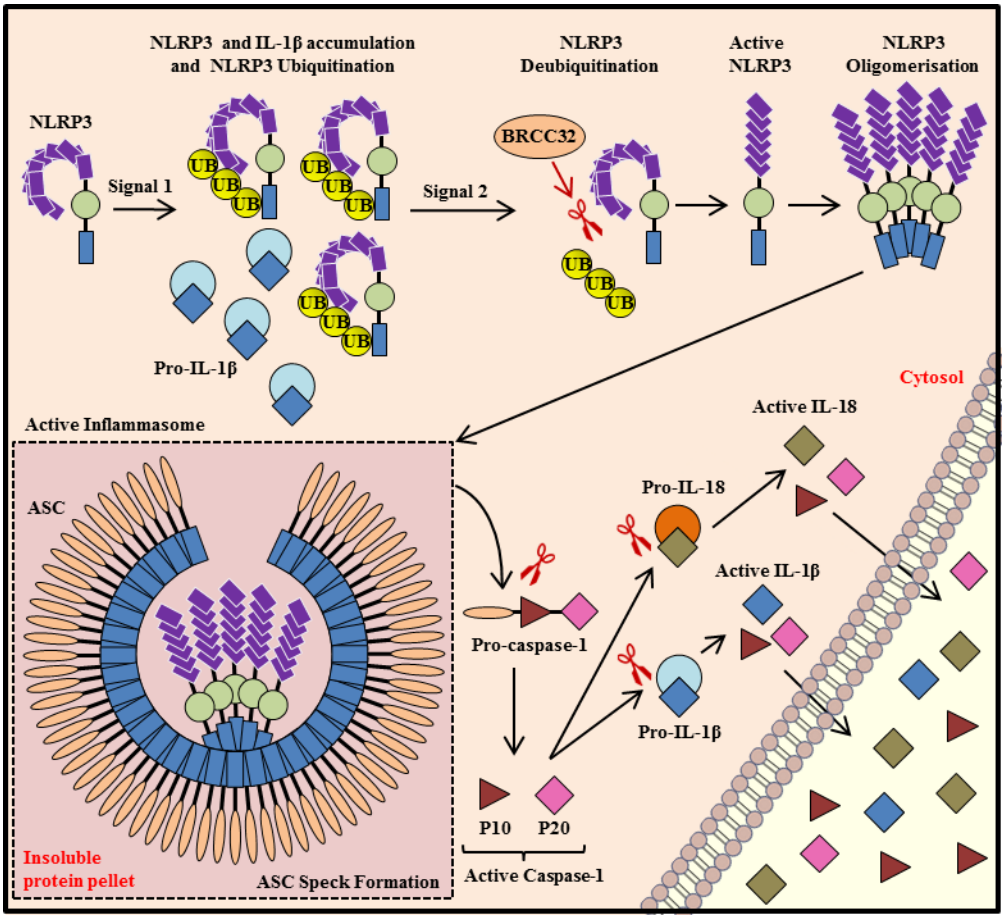

Figure 4.2 NLRP3 Inflammasome assembly and cytokine secretion

Red scissors indicate cleavage event. Dark dotted box represents the insoluble protein fraction of the cell. Yellow circles containing "UB" represent ubiquitination.

The work presented here does not specifically characterise the functional role of Pellino2 in the regulation of IRAK1. This is due to our inability to directly examine endogenous Pellino2, as no commercially available antibody could detect Pellino2. Future work will aim to address this issue by the generation of a flag-tagged Pellino2 knock-in mouse, which will give us the ability to specifically immunoprecipitate Pellino2 and examine its protein interactions with other inflammasome components, as well as examining the cellular localisation of Pellino2 following inflammasome assembly. Using this knock-in mouse, it will also be possible to examine post-translational modifications of Pellino2, such as ubiquitination and phosphorylation,

as well as determine the protein stability of Pellino2 following LPS stimulation which may provide invaluable insight into how Pellino2 is regulated.

Throughout this study, we have used IL-1β as the functional readout of inflammasome activation. However, both IL-18 activation and cellular pyroptosis are also regulated by NLRP3 inflammasome activation. IL-18 has been implicated in mediating a range of inflammatory diseases, including myocardial dysfunction (Mallat *et al.,* 2004; Woldbaek *et al.,* 2005) and inflammatory bowel disease (Banerjee and Bond, 2008). However, more recent studies have identified IL-18 as having protective effects during gastrointestinal diseases. *Nlrp3*$^{-/-}$ and *Nlrp6*$^{-/-}$ mice are more susceptible to DSS induced colitis, which is thought to be due to decreased IL-18 secretion (Doyle *et al.,* 2012; Elinav *et al.,* 2011; Hirota *et al.,* 2011). Further work is needed to fully disseminate the role of IL-18 in disease. The specialised form of inflammasome mediated cell death called pyroptosis is an important consequence of inflammasome activation. Two recent papers have demonstrated a novel role for the protein gasdermin D in mediating pyroptosis (Kayagaki *et al.,* 2015; Shi *et al.,* 2015). Gasdermin D is cleaved by either caspase-1 or caspase-11 upon inflammasome assembly, allowing the N-terminal domain of gasdermin D to drive pyroptosis. The precise mechanisms by which gasdermin D mediates pyroptosis remain to be fully elucidated. The work carried out in this thesis did not investigate IL-18 or pyroptosis in detail; however, future studies elucidating their relevance to the regulatory roles of Pellino 2 may provide further insight into the functioning of Pellino2 in NLRP3 signalling.

Dysregulation of the NLRP3 inflammasome and the resulting IL-1β release has been linked to the pathogenesis of a wide range of inflammatory diseases and is thus a potentially valuable therapeutic target. Diseases of aging are often associated with aberrant inflammasome activation. This is thought to be due to an accumulation of DAMPs such as amyloid-β, extracellular ATP and MSU which lead to chronic inflammasome activation (Kapetanovic *et al.*). For instance, NLRP3 activation has been linked with pathology in Alzheimer's disease (Heneka *et al.,* 2013) due to the ability of NLRP3 to sense amyloid-β, which stimulates the chronic activation of microglial cells (Halle *et al.,* 2008). NLRP3 deficiency was shown to reduce the

volume of amyloid-β plaques and thus protect from loss of memory in mice (Heneka *et al.*, 2013). Rheumatoid arthritis (RA) is another age-related disease and is associated with the chronic inflammation of joints; NLRP3 inflammasome activity has been shown to enhance joint destruction and further contributes to the pathology of RA (Walle *et al.*, 2014). These studies highlight the inflammasome as a potentially valuable therapeutic target in the treatment of a variety of pro-inflammatory diseases.

Anakinra, an IL-1 receptor antagonist has been used to successfully treat the symptoms of a variety of auto-inflammatory diseases, including RA (Bresnihan *et al.*, 1998). However, using Anakinra to suppress the activity of IL-1 has been linked with an increased risk of patients contracting serious infections due to a reduced ability to mount an effective immune response (Salliot *et al.*, 2009). Further, targeting circulating IL-1 does not address the underlying dysregulation of inflammasome activity, which may still function to propagate the disease by inducing pyroptosis and IL-18 secretion. Due to these issues, the ability to selectively target the inflammasome during inflammatory disease may prove to have advantageous clinical outcomes. A number of recent studies have examined small molecule inhibitors of components of the inflammasome in order to regulate its activation. CRID3 has been shown to inhibit ASC oligomerisation upon NLRP3 inflammasome activation (Coll and O'Neill, 2013, 2011) while the drug parthenolide directly inhibits NLRP3 by blocking its ATPase activity (Juliana *et al.*, 2010). Targeting the inflammasome as a therapeutic approach to disease management is still an emerging field and thus the delineation of new pathways which regulate inflammasome activation could prove vital to identifying potential drug targets.

Pellino2 may prove to be a viable therapeutic target, as it may serve to specifically regulate the NLRP3 inflammasome, while not affecting NF-κB signalling. Pellino2 deficiency does not entirely block the activity of the inflammasome, but rather hinders its full activation. Therefore, the blockade of Pellino2 may serve to regulate acute and perhaps chronic inflammasome activation without entirely abrogating its activity, which may prove beneficial in ameliorating the risk of contracting a secondary infection during drug treatment. However, in order to confirm the

potential for Pellino2 as a drug target, further studies need to be carried out describing the role of Pellino2 in human cells. To date, both Pellino1 and Pellino3 have been shown to have clinical relevance in human disease. Pellino1 was demonstrated to regulate the response of airway epithelial cells to rhinovirus (Bennett *et al.,* 2012) while Pellino3 was shown to be downregulated in the colon of patients with Crohn's disease (Yang *et al.,* 2013a). Assessing the levels of Pellino2 in patients exhibiting NLRP3 dependent inflammatory diseases such as atherosclerosis (Merhi-Soussi *et al.,* 2005) and gout (Tran *et al.,* 2013) may help delineate the role of Pellino2 in human disease. Should Pellino2 prove to have a similar function in human cells, the creation of a small molecule inhibitor of Pellino2 may be a viable method of suppressing the activity of Pellino2. Such a drug may prove useful in abating NLRP3 dependent IL-1β secrection, without fully inhibiting its signalling, hopefully resulting in a reduction of side effects usually seen with IL-1β blockade.

In conclusion, this thesis has described the importance of Pellino2 in facilitating robust NLRP3-dependent IL-1β secretion by affecting the ubiquitination state of NLRP3 during the priming signal. The possible role of IRAK1 as a regulator of NLRP3 activity has also been highlighted. Future work will be needed to describe in detail the precise mechanism by which Pellino2 modulates the activity of both IRAK1 and NLRP3 during this pathway. The biology of NLRP3 activation is a rapidly expanding and complex field and further understanding of the systems which regulate this receptor will have future clinical implications in the treatment of inflammatory diseases.

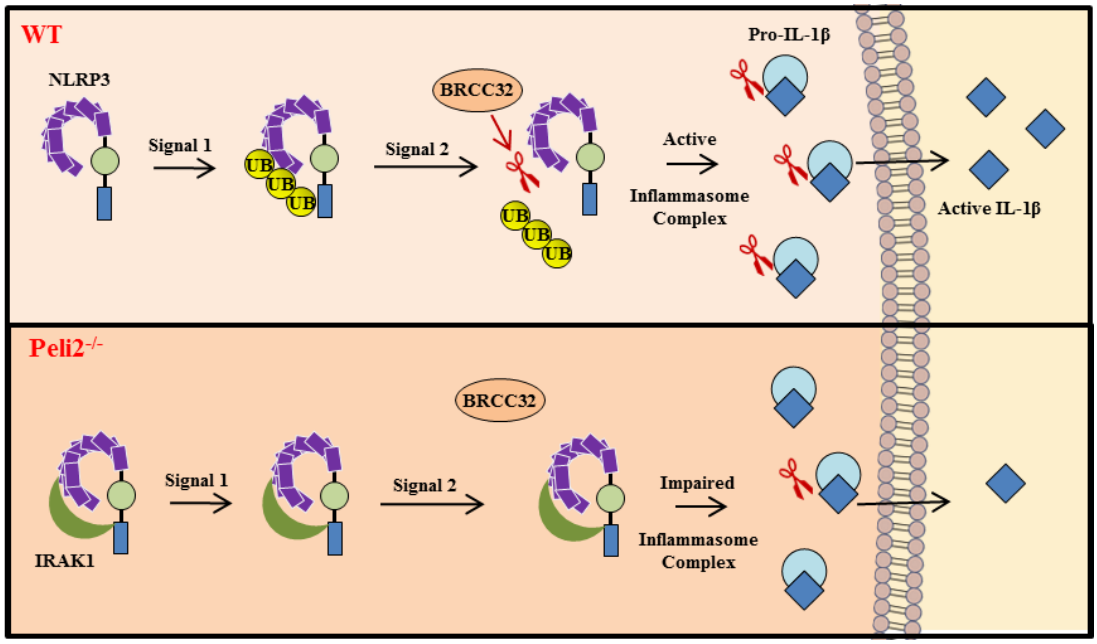

Figure 4.3 The effect of Pellino2-deficiency on NLRP3 Inflammasome assembly and cytokine secretion

Differences between WT and Pellino2 deficiency are highlighted in the discussion. Red scissors indicate a cleavage event. Yellow circles containing "UB" represent ubiquitination.

Chapter 5: Bibliography

Ablasser, A., Bauernfeind, F., Hartmann, G., Latz, E., Fitzgerald, K.A., Hornung, V., 2009. RIG-I dependent sensing of poly(dA-dT) via the induction of an RNA polymerase III transcribed RNA intermediate. *Nat. Immunol.*, **10**.

Adachi, O., Kawai, T., Takeda, K., Matsumoto, M., Tsutsui, H., Sakagami, M., Nakanishi, K., Akira, S., 1998. Targeted disruption of the MyD88 gene results in loss of IL-1- and IL-18-mediated function. *Immunity*, **9**, 143–150.

Akira, S., Uematsu, S., Takeuchi, O., 2006. Pathogen Recognition and Innate Immunity. *Cell*, **124**, 783–801.

Albrecht, M., Choubey, D., Lengauer, T., 2005. The HIN domain of IFI-200 proteins consists of two OB folds. *Biochem. Biophys. Res. Commun.*, **327**, 679–687.

Alexopoulou, L., Holt, A.C., Medzhitov, R., Flavell, R.A., 2001. Recognition of double-stranded RNA and activation of NF-κB by Toll-like receptor 3. *Nature*, **413**, 732–738.

Aliprantis, A.O., Yang, R.-B., Mark, M.R., Suggett, S., Devaux, B., Radolf, J.D., Klimpel, G.R., Godowski, P., Zychlinsky, A., 1999. Cell Activation and Apoptosis by Bacterial Lipoproteins Through Toll-like Receptor-2. *Science*, **285**, 736–739.

Anand, P.K., Malireddi, R.K.S., Lukens, J.R., Vogel, P., Bertin, J., Lamkanfi, M., Kanneganti, T.-D., 2012. NLRP6 negatively regulates innate immunity and host defence against bacterial pathogens. *Nature*, **488**, 389–393.

Anderson, K.V., Jürgens, G., Nüsslein-Volhard, C., 1985. Establishment of dorsal-ventral polarity in the Drosophila embryo: Genetic studies on the role of the Toll gene product. *Cell*, **42**, 779–789.

Balkhi, M.Y., Fitzgerald, K.A., Pitha, P.M., 2008. Functional Regulation of MyD88-Activated Interferon Regulatory Factor 5 by K63-Linked Polyubiquitination. *Mol. Cell. Biol.*, **28**, 7296–7308.

Bambou, J.-C., Giraud, A., Menard, S., Begue, B., Rakotobe, S., Heyman, M., Taddei, F., Cerf-Bensussan, N., Gaboriau-Routhiau, V., 2004. In Vitro and ex Vivo Activation of the TLR5 Signaling Pathway in Intestinal Epithelial Cells by a Commensal Escherichia coli Strain. *J. Biol. Chem.*, **279**, 42984–42992.

Banerjee, S., Bond, J.S., 2008. Prointerleukin-18 is activated by meprin beta in vitro and in vivo in intestinal inflammation. *J. Biol. Chem.*, **283**, 31371–31377.

Baroja-Mazo, A., Martín-Sánchez, F., Gomez, A.I., Martínez, C.M., Amores-Iniesta, J., Compan, V., Barberà-Cremades, M., Yagüe, J., Ruiz-Ortiz, E., Antón, J., Buján, S., Couillin, I., Brough, D., Arostegui, J.I., Pelegrín, P., 2014. The

NLRP3 inflammasome is released as a particulate danger signal that amplifies the inflammatory response. *Nat. Immunol.*, **15**, 738–748.

Bauernfeind, F., Bartok, E., Rieger, A., Franchi, L., Núñez, G., Hornung, V., 2011. Reactive oxygen species inhibitors block priming, but not activation of the NLRP3 inflammasome. *J. Immunol. Baltim. Md 1950*, **187**, 613–617.

Bauernfeind, F.G., Horvath, G., Stutz, A., Alnemri, E.S., MacDonald, K., Speert, D., Fernandes-Alnemri, T., Wu, J., Monks, B.G., Fitzgerald, K.A., Hornung, V., Latz, E., 2009. Cutting Edge: NF-κB Activating Pattern Recognition and Cytokine Receptors License NLRP3 Inflammasome Activation by Regulating NLRP3 Expression. *J. Immunol.*, **183**, 787–791.

Bauernfeind, F., Horvath, G., Stutz, A., Alnemri, E.S., MacDonald, K., Speert, D., Fernandes-Alnemri, T., Wu, J., Monks, B.G., Fitzgerald, K.A., Hornung, V., Latz, E., 2009. NF-kB activating pattern recognition and cytokine receptors license NLRP3 inflammasome activation by regulating NLRP3 expression. *J. Immunol. Baltim. Md 1950*, **183**, 787–791.

Baum, A., Sachidanandam, R., García-Sastre, A., 2010. Preference of RIG-I for short viral RNA molecules in infected cells revealed by next-generation sequencing. *Proc. Natl. Acad. Sci. U. S. A.*, **107**, 16303–16308.

Bell, J.K., Botos, I., Hall, P.R., Askins, J., Shiloach, J., Segal, D.M., Davies, D.R., 2005. The molecular structure of the Toll-like receptor 3 ligand-binding domain. *Proc. Natl. Acad. Sci. U. S. A.*, **102**, 10976–10980.

Bell, M.P., Svingen, P.A., Rahman, M.K., Xiong, Y., Faubion, W.A., 2007. Forkhead Box P3 Regulates TLR10 Expression in Human T Regulatory Cells. *J. Immunol.*, **179**, 1893–1900.

Bennett, J.A., Prince, L.R., Parker, L.C., Stokes, C.A., de Bruin, H.G., van den Berge, M., Heijink, I.H., Whyte, M.K., Sabroe, I., 2012. Pellino-1 Selectively Regulates Epithelial Cell Responses to Rhinovirus. *J. Virol.*, **86**, 6595–6604.

Berkeredjian-Ding, I.B., Wagner, M., Hornung, V., Giese, T., Schnurr, M., Endres, S., Hartmann, G., 2005. Plasmacytoid dendritic cells control TLR7 sensitivity of naive B cells via type I IFN. *J. Immunol.*, **174**, 4043–4050.

Berndsen, C.E., Wolberger, C., 2014. New insights into ubiquitin E3 ligase mechanism. *Nat. Struct. Mol. Biol.*, **21**, 301–307.

Beutler, B.A., 2011. Nobel Lecture: How Mammals Sense Infection: From Endotoxin to the Toll-like Receptors. *Nobel Media AB*,.

Bidoki, A.Z., Harsini, S., Sadr, M., Soltani, S., Mohammadzadeh, M., Najafi, S., Rezaei, N., 2016. NLRP3 gene polymorphisms in Iranian patients with recurrent aphthous stomatitis. *J. Oral Pathol. Med.*, **45**, 136–140.

Bieback, K., Lien, E., Klagge, I.M., Avota, E., Schneider-Schaulies, J., Duprex, W.P., Wagner, H., Kirschning, C.J., Ter Meulen, V., Schneider-Schaulies, S., 2002. Hemagglutinin protein of wild-type measles virus activates toll-like receptor 2 signaling. *J. Virol.*, **76**, 8729–8736.

Birmachu, W., Gleason, R.M., Bulbulian, B.J., Riter, C.L., Vasilakos, J.P., Lipson, K.E., Nikolsky, Y., 2007. Transcriptional networks in plasmacytoid dendritic cells stimulated with synthetic TLR 7 agonists. *BMC Immunol.*, **8**, 26.

Boyden, E.D., Dietrich, W.F., 2006. Nalp1b controls mouse macrophage susceptibility to anthrax lethal toxin. *Nat. Genet.*, **38**, 240–244.

Bradford, M.M., 1976. A rapid and sensitive method for the quantitation of microgram quantities of protein utilizing the principle of protein-dye binding. *Anal. Biochem.*, **72**, 248–254.

Bresnihan, B., Alvaro-Gracia, J.M., Cobby, M., Doherty, M., Domljan, Z., Emery, P., Nuki, G., Pavelka, K., Rau, R., Rozman, B., Watt, I., Williams, B., Aitchison, R., McCabe, D., Musikic, P., 1998. Treatment of rheumatoid arthritis with recombinant human interleukin-1 receptor antagonist. *Arthritis Rheum.*, **41**, 2196–2204.

Brown, G.D., Herre, J., Williams, D.L., Willment, J.A., Marshall, A.S.J., Gordon, S., 2003. Dectin-1 Mediates the Biological Effects of β-Glucans. *J. Exp. Med.*, **197**, 1119–1124.

Brown, G.D., Taylor, P.R., Reid, D.M., Willment, J.A., Williams, D.L., Martinez-Pomares, L., Wong, S.Y.C., Gordon, S., 2002. Dectin-1 Is A Major β-Glucan Receptor On Macrophages. *J. Exp. Med.*, **196**, 407–412.

Broz, P., Ruby, T., Belhocine, K., Bouley, D.M., Kayagaki, N., Dixit, V.M., Monack, D.M., 2012. Caspase-11 increases susceptibility to Salmonella infection in the absence of caspase-1. *Nature*, **490**, 288–291.

Bruey, J.-M., Bruey-Sedano, N., Luciano, F., Zhai, D., Balpai, R., Xu, C., Kress, C.L., Bailly-Maitre, B., Li, X., Osterman, A., Matsuzawa, S., Terskikh, A.V., Faustin, B., Reed, J.C., 2007. Bcl-2 and Bcl-XL Regulate Proinflammatory Caspase-1 Activation by Interaction with NALP1. *Cell*, **129**, 45–56.

Butler, M.P., Hanly, J.A., Moynagh, P.N., 2005. Pellino3 Is a Novel Upstream Regulator of p38 MAPK and Activates CREB in a p38-dependent Manner. *J. Biol. Chem.*, **280**, 27759–27768.

Butler, M.P., Hanly, J.A., Moynagh, P.N., 2007. Kinase-active Interleukin-1 Receptor-associated Kinases Promote Polyubiquitination and Degradation of the Pellino Family DIRECT EVIDENCE FOR PELLINO PROTEINS BEING UBIQUITIN-PROTEIN ISOPEPTIDE LIGASES. *J. Biol. Chem.*, **282**, 29729–29737.

Cai, X., Chen, J., Xu, H., Liu, S., Jiang, Q.-X., Halfmann, R., Chen, Z.J., 2014. Prion-like Polymerization Underlies Signal Transduction in Antiviral Immune Defense and Inflammasome Activation. *Cell*, **156**, 1207–1222.

Carswell, E.A., Old, L.J., Kassel, R.L., Green, S., Fiore, N., Williamson, B., 1975. An endotoxin-induced serum factor that causes necrosis of tumors. *Proc. Natl. Acad. Sci. U. S. A.*, **72**, 3666–3670.

Cavassani, K.A., Ishii, M., Wen, H., Schaller, M.A., Lincoln, P.M., Lukacs, N.W., Hogaboam, C.M., Kunkel, S.L., 2008. TLR3 is an endogenous sensor of tissue necrosis during acute inflammatory events. *J. Exp. Med.*, **205**, 2609–2621.

Chang, M., Jin, W., Chang, J.-H., Xiao, Y., Brittain, G.C., Yu, J., Zhou, X., Wang, Y.-H., Cheng, X., Li, P., Rabinovich, B.A., Hwu, P., Sun, S.-C., 2011. The ubiquitin ligase Peli1 negatively regulates T cell activation and prevents autoimmunity. *Nat. Immunol.*, **12**, 1002–1009.

Chang, M., Jin, W., Sun, S.-C., 2009a. Peli1 facilitates TRIF-dependent Toll-like receptor signaling and proinflammatory cytokine production. *Nat. Immunol.*, **10**, 1089–1095.

Chang, M., Jin, W., Sun, S.-C., 2009b. Peli1 facilitates TRIF-dependent Toll-like receptor signaling and proinflammatory cytokine production. *Nat. Immunol.*, **10**, 1089–1095.

Chau, V., Tobias, J.W., Bachmair, A., Marriott, D., Ecker, D.J., Gonda, D.K., Varshavsky, A., 1989. A multiubiquitin chain is confined to specific lysine in a targeted short-lived protein. *Science*, **243**, 1576–1583.

Chen, G.Y., 2014. Role of Nlrp6 and Nlrp12 in the maintenance of intestinal homeostasis. *Eur. J. Immunol.*, **44**, 321–327.

Chen, Y., Smith, M.R., Thirumalai, K., Zychlinsky, A., 1996. A bacterial invasin induces macrophage apoptosis by binding directly to ICE. *EMBO J.*, **15**, 3853–3860.

Chen, Z.J., 2005. Ubiquitin signalling in the NF-κB pathway. *Nat. Cell Biol.*, **7**, 758–765.

Chen, Z.J., Parent, L., Maniatis, T., 1996. Site-Specific Phosphorylation of IκBα by a Novel Ubiquitination-Dependent Protein Kinase Activity. *Cell*, **84**, 853–862.

Choe, J., Kelker, M.S., Wilson, I.A., 2005. Structural biology: Crystal structure of human toll-like receptor 3 (TLR3) ectodomain. *Science*, **309**, 581–585.

Choi, K.-C., Lee, Y.S., Lim, S., Choi, H.K., Lee, C.-H., Lee, E.-K., Hong, S., Kim, I.-H., Kim, S.-J., Park, S.H., 2006. Smad6 negatively regulates interleukin 1-

receptor–Toll-like receptor signaling through direct interaction with the adaptor Pellino-1. *Nat. Immunol.*, **7**, 1057–1065.

Choi, S.-H., Harkewicz, R., Lee, J.H., Boullier, A., Almazan, F., Li, A.C., Witztum, J.L., Bae, Y.S., Miller, Y.I., 2009. Lipoprotein accumulation in macrophages via toll-like receptor-4-dependent fluid phase uptake. *Circ. Res.*, **104**, 1355–1363.

Choubey, D., Walter, S., Geng, Y., Xin, H., 2000. Cytoplasmic localization of the interferon-inducible protein that is encoded by the AIM2 (absent in melanoma) gene from the 200-gene family. *FEBS Lett.*, **474**, 38–42.

Chow, J.C., Young, D.W., Golenbock, D.T., Christ, W.J., Gusovsky, F., 1999. Toll-like Receptor-4 Mediates Lipopolysaccharide-induced Signal Transduction. *J. Biol. Chem.*, **274**, 10689–10692.

Christensen, S.R., Shupe, J., Nickerson, K., Kashgarian, M., Flavell, R.A., Shlomchik, M.J., 2006. Toll-like Receptor 7 and TLR9 Dictate Autoantibody Specificity and Have Opposing Inflammatory and Regulatory Roles in a Murine Model of Lupus. *Immunity*, **25**, 417–428.

Chuang, T.-H., Ulevitch, R.J., 2001. Identification of hTLR10: a novel human Toll-like receptor preferentially expressed in immune cells. *Biochim. Biophys. Acta BBA - Gene Struct. Expr.*, **1518**, 157–161.

Chu, Z.-L., Pio, F., Xie, Z., Welsh, K., Krajewska, M., Krajewski, S., Godzik, A., Reed, J.C., 2001. A Novel Enhancer of the Apaf1 Apoptosome Involved in Cytochrome c-dependent Caspase Activation and Apoptosis. *J. Biol. Chem.*, **276**, 9239–9245.

Ciechanover, A., Elias, S., Heller, H., Hershko, A., 1982. "Covalent affinity" purification of ubiquitin-activating enzyme. *J. Biol. Chem.*, **257**, 2537–2542.

Ciehanover, A., Hod, Y., Hershko, A., 1978. A heat-stable polypeptide component of an ATP-dependent proteolytic system from reticulocytes. *Biochem. Biophys. Res. Commun.*, **81**, 1100–1105.

Coll, R.C., O'Neill, L.A.J., 2011. The Cytokine Release Inhibitory Drug CRID3 Targets ASC Oligomerisation in the NLRP3 and AIM2 Inflammasomes. *PLoS ONE*, **6**, e29539.

Coll, R.C., O'Neill, L.A.J., 2013. Correction: The Cytokine Release Inhibitory Drug CRID3 Targets ASC Oligomerisation in the NLRP3 and AIM2 Inflammasomes. *PLoS ONE*, **8**.

Conze, D.B., Wu, C.-J., Thomas, J.A., Landstrom, A., Ashwell, J.D., 2008a. Lys63-Linked Polyubiquitination of IRAK-1 Is Required for Interleukin-1 Receptor- and Toll-Like Receptor-Mediated NF-κB Activation. *Mol. Cell. Biol.*, **28**, 3538–3547.

Conze, D.B., Wu, C.-J., Thomas, J.A., Landstrom, A., Ashwell, J.D., 2008b. Lys63-Linked Polyubiquitination of IRAK-1 Is Required for Interleukin-1 Receptor- and Toll-Like Receptor-Mediated NF-κB Activation. *Mol. Cell. Biol.*, **28**, 3538–3547.

Cramer, T., Yamanishi, Y., Clausen, B.E., Förster, I., Pawlinski, R., Mackman, N., Haase, V.H., Jaenisch, R., Corr, M., Nizet, V., Firestein, G.S., Gerber, H.-P., Ferrara, N., Johnson, R.S., 2003. HIF-1α Is Essential for Myeloid Cell-Mediated Inflammation. *Cell*, **112**, 645–657.

Cruz, C.M., Rinna, A., Forman, H.J., Ventura, A.L.M., Persechini, P.M., Ojcius, D.M., 2007. ATP Activates a Reactive Oxygen Species-dependent Oxidative Stress Response and Secretion of Proinflammatory Cytokines in Macrophages. *J. Biol. Chem.*, **282**, 2871–2879.

Cullender, T.C., Chassaing, B., Janzon, A., Kumar, K., Muller, C.E., Werner, J.J., Angenent, L.T., Bell, M.E., Hay, A.G., Peterson, D.A., Walter, J., Vijay-Kumar, M., Gewirtz, A.T., Ley, R.E., 2013. Innate and Adaptive Immunity Interact to Quench Microbiome Flagellar Motility in the Gut. *Cell Host Microbe*, **14**, 571–581.

D'Costa, V.M., King, C.E., Kalan, L., Morar, M., Sung, W.W.L., Schwarz, C., Froese, D., Zazula, G., Calmels, F., Debruyne, R., Golding, G.B., Poinar, H.N., Wright, G.D., 2011. Antibiotic resistance is ancient. *Nature*, **477**, 457–461.

Demaria, O., Pagni, P.P., Traub, S., de Gassart, A., Branzk, N., Murphy, A.J., Valenzuela, D.M., Yancopoulos, G.D., Flavell, R.A., Alexopoulou, L., 2010. TLR8 deficiency leads to autoimmunity in mice. *J. Clin. Invest.*, **120**, 3651–3662.

De Nardo, D., De Nardo, C.M., Latz, E., 2014. New Insights into Mechanisms Controlling the NLRP3 Inflammasome and Its Role in Lung Disease. *Am. J. Pathol.*, **184**, 42–54.

Deng, L., Wang, C., Spencer, E., Yang, L., Braun, A., You, J., Slaughter, C., Pickart, C., Chen, Z.J., 2000. Activation of the IκB Kinase Complex by TRAF6 Requires a Dimeric Ubiquitin-Conjugating Enzyme Complex and a Unique Polyubiquitin Chain. *Cell*, **103**, 351–361.

DiDonato, J.A., Hayakawa, M., Rothwarf, D.M., Zandi, E., Karin, M., 1997. A cytokine-responsive IκB kinase that activates the transcription factor NF-κB. *Nature*, **388**, 548–554.

Diebold, S.S., Kaisho, T., Hemmi, H., Akira, S., Sousa, C.R. e, 2004. Innate Antiviral Responses by Means of TLR7-Mediated Recognition of Single-Stranded RNA. *Science*, **303**, 1529–1531.

Dinarello, C.A., 1991. Interleukin-1 and interleukin-1 antagonism. *Blood*, **77**, 1627–1652.

Dobrowolski, J.M., Sibley, L.D., 1996. Toxoplasma Invasion of Mammalian Cells Is Powered by the Actin Cytoskeleton of the Parasite. *Cell*, **84**, 933–939.

Dorner, M., Brandt, S., Tinguely, M., Zucol, F., Bourquin, J.-P., Zauner, L., Berger, C., Bernasconi, M., Speck, R.F., Nadal, D., 2009. Plasma cell toll-like receptor (TLR) expression differs from that of B cells, and plasma cell TLR triggering enhances immunoglobulin production. *Immunology*, **128**, 573–579.

Dostert, C., Pétrilli, V., Van Bruggen, R., Steele, C., Mossman, B.T., Tschopp, J., 2008. Innate Immune Activation Through Nalp3 Inflammasome Sensing of Asbestos and Silica. *Science*, **320**, 674–677.

Doyle, S.L., Campbell, M., Ozaki, E., Salomon, R.G., Mori, A., Kenna, P.F., Farrar, G.J., Kiang, A.-S., Humphries, M.M., Lavelle, E.C., O'Neill, L.A.J., Hollyfield, J.G., Humphries, P., 2012. NLRP3 has a protective role in age-related macular degeneration through the induction of IL-18 by drusen components. *Nat. Med.*, **18**, 791–798.

Dunne, A., Carpenter, S., Brikos, C., Gray, P., Strelow, A., Wesche, H., Morrice, N., O'Neill, L.A.J., 2010. IRAK1 and IRAK4 Promote Phosphorylation, Ubiquitination, and Degradation of MyD88 Adaptor-like (Mal). *J. Biol. Chem.*, **285**, 18276–18282.

Duong, B.H., Onizawa, M., Oses-Prieto, J.A., Advincula, R., Burlingame, A., Malynn, B.A., Ma, A., 2015. A20 Restricts Ubiquitination of Pro-Interleukin-1β Protein Complexes and Suppresses NLRP3 Inflammasome Activity. *Immunity*, **42**, 55–67.

Ea, C.-K., Deng, L., Xia, Z.-P., Pineda, G., Chen, Z.J., 2006. Activation of IKK by TNFα Requires Site-Specific Ubiquitination of RIP1 and Polyubiquitin Binding by NEMO. *Mol. Cell*, **22**, 245–257.

Edelmann, K.H., Richardson-Burns, S., Alexopoulou, L., Tyler, K.L., Flavell, R.A., Oldstone, M.B.A., 2004. Does Toll-like receptor 3 play a biological role in virus infections? *Virology*, **322**, 231–238.

Edwards, A.D., Diebold, S.S., Slack, E.M.C., Tomizawa, H., Hemmi, H., Kaisho, T., Akira, S., Sousa, C.R. e, 2003. Toll-like receptor expression in murine DC subsets: lack of TLR7 expression by CD8α+ DC correlates with unresponsiveness to imidazoquinolines. *Eur. J. Immunol.*, **33**, 827–833.

Elinav, E., Strowig, T., Kau, A.L., Henao-Mejia, J., Thaiss, C.A., Booth, C.J., Peaper, D.R., Bertin, J., Eisenbarth, S.C., Gordon, J.I., Flavell, R.A., 2011. NLRP6 Inflammasome Regulates Colonic Microbial Ecology and Risk for Colitis. *Cell*, **145**, 745–757.

Enesa, K., Ordureau, A., Smith, H., Barford, D., Cheung, P.C.F., Patterson-Kane, J., Arthur, J.S.C., Cohen, P., 2012. Pellino1 Is Required for Interferon Production by Viral Double-stranded RNA. *J. Biol. Chem.*, **287**, 34825–34835.

Farhat, K., Riekenberg, S., Heine, H., Debarry, J., Lang, R., Mages, J., Buwitt-Beckmann, U., Röschmann, K., Jung, G., Wiesmüller, K.-H., Ulmer, A.J., 2008. Heterodimerization of TLR2 with TLR1 or TLR6 expands the ligand spectrum but does not lead to differential signaling. *J. Leukoc. Biol.*, **83**, 692–701.

Faustin, B., Lartigue, L., Bruey, J.-M., Luciano, F., Sergienko, E., Bailly-Maitre, B., Volkmann, N., Hanein, D., Rouiller, I., Reed, J.C., 2007. Reconstituted NALP1 Inflammasome Reveals Two-Step Mechanism of Caspase-1 Activation. *Mol. Cell*, **25**, 713–724.

Feldmeyer, L., Keller, M., Niklaus, G., Hohl, D., Werner, S., Beer, H.-D., 2007. The Inflammasome Mediates UVB-Induced Activation and Secretion of Interleukin-1β by Keratinocytes. *Curr. Biol.*, **17**, 1140–1145.

Fenchel, T., Thar, R., 2004. "Candidatus Ovobacter propellens": a large conspicuous prokaryote with an unusual motility behaviour. *FEMS Microbiol. Ecol.*, **48**, 231–238.

Fernandes-Alnemri, T., Kang, S., Anderson, C., Sagara, J., Fitzgerald, K.A., Alnemri, E.S., 2013. Toll-Like Receptor Signaling Licenses IRAK1 For Rapid Activation Of The NLRP3 Inflammasome. *J. Immunol. Baltim. Md 1950*, **191**, 3995–3999.

Fernandes-Alnemri, T., Yu, J.-W., Juliana, C., Solorzano, L., Kang, S., Wu, J., Datta, P., McCormick, M., Huang, L., McDermott, E., Eisenlohr, L., Landel, C.P., Alnemri, E.S., 2010. The AIM2 inflammasome is critical for innate immunity against Francisella tularensis. *Nat. Immunol.*, **11**, 385–393.

Fernandes-Alnemri, T., Yu, J.-W., Wu, J., Datta, P., Alnemri, E.S., 2009. AIM2 activates the inflammasome and cell death in response to cytoplasmic DNA. *Nature*, **458**, 509–513.

Ferwerda, G., Kramer, M., de Jong, D., Piccini, A., Joosten, L.A., DevesaGiner, I., Girardin, S.E., Adema, G.J., van der Meer, J.W.M., Kullberg, B.-J., Rubartelli, A., Netea, M.G., 2008. Engagement of NOD2 has a dual effect on proIL-1β mRNA transcription and secretion of bioactive IL-1β. *Eur. J. Immunol.*, **38**, 184–191.

Fink, S.L., Cookson, B.T., 2006. Caspase-1-dependent pore formation during pyroptosis leads to osmotic lysis of infected host macrophages. *Cell. Microbiol.*, **8**, 1812–1825.

Fitzgerald, K.A., McWhirter, S.M., Faia, K.L., Rowe, D.C., Latz, E., Golenbock, D.T., Coyle, A.J., Liao, S.-M., Maniatis, T., 2003. IKKε and TBK1 are essential components of the IRF3 signaling pathway. *Nat. Immunol.*, **4**, 491–496.

Fitzgerald, K.A., Palsson-McDermott, E.M., Bowie, A.G., Jefferies, C.A., Mansell, A.S., Brady, G., Brint, E., Dunne, A., Gray, P., Harte, M.T., McMurray, D.,

Smith, D.E., Sims, J.E., Bird, T.A., O'Neill, L.A.J., 2001. Mal (MyD88-adapter-like) is required for Toll-like receptor-4 signal transduction. *Nature*, **413**, 78–83.

Flynn, J.L., Goldstein, M.M., Chan, J., Triebold, K.J., Pfeffer, K., Lowenstein, C.J., Schrelber, R., Mak, T.W., Bloom, B.R., 1995. Tumor necrosis factor-α is required in the protective immune response against mycobacterium tuberculosis in mice. *Immunity*, **2**, 561–572.

Franchi, L., Amer, A., Body-Malapel, M., Kanneganti, T.-D., Özören, N., Jagirdar, R., Inohara, N., Vandenabeele, P., Bertin, J., Coyle, A., Grant, E.P., Núñez, G., 2006. Cytosolic flagellin requires Ipaf for activation of caspase-1 and interleukin 1β in salmonella-infected macrophages. *Nat. Immunol.*, **7**, 576–582.

Franchi, L., Núñez, G., 2008. The Nlrp3 inflammasome is critical for aluminium hydroxide-mediated IL-1beta secretion but dispensable for adjuvant activity. *Eur. J. Immunol.*, **38**, 2085–2089.

Fujiuchi, N., Aglipay, J.A., Ohtsuka, T., Maehara, N., Sahin, F., Su, G.H., Lee, S.W., Ouchi, T., 2004. Requirement of IFI16 for the Maximal Activation of p53 Induced by Ionizing Radiation. *J. Biol. Chem.*, **279**, 20339–20344.

Galán, J.E., Wolf-Watz, H., 2006. Protein delivery into eukaryotic cells by type III secretion machines. *Nature*, **444**, 567–573.

Ganguly, D., Chamilos, G., Lande, R., Gregorio, J., Meller, S., Facchinetti, V., Homey, B., Barrat, F.J., Zal, T., Gilliet, M., 2009. Self-RNA–antimicrobial peptide complexes activate human dendritic cells through TLR7 and TLR8. *J. Exp. Med.*, **206**, 1983–1994.

Ganley-Leal, L.M., Liu, X., Wetzler, L.M., 2006. Toll-like receptor 2-mediated human B cell differentiation. *Clin. Immunol.*, **120**, 272–284.

Gantner, B.N., Simmons, R.M., Canavera, S.J., Akira, S., Underhill, D.M., 2003. Collaborative Induction of Inflammatory Responses by Dectin-1 and Toll-like Receptor 2. *J. Exp. Med.*, **197**, 1107–1117.

Ge, J., Gong, Y.-N., Xu, Y., Shao, F., 2012. Preventing bacterial DNA release and absent in melanoma 2 inflammasome activation by a Legionella effector functioning in membrane trafficking. *Proc. Natl. Acad. Sci. U. S. A.*, **109**, 6193–6198.

Gerlach, B., Cordier, S.M., Schmukle, A.C., Emmerich, C.H., Rieser, E., Haas, T.L., Webb, A.I., Rickard, J.A., Anderton, H., Wong, W.W.-L., Nachbur, U., Gangoda, L., Warnken, U., Purcell, A.W., Silke, J., Walczak, H., 2011. Linear ubiquitination prevents inflammation and regulates immune signalling. *Nature*, **471**, 591–596.

Girardin, S.E., Boneca, I.G., Viala, J., Chamaillard, M., Labigne, A., Thomas, G., Philpott, D.J., Sansonetti, P.J., 2003. Nod2 is a general sensor of peptidoglycan through muramyl dipeptide (MDP) detection. *J. Biol. Chem.*, **278**, 8869–8872.

Gitlin, L., Barchet, W., Gilfillan, S., Cella, M., Beutler, B., Flavell, R.A., Diamond, M.S., Colonna, M., 2006. Essential role of mda-5 in type I IFN responses to polyriboinosinic:polyribocytidylic acid and encephalomyocarditis picornavirus. *Proc. Natl. Acad. Sci.*, **103**, 8459–8464.

Gong, Y.-N., Wang, X., Wang, J., Yang, Z., Li, S., Yang, J., Liu, L., Lei, X., Shao, F., 2010. Chemical probing reveals insights into the signaling mechanism of inflammasome activation. *Cell Res.*, **20**, 1289–1305.

Gong, Z., Zhou, J., Li, H., Gao, Y., Xu, C., Zhao, S., Chen, Y., Cai, W., Wu, J., 2015. Curcumin suppresses NLRP3 inflammasome activation and protects against LPS-induced septic shock. *Mol. Nutr. Food Res.*, n/a–n/a.

Gorbea, C., Makar, K.A., Pauschinger, M., Pratt, G., Bersola, J.L.F., Varela, J., David, R.M., Banks, L., Huang, C.-H., Li, H., Schultheiss, H.-P., Towbin, J.A., Vallejo, J.G., Bowles, N.E., 2010. A Role for Toll-like Receptor 3 Variants in Host Susceptibility to Enteroviral Myocarditis and Dilated Cardiomyopathy. *J. Biol. Chem.*, **285**, 23208–23223.

Grenier, J.M., Wang, L., Manji, G.A., Huang, W.-J., Al-Garawi, A., Kelly, R., Carlson, A., Merriam, S., Lora, J.M., Briskin, M., DiStefano, P.S., Bertin, J., 2002. Functional screening of five PYPAF family members identifies PYPAF5 as a novel regulator of NF-κB and caspase-1. *FEBS Lett.*, **530**, 73–78.

Großhans, J., Schnorrer, F., Nüsslein-Volhard, C., 1999. Oligomerisation of Tube and Pelle leads to nuclear localisation of Dorsal. *Mech. Dev.*, **81**, 127–138.

Gross, O., Poeck, H., Bscheider, M., Dostert, C., Hannesschläger, N., Endres, S., Hartmann, G., Tardivel, A., Schweighoffer, E., Tybulewicz, V., Mocsai, A., Tschopp, J., Ruland, J., 2009. Syk kinase signalling couples to the Nlrp3 inflammasome for anti-fungal host defence. *Nature*, **459**, 433–436.

Guan, K., Wei, C., Zheng, Z., Song, T., Wu, F., Zhang, Y., Cao, Y., Ma, S., Chen, W., Xu, Q., Xia, W., Gu, J., He, X., Zhong, H., 2015. MAVS Promotes Inflammasome Activation by Targeting ASC for K63-Linked Ubiquitination via the E3 Ligase TRAF3. *J. Immunol. Baltim. Md 1950*, **194**, 4880–4890.

Guan, Y., Ranoa, D.R.E., Jiang, S., Mutha, S.K., Li, X., Baudry, J., Tapping, R.I., 2010. Human TLRs 10 and 1 Share Common Mechanisms of Innate Immune Sensing but Not Signaling. *J. Immunol.*, **184**, 5094–5103.

Guilliams, M., Ginhoux, F., Jakubzick, C., Naik, S.H., Onai, N., Schraml, B.U., Segura, E., Tussiwand, R., Yona, S., 2014. Dendritic cells, monocytes and

macrophages: a unified nomenclature based on ontogeny. *Nat. Rev. Immunol.*, **14**, 571–578.

Gunn, J.S., Lim, K.B., Krueger, J., Kim, K., Guo, L., Hackett, M., Miller, S.I., 1998. PmrA–PmrB-regulated genes necessary for 4-aminoarabinose lipid A modification and polymyxin resistance. *Mol. Microbiol.*, **27**, 1171–1182.

Guo, H., Callaway, J.B., Ting, J.P.-Y., 2015. Inflammasomes: mechanism of action, role in disease, and therapeutics. *Nat. Med.*, **21**, 677–687.

Guo, L., Lim, K.B., Poduje, C.M., Daniel, M., Gunn, J.S., Hackett, M., Miller, S.I., 1998. Lipid A Acylation and Bacterial Resistance against Vertebrate Antimicrobial Peptides. *Cell*, **95**, 189–198.

Hajjar, A.M., Ernst, R.K., Tsai, J.H., Wilson, C.B., Miller, S.I., 2002. Human Toll-like receptor 4 recognizes host-specific LPS modifications. *Nat. Immunol.*, **3**, 354–359.

Halle, A., Hornung, V., Petzold, G.C., Stewart, C.R., Monks, B.G., Reinheckel, T., Fitzgerald, K.A., Latz, E., Moore, K.J., Golenbock, D.T., 2008. The NALP3 inflammasome is involved in the innate immune response to amyloid-β. *Nat. Immunol.*, **9**, 857–865.

Hara, H., Tsuchiya, K., Kawamura, I., Fang, R., Hernandez-Cuellar, E., Shen, Y., Mizuguchi, J., Schweighoffer, E., Tybulewicz, V., Mitsuyama, M., 2013. Phosphorylation of the adaptor ASC acts as a molecular switch that controls the formation of speck-like aggregates and inflammasome activity. *Nat. Immunol.*, **14**, 1247–1255.

Hardarson, H.S., Baker, J.S., Yang, Z., Purevjav, E., Huang, C.-H., Alexopoulou, L., Li, N., Flavell, R.A., Bowles, N.E., Vallejo, J.G., 2007. Toll-like receptor 3 is an essential component of the innate stress response in virus-induced cardiac injury. *Am. J. Physiol. - Heart Circ. Physiol.*, **292**, H251–H258.

Hardiman, G., Rock, F.L., Balasubramanian, S., Kastelein, R.A., Bazan, J.F., 1996. Molecular characterization and modular analysis of human MyD88. *Oncogene*, **13**, 2467–2475.

Hasan, U., Chaffois, C., Gaillard, C., Saulnier, V., Merck, E., Tancredi, S., Guiet, C., Brière, F., Vlach, J., Lebecque, S., Trinchieri, G., Bates, E.E.M., 2005. Human TLR10 Is a Functional Receptor, Expressed by B Cells and Plasmacytoid Dendritic Cells, Which Activates Gene Transcription through MyD88. *J. Immunol.*, **174**, 2942–2950.

Hawn, T.R., Scholes, D., Li, S.S., Wang, H., Yang, Y., Roberts, P.L., Stapleton, A.E., Janer, M., Aderem, A., Stamm, W.E., Zhao, L.P., Hooton, T.M., 2009. Toll-Like Receptor Polymorphisms and Susceptibility to Urinary Tract Infections in Adult Women. *PLoS ONE*, **4**, e5990.

Hawn, T.R., Verbon, A., Lettinga, K.D., Zhao, L.P., Li, S.S., Laws, R.J., Skerrett, S.J., Beutler, B., Schroeder, L., Nachman, A., Ozinsky, A., Smith, K.D., Aderem, A., 2003. A Common Dominant TLR5 Stop Codon Polymorphism Abolishes Flagellin Signaling and Is Associated with Susceptibility to Legionnaires' Disease. *J. Exp. Med.*, **198**, 1563–1572.

Hayashi, F., Means, T.K., Luster, A.D., 2003. Toll-like receptors stimulate human neutrophil function. *Blood*, **102**, 2660–2669.

Hayashi, F., Smith, K.D., Ozinsky, A., Hawn, T.R., Yi, E.C., Goodlett, D.R., Eng, J.K., Akira, S., Underhill, D.M., Aderem, A., 2001. The innate immune response to bacterial flagellin is mediated by Toll-like receptor 5. *Nature*, **410**, 1099–1103.

Heil, F., Ahmad-Nejad, P., Hemmi, H., Hochrein, H., Ampenberger, F., Gellert, T., Dietrich, H., Lipford, G., Takeda, K., Akira, S., Wagner, H., Bauer, S., 2003. The Toll-like receptor 7 (TLR7)-specific stimulus loxoribine uncovers a strong relationship within the TLR7, 8 and 9 subfamily. *Eur. J. Immunol.*, **33**, 2987–2997.

Heil, F., Hemmi, H., Hochrein, H., Ampenberger, F., Kirschning, C., Akira, S., Lipford, G., Wagner, H., Bauer, S., 2004. Species-Specific Recognition of Single-Stranded RNA via Toll-like Receptor 7 and 8. *Science*, **303**, 1526–1529.

Heine, H., Kirschning, C.J., Lien, E., Monks, B.G., Rothe, M., Golenbock, D.T., 1999. Cutting Edge: Cells That Carry A Null Allele for Toll-Like Receptor 2 Are Capable of Responding to Endotoxin. *J. Immunol.*, **162**, 6971–6975.

Hemmi, H., Kaisho, T., Takeda, K., Akira, S., 2003. The roles of Toll-like receptor 9, MyD88, and DNA-dependent protein kinase catalytic subunit in the effects of two distinct CpG DNAs on dendritic cell subsets. *J. Immunol. Baltim. Md 1950*, **170**, 3059–3064.

Hemmi, H., Kaisho, T., Takeuchi, O., Sato, S., Sanjo, H., Hoshino, K., Horiuchi, T., Tomizawa, H., Takeda, K., Akira, S., 2002. Small anti-viral compounds activate immune cells via the TLR7 MyD88–dependent signaling pathway. *Nat. Immunol.*, **3**, 196–200.

Hemmi, H., Takeuchi, O., Kawai, T., Kaisho, T., Sato, S., Sanjo, H., Matsumoto, M., Hoshino, K., Wagner, H., Takeda, K., Akira, S., 2000. A Toll-like receptor recognizes bacterial DNA. *Nature*, **408**, 740–745.

Heneka, M.T., Kummer, M.P., Stutz, A., Delekate, A., Schwartz, S., Vieira-Saecker, A., Griep, A., Axt, D., Remus, A., Tzeng, T.-C., Gelpi, E., Halle, A., Korte, M., Latz, E., Golenbock, D.T., 2013. NLRP3 is activated in Alzheimer/'s disease and contributes to pathology in APP/PS1 mice. *Nature*, **493**, 674–678.

Hershko, A., Ciechanover, A., Heller, H., Haas, A.L., Rose, I.A., 1980. Proposed role of ATP in protein breakdown: conjugation of protein with multiple chains of the polypeptide of ATP-dependent proteolysis. *Proc. Natl. Acad. Sci. U. S. A.*, **77**, 1783–1786.

Hershko, A., Heller, H., Elias, S., Ciechanover, A., 1983. Components of ubiquitin-protein ligase system. Resolution, affinity purification, and role in protein breakdown. *J. Biol. Chem.*, **258**, 8206–8214.

Hewinson, J., Moore, S.F., Glover, C., Watts, A.G., MacKenzie, A.B., 2008. A Key Role for Redox Signaling in Rapid P2X7 Receptor-Induced IL-1β Processing in Human Monocytes. *J. Immunol.*, **180**, 8410–8420.

He, Y., Franchi, L., Núñez, G., 2013. The protein kinase PKR is critical for LPS-induced iNOS production but dispensable for inflammasome activation in macrophages. *Eur. J. Immunol.*, **43**, 1147–1152.

Hirota, S.A., Ng, J., Lueng, A., Khajah, M., Parhar, K., Li, Y., Lam, V., Potentier, M.S., Ng, K., Bawa, M., McCafferty, D.-M., Rioux, K.P., Ghosh, S., Xavier, R.J., Colgan, S.P., Tschopp, J., Muruve, D., MacDonald, J.A., Beck, P.L., 2011. NLRP3 inflammasome plays a key role in the regulation of intestinal homeostasis. *Inflamm. Bowel Dis.*, **17**, 1359–1372.

Hochrein, H., Schlatter, B., O'Keeffe, M., Wagner, C., Schmitz, F., Schiemann, M., Bauer, S., Suter, M., Wagner, H., 2004. Herpes simplex virus type-1 induces IFN-α production via Toll-like receptor 9-dependent and -independent pathways. *Proc. Natl. Acad. Sci. U. S. A.*, **101**, 11416–11421.

Hochstrasser, M., 2006. Lingering Mysteries of Ubiquitin-Chain Assembly. *Cell*, **124**, 27–34.

Hoebe, K., Du, X., Georgel, P., Janssen, E., Tabeta, K., Kim, S.O., Goode, J., Lin, P., Mann, N., Mudd, S., Crozat, K., Sovath, S., Han, J., Beutler, B., 2003. Identification of Lps2 as a key transducer of MyD88-independent TIR signalling. *Nature*, **424**, 743–748.

Hoebe, K., Georgel, P., Rutschmann, S., Du, X., Mudd, S., Crozat, K., Sovath, S., Shamel, L., Hartung, T., Zähringer, U., Beutler, B., 2005. CD36 is a sensor of diacylglycerides. *Nature*, **433**, 523–527.

Honda, K., Yanai, H., Negishi, H., Asagiri, M., Sato, M., Mizutani, T., Shimada, N., Ohba, Y., Takaoka, A., Yoshida, N., Taniguchi, T., 2005. IRF-7 is the master regulator of type-I interferon-dependent immune responses. *Nature*, **434**, 772–777.

Hornung, V., Ablasser, A., Charrel-Dennis, M., Bauernfeind, F., Horvath, G., Caffrey, D.R., Latz, E., Fitzgerald, K.A., 2009. AIM2 recognizes cytosolic dsDNA and forms a caspase-1-activating inflammasome with ASC. *Nature*, **458**, 514–518.

Hornung, V., Bauernfeind, F., Halle, A., Samstad, E.O., Kono, H., Rock, K.L., Fitzgerald, K.A., Latz, E., 2008. Silica crystals and aluminum salts activate the NALP3 inflammasome through phagosomal destabilization. *Nat. Immunol.*, **9**, 847–856.

Horvath, G.L., Schrum, J.E., De Nardo, C.M., Latz, E., 2011. Intracellular sensing of microbes and danger signals by the inflammasomes. *Immunol. Rev.*, **243**, 119–135.

Hoshino, K., Takeuchi, O., Kawai, T., Sanjo, H., Ogawa, T., Takeda, Y., Takeda, K., Akira, S., 1999. Cutting Edge: Toll-Like Receptor 4 (TLR4)-Deficient Mice Are Hyporesponsive to Lipopolysaccharide: Evidence for TLR4 as the Lps Gene Product. *J. Immunol.*, **162**, 3749–3752.

Hotta, K., Takahashi, H., Asakura, T., Saitoh, B., Takatori, N., Satou, Y., Satoh, N., 2000. Characterization of Brachyury-Downstream Notochord Genes in the Ciona intestinalis Embryo. *Dev. Biol.*, **224**, 69–80.

Hsu, H., Huang, J., Shu, H.-B., Baichwal, V., Goeddel, D.V., 1996. TNF-Dependent Recruitment of the Protein Kinase RIP to the TNF Receptor-1 Signaling Complex. *Immunity*, **4**, 387–396.

Hua, K.-F., Yang, F.-L., Chiu, H.-W., Chou, J.-C., Dong, W.-C., Lin, C.-N., Lin, C.-Y., Wang, J.-T., Li, L.-H., Chiu, H.-W., Chiu, Y.-C., Wu, S.-H., 2015. Capsular polysaccharide is involved in NLRP3 inflammasome activation by Klebsiella pneumoniae serotype K1. *Infect. Immun.*, IAI.00125–15.

Hu, B., Elinav, E., Huber, S., Strowig, T., Hao, L., Hafemann, A., Jin, C., Wunderlich, C., Wunderlich, T., Eisenbarth, S.C., Flavell, R.A., 2013. Microbiota-induced activation of epithelial IL-6 signaling links inflammasome-driven inflammation with transmissible cancer. *Proc. Natl. Acad. Sci.*, **110**, 9862–9867.

Humphries, F., Moynagh, P.N., 2015. Molecular and physiological roles of Pellino E3 ubiquitin ligases in immunity. *Immunol. Rev.*, **266**, 93–108.

Hu, Z., Yan, C., Liu, P., Huang, Z., Ma, R., Zhang, C., Wang, R., Zhang, Y., Martinon, F., Miao, D., Deng, H., Wang, J., Chang, J., Chai, J., 2013. Crystal Structure of NLRC4 Reveals Its Autoinhibition Mechanism. *Science*, **341**, 172–175.

Inohara, N., Ogura, Y., Chen, F.F., Muto, A., Nuñez, G., 2001. Human Nod1 Confers Responsiveness to Bacterial Lipopolysaccharides. *J. Biol. Chem.*, **276**, 2551–2554.

Iyer, S.S., He, Q., Janczy, J.R., Elliott, E.I., Zhong, Z., Olivier, A.K., Sadler, J.J., Knepper-Adrian, V., Han, R., Qiao, L., Eisenbarth, S.C., Nauseef, W.M., Cassel, S.L., Sutterwala, F.S., 2013. Mitochondrial Cardiolipin Is Required for Nlrp3 Inflammasome Activation. *Immunity*, **39**, 311–323.

Janeway, C.A., 1989. Approaching the Asymptote? Evolution and Revolution in Immunology. Cold Spring Harb. Symp. Quant. Biol. 54, 1–13.

Jensen, L.E., Whitehead, A.S., 2003a. Pellino3, a Novel Member of the Pellino Protein Family, Promotes Activation of c-Jun and Elk-1 and May Act as a Scaffolding Protein. *J. Immunol.*, **171**, 1500–1506.

Jensen, L.E., Whitehead, A.S., 2003b. Pellino2 activates the mitogen activated protein kinase pathway. *FEBS Lett.*, **545**, 199–202.

Jiang, Z., Johnson, H.J., Nie, H., Qin, J., Bird, T.A., Li, X., 2003. Pellino 1 Is Required for Interleukin-1 (IL-1)-mediated Signaling through Its Interaction with the IL-1 Receptor-associated Kinase 4 (IRAK4)-IRAK-Tumor Necrosis Factor Receptor-associated Factor 6 (TRAF6) Complex. *J. Biol. Chem.*, **278**, 10952–10956.

Jin, J., Li, X., Gygi, S.P., Harper, J.W., 2007. Dual E1 activation systems for ubiquitin differentially regulate E2 enzyme charging. *Nature*, **447**, 1135–1138.

Jin, M.S., Kim, S.E., Heo, J.Y., Lee, M.E., Kim, H.M., Paik, S.-G., Lee, H., Lee, J.-O., 2007. Crystal Structure of the TLR1-TLR2 Heterodimer Induced by Binding of a Tri-Acylated Lipopeptide. *Cell*, **130**, 1071–1082.

Jin, T., Perry, A., Jiang, J., Smith, P., Curry, J.A., Unterholzner, L., Jiang, Z., Horvath, G., Rathinam, V.A., Johnstone, R.W., Hornung, V., Latz, E., Bowie, A.G., Fitzgerald, K.A., Xiao, T.S., 2012. Structures of the HIN Domain:DNA Complexes Reveal Ligand Binding and Activation Mechanisms of the AIM2 Inflammasome and IFI16 Receptor. *Immunity*, **36**, 561–571.

Jin, T., Perry, A., Smith, P., Jiang, J., Xiao, T.S., 2013. Structure of the Absent in Melanoma 2 (AIM2) Pyrin Domain Provides Insights into the Mechanisms of AIM2 Autoinhibition and Inflammasome Assembly. *J. Biol. Chem.*, **288**, 13225–13235.

Jin, Y., Mailloux, C.M., Gowan, K., Riccardi, S.L., LaBerge, G., Bennett, D.C., Fain, P.R., Spritz, R.A., 2007. NALP1 in Vitiligo-Associated Multiple Autoimmune Disease. *N. Engl. J. Med.*, **356**, 1216–1225.

Juliana, C., Fernandes-Alnemri, T., Kang, S., Farias, A., Qin, F., Alnemri, E.S., 2012. Non-transcriptional Priming and Deubiquitination Regulate NLRP3 Inflammasome Activation. *J. Biol. Chem.*, **287**, 36617–36622.

Juliana, C., Fernandes-Alnemri, T., Wu, J., Datta, P., Solorzano, L., Yu, J.-W., Meng, R., Quong, A.A., Latz, E., Scott, C.P., Alnemri, E.S., 2010. Anti-inflammatory Compounds Parthenolide and Bay 11-7082 Are Direct Inhibitors of the Inflammasome. *J. Biol. Chem.*, **285**, 9792–9802.

Kagan, J.C., Su, T., Horng, T., Chow, A., Akira, S., Medzhitov, R., 2008. TRAM couples endocytosis of Toll-like receptor 4 to the induction of interferon-β. *Nat. Immunol.*, **9**, 361–368.

Kahlenberg, J.M., Dubyak, G.R., 2004. Differing caspase-1 activation states in monocyte versus macrophage models of IL-1β processing and release. *J. Leukoc. Biol.*, **76**, 676–684.

Kahlenberg, J.M., Thacker, S.G., Berthier, C.C., Cohen, C.D., Kretzler, M., Kaplan, M.J., 2011. Inflammasome Activation of IL-18 Results in Endothelial Progenitor Cell Dysfunction in Systemic Lupus Erythematosus. *J. Immunol.*, **187**, 6143–6156.

Kamio, Y., Nikaido, H., 1976. Outer membrane of Salmonella typhimurium: accessibility of phospholipid head groups to phospholipase c and cyanogen bromide activated dextran in the external medium. *Biochemistry (Mosc.)*, **15**, 2561–2570.

Kanayama, A., Seth, R.B., Sun, L., Ea, C.-K., Hong, M., Shaito, A., Chiu, Y.-H., Deng, L., Chen, Z.J., 2004. TAB2 and TAB3 Activate the NF-κB Pathway through Binding to Polyubiquitin Chains. *Mol. Cell*, **15**, 535–548.

Kang, J.Y., Nan, X., Jin, M.S., Youn, S.-J., Ryu, Y.H., Mah, S., Han, S.H., Lee, H., Paik, S.-G., Lee, J.-O., 2009. Recognition of Lipopeptide Patterns by Toll-like Receptor 2-Toll-like Receptor 6 Heterodimer. *Immunity*, **31**, 873–884.

Kang, S., Fernandes-Alnemri, T., Rogers, C., Mayes, L., Wang, Y., Dillon, C., Roback, L., Kaiser, W., Oberst, A., Sagara, J., Fitzgerald, K.A., Green, D.R., Zhang, J., Mocarski, E.S., Alnemri, E.S., 2015. Caspase-8 scaffolding function and MLKL regulate NLRP3 inflammasome activation downstream of TLR3. *Nat. Commun.*, **6**.

Kapetanovic, R., Bokil, N.J., Sweet, M.J., n.d. Innate immune perturbations, accumulating DAMPs and inflammasome dysregulation: A ticking time bomb in ageing. *Ageing Res. Rev.*,.

Kapsenberg, M.L., 2003. Dendritic-cell control of pathogen-driven T-cell polarization. *Nat. Rev. Immunol.*, **3**, 984–993.

Karikó, K., Ni, H., Capodici, J., Lamphier, M., Weissman, D., 2004. mRNA Is an Endogenous Ligand for Toll-like Receptor 3. *J. Biol. Chem.*, **279**, 12542–12550.

Kawai, T., Akira, S., 2009. The roles of TLRs, RLRs and NLRs in pathogen recognition ARTICLE. *Int. Immunol.*, **21**, 317–337.

Kawai, T., Sato, S., Ishii, K.J., Coban, C., Hemmi, H., Yamamoto, M., Terai, K., Matsuda, M., Inoue, J., Uematsu, S., Takeuchi, O., Akira, S., 2004. Interferon-α induction through Toll-like receptors involves a direct interaction of IRF7 with MyD88 and TRAF6. *Nat. Immunol.*, **5**, 1061–1068.

Kawai, T., Takahashi, K., Sato, S., Coban, C., Kumar, H., Kato, H., Ishii, K.J., Takeuchi, O., Akira, S., 2005. IPS-1, an adaptor triggering RIG-I- and Mda5-mediated type I interferon induction. *Nat. Immunol.*, **6**, 981–988.

Kayagaki, N., Stowe, I.B., Lee, B.L., O'Rourke, K., Anderson, K., Warming, S., Cuellar, T., Haley, B., Roose-Girma, M., Phung, Q.T., Liu, P.S., Lill, J.R., Li, H., Wu, J., Kummerfeld, S., Zhang, J., Lee, W.P., Snipas, S.J., Salvesen, G.S., Morris, L.X., Fitzgerald, L., Zhang, Y., Bertram, E.M., Goodnow, C.C., Dixit, V.M., 2015. Caspase-11 cleaves gasdermin D for non-canonical inflammasome signaling. *Nature*, **advance online publication**.

Kayagaki, N., Warming, S., Lamkanfi, M., Walle, L.V., Louie, S., Dong, J., Newton, K., Qu, Y., Liu, J., Heldens, S., Zhang, J., Lee, W.P., Roose-Girma, M., Dixit, V.M., 2011. Non-canonical inflammasome activation targets caspase-11. *Nature*, **479**, 117–121.

Kayagaki, N., Wong, M.T., Stowe, I.B., Ramani, S.R., Gonzalez, L.C., Akashi-Takamura, S., Miyake, K., Zhang, J., Lee, W.P., Muszyński, A., Forsberg, L.S., Carlson, R.W., Dixit, V.M., 2013. Noncanonical Inflammasome Activation by Intracellular LPS Independent of TLR4. *Science*, **341**, 1246–1249.

Keller, M., Rüegg, A., Werner, S., Beer, H.-D., 2008. Active Caspase-1 Is a Regulator of Unconventional Protein Secretion. *Cell*, **132**, 818–831.

Kerkhof, P. van, Govers, R., Santos, C.M.A. dos, Strous, G.J., 2000. Endocytosis and Degradation of the Growth Hormone Receptor Are Proteasome-dependent. *J. Biol. Chem.*, **275**, 1575–1580.

Kerur, N., Veettil, M.V., Sharma-Walia, N., Bottero, V., Sadagopan, S., Otageri, P., Chandran, B., 2011. IFI16 Acts as a Nuclear Pathogen Sensor to Induce the Inflammasome in Response to Kaposi Sarcoma-Associated Herpesvirus Infection. *Cell Host Microbe*, **9**, 363–375.

Khare, S., Dorfleutner, A., Bryan, N.B., Yun, C., Radian, A.D., de Almeida, L., Rojanasakul, Y., Stehlik, C., 2012. An NLRP7-Containing Inflammasome Mediates Recognition of Microbial Lipopeptides in Human Macrophages. *Immunity*, **36**, 464–476.

Kim, H.M., Park, B.S., Kim, J.-I., Kim, S.E., Lee, J., Oh, S.C., Enkhbayar, P., Matsushima, N., Lee, H., Yoo, O.J., Lee, J.-O., 2007. Crystal Structure of the TLR4-MD-2 Complex with Bound Endotoxin Antagonist Eritoran. *Cell*, **130**, 906–917.

Kim, J.W., Choi, E.J., Joe, C.O., 2000. Activation of death-inducing signaling complex (DISC) by pro-apoptotic C-terminal fragment of RIP. *Oncogene*, **19**, 4491–4499.

Kim, S., Bauernfeind, F., Ablasser, A., Hartmann, G., Fitzgerald, K.A., Latz, E., Hornung, V., 2010. Listeria monocytogenes is sensed by the NLRP3 and AIM2 Inflammasome. *Eur. J. Immunol.*, **40**, 1545–1551.

Kim, T.W., Yu, M., Zhou, H., Cui, W., Wang, J., DiCorleto, P., Fox, P., Xiao, H., Li, X., 2012a. Pellino 2 Is critical for Toll-like Receptor/Interleukin-1 Receptor (TLR/IL-1R)-mediated Post-transcriptional Control. *J. Biol. Chem.*, **287**, 25686–25695.

Kim, T.W., Yu, M., Zhou, H., Cui, W., Wang, J., DiCorleto, P., Fox, P., Xiao, H., Li, X., 2012b. Pellino 2 Is critical for Toll-like Receptor/Interleukin-1 Receptor (TLR/IL-1R)-mediated Post-transcriptional Control. *J. Biol. Chem.*, **287**, 25686–25695.

Kindberg, E., Vene, S., Mickiene, A., Lundkvist, Å., Lindquist, L., Svensson, L., 2011. A Functional Toll-Like Receptor 3 Gene (TLR3) May Be a Risk Factor for Tick-borne Encephalitis Virus (TBEV) Infection. *J. Infect. Dis.*, **203**, 523–528.

Kirisako, T., Kamei, K., Murata, S., Kato, M., Fukumoto, H., Kanie, M., Sano, S., Tokunaga, F., Tanaka, K., Iwai, K., 2006. A ubiquitin ligase complex assembles linear polyubiquitin chains. *EMBO J.*, **25**, 4877–4887.

Kischkel, F.C., Hellbardt, S., Behrmann, I., Germer, M., Pawlita, M., Krammer, P.H., Peter, M.E., 1995. Cytotoxicity-dependent APO-1 (Fas/CD95)-associated proteins form a death-inducing signaling complex (DISC) with the receptor. *EMBO J.*, **14**, 5579–5588.

Kleessen, B., Kroesen, A.J., Buhr, H.J., Blaut, M., 2002. Mucosal and invading bacteria in patients with inflammatory bowel disease compared with controls. *Scand. J. Gastroenterol.*, **37**, 1034–1041.

Klimosch, S.N., Försti, A., Eckert, J., Knežević, J., Bevier, M., Schönfels, W. von, Heits, N., Walter, J., Hinz, S., Lascorz, J., Hampe, J., Hartl, D., Frick, J.-S., Hemminki, K., Schafmayer, C., Weber, A.N.R., 2013. Functional TLR5 Genetic Variants Affect Human Colorectal Cancer Survival. *Cancer Res.*, **73**, 7232–7242.

Knodler, L.A., Crowley, S.M., Sham, H.P., Yang, H., Wrande, M., Ma, C., Ernst, R.K., Steele-Mortimer, O., Celli, J., Vallance, B.A., 2014. Noncanonical Inflammasome Activation of Caspase-4/Caspase-11 Mediates Epithelial Defenses against Enteric Bacterial Pathogens. *Cell Host Microbe*, **16**, 249–256.

Kofoed, E.M., Vance, R.E., 2011. Innate immune recognition of bacterial ligands by NAIPs determines inflammasome specificity. *Nature*, **477**, 592–595.

Kuida, K., Lippke, J.A., Ku, G., Harding, M.W., Livingston, D.J., Su, M.S., Flavell, R.A., 1995. Altered cytokine export and apoptosis in mice deficient in interleukin-1 beta converting enzyme. *Science*, **267**, 2000–2003.

Kumar, H., Kawai, T., Kato, H., Sato, S., Takahashi, K., Coban, C., Yamamoto, M., Uematsu, S., Ishii, K.J., Takeuchi, O., Akira, S., 2006. Essential role of IPS-1 in innate immune responses against RNA viruses. *J. Exp. Med.*, **203**, 1795–1803.

Kurt-Jones, E.A., Popova, L., Kwinn, L., Haynes, L.M., Jones, L.P., Tripp, R.A., Walsh, E.E., Freeman, M.W., Golenbock, D.T., Anderson, L.J., Finberg, R.W., 2000. Pattern recognition receptors TLR4 and CD14 mediate response to respiratory syncytial virus. *Nat. Immunol.*, **1**, 398–401.

Kurtz, J., 2005. Specific memory within innate immune systems. *Trends Immunol.*, **26**, 186–192.

Kutikhin, A.G., Yuzhalin, A.E., 2012. C-type lectin receptors and RIG-I-like receptors: new points on the oncogenomics map. *Cancer Manag. Res.*, **4**, 39–53.

Laemmli, U.K., 1970. Cleavage of structural proteins during the assembly of the head of bacteriophage T4. *Nature*, **227**, 680–685.

Lagathu, C., Yvan-Charvet, L., Bastard, J.-P., Maachi, M., Quignard-Boulangé, A., Capeau, J., Caron, M., 2006. Long-term treatment with interleukin-1β induces insulin resistance in murine and human adipocytes. *Diabetologia*, **49**, 2162–2173.

Lamkanfi, M., Dixit, V.M., 2014. Mechanisms and Functions of Inflammasomes. *Cell*, **157**, 1013–1022.

Lamping, N., Dettmer, R., Schröder, N.W., Pfeil, D., Hallatschek, W., Burger, R., Schumann, R.R., 1998. LPS-binding protein protects mice from septic shock caused by LPS or gram-negative bacteria. *J. Clin. Invest.*, **101**, 2065–2071.

Lanier, L.L., Sun, J.C., 2009. Do the terms innate and adaptive immunity create conceptual barriers? *Nat. Rev. Immunol.*, **9**, 302–303.

Latz, E., Verma, A., Visintin, A., Gong, M., Sirois, C.M., Klein, D.C.G., Monks, B.G., McKnight, C.J., Lamphier, M.S., Duprex, W.P., Espevik, T., Golenbock, D.T., 2007. Ligand-induced conformational changes allosterically activate Toll-like receptor 9. *Nat. Immunol.*, **8**, 772–779.

Latz, E., Xiao, T.S., Stutz, A., 2013. Activation and regulation of the inflammasomes. *Nat. Rev. Immunol.*, **13**.

Lee, G.-S., Subramanian, N., Kim, A.I., Aksentijevich, I., Goldbach-Mansky, R., Sacks, D.B., Germain, R.N., Kastner, D.L., Chae, J.J., 2012. The calcium-sensing receptor regulates the NLRP3 inflammasome through Ca2+ and cAMP. *Nature*, **492**, 123–127.

Lee, J., Li, L., Gretz, N., Gebert, J., Dihlmann, S., 2012. Absent in Melanoma 2 (AIM2) is an important mediator of interferon-dependent and -independent

HLA-DRA and HLA-DRB gene expression in colorectal cancers. *Oncogene*, **31**, 1242–1253.

Lee, S.M.Y., Kok, K.-H., Jaume, M., Cheung, T.K.W., Yip, T.-F., Lai, J.C.C., Guan, Y., Webster, R.G., Jin, D.-Y., Peiris, J.S.M., 2014. Toll-like receptor 10 is involved in induction of innate immune responses to influenza virus infection. *Proc. Natl. Acad. Sci.*, **111**, 3793–3798.

Lee, Y.H., Bae, S.-C., 2016. Association between functional NLRP3 polymorphisms and susceptibility to autoimmune and inflammatory diseases: a meta-analysis. *Lupus*,.

Le Goffic, R., Balloy, V., Lagranderie, M., Alexopoulou, L., Escriou, N., Flavell, R., Chignard, M., Si-Tahar, M., 2006. Detrimental contribution of the Toll-like receptor (TLR)3 to influenza A virus-induced acute pneumonia. *PLoS Pathog.*, **2**, e53.

Lemaitre, B., Nicolas, E., Michaut, L., Reichhart, J.M., Hoffmann, J.A., 1996. The dorsoventral regulatory gene cassette spätzle/Toll/cactus controls the potent antifungal response in Drosophila adults. *Cell*, **86**, 973–983.

Lien, E., Sellati, T.J., Yoshimura, A., Flo, T.H., Rawadi, G., Finberg, R.W., Carroll, J.D., Espevik, T., Ingalls, R.R., Radolf, J.D., Golenbock, D.T., 1999. Toll-like Receptor 2 Functions as a Pattern Recognition Receptor for Diverse Bacterial Products. *J. Biol. Chem.*, **274**, 33419–33425.

Lightfield, K.L., Persson, J., Brubaker, S.W., Witte, C.E., von Moltke, J., Dunipace, E.A., Henry, T., Sun, Y.-H., Cado, D., Dietrich, W.F., Monack, D.M., Tsolis, R.M., Vance, R.E., 2008. Critical function for Naip5 in inflammasome activation by a conserved carboxy-terminal domain of flagellin. *Nat. Immunol.*, **9**, 1171–1178.

Lin, C.-C., Huoh, Y.-S., Schmitz, K.R., Jensen, L.E., Ferguson, K.M., 2008. Pellino Proteins Contain a Cryptic FHA Domain that Mediates Interaction with Phosphorylated IRAK1. *Structure*, **16**, 1806–1816.

Lin, K.-M., Hu, W., Troutman, T.D., Jennings, M., Brewer, T., Li, X., Nanda, S., Cohen, P., Thomas, J.A., Pasare, C., 2014. IRAK-1 bypasses priming and directly links TLRs to rapid NLRP3 inflammasome activation. *Proc. Natl. Acad. Sci. U. S. A.*, **111**, 775–780.

Lin, S.-C., Lo, Y.-C., Wu, H., 2010. Helical assembly in the MyD88–IRAK4–IRAK2 complex in TLR/IL-1R signalling. *Nature*, **465**, 885–890.

Li, P., Allen, H., Banerjee, S., Franklin, S., Herzog, L., Johnston, C., McDowell, J., Paskind, M., Rodman, L., Salfeld, J., Towne, E., Tracey, D., Wardwell, S., Wei, F.-Y., Wong, W., Kamen, R., Seshadri, T., 1995. Mice deficient in IL-1β-converting enzyme are defective in production of mature IL-1β and resistant to endotoxic shock. *Cell*, **80**, 401–411.

Li, S., Strelow, A., Fontana, E.J., Wesche, H., 2002. IRAK-4: A novel member of the IRAK family with the properties of an IRAK-kinase. *Proc. Natl. Acad. Sci.*, **99**, 5567–5572.

Liu, Y., Dong, W., Chen, L., Xiang, R., Xiao, H., De, G., Wang, Z., Qi, Y., 2004. BCL10 Mediates Lipopolysaccharide/Toll-like Receptor-4 Signaling through Interaction with Pellino2. *J. Biol. Chem.*, **279**, 37436–37444.

Liu, Z., Hsu, H., Goeddel, D.V., Karin, M., 1996. Dissection of TNF Receptor 1 Effector Functions: JNK Activation Is Not Linked to Apoptosis While NF-κB Activation Prevents Cell Death. *Cell*, **87**, 565–576.

Loo, Y.-M., Gale, M., 2011. Immune signaling by RIG-I-like receptors. *Immunity*, **34**, 680–692.

Lopez-Castejon, G., Brough, D., 2011. Understanding the mechanism of IL-1β secretion. *Cytokine Growth Factor Rev.*, **22**, 189–195.

Lu, A., Magupalli, V.G., Ruan, J., Yin, Q., Atianand, M.K., Vos, M.R., Schröder, G.F., Fitzgerald, K.A., Wu, H., Egelman, E.H., 2014. Unified Polymerization Mechanism for the Assembly of ASC-Dependent Inflammasomes. *Cell*, **156**, 1193–1206.

Ludlow, L.E.A., Johnstone, R.W., Clarke, C.J.P., 2005. The HIN-200 family: More than interferon-inducible genes? *Exp. Cell Res.*, **308**, 1–17.

Madrzak, J., Fiedler, M., Johnson, C.M., Ewan, R., Knebel, A., Bienz, M., Chin, J.W., 2015. Ubiquitination of the Dishevelled DIX domain blocks its head-to-tail polymerization. *Nat. Commun.*, **6**, 6718.

Mallat, Z., Heymes, C., Corbaz, A., Logeart, D., Alouani, S., Cohen-Solal, A., Seidler, T., Hasenfuss, G., Chvatchko, Y., Shah, A.M., Tedgui, A., 2004. Evidence for altered interleukin 18 (IL)-18 pathway in human heart failure. *FASEB J. Off. Publ. Fed. Am. Soc. Exp. Biol.*, **18**, 1752–1754.

Mao, K., Chen, S., Chen, M., Ma, Y., Wang, Y., Huang, B., He, Z., Zeng, Y., Hu, Y., Sun, S., Li, J., Wu, X., Wang, X., Strober, W., Chen, C., Meng, G., Sun, B., 2013. Nitric oxide suppresses NLRP3 inflammasome activation and protects against LPS-induced septic shock. *Cell Res.*, **23**, 201–212.

Mariathasan, S., Newton, K., Monack, D.M., Vucic, D., French, D.M., Lee, W.P., Roose-Girma, M., Erickson, S., Dixit, V.M., 2004. Differential activation of the inflammasome by caspase-1 adaptors ASC and Ipaf. *Nature*, **430**, 213–218.

Mariathasan, S., Weiss, D.S., Newton, K., McBride, J., O'Rourke, K., Roose-Girma, M., Lee, W.P., Weinrauch, Y., Monack, D.M., Dixit, V.M., 2006. Cryopyrin activates the inflammasome in response to toxins and ATP. *Nature*, **440**, 228–232.

Martin, M.U., Kollewe, C., 2001. Interleukin-1 receptor-associated kinase-1 (IRAK-1): A self-regulatory adapter molecule in the signaling cascade of the Toll/IL-1 receptor family. *Signal Transduct.*, **1**, 37–50.

Martinon, F., Agostini, L., Meylan, E., Tschopp, J., 2004. Identification of Bacterial Muramyl Dipeptide as Activator of the NALP3/Cryopyrin Inflammasome. *Curr. Biol.*, **14**, 1929–1934.

Martinon, F., Burns, K., Tschopp, J., 2002. The Inflammasome: A Molecular Platform Triggering Activation of Inflammatory Caspases and Processing of proIL-β. *Mol. Cell*, **10**, 417–426.

Martinon, F., Mayor, A., Tschopp, J., 2009. The Inflammasomes: Guardians of the Body. *Annu. Rev. Immunol.*, **27**, 229–265.

Martinon, F., Pétrilli, V., Mayor, A., Tardivel, A., Tschopp, J., 2006. Gout-associated uric acid crystals activate the NALP3 inflammasome. *Nature*, **440**, 237–241.

Masumoto, J., Dowds, T.A., Schaner, P., Chen, F.F., Ogura, Y., Li, M., Zhu, L., Katsuyama, T., Sagara, J., Taniguchi, S., Gumucio, D.L., Núñez, G., Inohara, N., 2003. ASC is an activating adaptor for NF-κB and caspase-8-dependent apoptosis. *Biochem. Biophys. Res. Commun.*, **303**, 69–73.

Masumoto, J., Taniguchi, S., Ayukawa, K., Sarvotham, H., Kishino, T., Niikawa, N., Hidaka, E., Katsuyama, T., Higuchi, T., Sagara, J., 1999. ASC, a novel 22-kDa protein, aggregates during apoptosis of human promyelocytic leukemia HL-60 cells. *J. Biol. Chem.*, **274**, 33835–33838.

Matusiak, M., Opdenbosch, N.V., Walle, L.V., Sirard, J.-C., Kanneganti, T.-D., Lamkanfi, M., 2015. Flagellin-induced NLRC4 phosphorylation primes the inflammasome for activation by NAIP5. *Proc. Natl. Acad. Sci.*, **112**, 1541–1546.

Medzhitov, R., 2008. Origin and physiological roles of inflammation. *Nature*, **454**, 428–435.

Medzhitov, R., Janeway, C.J., 2000. Innate immune recognition: mechanisms and pathways. *Immunol. Rev.*, **173**, 89–97.

Medzhitov, R., Preston-Hurlburt, P., Janeway, C.A., 1997. A human homologue of the Drosophila Toll protein signals activation of adaptive immunity. *Nature*, **388**, 394–397.

Merhi-Soussi, F., Kwak, B.R., Magne, D., Chadjichristos, C., Berti, M., Pelli, G., James, R.W., Mach, F., Gabay, C., 2005. Interleukin-1 plays a major role in vascular inflammation and atherosclerosis in male apolipoprotein E-knockout mice. *Cardiovasc. Res.*, **66**, 583–593.

Meylan, E., Burns, K., Hofmann, K., Blancheteau, V., Martinon, F., Kelliher, M., Tschopp, J., 2004. RIP1 is an essential mediator of Toll-like receptor 3–induced NF-κB activation. *Nat. Immunol.*, **5**, 503–507.

Meylan, E., Curran, J., Hofmann, K., Moradpour, D., Binder, M., Bartenschlager, R., Tschopp, J., 2005. Cardif is an adaptor protein in the RIG-I antiviral pathway and is targeted by hepatitis C virus. *Nature*, **437**, 1167–1172.

Meylan, E., Tschopp, J., 2008. IRAK2 takes its place in TLR signaling. *Nat. Immunol.*, **9**, 581–582.

Miao, E.A., Leaf, I.A., Treuting, P.M., Mao, D.P., Dors, M., Sarkar, A., Warren, S.E., Wewers, M.D., Aderem, A., 2010a. Caspase-1-induced pyroptosis is an innate immune effector mechanism against intracellular bacteria. *Nat. Immunol.*, **11**, 1136–1142.

Miao, E.A., Mao, D.P., Yudkovsky, N., Bonneau, R., Lorang, C.G., Warren, S.E., Leaf, I.A., Aderem, A., 2010b. Innate immune detection of the type III secretion apparatus through the NLRC4 inflammasome. *Proc. Natl. Acad. Sci.*, **107**, 3076–3080.

Mills, K.H.G., 2011. TLR-dependent T cell activation in autoimmunity. *Nat. Rev. Immunol.*, **11**, 807–822.

Mills, K.H.G., Dungan, L.S., Jones, S.A., Harris, J., 2013. The role of inflammasome-derived IL-1 in driving IL-17 responses. *J. Leukoc. Biol.*, **93**, 489–497.

Mogensen, T.H., 2009. Pathogen Recognition and Inflammatory Signaling in Innate Immune Defenses. *Clin. Microbiol. Rev.*, **22**, 240–273.

Mori, Y., Yin, J., Rashid, A., Leggett, B.A., Young, J., Simms, L., Kuehl, P.M., Langenberg, P., Meltzer, S.J., Stine, O.C., 2001. Instabilotyping Comprehensive Identification of Frameshift Mutations Caused by Coding Region Microsatellite Instability. *Cancer Res.*, **61**, 6046–6049.

Muñoz-Planillo, R., Kuffa, P., Martínez-Colón, G., Smith, B.L., Rajendiran, T.M., Núñez, G., 2013. K+ efflux is the Common Trigger of NLRP3 inflammasome Activation by Bacterial Toxins and Particulate Matter. *Immunity*, **38**, 1142–1153.

Muruve, D.A., Pétrilli, V., Zaiss, A.K., White, L.R., Clark, S.A., Ross, P.J., Parks, R.J., Tschopp, J., 2008. The inflammasome recognizes cytosolic microbial and host DNA and triggers an innate immune response. *Nature*, **452**, 103–107.

Nagata, S., Golstein, P., 1995. The Fas death factor. *Science*, **267**, 1449–1456.

Napetschnig, J., Wu, H., 2013. Molecular Basis of NF-κB Signaling. *Annu. Rev. Biophys.*, **42**, 443–468.

Nguyen, M.D., Julien, J.-P., Rivest, S., 2002. Innate immunity: the missing link in neuroprotection and neurodegeneration? *Nat. Rev. Neurosci.*, **3**, 216–227.

Nickerson, K.M., Christensen, S.R., Shupe, J., Kashgarian, M., Kim, D., Elkon, K., Shlomchik, M.J., 2010. TLR9 Regulates TLR7- and MyD88-Dependent Autoantibody Production and Disease in a Murine Model of Lupus. *J. Immunol.*, **184**, 1840–1848.

Nishiya, T., DeFranco, A.L., 2004. Ligand-regulated chimeric receptor approach reveals distinctive subcellular localization and signaling properties of the Toll-like receptors. *J. Biol. Chem.*, **279**, 19008–19017.

Nutt, S.L., Hodgkin, P.D., Tarlinton, D.M., Corcoran, L.M., 2015. The generation of antibody-secreting plasma cells. *Nat. Rev. Immunol.*, **15**, 160–171.

Ogura, Y., Bonen, D.K., Inohara, N., Nicolae, D.L., Chen, F.F., Ramos, R., Britton, H., Moran, T., Karaliuskas, R., Duerr, R.H., Achkar, J.-P., Brant, S.R., Bayless, T.M., Kirschner, B.S., Hanauer, S.B., Nuñez, G., Cho, J.H., 2001a. A frameshift mutation in NOD2 associated with susceptibility to Crohn's disease. *Nature*, **411**, 603–606.

Ogura, Y., Inohara, N., Benito, A., Chen, F.F., Yamaoka, S., Núñez, G., 2001b. Nod2, a Nod1/Apaf-1 Family Member That Is Restricted to Monocytes and Activates NF-κB. *J. Biol. Chem.*, **276**, 4812–4818.

Ohashi, K., Burkart, V., Flohé, S., Kolb, H., 2000. Cutting Edge: Heat Shock Protein 60 Is a Putative Endogenous Ligand of the Toll-Like Receptor-4 Complex. *J. Immunol.*, **164**, 558–561.

Ohnishi, H., Tochio, H., Kato, Z., Orii, K.E., Li, A., Kimura, T., Hiroaki, H., Kondo, N., Shirakawa, M., 2009. Structural basis for the multiple interactions of the MyD88 TIR domain in TLR4 signaling. *Proc. Natl. Acad. Sci.*, **106**, 10260–10265.

Okamura, Y., Watari, M., Jerud, E.S., Young, D.W., Ishizaka, S.T., Rose, J., Chow, J.C., Strauss, J.F., 2001. The Extra Domain A of Fibronectin Activates Toll-like Receptor 4. *J. Biol. Chem.*, **276**, 10229–10233.

Oldenburg, M., Krüger, A., Ferstl, R., Kaufmann, A., Nees, G., Sigmund, A., Bathke, B., Lauterbach, H., Suter, M., Dreher, S., Koedel, U., Akira, S., Kawai, T., Buer, J., Wagner, H., Bauer, S., Hochrein, H., Kirschning, C.J., 2012. TLR13 Recognizes Bacterial 23S rRNA Devoid of Erythromycin Resistance–Forming Modification. *Science*, **337**, 1111–1115.

Oliveira-Nascimento, L., Massari, P., Wetzler, L.M., 2012. The Role of TLR2 in Infection and Immunity. *Front. Immunol.*, **3**.

O'Neill, L.A.J., Golenbock, D., Bowie, A.G., 2013. The history of Toll-like receptors — redefining innate immunity. *Nat. Rev. Immunol.*, **13**, 453–460.

Perry, A.K., Chen, G., Zheng, D., Tang, H., Cheng, G., 2005. The host type I interferon response to viral and bacterial infections. *Cell Res.*, **15**, 407–422.

Peterson, L.W., Artis, D., 2014. Intestinal epithelial cells: regulators of barrier function and immune homeostasis. *Nat. Rev. Immunol.*, **14**, 141–153.

Pétrilli, V., Papin, S., Dostert, C., Mayor, A., Martinon, F., Tschopp, J., 2007. Activation of the NALP3 inflammasome is triggered by low intracellular potassium concentration. *Cell Death Differ.*, **14**, 1583–1589.

Pickart, C.M., Fushman, D., 2004. Polyubiquitin chains: polymeric protein signals. *Curr. Opin. Chem. Biol.*, **8**, 610–616.

Pierini, R., Juruj, C., Perret, M., Jones, C.L., Mangeot, P., Weiss, D.S., Henry, T., 2012. AIM2/ASC triggers caspase-8-dependent apoptosis in Francisella-infected caspase-1-deficient macrophages. *Cell Death Differ.*, **19**, 1709–1721.

Pifer, R., Benson, A., Sturge, C.R., Yarovinsky, F., 2011. UNC93B1 Is Essential for TLR11 Activation and IL-12-dependent Host Resistance to Toxoplasma gondii. *J. Biol. Chem.*, **286**, 3307–3314.

Pifer, R., Yarovinsky, F., 2011. Innate responses to Toxoplasma gondii in mice and humans. *Trends Parasitol.*, **27**, 388–393.

Plattner, F., Yarovinsky, F., Romero, S., Didry, D., Carlier, M.-F., Sher, A., Soldati-Favre, D., 2008. Toxoplasma Profilin Is Essential for Host Cell Invasion and TLR11-Dependent Induction of an Interleukin-12 Response. *Cell Host Microbe*, **3**, 77–87.

Poeck, H., Bscheider, M., Gross, O., Finger, K., Roth, S., Rebsamen, M., Hannesschläger, N., Schlee, M., Rothenfusser, S., Barchet, W., Kato, H., Akira, S., Inoue, S., Endres, S., Peschel, C., Hartmann, G., Hornung, V., Ruland, J., 2010. Recognition of RNA virus by RIG-I results in activation of CARD9 and inflammasome signaling for interleukin 1β production. *Nat. Immunol.*, **11**, 63–69.

Poltorak, A., He, X., Smirnova, I., Liu, M.-Y., Huffel, C.V., Du, X., Birdwell, D., Alejos, E., Silva, M., Galanos, C., Freudenberg, M., Ricciardi-Castagnoli, P., Layton, B., Beutler, B., 1998. Defective LPS Signaling in C3H/HeJ and C57BL/10ScCr Mice: Mutations in Tlr4 Gene. *Science*, **282**, 2085–2088.

Pontillo, A., Girardelli, M., Kamada, A.J., Pancotto, J.A. t, Donadi, E.A., Crovella, S., Sandrin-Garcia, P., 2012. Polimorphisms in Inflammasome Genes Are Involved in the Predisposition to Systemic Lupus Erythematosus. *Autoimmunity*, **45**, 271–278.

Pope, M., Haase, A.T., 2003. Transmission, acute HIV-1 infection and the quest for strategies to prevent infection. *Nat. Med.*, **9**, 847–852.

Pothlichet, J., Meunier, I., Davis, B.K., Ting, J.P.-Y., Skamene, E., von Messling, V., Vidal, S.M., 2013. Type I IFN Triggers RIG-I/TLR3/NLRP3-dependent Inflammasome Activation in Influenza A Virus Infected Cells. *PLoS Pathog*, **9**, e1003256.

Proell, M., Gerlic, M., Mace, P.D., Reed, J.C., Riedl, S.J., 2013. The CARD plays a critical role in ASC foci formation and inflammasome signaling. *Biochem. J.*, **449**, 613–621.

Prothmann, C., Armstrong, N.J., Roth, S., Rupp, R.A.W., 2006. Vertebrate rel proteins exhibit dorsal-like activities in early Drosophila embryogenesis. *Dev. Dyn.*, **235**, 949–957.

Pruitt, J.H., Copeland, E.M., Moldawer, L.L., 1995. Interleukin-1 and interleukin-1 antagonism in sepsis, systemic inflammatory response syndrome, and septic shock. *Shock Augusta Ga*, **3**, 235–251.

Pugin, J., Schürer-Maly, C.C., Leturcq, D., Moriarty, A., Ulevitch, R.J., Tobias, P.S., 1993. Lipopolysaccharide activation of human endothelial and epithelial cells is mediated by lipopolysaccharide-binding protein and soluble CD14. *Proc. Natl. Acad. Sci.*, **90**, 2744–2748.

Py, B.F., Kim, M.-S., Vakifahmetoglu-Norberg, H., Yuan, J., 2013. Deubiquitination of NLRP3 by BRCC3 Critically Regulates Inflammasome Activity. *Mol. Cell*, **49**, 331–338.

Qiao, Y., Wang, P., Qi, J., Zhang, L., Gao, C., 2012. TLR-induced NF-κB activation regulates NLRP3 expression in murine macrophages. *FEBS Lett.*, **586**, 1022–1026.

Qu, Y., Misaghi, S., Izrael-Tomasevic, A., Newton, K., Gilmour, L.L., Lamkanfi, M., Louie, S., Kayagaki, N., Liu, J., Kömüves, L., Cupp, J.E., Arnott, D., Monack, D., Dixit, V.M., 2012. Phosphorylation of NLRC4 is critical for inflammasome activation. *Nature*, **490**, 539–542.

Raetz, C.R.H., Whitfield, C., 2002. Lipopolysaccharide Endotoxins. *Annu. Rev. Biochem.*, **71**, 635–700.

Raetz, M., Kibardin, A., Sturge, C.R., Pifer, R., Li, H., Burstein, E., Ozato, K., Larin, S., Yarovinsky, F., 2013. Cooperation of TLR12 and TLR11 in the IRF8-Dependent IL-12 Response to Toxoplasma gondii Profilin. *J. Immunol.*, **191**, 4818–4827.

Ramadan, K., Meerang, M., 2011. Degradation-linked ubiquitin signal and proteasome are integral components of DNA double strand break repair: New perspectives for anti-cancer therapy. *FEBS Lett.*, Ubiquitin Family Proteins in DNA Damage Response **585**, 2868–2875.

Ramos, H.C., Rumbo, M., Sirard, J.-C., 2004. Bacterial flagellins: mediators of pathogenicity and host immune responses in mucosa. *Trends Microbiol.*, **12**, 509–517.

Rathinam, V.A.K., Vanaja, S.K., Waggoner, L., Sokolovska, A., Becker, C., Stuart, L.M., Leong, J.M., Fitzgerald, K.A., 2012. TRIF Licenses Caspase-11-Dependent NLRP3 Inflammasome Activation by Gram-Negative Bacteria. *Cell*, **150**, 606–619.

Resch, K., Jockusch, H., Schmitt-John, T., 2001. Assignment of homologous genes, Peli1/PELI1 and Peli2/PELI2, for the Pelle adaptor protein Pellino to mouse chromosomes 11 and 14 and human chromosomes 2p13.3 and 14q21, respectively, by physical and radiation hybrid mapping. *Cytogenet. Cell Genet.*, **92**, 172–174.

Reubold, T.F., Hahne, G., Wohlgemuth, S., Eschenburg, S., 2014. Crystal structure of the leucine-rich repeat domain of the NOD-like receptor NLRP1: Implications for binding of muramyl dipeptide. *FEBS Lett.*, **588**, 3327–3332.

Rich, T., Allen, R.L., Lucas, A.-M., Stewart, A., Trowsdale, J., 2000. Pellino-related sequences from Caenorhabditis elegans and Homo sapiens. *Immunogenetics*, **52**, 145–149.

Rittirsch, D., Flierl, M.A., Ward, P.A., 2008. Harmful molecular mechanisms in sepsis. *Nat. Rev. Immunol.*, **8**, 776–787.

Roberts, R.L., Topless, R.K.G., Phipps-Green, A.J., Gearry, R.B., Barclay, M.L., Merriman, T.R., 2010. Evidence of interaction of CARD8 rs2043211 with NALP3 rs35829419 in Crohn's disease. *Genes Immun.*, **11**, 351–356.

Rock, F.L., Hardiman, G., Timans, J.C., Kastelein, R.A., Bazan, J.F., 1998. A family of human receptors structurally related to Drosophila Toll. *Proc. Natl. Acad. Sci.*, **95**, 588–593.

Rodgers, M.A., Bowman, J.W., Fujita, H., Orazio, N., Shi, M., Liang, Q., Amatya, R., Kelly, T.J., Iwai, K., Ting, J., Jung, J.U., 2014. The linear ubiquitin assembly complex (LUBAC) is essential for NLRP3 inflammasome activation. *J. Exp. Med.*, **211**, 1333–1347.

Romani, L., Fallarino, F., De Luca, A., Montagnoli, C., D'Angelo, C., Zelante, T., Vacca, C., Bistoni, F., Fioretti, M.C., Grohmann, U., Segal, B.H., Puccetti, P., 2008. Defective tryptophan catabolism underlies inflammation in mouse chronic granulomatous disease. *Nature*, **451**, 211–215.

Rossol, M., Pierer, M., Raulien, N., Quandt, D., Meusch, U., Rothe, K., Schubert, K., Schöneberg, T., Schaefer, M., Krügel, U., Smajilovic, S., Bräuner-Osborne, H., Baerwald, C., Wagner, U., 2012. Extracellular Ca2+ is a danger signal activating the NLRP3 inflammasome through G protein-coupled calcium sensing receptors. *Nat. Commun.*, **3**, 1329.

Rowe, D.C., McGettrick, A.F., Latz, E., Monks, B.G., Gay, N.J., Yamamoto, M., Akira, S., O'Neill, L.A., Fitzgerald, K.A., Golenbock, D.T., 2006. The myristoylation of TRIF-related adaptor molecule is essential for Toll-like receptor 4 signal transduction. *Proc. Natl. Acad. Sci.*, **103**, 6299–6304.

Sahillioglu, A.C., Sumbul, F., Ozoren, N., Haliloglu, T., 2014. Structural and Dynamics Aspects of ASC Speck Assembly. *Structure*, **22**, 1722–1734.

Salliot, C., Dougados, M., Gossec, L., 2009. Risk of serious infections during rituximab, abatacept and anakinra treatments for rheumatoid arthritis: meta-analyses of randomised placebo-controlled trials. *Ann. Rheum. Dis.*, **68**, 25–32.

Sampath, V., Garland, J.S., Le, M., Patel, A.L., Konduri, G.G., Cohen, J.D., Simpson, P.M., Hines, R.N., 2012. A TLR5 (g.1174C > T) variant that encodes a stop codon (R392X) is associated with bronchopulmonary dysplasia. *Pediatr. Pulmonol.*, **47**, 460–468.

Sato, S., Sugiyama, M., Yamamoto, M., Watanabe, Y., Kawai, T., Takeda, K., Akira, S., 2003. Toll/IL-1 Receptor Domain-Containing Adaptor Inducing IFN-β (TRIF) Associates with TNF Receptor-Associated Factor 6 and TANK-Binding Kinase 1, and Activates Two Distinct Transcription Factors, NF-κB and IFN-Regulatory Factor-3, in the Toll-Like Receptor Signaling. *J. Immunol.*, **171**, 4304–4310.

Sauer, J.-D., Witte, C.E., Zemansky, J., Hanson, B., Lauer, P., Portnoy, D.A., 2010. Listeria monocytogenes that lyse in the macrophage cytosol trigger AIM2-mediated pyroptosis. *Cell Host Microbe*, **7**, 412–419.

Schauvliege, R., Janssens, S., Beyaert, R., 2006. Pellino proteins are more than scaffold proteins in TLR/IL-1R signalling: A role as novel RING E3–ubiquitin-ligases. *FEBS Lett.*, **580**, 4697–4702.

Schauvliege, R., Janssens, S., Beyaert, R., 2007. Pellino Proteins: Novel Players in TLR and IL-1R Signalling. *J. Cell. Mol. Med.*, **11**, 453–461.

Schoenemeyer, A., Barnes, B.J., Mancl, M.E., Latz, E., Goutagny, N., Pitha, P.M., Fitzgerald, K.A., Golenbock, D.T., 2005. The Interferon Regulatory Factor, IRF5, Is a Central Mediator of Toll-like Receptor 7 Signaling. *J. Biol. Chem.*, **280**, 17005–17012.

Schroder, K., Tschopp, J., 2010. The Inflammasomes. *Cell*, **140**, 821–832.

Sedimbi, S.K., Hägglöf, T., Karlsson, M.C.I., 2013. IL-18 in inflammatory and autoimmune disease. *Cell. Mol. Life Sci.*, **70**, 4795–4808.

Semenza, G.L., Wang, G.L., 1992. A nuclear factor induced by hypoxia via de novo protein synthesis binds to the human erythropoietin gene enhancer at a site required for transcriptional activation. *Mol. Cell. Biol.*, **12**, 5447–5454.

Seppälä, I.J., Mäkelä, O., 1984. Adjuvant effect of bacterial LPS and/or alum precipitation in responses to polysaccharide and protein antigens. *Immunology*, **53**, 827–836.

Seth, R.B., Sun, L., Ea, C.-K., Chen, Z.J., 2005. Identification and Characterization of MAVS, a Mitochondrial Antiviral Signaling Protein that Activates NF-κB and IRF3. *Cell*, **122**, 669–682.

Sharma, S., tenOever, B.R., Grandvaux, N., Zhou, G.-P., Lin, R., Hiscott, J., 2003. Triggering the Interferon Antiviral Response Through an IKK-Related Pathway. *Science*, **300**, 1148–1151.

Shi, J., Zhao, Y., Wang, K., Shi, X., Wang, Y., Huang, H., Zhuang, Y., Cai, T., Wang, F., Shao, F., 2015. Cleavage of GSDMD by inflammatory caspases determines pyroptotic cell death. *Nature*, **advance online publication**.

Shi, J., Zhao, Y., Wang, Y., Gao, W., Ding, J., Li, P., Hu, L., Shao, F., 2014. Inflammatory caspases are innate immune receptors for intracellular LPS. *Nature*, **514**, 187–192.

Siednienko, J., Jackson, R., Mellett, M., Delagic, N., Yang, S., Wang, B., Tang, L.S., Callanan, J.J., Mahon, B.P., Moynagh, P.N., 2012. Pellino3 targets the IRF7 pathway and facilitates autoregulation of TLR3- and viral-induced expression of type I interferons. *Nat. Immunol.*, **13**, 1055–1062.

Sironi, M., Biasin, M., Cagliani, R., Forni, D., Luca, M.D., Saulle, I., Caputo, S.L., Mazzotta, F., Macías, J., Pineda, J.A., Caruz, A., Clerici, M., 2012. A Common Polymorphism in TLR3 Confers Natural Resistance to HIV-1 Infection. *J. Immunol.*, **188**, 818–823.

Srikrishna, G., Freeze, H.H., 2009. Endogenous Damage-Associated Molecular Pattern Molecules at the Crossroads of Inflammation and Cancer. *Neoplasia N. Y. N*, **11**, 615–628.

Studier, F.W., 1973. Analysis of bacteriophage T7 early RNAs and proteins on slab gels. *J. Mol. Biol.*, **79**, 237–248.

Sugarman, B.J., Aggarwal, B.B., Hass, P.E., Figari, I.S., Palladino, M.A., Shepard, H.M., 1985. Recombinant human tumor necrosis factor-alpha: effects on proliferation of normal and transformed cells in vitro. *Science*, **230**, 943–945.

Sui, J., Li, H., Fang, Y., Liu, Y., Li, M., Zhong, B., Yang, F., Zou, Q., Wu, Y., 2012. NLRP1 gene polymorphism influences gene transcription and is a risk factor for rheumatoid arthritis in Han Chinese. *Arthritis Rheum.*, **64**, 647–654.

Sun, L., Deng, L., Ea, C.-K., Xia, Z.-P., Chen, Z.J., 2004. The TRAF6 Ubiquitin Ligase and TAK1 Kinase Mediate IKK Activation by BCL10 and MALT1 in T Lymphocytes. *Mol. Cell*, **14**, 289–301.

Tabeta, K., Georgel, P., Janssen, E., Du, X., Hoebe, K., Crozat, K., Mudd, S., Shamel, L., Sovath, S., Goode, J., Alexopoulou, L., Flavell, R.A., Beutler, B., 2004. Toll-like receptors 9 and 3 as essential components of innate immune defense against mouse cytomegalovirus infection. *Proc. Natl. Acad. Sci. U. S. A.*, **101**, 3516–3521.

Takaoka, A., Wang, Z., Choi, M.K., Yanai, H., Negishi, H., Ban, T., Lu, Y., Miyagishi, M., Kodama, T., Honda, K., Ohba, Y., Taniguchi, T., 2007. DAI (DLM-1/ZBP1) is a cytosolic DNA sensor and an activator of innate immune response. *Nature*, **448**, 501–505.

Takeuchi, O., Hoshino, K., Kawai, T., Sanjo, H., Takada, H., Ogawa, T., Takeda, K., Akira, S., 1999. Differential Roles of TLR2 and TLR4 in Recognition of Gram-Negative and Gram-Positive Bacterial Cell Wall Components. *Immunity*, **11**, 443–451.

Tan, E.M., Cohen, A.S., Fries, J.F., Masi, A.T., Mcshane, D.J., Rothfield, N.F., Schaller, J.G., Talal, N., Winchester, R.J., 1982. The 1982 revised criteria for the classification of systemic lupus erythematosus. *Arthritis Rheum.*, **25**, 1271–1277.

Tannahill, G.M., Curtis, A.M., Adamik, J., Palsson-Mcdermott, E.M., McGettrick, A.F., Goel, G., Frezza, C., Bernard, N.J., Kelly, B., Foley, N.H., Zheng, L., Gardet, A., Tong, Z., Jany, S.S., Corr, S.C., Haneklaus, M., Caffrey, B.E., Pierce, K., Walmsley, S., Beasley, F.C., Cummins, E., Nizet, V., Whyte, M., Taylor, C.T., Lin, H., Masters, S.L., Gottlieb, E., Kelly, V.P., Clish, C., Auron, P.E., Xavier, R.J., O'Neill, L.A.J., 2013. Succinate is an inflammatory signal that induces IL-1β through HIF-1α. *Nature*, **496**, 238–242.

Tan, R.S.T., Ho, B., Leung, B.P., Ding, J.L., 2014. TLR Cross-talk Confers Specificity to Innate Immunity. *Int. Rev. Immunol.*, **33**, 443–453.

Tartaglia, L.A., Ayres, T.M., Wong, G.H.W., Goeddel, D.V., 1993. A novel domain within the 55 kd TNF receptor signals cell death. *Cell*, **74**, 845–853.

Tran, T.H., Pham, J.T., Shafeeq, H., Manigault, K.R., Arya, V., 2013. Role of interleukin-1 inhibitors in the management of gout. *Pharmacotherapy*, **33**, 744–753.

Trujillo, M., Shirasu, K., 2010. Ubiquitination in plant immunity. *Curr. Opin. Plant Biol.*, **13**, 402–408.

Tschopp, J., Martinon, F., Burns, K., 2003. NALPs: a novel protein family involved in inflammation. *Nat. Rev. Mol. Cell Biol.*, **4**, 95–104.

Tsukumo, D.M.L., Carvalho-Filho, M.A., Carvalheira, J.B.C., Prada, P.O., Hirabara, S.M., Schenka, A.A., Araújo, E.P., Vassallo, J., Curi, R., Velloso, L.A., Saad, M.J.A., 2007. Loss-of-Function Mutation in Toll-Like Receptor 4 Prevents Diet-Induced Obesity and Insulin Resistance. *Diabetes*, **56**, 1986–1998.

Tzieply, N., Kuhn, A.-M., Morbitzer, D., Namgaladze, D., Heeg, A., Schaefer, L., von Knethen, A., Jensen, L.E., Brüne, B., 2012. OxLDL inhibits LPS-induced IFNβ expression by Pellino3- and IRAK1/4-dependent modification of TANK. *Cell. Signal.*, **24**, 1141–1149.

Underhill, D.M., Ozinsky, A., Hajjar, A.M., Stevens, A., Wilson, C.B., Bassetti, M., Aderem, A., 1999. The Toll-like receptor 2 is recruited to macrophage phagosomes and discriminates between pathogens. *Nature*, **401**, 811–815.

Underhill, D.M., Rossnagle, E., Lowell, C.A., Simmons, R.M., 2005. Dectin-1 activates Syk tyrosine kinase in a dynamic subset of macrophages for reactive oxygen production. *Blood*, **106**, 2543–2550.

Unterholzner, L., Keating, S.E., Baran, M., Horan, K.A., Jensen, S.B., Sharma, S., Sirois, C.M., Jin, T., Latz, E., Xiao, T.S., Fitzgerald, K.A., Paludan, S.R., Bowie, A.G., 2010. IFI16 is an innate immune sensor for intracellular DNA. *Nat. Immunol.*, **11**, 997–1004.

Vajjhala, P.R., Kaiser, S., Smith, S.J., Ong, Q.-R., Soh, S.L., Stacey, K.J., Hill, J.M., 2014. Identification of multifaceted binding modes for pyrin and ASC pyrin domains gives insights into pyrin inflammasome assembly. *J. Biol. Chem.*, **289**, 23504–23519.

Vallabhapurapu, S., Karin, M., 2009. Regulation and Function of NF-κB Transcription Factors in the Immune System. *Annu. Rev. Immunol.*, **27**, 693–733.

van de Veerdonk, F.L., Netea, M.G., Dinarello, C.A., Joosten, L.A.B., 2011. Inflammasome activation and IL-1β and IL-18 processing during infection. *Trends Immunol.*, **32**, 110–116.

van de Veerdonk, F.L., Smeekens, S.P., Joosten, L.A.B., Kullberg, B.J., Dinarello, C.A., van der Meer, J.W.M., Netea, M.G., 2010. Reactive oxygen species–independent activation of the IL-1β inflammasome in cells from patients with chronic granulomatous disease. *Proc. Natl. Acad. Sci. U. S. A.*, **107**, 3030–3033.

Van Opdenbosch, N., Gurung, P., Vande Walle, L., Fossoul, A., Kanneganti, T.-D., Lamkanfi, M., 2014. Activation of the NLRP1b inflammasome independently of ASC-mediated caspase-1 autoproteolysis and speck formation. *Nat. Commun.*, **5**.

Viaud, S., Saccheri, F., Mignot, G., Yamazaki, T., Daillère, R., Hannani, D., Enot, D.P., Pfirschke, C., Engblom, C., Pittet, M.J., Schlitzer, A., Ginhoux, F., Apetoh, L., Chachaty, E., Woerther, P.-L., Eberl, G., Bérard, M., Ecobichon, C., Clermont, D., Bizet, C., Gaboriau-Routhiau, V., Cerf-Bensussan, N., Opolon, P., Yessaad, N., Vivier, E., Ryffel, B., Elson, C.O., Doré, J., Kroemer, G., Lepage, P., Boneca, I.G., Ghiringhelli, F., Zitvogel, L., 2013. The intestinal microbiota modulates the anticancer immune effects of cyclophosphamide. *Science*, **342**, 971–976.

Vince, J.E., Pantaki, D., Feltham, R., Mace, P.D., Cordier, S.M., Schmukle, A.C., Davidson, A.J., Callus, B.A., Wong, W.W.-L., Gentle, I.E., Carter, H., Lee, E.F., Walczak, H., Day, C.L., Vaux, D.L., Silke, J., 2009. TRAF2 Must Bind to Cellular Inhibitors of Apoptosis for Tumor Necrosis Factor (TNF) to Efficiently Activate NF-κB and to Prevent TNF-induced Apoptosis. *J. Biol. Chem.*, **284**, 35906–35915.

Vladimer, G.I., Weng, D., Paquette, S.W.M., Vanaja, S.K., Rathinam, V.A.K., Aune, M.H., Conlon, J.E., Burbage, J.J., Proulx, M.K., Liu, Q., Reed, G., Mecsas, J.C., Iwakura, Y., Bertin, J., Goguen, J.D., Fitzgerald, K.A., Lien, E., 2012. The NLRP12 Inflammasome Recognizes Yersinia pestis. *Immunity*, **37**, 96–107.

Walev, I., Reske, K., Palmer, M., Valeva, A., Bhakdi, S., 1995. Potassium-inhibited processing of IL-1 beta in human monocytes. *EMBO J.*, **14**, 1607–1614.

Walle, L.V., Van Opdenbosch, N., Jacques, P., Fossoul, A., Verheugen, E., Vogel, P., Beyaert, R., Elewaut, D., Kanneganti, T.-D., van Loo, G., Lamkanfi, M., 2014. Negative regulation of the NLRP3 inflammasome by A20 protects against arthritis. *Nature*, **advance online publication**.

Wang, C., Deng, L., Hong, M., Akkaraju, G.R., Inoue, J., Chen, Z.J., 2001. TAK1 is a ubiquitin-dependent kinase of MKK and IKK. *Nature*, **412**, 346–351.

Wang, L.F., Ding, Y.J., Zhao, Q., Zhang, X.L., 2015. Investigation on the association between NLRP3 gene polymorphisms and susceptibility to primary gout. *Genet. Mol. Res. GMR*, **14**, 16410–16414.

Wang, T., Town, T., Alexopoulou, L., Anderson, J.F., Fikrig, E., Flavell, R.A., 2004. Toll-like receptor 3 mediates West Nile virus entry into the brain causing lethal encephalitis. *Nat. Med.*, **10**, 1366–1373.

Warner, N., Núñez, G., 2013. MyD88: A Critical Adaptor Protein in Innate Immunity Signal Transduction. *J. Immunol.*, **190**, 3–4.

Weber, F., Wagner, V., Rasmussen, S.B., Hartmann, R., Paludan, S.R., 2006. Double-Stranded RNA Is Produced by Positive-Strand RNA Viruses and DNA Viruses but Not in Detectable Amounts by Negative-Strand RNA Viruses. *J. Virol.*, **80**, 5059–5064.

Wertz, I.E., O'Rourke, K.M., Zhou, H., Eby, M., Aravind, L., Seshagiri, S., Wu, P., Wiesmann, C., Baker, R., Boone, D.L., Ma, A., Koonin, E.V., Dixit, V.M., 2004. De-ubiquitination and ubiquitin ligase domains of A20 downregulate NF-κB signalling. *Nature*, **430**, 694–699.

Wijk, S.J.L. van, Timmers, H.T.M., 2010. The family of ubiquitin-conjugating enzymes (E2s): deciding between life and death of proteins. *FASEB J.*, **24**, 981–993.

Willingham, S.B., Allen, I.C., Bergstralh, D.T., Brickey, W.J., Huang, M.T.-H., Taxman, D.J., Duncan, J.A., Ting, J.P.-Y., 2009. NLRP3 (NALP3, cryopyrin) facilitates in vivo caspase-1, necrosis, & HMGB1 release via inflammasome-dependent and –independent pathways. *J. Immunol. Baltim. Md 1950*, **183**, 2008–2015.

Woldbaek, P.R., Sande, J.B., Strømme, T.A., Lunde, P.K., Djurovic, S., Lyberg, T., Christensen, G., Tønnessen, T., 2005. Daily administration of interleukin-18 causes myocardial dysfunction in healthy mice. *Am. J. Physiol. Heart Circ. Physiol.*, **289**, H708–714.

Wollaston, W.H., 1797. On Gouty and Urinary Concretions. By William Hyde Wollaston, M. D. F. R. S. *Philos. Trans. R. Soc. Lond.*, **87**, 386–400.

Wright, S.D., Ramos, R.A., Tobias, P.S., Ulevitch, R.J., Mathison, J.C., 1990. CD14, a receptor for complexes of lipopolysaccharide (LPS) and LPS binding protein. *Science*, **249**, 1431–1433.

Wu, Y., Zheng, Z., Jiang, Y., Chess, L., Jiang, H., 2009. The specificity of T cell regulation that enables self-nonself discrimination in the periphery. *Proc. Natl. Acad. Sci. U. S. A.*, **106**, 534–539.

Xiao, H., Qian, W., Staschke, K., Qian, Y., Cui, G., Deng, L., Ehsani, M., Wang, X., Qian, Y.-W., Chen, Z.J., Gilmour, R., Jiang, Z., Li, X., 2008. Pellino 3b Negatively Regulates Interleukin-1-induced TAK1-dependent NFκB Activation. *J. Biol. Chem.*, **283**, 14654–14664.

Xiao, Y., Jin, J., Chang, M., Chang, J.-H., Hu, H., Zhou, X., Brittain, G.C., Stansberg, C., Torkildsen, Ø., Wang, X., Brink, R., Cheng, X., Sun, S.-C., 2013. Peli1 promotes microglia-mediated CNS inflammation by regulating Traf3 degradation. *Nat. Med.*, **19**, 595–602.

Xu, H., Barnes, G.T., Yang, Q., Tan, G., Yang, D., Chou, C.J., Sole, J., Nichols, A., Ross, J.S., Tartaglia, L.A., Chen, H., 2003. Chronic inflammation in fat plays a crucial role in the development of obesity-related insulin resistance. *J. Clin. Invest.*, **112**, 1821–1830.

Xu, Y., Tao, X., Shen, B., Horng, T., Medzhitov, R., Manley, J.L., Tong, L., 2000. Structural basis for signal transduction by the Toll/interleukin-1 receptor domains. *Nature*, **408**, 111–115.

Yamamoto, M., Sato, S., Hemmi, H., Hoshino, K., Kaisho, T., Sanjo, H., Takeuchi, O., Sugiyama, M., Okabe, M., Takeda, K., Akira, S., 2003a. Role of Adaptor TRIF in the MyD88-Independent Toll-Like Receptor Signaling Pathway. *Science*, **301**, 640–643.

Yamamoto, M., Sato, S., Hemmi, H., Sanjo, H., Uematsu, S., Kaisho, T., Hoshino, K., Takeuchi, O., Kobayashi, M., Fujita, T., Takeda, K., Akira, S., 2002. Essential role for TIRAP in activation of the signalling cascade shared by TLR2 and TLR4. *Nature*, **420**, 324–329.

Yamamoto, M., Sato, S., Hemmi, H., Uematsu, S., Hoshino, K., Kaisho, T., Takeuchi, O., Takeda, K., Akira, S., 2003b. TRAM is specifically involved in the Toll-like receptor 4–mediated MyD88-independent signaling pathway. *Nat. Immunol.*, **4**, 1144–1150.

Yamamoto, M., Yaginuma, K., Tsutsui, H., Sagara, J., Guan, X., Seki, E., Yasuda, K., Yamamoto, M., Akira, S., Nakanishi, K., Noda, T., Taniguchi, S., 2004. ASC is essential for LPS-induced activation of procaspase-1 independently of TLR-associated signal adaptor molecules. *Genes Cells*, **9**, 1055–1067.

Yamaoka, S., Courtois, G., Bessia, C., Whiteside, S.T., Weil, R., Agou, F., Kirk, H.E., Kay, R.J., Israël, A., 1998. Complementation cloning of NEMO, a component of the IkappaB kinase complex essential for NF-kappaB activation. *Cell*, **93**, 1231–1240.

Yamin, T.-T., Miller, D.K., 1997. The Interleukin-1 Receptor-associated Kinase Is Degraded by Proteasomes following Its Phosphorylation. *J. Biol. Chem.*, **272**, 21540–21547.

Yang, R.-B., Mark, M.R., Gray, A., Huang, A., Xie, M.H., Zhang, M., Goddard, A., Wood, W.I., Gurney, A.L., Godowski, P.J., 1998. Toll-like receptor-2 mediates lipopolysaccharide-induced cellular signalling. *Nature*, **395**, 284–288.

Yang, S., Sugawara, S., Monodane, T., Nishijima, M., Adachi, Y., Akashi, S., Miyake, K., Hase, S., Takada, H., 2001. Micrococcus luteus Teichuronic Acids Activate Human and Murine Monocytic Cells in a CD14- and Toll-Like Receptor 4-Dependent Manner. *Infect. Immun.*, **69**, 2025–2030.

Yang, S., Wang, B., Humphries, F., Hogan, A.E., O'Shea, D., Moynagh, P.N., 2014. The E3 Ubiquitin Ligase Pellino3 Protects against Obesity-Induced Inflammation and Insulin Resistance. *Immunity*, **41**, 973–987.

Yang, S., Wang, B., Humphries, F., Jackson, R., Healy, M.E., Bergin, R., Aviello, G., Hall, B., McNamara, D., Darby, T., Quinlan, A., Shanahan, F., Melgar, S., Fallon, P.G., Moynagh, P.N., 2013a. Pellino3 ubiquitinates RIP2 and mediates Nod2-induced signaling and protective effects in colitis. *Nat. Immunol.*, **14**, 927–936.

Yang, S., Wang, B., Tang, L.S., Siednienko, J., Callanan, J.J., Moynagh, P.N., 2013b. Pellino3 targets RIP1 and regulates the pro-apoptotic effects of TNF-α. *Nat. Commun.*, **4**, 2583.

Yarovinsky, F., Zhang, D., Andersen, J.F., Bannenberg, G.L., Serhan, C.N., Hayden, M.S., Hieny, S., Sutterwala, F.S., Flavell, R.A., Ghosh, S., Sher, A., 2005. TLR11 Activation of Dendritic Cells by a Protozoan Profilin-Like Protein. *Science*, **308**, 1626–1629.

Yonekura, K., Maki-Yonekura, S., Namba, K., 2003. Complete atomic model of the bacterial flagellar filament by electron cryomicroscopy. *Nature*, **424**, 643–650.

Yoneyama, M., Kikuchi, M., Natsukawa, T., Shinobu, N., Imaizumi, T., Miyagishi, M., Taira, K., Akira, S., Fujita, T., 2004. The RNA helicase RIG-I has an essential function in double-stranded RNA-induced innate antiviral responses. *Nat. Immunol.*, **5**, 730–737.

Yu, K.-Y., Kwon, H.-J., Norman, D.A.M., Vig, E., Goebl, M.G., Harrington, M.A., 2002. Cutting Edge: Mouse Pellino-2 Modulates IL-1 and Lipopolysaccharide Signaling. *J. Immunol.*, **169**, 4075–4078.

Zandi, E., Rothwarf, D.M., Delhase, M., Hayakawa, M., Karin, M., 1997. The IκB Kinase Complex (IKK) Contains Two Kinase Subunits, IKKα and IKKβ, Necessary for IκB Phosphorylation and NF-κB Activation. *Cell*, **91**, 243–252.

Zhang, S.-Y., Jouanguy, E., Ugolini, S., Smahi, A., Elain, G., Romero, P., Segal, D., Sancho-Shimizu, V., Lorenzo, L., Puel, A., Picard, C., Chapgier, A., Plancoulaine, S., Titeux, M., Cognet, C., Bernuth, H. von, Ku, C.-L., Casrouge, A., Zhang, X.-X., Barreiro, L., Leonard, J., Hamilton, C., Lebon, P., Héron, B., Vallée, L., Quintana-Murci, L., Hovnanian, A., Rozenberg, F., Vivier, E., Geissmann, F., Tardieu, M., Abel, L., Casanova, J.-L., 2007. TLR3 Deficiency in Patients with Herpes Simplex Encephalitis. *Science*, **317**, 1522–1527.

Zhao, Y., Yang, J., Shi, J., Gong, Y.-N., Lu, Q., Xu, H., Liu, L., Shao, F., 2011. The NLRC4 inflammasome receptors for bacterial flagellin and type III secretion apparatus. *Nature*, **477**, 596–600.

Zheng, C., Kabaleeswaran, V., Wang, Y., Cheng, G., Wu, H., 2010. Crystal structures of the TRAF2: cIAP2 and the TRAF1: TRAF2: cIAP2 complexes – affinity, specificity and regulation. *Mol. Cell*, **38**, 101–113.

Zhong, Z., Zhai, Y., Liang, S., Mori, Y., Han, R., Sutterwala, F.S., Qiao, L., 2013. TRPM2 links oxidative stress to NLRP3 inflammasome activation. *Nat. Commun.*, **4**, 1611.

Zhou, R., Yazdi, A.S., Menu, P., Tschopp, J., 2011. A role for mitochondria in NLRP3 inflammasome activation. *Nature*, **469**, 221–225.

Zhou, Y., Guo, M., Wang, X., Li, J., Wang, Y., Ye, L., Dai, M., Zhou, L., Persidsky, Y., Ho, W., 2013. TLR3 activation efficiency by high or low molecular mass poly I:C. *Innate Immun.*, **19**, 184–192.

Żurawek, M., Fichna, M., Januszkiewicz-Lewandowska, D., Gryczyńska, M., Fichna, P., Nowak, J., 2010. A coding variant in NLRP1 is associated with autoimmune Addison's disease. *Hum. Immunol.*, **71**, 530–534.